

UNCLASSIFIED

AD 256 584

*Reproduced
by the*

**ARMED SERVICES TECHNICAL INFORMATION AGENCY
ARLINGTON HALL STATION
ARLINGTON 12, VIRGINIA**



UNCLASSIFIED

NOTICE: When government or other drawings, specifications or other data are used for any purpose other than in connection with a definitely related government procurement operation, the U. S. Government thereby incurs no responsibility, nor any obligation whatsoever; and the fact that the Government may have formulated, furnished, or in any way supplied the said drawings, specifications, or other data is not to be regarded by implication or otherwise as in any manner licensing the holder or any other person or corporation, or conveying any rights or permission to manufacture, use or sell any patented invention that may in any way be related thereto.

RADC-TR-61-58
ASTIA Document No. AD-

CORNELL AERONAUTICAL LABORATORY, INC.

256-584

INVESTIGATION OF DIGITAL DATA COMMUNICATION SYSTEMS

Prepared by:
John G. Lawton

Report No. UA-1420-S-1
Contract No. AF 30(602)-2210

3 January 1961

Prepared for:

Home Air Development Center
Air Research and Development Command
United States Air Force
Griffiss Air Force Base
New York

B U F F A L O , N E W Y O R K

PATENT NOTICE: When Government drawings, specifications, or other data are used for any purpose other than in connection with a definitely related Government procurement operation, the United States Government thereby incurs no responsibility nor any obligation whatsoever and the fact that the Government may have formulated, furnished, or in any way supplied the said drawings, specifications or other data is not to be regarded by implication or otherwise as in any manner licensing the holder or any other person or corporation, or conveying any rights or permission to manufacture, use, or sell any patented invention that may in any way be related thereto.

Qualified requestors may obtain copies of this report from the ASTIA Document Service Center, Dayton, Ohio. ASTIA Services for the Department of Defense contractors are available through the "Field of Interest Register" on a "need-to-know" certified by the cognizant military agency of their project or contract.

RADC-TR-61-58
ASTIA Document No. AD-

3 JANUARY 1961

INVESTIGATION OF DIGITAL DATA
COMMUNICATION SYSTEMS

Prepared by:
John G. Lawton

CORNELL AERONAUTICAL LABORATORY, INC.
BUFFALO, NEW YORK

Report No. UA-1420-S-1
Contract No. AF 30(602)-2210

Project Number 4519
Task Number 45568

Prepared for:
ROME AIR DEVELOPMENT CENTER
AIR RESEARCH AND DEVELOPMENT COMMAND
UNITED STATES AIR FORCE
GRIFFISS AIR FORCE BASE
NEW YORK

FOREWORD

This report covers the work performed during the period February - December 1960 by the Cornell Aeronautical Laboratory, Inc., Buffalo, New York, under Air Force Contract AF 30(602)-2210. The contract was initiated by the Advanced Development Laboratory of the Directorate of Communications, the Rome Air Development Center, Griffiss Air Force Base, New York. The work was performed under the cognizance and direction of Mr. Alfred S. Kobos. The assistance and encouragement received from RADC personnel, in particular Messrs. Miles H. Bickelhaupt, Alfred S. Kobos and Lt. Jack K. Wolf, is gratefully acknowledged.

The material which is presented in this report is the result of the joint efforts of the personnel assigned to this project at the Cornell Aeronautical Laboratory. The Project Engineer at the C.A.L. is Dr. John G. Lawton and the major contributors to this effort are: Messrs. Harold D. Becker, Ting T. Chang, Richard E. Cleary, Eugene A. Trabka, Ned B. Smith.

ABSTRACT

This report covers analyses on a variety of topics related to the transmission of digital data. The performance of several types of Phase Shift Keyed (PSK) systems, as determined by the relationship of the error probability to signal-to-noise ratio, is examined. Coherent, differentially coherent, binary and m-state PSK systems, and the effects of frequency offset, cross-talk and thermal noise on the performance of these systems are considered. The performance of m-state differentially coherent multiplexed PSK data links operating over a Rayleigh fading tropospheric scatter link is analyzed.

The properties of impulse noise are examined and the effect of impulse noise on digital systems using close-packed codes are investigated.

"Moment detection", which refers to a decision technique based on the use of temporal moments, m_k , of the received waveform, ($m_k = \int_0^T t^k y(t) dt$), is investigated both analytically and experimentally.

TABLE OF CONTENTS

<u>SECTION</u>	<u>PAGE</u>
TITLE PAGE	1
FOREWORD	ii
ABSTRACT	iii
TABLE OF CONTENTS	iv
LIST OF ILLUSTRATIONS	v
LIST OF APPENDICES	vi
I INTRODUCTION	1
II ANALYSIS OF PHASE SHIFT KEYED SYSTEMS	4
III ANALYSIS OF DIFFERENTIAL COHERENT PHASE SHIFT KEYED (DGPSK) DATA SYSTEMS OPERATING OVER A FADING FM TROPOSPHERIC SCATTER CIRCUIT	24
IV COMMENTS ON AN ARTICLE ENTITLED "IDEAL BINARY PULSE TRANSMISSION BY AM AND FM"	27
V PROPERTIES OF IMPULSE NOISE AND THE EFFECT OF IMPULSE NOISE ON DIGITAL DATA COMMUNICATIONS SYSTEMS USING CLOSE PACKED CODES	30
VI MOMENT DETECTION	35
BIBLIOGRAPHY	40
GLOSSARY	50

LIST OF ILLUSTRATIONS

<u>FIGURE</u>	<u>PAGE</u>
II-1 Phasor Representation of m-State PSK Signals	5
II-2 Block Diagram of m-State PSK Transmitter	6
II-3 Waveforms Produced by Unchanging Data in PSK Systems	7
II-4 Cross-Correlation Embodiment of the Maximum Likelihood Receiver	9
II-5 Matched Filter Embodiment of Maximum Likelihood Receiver	11
II-6 A "Practical" Receiver	11
II-7 Error Probability of a BGPPSKS With Frequency Error	15
II-8 Probability Density of Phase Difference	18
II-9 Probability of Character Error in m-State DCPSKS	19
II-10 Sub-Channel Error Probability in an $m = 4$ DCPSKS	21
II-11 Character Error Probability in an m-State DCPSKS with Frequency Error	23
V-1 Probability Density of "Rectangular" Poisson Noise	32
V-2 Word Error Probability vs. Expected Number of Letter Errors per Word (Completely Overlapped by a Burst)	33
V-3 Comparison of Word Error Probability with Original and Modified Assumptions	34

LIST OF APPENDICES

APPENDIX

I DERIVATION OF RESULTS USED IN CHAPTER II

- (a) DETECT MEMO NO. 5A - "Embodiments of the Maximum Likelihood Receiver for Detection of Coherent Phase Shift Keyed Signals" by Eugene A. Trabka.
- (b) DETECT MEMO NO. 12 - "Error Probability (in the presence of sampling time errors) of the Cross Correlation Embodiments of a Maximum Likelihood Receiver for Binary Coherent Gated Phase Shift Keyed Systems (BCGPSKS)" by Eugene A. Trabka.
- (c) DETECT MEMO NO. 15 - "Comments on m-State Coherent Digital Communications Systems" by Eugene A. Trabka.
- (d) DETECT MEMO NO. 7A - "Error Probabilities for Coherent Pulsed Phase-Shift Keyed Systems (CPPSKS) with Frequency and Sampling Time Errors" by Eugene A. Trabka.
- (e) DETECT MEMO NO. 8A - "Error Probability in a Binary Coherent Pulsed Phase Shift Keyed System (BCPPSKS) with Cross Talk from Adjacent Multiplexed Channels" by Eugene A. Trabka.
- (f) DETECT MEMO NO. 10(a) - "Double Bit Matched Filter (DBMF) Reception of Differentially Coherent Binary Phase Shift Keyed (DCBPSK) Signals"
 - (b) "The Equivalence of Integrate, Delay and Phase Comparison and DBMF Receivers for DCBPSK Systems" by John G. Lawton.

I LIST OF APPENDICES (CONTD.)

APPENDIX

- I (g) DETECT MEMO NO. 2A - "Error Probabilities of Multiple-State Differentially Coherent Phase Shift Keyed Systems in the Presence of White Gaussian Noise" by John T. Fleck and Eugene A. Trabka.
- I (h) DETECT MEMO NO. 11 - "Error Probabilities of m-State Differentially Coherent Phase Shift Keyed Systems (DCPSKS) with a Frequency Offset of the Received Signals" by Eugene A. Trabka.

II ILLUSTRATION OF RESULTS USED IN CHAPTER III

- I (a) DETECT MEMO NO. 13 - "Analysis of a Differentially Coherent Phase Shift Keyed (DCPSK) Digital Data Systems Operating over a Fading FM Tropospheric Scatter Circuit" by Harold E. Becker.

III ILLUSTRATION OF RESULTS USED IN CHAPTER V

- I (a) DETECT MEMO NO. 6 - "Some Properties of Impulse Noise" by Richard E. Cleary.
- I (b) DETECT MEMO NO. 3A - "Error Probability of a System Using Close Packed Codes in the Presence of Impulse Noise" by Richard E. Cleary.
- I (c) ALLENHUM TO DETECT MEMO NO. 3 - "Error Probability of a System Using Close Packed Codes in the Presence of Impulse Noise" by Richard E. Cleary and Peter Crimi.

LIST OF APPENDICES (CONTD.)

APPENDIX

IV DERIVATION OF RESULTS USED IN CHAPTER VI

- (a) DETECT MEMO NO. 1A - "Moment Detection in the Presence of White Gaussian Noise" by T. T. Chang.
- (b) DETECT MEMO NO. 4 - "Optimum Decision Based on Multiple Moment Detection" by T. T. Chang.
- (c) DETECT MEMO NO. 9 - "Analysis of the Effects of Impulse Noise on Moment Detection" by T. T. Chang.
- (d) DETECT MEMO NO. 14 - "Experimental Investigation of Moment Detection" by Ned B. Smith.

I. INTRODUCTION

The need for rapid, reliable, digital communications systems spanning very large distances, has assumed great importance during the last few years. In some cases, such as the telemetering of data from space probes, it has been practical to design the digital communications system "from the ground up" for the particular task at hand. In other cases, such as the transmission of data over long distance telephone facilities, the economic necessity of utilizing the vast existing plant imposes particular restrictions on the data system employed.

In view of the fundamental differences of the various environments encountered, it has not been possible to conceive of a universally suitable digital communications system. Even for a single environment, the precise form which an "optimum" system should take is, in general, unknown; in fact, it is doubtful that agreement on what constitutes an optimum system could be obtained. Although a universally accepted method of comparing different digital communications systems does not exist, it is often possible to compare systems on a relative or "all other parameters being equal" basis.

The present report covers that part of a continuing investigation of methods for the transmission and detection of digital data which was performed during the period February - December 1960, under Air Force Contract No. AF-30(602)-2210. This contract is concerned with a variety of fundamental investigations which fall into the following two broad categories:

- 1) Investigations aimed at determining the limitations imposed on the performance of various systems by deleterious phenomena, such as fading, phase distortion, noise, synchronization errors, etc.
- 2) The postulation and/or examination of promising new techniques, such as m-state (as distinguished from 2-state or binary) digital communications systems, new modulation and decision techniques, etc.

As several of the topics covered are not closely related, and since they were treated by separate investigations, they are reported herein by means of independent Chapters and Appendices. Major project effort

was devoted to these separate studies, and their results and derivations were documented in DETECT* memoranda upon completion of the individual studies. In view of the above, it seems appropriate to restrict the body of this report primarily to a summary of the results obtained and to leave the derivations of these results in the DETECT memoranda which form appendices of this report.

This Laboratory had under a previous contract, AF 30(602)-1702, investigated the performance of various binary data transmission systems in the presence of additive white Gaussian noise. A major portion of that analysis ** was concerned with coherent and differentially coherent binary phase-shift keyed systems. Under the present contract, this analysis has been extended to cover:

- a) multiple state as well as binary phase-shift keyed systems;
- b) the effects of frequency offset between transmitter and receiver, synchronization errors, and crosstalk;
- c) various embodiments of receivers for the reception of these signals;

The results of this phase of the work are reported in Chapter II of this report, while the derivations and proofs are contained in Appendix I.

Chapter III reports the results of applying the above analysis to the investigation of the performance of digital data links in which DCPSK channels are multiplexed and transmitted over a Rayleigh fading FM tropospheric scatter link. Appendix II contains the derivation of these results.

Chapter IV is devoted to comments on an article entitled, "Ideal Binary Pulse Transmission by AM and FM," *** which reached conclusions incompatible with prior work at this Laboratory.

* Effort under this contract has, within the Cornell Aeronautical Laboratory, been designated as Project DETECT.

** See Bibliography - Becker I.

*** Sunde I.

Chapter V discusses some of the properties of impulse noise and reports the results of an investigation of the effects of impulse noise on the error probability of digital communications systems using close-packed codes. Appendix III contains the derivations of the results noted in that chapter.

"Moment detection" is the name given to a decision technique based on the utilization of temporal moments by a group at Rutgers University who proposed this technique. Under the present program, the performance attainable by "moment detection" has been investigated both analytically and experimentally. The results of these investigations are reported in Chapter VI of this report and the derivations and proofs are contained in Appendix IV.

Because material contained in the appendices, most of which was originally issued in DETECT memoranda, was written by various authors, the meaning of symbols may vary somewhat among the appendices. A consistent notation is, however, used in every individual appendix and throughout the body of this report. It was felt that any attempt to change notation so as to enforce complete consistency would probably be unsuccessful. In several instances it was felt desirable to make changes in DETECT memoranda before incorporating them into the appendices of this report; such memoranda are identified by the letter "A" after the memorandum number.

II. ANALYSIS OF PHASE-SHIFT KEYED SYSTEMS

Previous analyses* have shown that among binary systems operating in the presence of white Gaussian noise, phase-shift keyed systems attain smaller error probabilities than other systems. Differentially coherent phase-shift keyed systems** are currently in use or contemplated for use over wire lines, H.F. radio, and troposcatter links and PSK systems using phase-locked loops have been used for telemetry from space probes.***

Since, in practice, these systems often do not use a binary alphabet and are subject to disturbances other than white Gaussian noise, it is of interest to investigate phase-shift keyed systems further. This report extends the analyses to include m -state coherent phase-shift keyed (CPSK) and differentially coherent phase-shift keyed (DCPSK) systems, as well as the effects of synchronization errors and frequency offset between transmitter and receiver. Details of the analyses which have been performed on these systems will be found in Appendix I and the results obtained there are discussed below.

Figure II-1 is a phasor representation of the transmitted signals (characters) of an m -state PSK system for the case $m = 8$. In the case of CPSK systems, the reference phasor represents an absolute reference, whereas in the case of a DCPSK system it represents the phase of the signal transmitted during the previous signal interval. Note that it is not, in general, possible to distinguish CPSK from DCPSK signals without additional information.

* Becker I, Reiger I, Cahn I.

** A coherent phase-shift keyed system is one in which the absolute phase of the signal corresponds to the data; a differentially coherent phase-shift keyed system is one where the phase difference between successive signals corresponds to the data.

*** Taber I, Sanders I

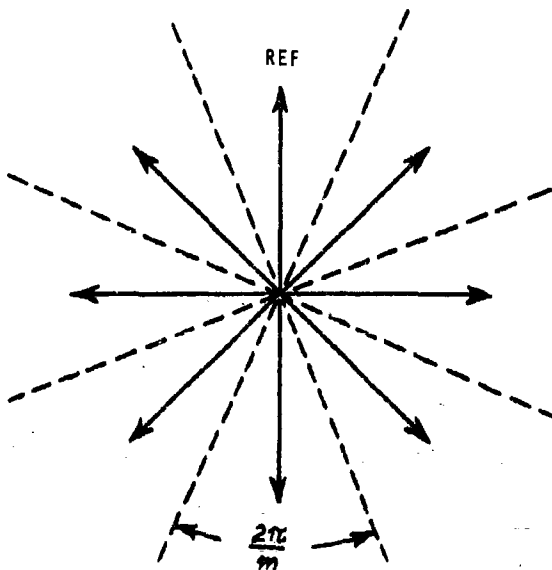


Figure II-1 PHASOR REPRESENTATION OF m -STATE PSK SIGNALS

Figure II-2 is a block diagram of an m -state PSK transmitter. An oscillator produces a continuous sinusoidal wave form which is phase-shifted so that the m phase-shifted signals shown in Figure II-1 are applied to the input of m gates. The gates are controlled by a logic circuit such that only one gate is open during any signal interval. The logic circuit selects the proper gate in accordance with the input data and whether GPSK or DCPSK operation is desired. Synchronization of the data rate and gate operation is required and may be performed either externally or within the logic circuit. The operating frequency ω_0 may also be related to the signalling speed* such that each signal interval contains an integral number of cycles. If there are

* Signalling speed is defined as the rate at which elementary signals are transmitted regardless of the information content, thus an $m = 8$ state system operating at a signalling speed of 1000 baud would have a signal duration of 1 millisecond and could convey at most $1000 \log_2 8 = 3000$ bits of information per second.

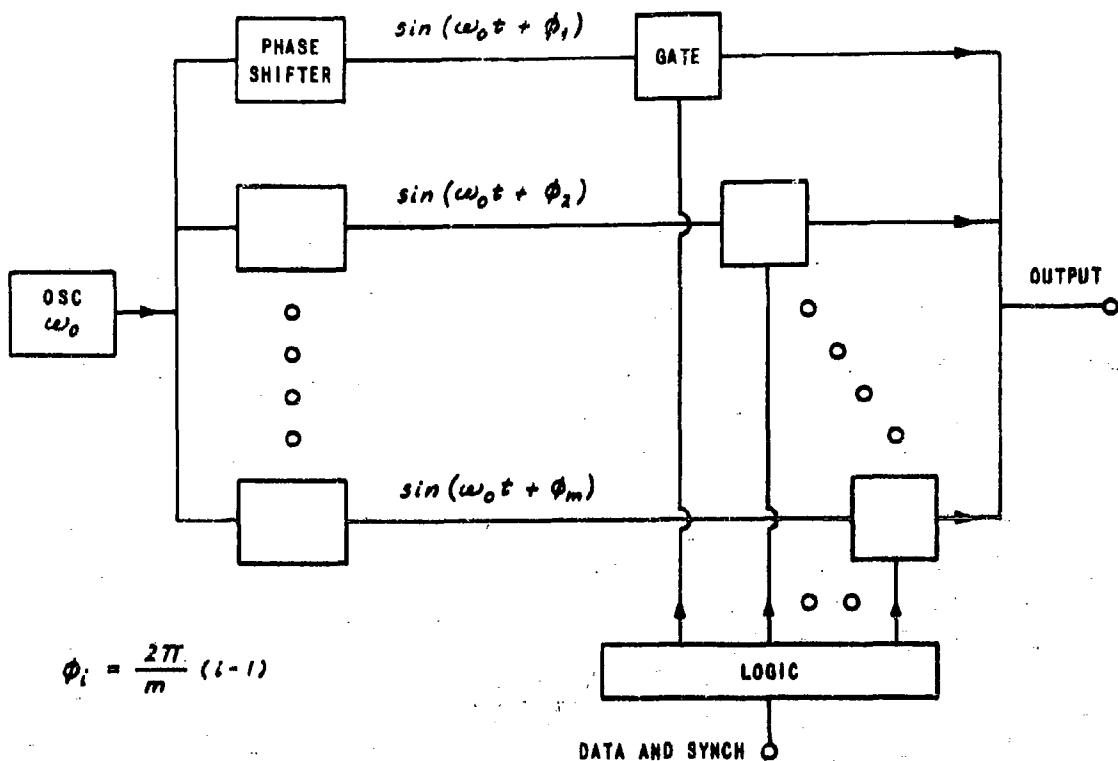
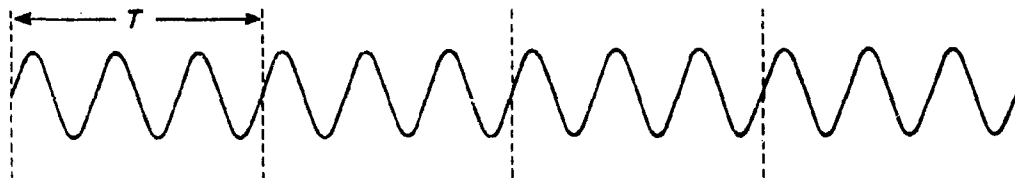


Figure III-2 BLOCK DIAGRAM OF m -STATE PSK TRANSMITTER

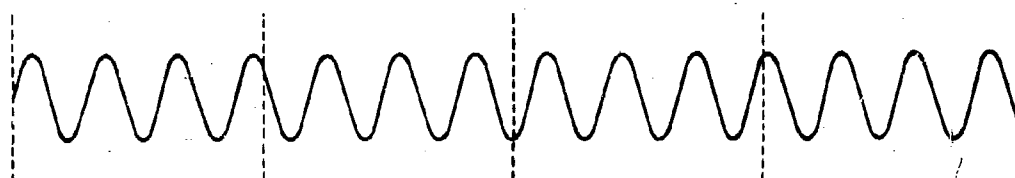
an integral number of cycles per signal interval, certain aspects of the analysis are greatly facilitated. This assumption has been made in several places in the analyses but is not required in the proof of the major results obtained in connection with DCPSK systems.

It is possible to conceive of a PSK system which operates in a manner somewhat different from the system described above. In order to distinguish between these systems, the system described above will be called a gated PSK system, since the transmitted signals are obtained by gating of continuous phase-shifted sinusoids, and the alternate system will be called a pulsed PSK system. In an m -state pulsed PSK system the signals are pulsed sinusoids

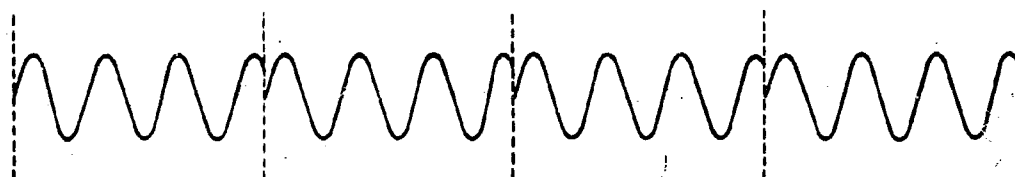
with m distinct starting phases. The difference between the signals of these systems is illustrated in Figure II-3.



a) GATED OR PULSED PSK SYSTEM WITH INTEGRAL NUMBER OF CYCLES PER SIGNAL INTERVAL



b) GATED PSK SYSTEM WITH NONINTEGRAL NUMBER OF CYCLES PER SIGNAL INTERVAL



c) PULSED PSK SYSTEM WITH NONINTEGRAL NUMBER OF CYCLES PER SIGNAL INTERVAL

Figure II-3 WAVEFORMS PRODUCED BY UNCHANGING DATA IN PSK SYSTEMS

If each signal interval contains an integral number of cycles, then the two PSK systems are equivalent, otherwise the two systems are not strictly equivalent. In particular, it is possible to consider the pulsed CPSK system operating with a frequency difference between transmitter and receiver. Operation can be maintained in the presence of an unknown frequency difference only if starting phase coherence is maintained. This may be the case, for instance, when the frequency-determining elements of the transmitter and receiver are "detuned" with respect to each other, but would not be the case when the frequency difference is due to "offset" of heterodyning oscillators. This does not appear reasonable for the gated CPSK system because,

in this system, a phase error would accumulate in accordance with $\Delta\phi(t) = \int_0^t \Delta\omega(\tau) d\tau$. In practice, where frequency errors occur with a gated CPSK system, some power is transmitted at the carrier frequency to establish a phase reference, and a frequency-following scheme using a phase-locked loop is usually employed.

It is, of course, necessary that the transmitter and receiver of a PSK system be designed so as to be compatible, i.e., both components must be designed either for gated or pulsed PSK operation. From an analytical point of view, these systems are equivalent to a considerable extent and closely analogous embodiments of the various receivers are possible. As far as is known, only gated CPSK systems have been used in practice. This is probably due to the greater simplicity of the resulting hardware and the ability to approach the performance of a true coherent system by the use of a transmitted reference signal.

Sections (a) and (b) of Appendix I describe several embodiments of the maximum likelihood receiver for the detection of CPSK signals in white Gaussian noise.

Figure II-4 shows the block diagram of the cross-correlation embodiment of a maximum likelihood receiver based on the theory of these receivers as described in Appendix I(c) and by several other authors.*

* Woodward I, Peterson I, Davenport I

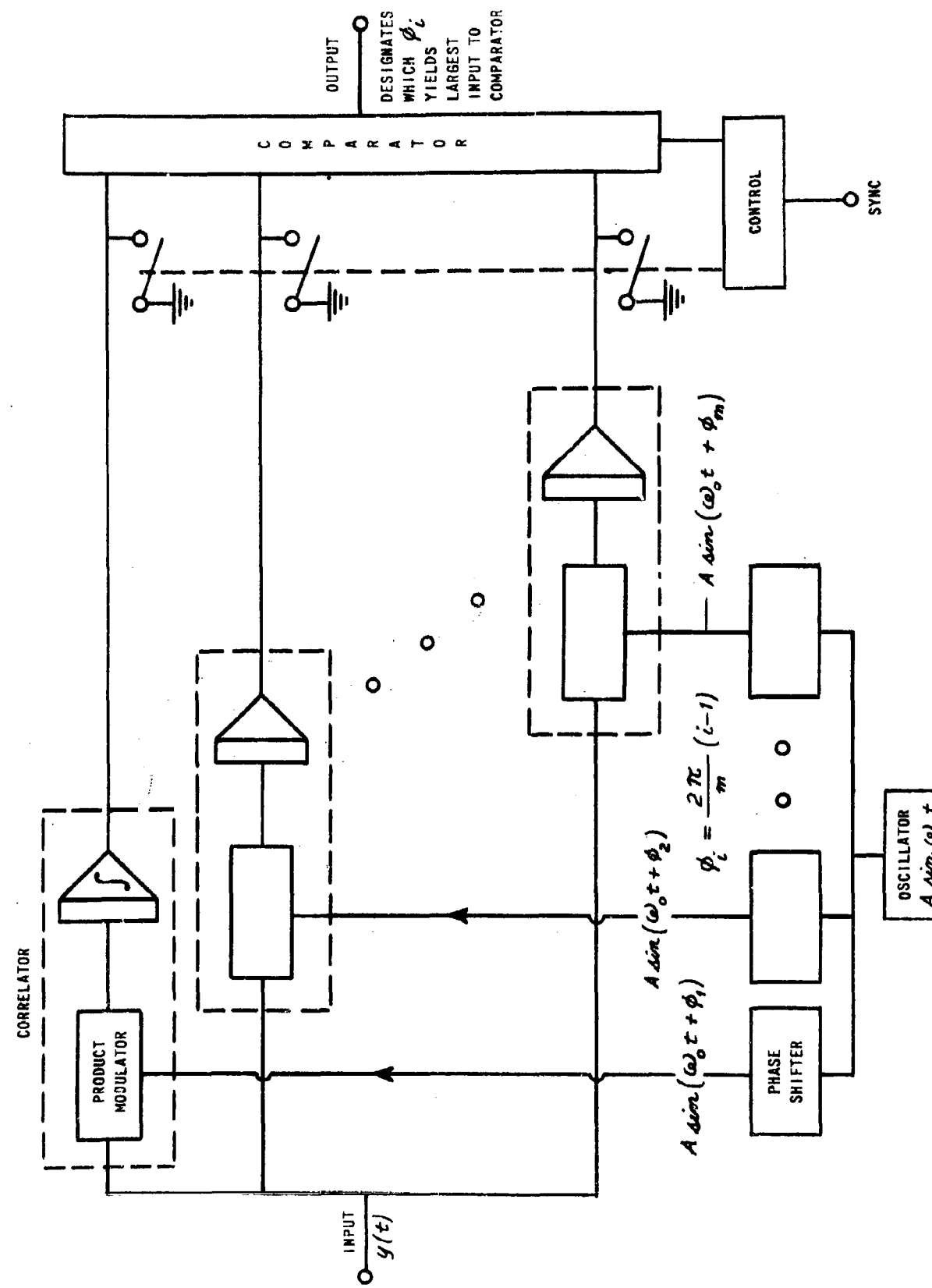


Figure II-4 CROSS-CORRELATION EMBODIMENT OF MAXIMUM LIKELIHOOD RECEIVER

Figure II-5 is the block diagram of a matched filter embodiment. This receiver is applicable to the pulsed CPSK systems and to the gated CPSK systems only if each signal interval contains exactly an integral number of cycles and the start of the signal intervals is phase-locked to the reference signal phase. If each signal interval of a gated CPSK system does not contain an integral number of cycles, then the signals contained in adjacent signal intervals will differ in their respective starting phases, even when the data corresponding to the two signal intervals does not change. This would require that different matched filters be used for adjacent signal intervals and make the matched filter embodiment rather impractical. The transmitter, Figure II-2, and the cross-correlation receiver, Figure II-4, however, do not require an integral number of cycles per signal interval.

Upon noting the m -fold repetition of most of the components of the cross-correlation and the matched filter receivers (Figures II-4 and II-5), one is led to inquire whether equivalent performance could not be obtained from a simpler receiver. Figure II-6 shows the block diagram of a more practical receiver, the performance of which approaches that of a true maximum likelihood receiver if the number of cycles per signal interval is large.

If $\omega_0 T \gg 2\pi$ the error probability of the m -state CPSK system is given by

$$P(m) = 1 - \frac{2}{\pi} \int_0^{\infty} \left[e^{-\left(u - \sqrt{\frac{E}{N_0}}\right)^2} \int_0^{u \tan \frac{\pi}{m}} e^{-v^2} dv \right] du \quad \text{Ia-21*}$$

It has been possible to evaluate the integral in Eq. Ia-21 in closed form only for $m = 2$ and 4 yielding

$$P(2) = \frac{1}{2} \left\{ 1 - \operatorname{erf} \sqrt{\frac{E}{N_0}} \right\} \quad \text{Ia-22}$$

* The notation Ia-21, etc., indicates that this equation is derived in Appendix Ia and is there designated as Equation 21.

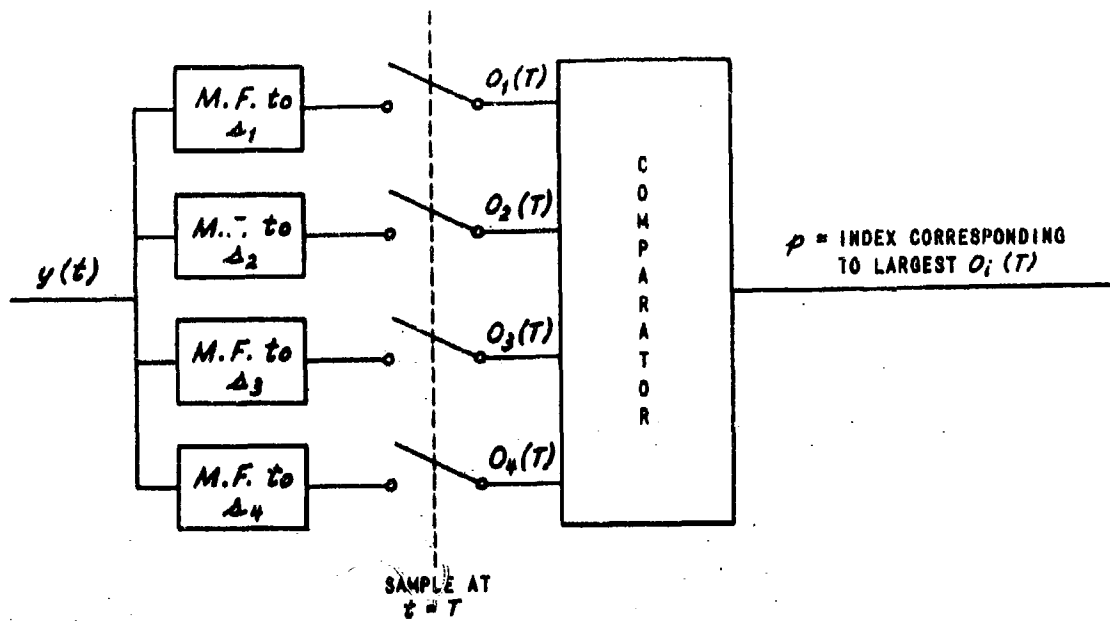


Figure II-5 MATCHED FILTER EMBODIMENT OF MAXIMUM LIKELIHOOD RECEIVER

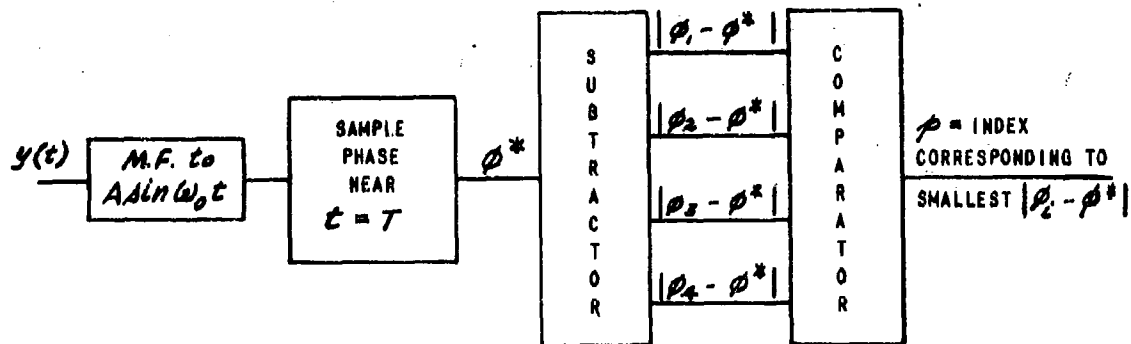


Figure II-6 A "PRACTICAL" RECEIVER

$$P(4) = \frac{3}{4} - \frac{1}{2} \operatorname{erf} \sqrt{\frac{E}{2N_0}} - \frac{1}{4} \operatorname{erf}^2 \left\{ \sqrt{\frac{E}{2N_0}} \right\} \quad \text{Ia-23}$$

where ESignal Energy (joules) per signal interval

No.....Noise power density (watts per cps) of the one-sided spectrum

$$\operatorname{erf} x = \frac{2}{\sqrt{\pi}} \int_0^x e^{-t^2} dt$$

Gilbert* has obtained an approximate formula for the error probability of coherent systems which is valid for $\sqrt{\frac{2E}{N_0}} \gg 1$. Although Gilbert did not specifically consider PSK systems, his approach, which is discussed in Appendix I(c), may be applied to these systems and yields

$$P(m) \cong 1 - \operatorname{erf} \left\{ \sqrt{\frac{E}{N_0}} \sin \frac{\pi}{m} \right\} .$$

It is always of interest to determine the sensitivity of a system to disturbances, or operation under conditions differing from those for which it was designed. Frequently it is not possible to carry through a statistically optimized design because the necessary statistics are not available. Under these conditions, knowledge of the sensitivity to variation of various parameters can be valuable. In this vein the sensitivities of the cross-correlation (Figure II-4), the matched-filter (Figure II-5), and the practical (Figure II-6) receivers to timing errors of the synchronization between transmitter and receiver were examined. Although these receivers give equivalent performance in the absence of synchronization errors, it is found that the matched-filter receiver is more sensitive to synchronization errors than the cross-correlation or the "practical" receivers. An equation for the error probability of the m-state "practical" receiver in the presence of timing errors is derived in Appendix I(d).

* Gilbert I

For $m = 2$ this equation reduces to

$$P(2) = \frac{1}{4} \left[2 - \operatorname{erf} \sqrt{\frac{E}{N_0}} - \operatorname{erf} \left\{ \left(1 - 2 \left| \frac{\Delta T}{T} \right| \right) \sqrt{\frac{E}{N_0}} \right\} \right]$$

Ib-16

Id-21

which also applies to the two-state cross-correlation receiver as is shown in Appendix I(b). However, the probability of error of the matched-filter receiver under these conditions is

$$P(2) = \frac{1}{4} \left[2 - \operatorname{erf} \left\{ \sqrt{\frac{E}{N_0}} \cos(\omega_0 \Delta T) \right\} - \operatorname{erf} \left\{ \left(1 - 2 \left| \frac{\Delta T}{T} \right| \right) \sqrt{\frac{E}{N_0}} \cos(\omega_0 \Delta T) \right\} \right] \quad \text{Id-28}$$

It will be noted that (for large E/N_0) the error probability of the cross-correlation and practical receivers is much less sensitive to $|\Delta T|$ than is the error probability of the matched-filter receiver. $P(2)$ as given by Equation Id-21 is monotonic with $|\Delta T|$ while $P(2)$ as given by Equation Id-28 is oscillatory. This behavior is plausible on physical grounds. It is a manifestation of the characteristics of the output voltage of the matched filter which oscillates with relatively constant phase at its resonant frequency. Hence, the error probability of the matched-filter receiver, which bases its decision on output voltage, reflects this oscillatory nature, whereas the error probability of the "practical" receiver, which bases its decision on output phase, reflects the more steady nature of the output phase. In the case of the cross-correlation receiver the output is governed primarily by the degree of overlap between the received signal and the interval of integration.

Although the analysis was not carried out for $m \neq 2$, the above arguments indicate that the cross-correlation and the practical receiver will retain their smaller sensitivity to $|\Delta T|$ compared to the matched-filter receiver for $m \neq 2$. A description of a particular realization of the "practical" receiver will be found in Appendix I(d). The receiver which is there described uses an "integrate and dump" technique for the realization of the matched filter and a zero-crossing phase detector for the determination of the phase of the filter output.

A comparison of the performance of the matched-filter and the "practical" receivers operated in a pulsed CPM system shows that these receivers give identical performance in the presence of frequency error* (and zero timing error). Appendix I(d) derives a formal expression for the error probability of an m-state "practical" receiver operating in the presence of sampling time and frequency errors. This expression is evaluated for $m = 2$. The corresponding expression for the matched-filter receiver yields equivalent performance only if $\frac{\omega_0}{2\pi} \Delta T = \nu$ = an integer.

It is well known that ideal PSK channels can be frequency-multiplexed without cross-talk provided that the frequency separation between channels is an integral multiple of $\frac{1}{T}$ cps, where T is the duration of an elementary signal interval. If there exists a frequency offset between transmitter and receiver then, not only is the response to the desired signal reduced, but cross-talk will also occur. Appendix I(e) determines the error probability of a Binary Coherent Pulsed Phase Shift-Keyed System (BCPPSKS) when cross-talk is due to two adjacent channels separated by $\frac{1}{T}$ cps, and the receiver is offset in frequency by Δf cps. The result is reproduced as Figure II-7.

The need for an absolute phase reference for the demodulation of CPSK signals poses a serious practical problem. Two approaches to the solution of this problem have been used. One is to expend a finite portion of the transmitted power to the transmission of a reference signal, which may be recovered with a very narrow band receiver. In practice, such a receiver usually takes the form of a "phase-locked loop", ** i.e., a phase reference signal is locally generated by an oscillator, the phase of which is controlled by the received signal. The other approach is to encode the information to be transmitted in accordance with DCPSK logic. It will be recalled that DCPSK logic encodes the m discrete signals as m discrete phase shifts between successive signals. At the transmitter an absolute phase reference may be used and at the receiver a reference oscillator may be phase-locked by the received signal in the manner described below. The frequency of the incoming

* The conditions under which a pulsed CPM system can be operated in the presence of a frequency error were discussed on page 7.

** Taber I, Sanders J.

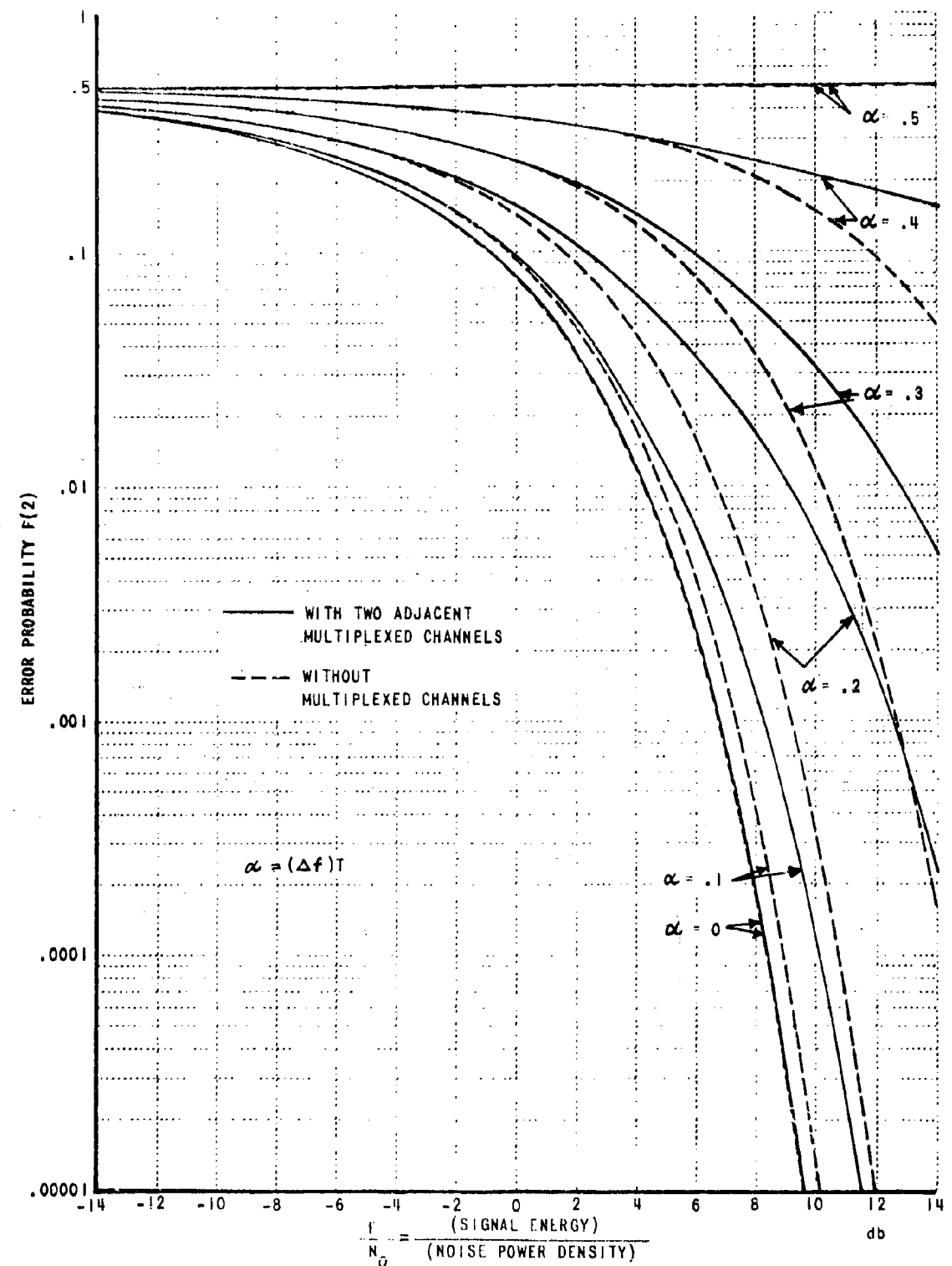


Figure II-7 ERROR PROBABILITY OF A BCPPSKS WITH FREQUENCY ERROR

signal is multiplied by m in such a manner that, in the absence of noise, a signal of constant phase results regardless of which of the m phases the input signal assumes. This signal is then passed through a very narrow band filter, which again may take the form of a phase-locked loop, and the reference signal is finally obtained by a phase-locked frequency divider. Note that the phase of the reference signal so obtained is known only to correspond to one of the m possible transmitted phases. However, for the reception of DCPSK signals, knowledge of absolute phase is not required.

The minimum bandwidth which can be used in recovering the reference signals with either of the above systems (i.e., the system where some power is expended for the transmission of the reference signal and the DCPSK system) is determined by the stability of the transmission medium and equipments.

The operation of a DCPSK system operating in the manner described above has not yet been evaluated. It has been mentioned primarily to point out that DCPSK systems are not restricted to the use of the previous signal as a phase reference. It is also noted that with a DCPSK system in which the reference phase is derived over a large number of signal intervals one would expect a marked decrease in the conditional probability of error given that the adjacent datum is in error, i.e., a reduction in the tendency for errors to occur in pairs which one expects when only the previous signal is used as a phase reference.

The results of analyses of LCPSK systems which derive their reference phase from only the previous signal interval will now be described.

Previous analysis* derived the error probability of various binary communications systems operating in the presence of additive white Gaussian noise, and noted that the LCPSK system required exactly 1/2 the signal energy of a noncoherent Frequency Shift-Keyed System to obtain the same error probability.

* Becker I

These error probabilities are

$$P(1)_{\text{BDCPSK}} = \frac{1}{2} e^{-E/N_0} \quad \text{If-1a}$$

$$P(2)_{\text{FSK}} = \frac{1}{2} e^{-E/2N_0} \quad \text{If-1b}$$

where E Signal energy (joules) per received bit
 N_0 Noise power density (watts/cps)

The reasons for the relationship are examined in Appendix I(f). It is concluded that Equation If-1b is applicable to all noncoherent binary systems which use orthogonal ($\rho=0$) signals having equal energy. The four possible waveforms produced by a BDCPSK system during two signal intervals can be divided into two sets containing two members each, according to whether or not there is a phase change between succeeding signal intervals. The two sets of signals satisfy the conditions for applicability of Equation If-1b. Upon noting that the energy in each waveform corresponds to two bits, the relationship of Equation If-1a to Equation If-1b follows. The performance of a receiver, called a Double-Bit Matched-Filter Receiver, which employs two filters, one matched to the constant phase and the other to the phase reversal set, and envelope detectors is examined, compared with and found to be equivalent to that of a BDCPSK receiver which compares the phases of the signals received during adjacent signal intervals.

In Appendix I(g) the character error probability of m -state BCPKS systems operating in the presence of white Gaussian noise is analyzed. The probability is equal to the probability that the phase difference of two vectors of equal magnitude which are independently perturbed by Gaussian noise differ by more than π/m from the phase difference of their means. An expression, Equation Ig-81, for the probability density, $h(\hat{\alpha})$, of this phase difference is obtained.* The behavior of $h(\hat{\alpha})$ is shown in Figure II-8. This expression was integrated, by cyclic summation, to yield the character error probability $P_e(m)$. Figure II-9 shows the results of this computation. For

* Note that here $\hat{\alpha}$ is calculated for the symbol α used in Appendix I(f), since the symbol α was used previously in this chapter.

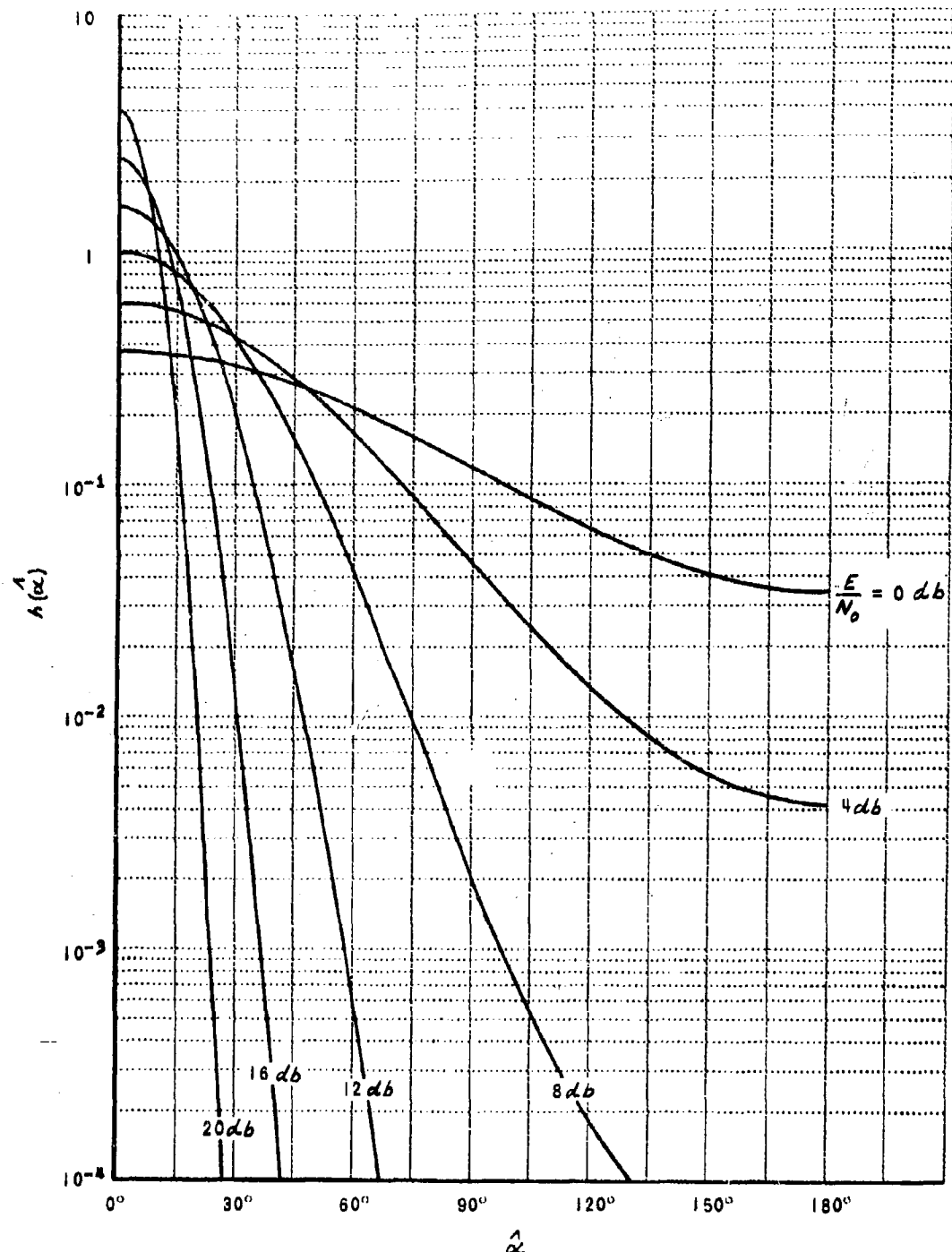


Figure II-8 PROBABILITY DENSITY OF PHASE DIFFERENCE

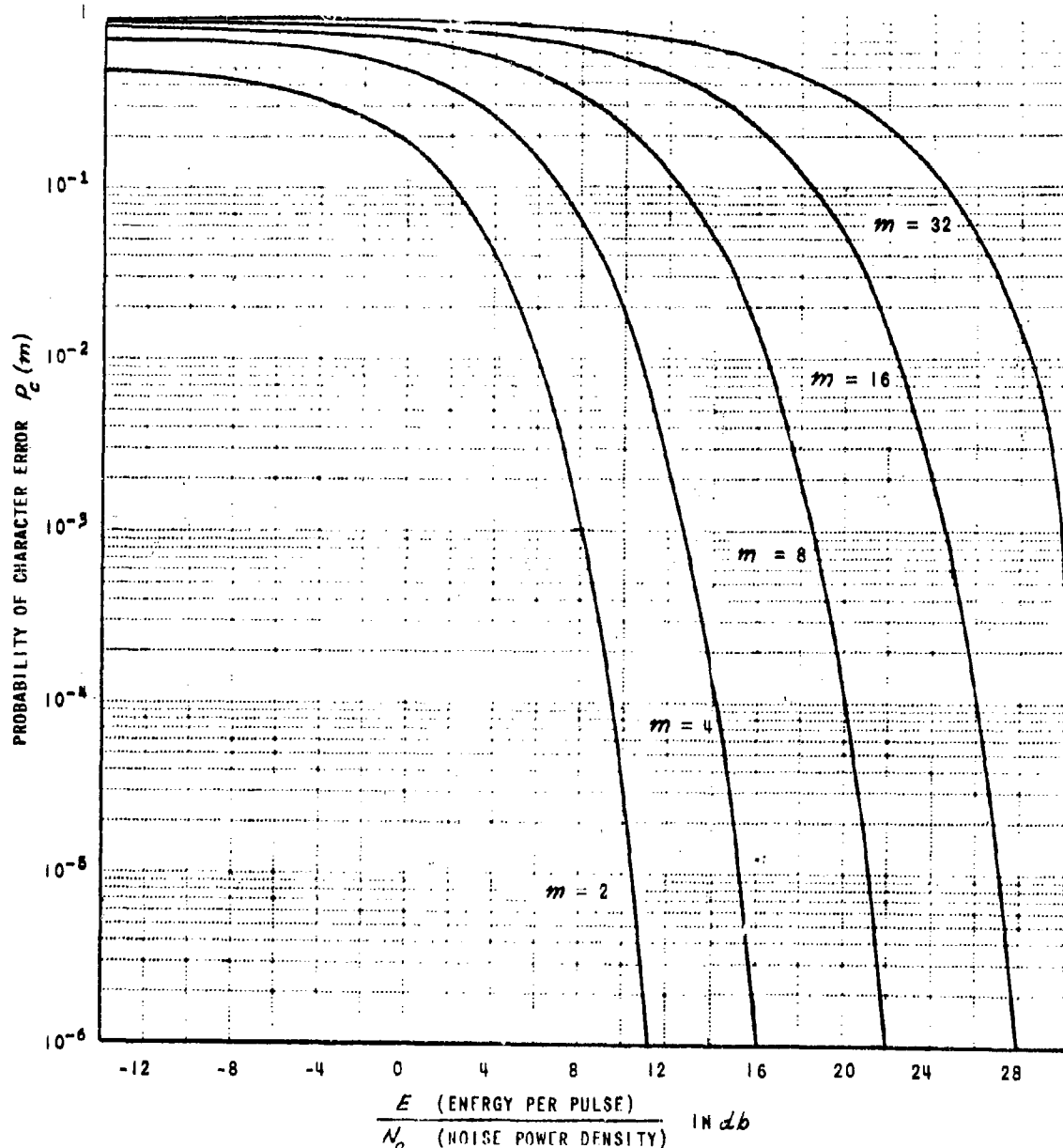


Figure II-9 PROBABILITY OF CHARACTER ERROR IN m - STATE DCPSKS

the case $m = 2$ it is possible to perform the integration in closed form yielding Equation Ig-54, the error probability of a BDCPSK in agreement with earlier analysis.*

A simple approximate formula, Equation Ig-80, was obtained from which extensive tabulations of $P_c(m)$ were prepared. Cross-checks against the more limited tabulation of $P_c(m)$ obtained from the exact formulation shows excellent agreement in all cases in which $E/N_0 > 0 \text{ db}$. Tabulations permitting the determination of the error probability for cases not illustrated in the figure are included in Appendix I(g).

It is possible to generate 4-state DCPSK signals by combining two 2-state (BDCPSK) signals in quadrature. The error probability $P_{\text{sub}}(4)$ of these sub-channels has been computed from Equation Ig-145 and plotted. Since

$$P_{\text{sub}}(4) < P_c(4) < 2P_{\text{sub}}(4)$$

Ig-146

and $P_{\text{sub}}(4)$ was computed by a different approach from that used for the computation of $P_c(4)$ (which is obtained from $h(\hat{\alpha})$), Equation Ig-146 serves as an excellent check on the computation of $P_c(m)$ as can be seen from Figure II-10. The computation of $P_{\text{sub}}(4)$ yielded as an intermediate result a tractable integral expression, Equation Ig-137, for the probability that the dot product of arbitrary two-dimensional vectors perturbed by independent samples of a two-dimensional Gaussian process is negative (i.e., that the phase difference between these vectors exceed $\pi/2$ in absolute value). This result may be of interest in areas not related to the present effort; it may also be specialized to identical vectors, perturbed by independent Gaussian noise, yielding the error probability of a binary DCPSK, Equation Ig-142, in agreement with previous analyses.

* Becker I

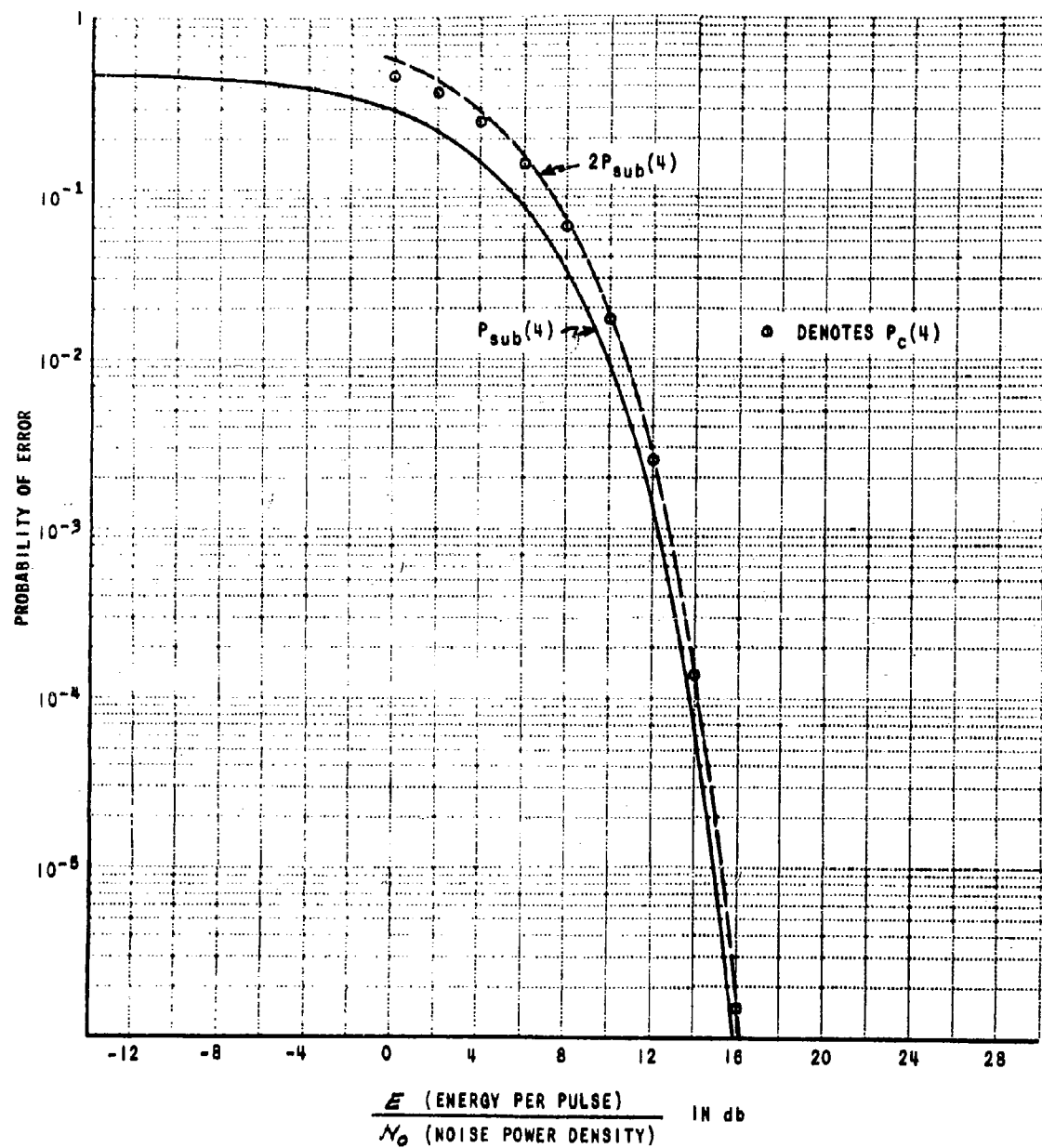


Figure II-10 SUB-CHANNEL ERROR PROBABILITY IN AN $m = 4$ DCPSK

Appendix I(h) determines the error probability of m -state DCPSK systems operating with a frequency "offset", i.e., a difference in the frequency of the received signal and the design frequency of the receiver. Such frequency errors may, in this case, be due to numerous causes such as Doppler shift, and frequency differences in heterodyning oscillators. Although it is impossible to make a universally applicable estimate of the magnitude of the frequency error likely to be encountered in practice, it may be well to bear in mind that a communications system which is designed to yield toll quality telephone service cannot tolerate a shift of more than a very small number of cps.

The results of this analysis are presented graphically in Figure II-11 (a more extensive tabulation is contained in Appendix I(b)). The parameter $\alpha = \frac{4f}{\sqrt{T}}$ of that figure is seen to correspond to the number of cycles gained or lost during one signal interval due to the frequency offset. In an m -state system the phase difference must be determined to within $\frac{\pi}{m}$ radians or $\frac{1}{2m}$ cycles. It will be noted that for $\alpha > \frac{1}{2m}$ the error probability approaches unity for E/N_0 sufficiently large. This merely reflects the fact that the phase error, as measured by the number of cycles gained (or lost) per signal interval in the absence of noise exceeds the decision threshold.

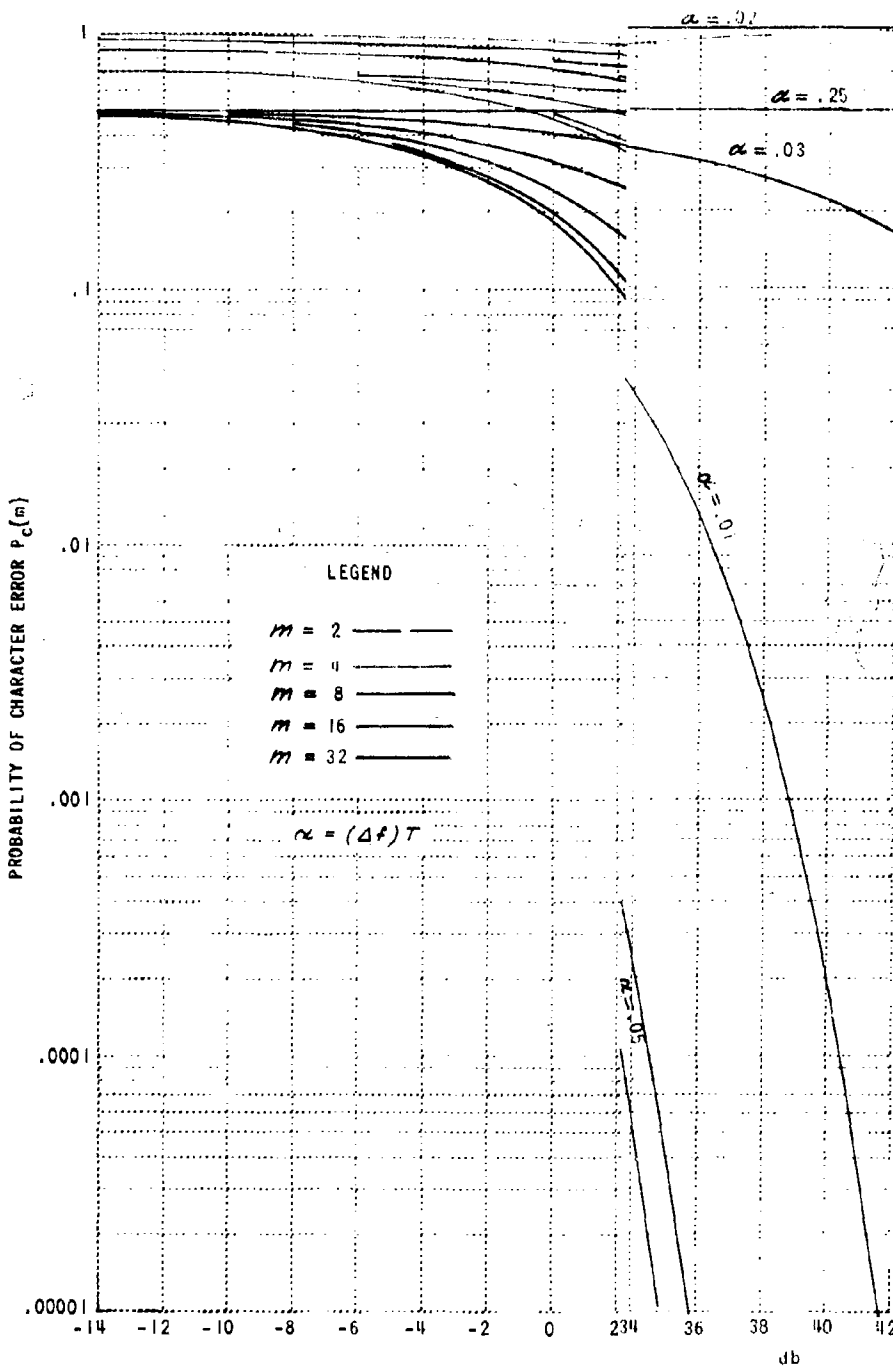
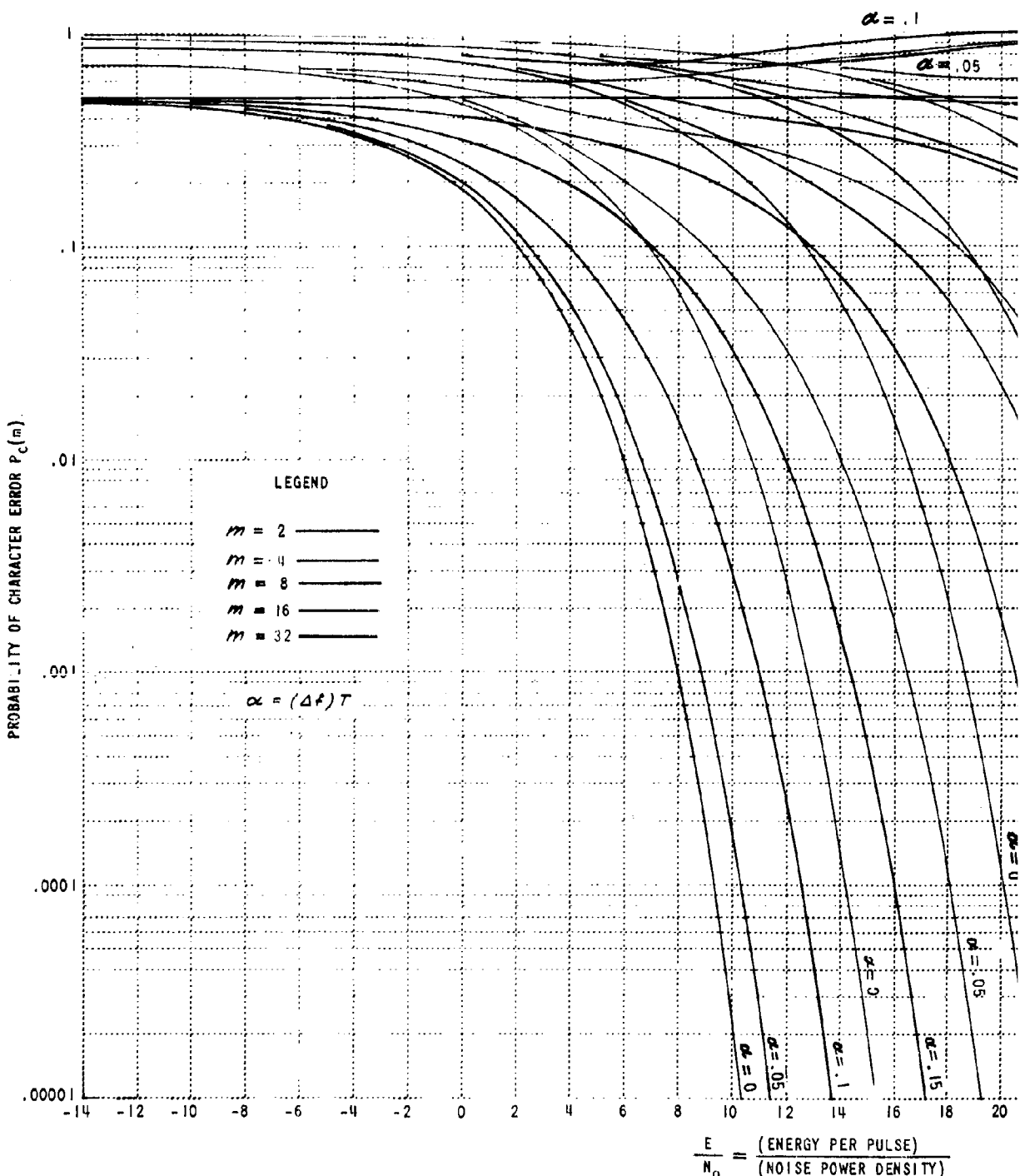
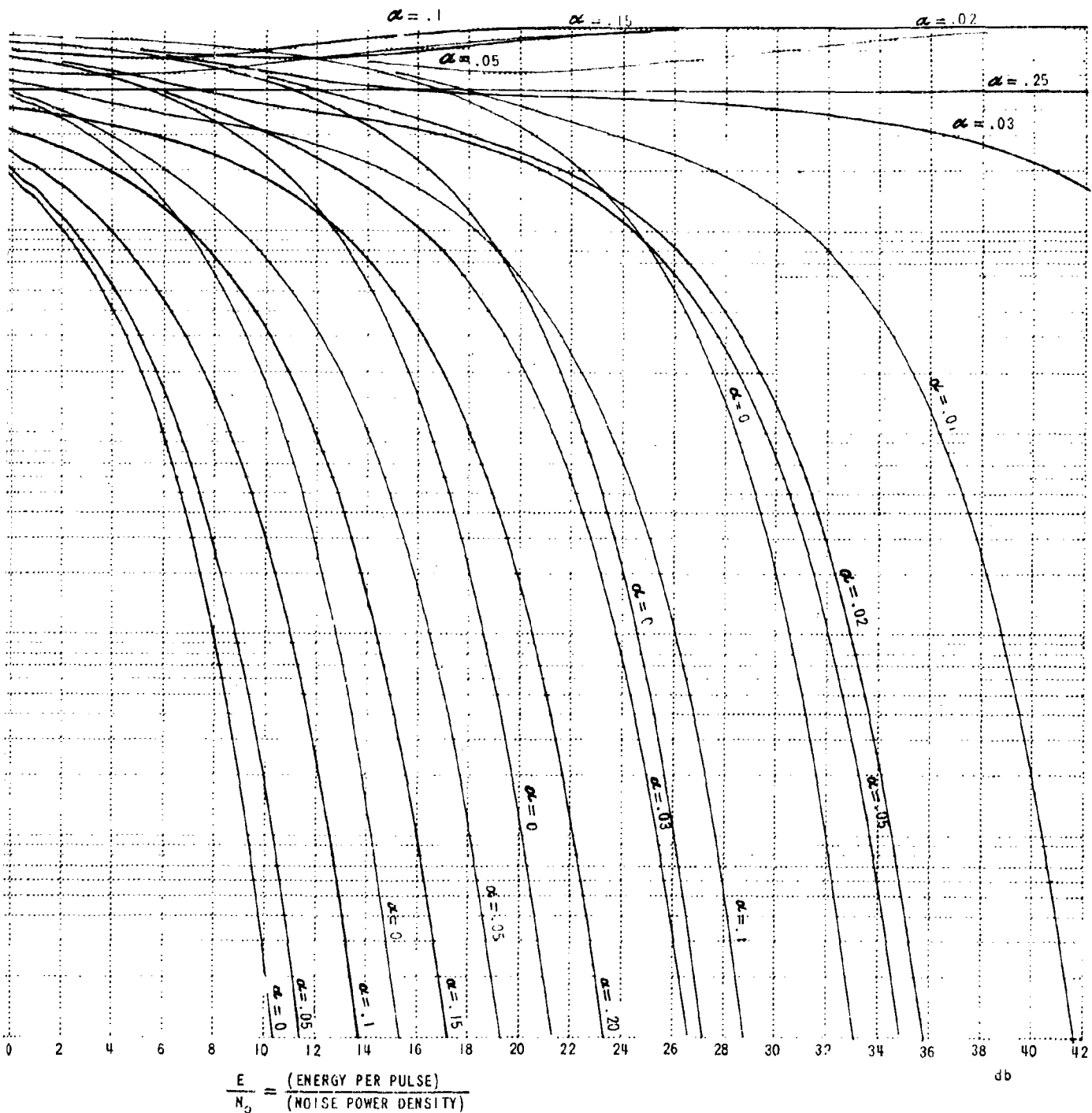


Figure II-11



1

Figure II-11 ERROR PROBABILITY OF m -STATE DPSKS WITH



I-11 ERROR PROBABILITY OF m -STATE DPSKS WITH FREQUENCY ERROR

2

- III. ANALYSIS OF DIFFERENTIALLY COHERENT PHASE SHIFT KEYED (DCPSK) DIGITAL DATA SYSTEMS OPERATING OVER A FADING FM TROPOSPHERIC SCATTER CIRCUIT

Analysis of a typical tropospheric scatter link using the parameters of the AN/GSC-4* shows that all but a negligible fraction of the errors occur when the received carrier-to-noise power ratio fades well below the FM improvement threshold. It is, therefore, of utmost importance to prevent deep fades; diversity reception is the primary means of achieving this. The effectiveness of various orders of diversity in improving the system's performance is examined and the results are shown in Table II of Appendix II(a). For an optimum coherent diversity** combiner, one finds that the ratio of the probability density of the signal-to-noise ratio obtained without diversity to that obtained with m -fold diversity is given by

$$\frac{P(W, \text{No Diversity})}{P(W, m \text{ Fold Diversity})} = \frac{1}{(m-1)!} \left(\frac{W}{R_0}\right)^{m-1}$$

where: W is the signal-to-noise ratio at the output of the combiner,
 R_0 is the mean signal-to-noise ratio at the input to the combiner.

In the above equation all inputs are assumed to have independent Rayleigh fading statistics with equal means and, from this equation, it is seen that optimum diversity combination results in a decreased probability of $\frac{W}{R_0}$ whenever $\frac{W}{R_0} < [(m-1)!]^{1/m-1}$ and vice versa.

The circuit analyzed is assumed to be channelized in accordance with conventional frequency division multiplex practice. Thus, each data link is

* Clabaugh I

** Brilliant II

assigned to one of 77 voice channels, each 4 kc's wide. It will be noted that the six tones require only $6 \times 300 = 1800$ cps, thus a sizeable fraction of the available bandwidth is taken up by guard bands. Channelization on the basis of voice channels, which is reasonable under certain circumstances, may not be desirable under other circumstances.

The FM link is assumed to employ pre-emphasis in accordance with accepted procedures, the aim of which is to achieve equivalent intelligibility of voice transmission over all channels. It may reasonably be assumed that the quality of voice signals is subjectively judged primarily on the signal-to-noise ratio attained during the large fraction of time that the system operates above the FM improvement threshold. During this time, the noise power density at the output of the FM system is proportional to the square of frequency, and signal pre-emphasis is employed to compensate for this. The quality of a data link may be judged primarily on the basis of its error probability. As almost all errors occur during the small fraction of time during which the system operates below the FM improvement threshold, a pure data system should be equalized on that basis (assuming all data to be equally important). Well below threshold, the noise-power density is found to be independent of frequency and pre-emphasis should, therefore, be avoided. If a system is used for the transmission of both data and voice, then a compromise based on the relative importance of the two modulations must be reached. If one system carries both data and voice and if pre-emphasis is used, then the data should be assigned to the highest frequency channels since this will result in the lowest error rate and since, in view of the pre-emphasis, it does not matter which channels are used for the transmission of voice. If pre-emphasis is not used, then the performance of the data link is independent of which channels are used for this purpose, but the lower frequency channels will give improved performance when used for the transmission of voice. Therefore, it is seen that, regardless of the degree of pre-emphasis, data should always be sent over the high-frequency channels and voice over the lower frequency channels. It is to be noted that, in a frequency division multiplex system, the function of the usual pre-emphasis circuit can be obtained, approximately, by adjustment of the signal levels in the various channels. The availability of independent adjustments offers a great deal of operational

flexibility. Thus, one may increase the deviation assigned to a channel carrying "more important" data at the expense of the other channels. Again, when the tropospheric conditions are unfavorable, it may be possible by removing some of the channels and increasing the deviation of the remaining channels to retain acceptable error probabilities.

IV COMMENTS ON AN ARTICLE ENTITLED "IDEAL BINARY PULSE TRANSMISSION
BY AM AND FM"

It can be shown by very general arguments that a binary communications system operating with a given average signal energy can attain the lowest possible error probability in the presence of white additive Gaussian noise only if the two signals are the negative of each other. Appendix I(c) discusses the major points needed for proof of the above statement; a detailed proof will be found in a previous Cornell Aeronautical Laboratory Report.* It is to be noted that the precise form of the signals was not specified and that binary PSK signals meet the criterion. Therefore, under the assumed conditions, no binary data transmission system can attain a lower error probability than a binary PSK system used with an optimum (maximum likelihood or coherent matched filter) receiver.

The November 1959 issue of the Bell System Technical Journal contains an article entitled "Ideal Binary Pulse Transmission by AM and FM" by E. D. Sunde of the Bell Telephone Laboratory (BTL).** This paper contains a very detailed and extensive investigation into the problems associated with the transmission of binary data by means of amplitude or frequency modulation of a carrier. In this paper, Sunde concludes that an FM system with optimum pre- and post-detection filtering could be superior to the binary PSK system with an optimum receiver and could, in particular, attain a lower error probability. This conclusion is evidently incompatible with accepted theory; therefore, Sunde's paper was closely examined for possible errors and the results of our examination were discussed with Mr. Sunde during a visit to the Bell Telephone Laboratories. As a result of this discussion, Mr. Sunde agreed that our previous conclusions remain unimpaired.

The difference between Sunde's and our previous results arises, not from errors in the formal mathematics used to derive these results, but from two premises used by Sunde which, it was agreed, are not tenable.

* Becker I

** Sunde II

The first of these concerns the comparison of digital data transmission systems on the basis of signal-to-noise ratios. The following paragraph appears on page 1409 of the referenced article: "Comparison of binary FM and AM on the basis of signal-to-noise ratios is legitimate provided that, for a given N_o/S_o , the error probability is the same in FM and AM. For high signal-to-noise ratios, this is approximately the case, since the normal law (171) is then closely approximated in FM⁹. On this premise, comparison on the basis of signal-to-noise ratios is legitimate for small error probabilities."^{*} However, the premise cannot be defended since it has not been shown that a given N_o/S_o results in the same error probabilities for FM and AM. A close approximation to the normal law is not sufficient to assure this. In order to obtain identical error probabilities at large signal-to-noise ratios, the tails of the probability density function must be identical with those of a normal distribution. Small deviations in the tails of the probability density function can lead to orders of magnitude of difference in the error probability, as can be easily demonstrated. This behavior can be explained in a somewhat different manner as follows: the probability of error, P_{error} , may be expressed as the difference between unity and the probability of being correct.

$$P_{\text{error}} = 1 - P_{\text{correct}}$$

If two distributions are nearly identical, then the two resulting values of P_{correct} will be nearly identical for large E/N_o ; in fact, they will both approach unity. The ratio of the differences between the two values of P_{correct} and unity may, however, be very large (or very small).

The second premise concerns the manner in which the signal-to-noise ratio in an FM system is computed. Equation (209) of Sunde's paper gives the output voltage of the FM system due to a single interfering sinusoid, relative to the output due to the desired signal at the sampling points. Equation (212) is an approximation to (209) which is valid, provided the amplitude and rate of change of the interfering signal are small compared to the desired signal. Equation

* Sunde's Reference 9 corresponds to Rice II in this report.

(225) or (116) gives the r.m.s. ... of (212) for a uniform distribution of the phase of the interfering signal. The expressions, Equations (118) and (119), for the noise power-to signal power ratios at the output of an FM system operating in the presence of white Gaussian noise are obtained formally by integrating Equation (225) or (116) over all frequencies. However, in order to justify this step, one must prove that the approximations made in going from Equation (209) to Equation (212) are still valid in this case. Gaussian noise of nonzero power, no matter how small, will violate these assumptions with nonzero probability. When these assumptions are violated, a noise peak which is very large compared to the noise at other times can be generated. It is conventional, in connection with FM systems, to speak of the noise capturing the phase of the waveform under these circumstances. Because of square law weighting, the contribution of these large peaks to the mean square output noise is accentuated. If the contribution of the noise peaks is neglected, an optimistic result will be obtained.

The assumption of the signal retaining control of the carrier phase at all times is consistently made throughout the paper, e.g., in computing the effects of a post-detection filter. Again, it can be easily demonstrated that changes of orders of magnitude in the computed error probability can result when second-order terms are neglected.

After discussing the above, Mr. Sunde readily agreed that the lowest error probability attainable with FM in white Gaussian noise must be greater than that attainable with coherent PSK. This leaves the question of determination of the error probability of the optimum binary FM system open to further investigation which should be greatly aided by Sunde's work.*

* The expression for the error probability of noncoherent FSK given in the referenced C.A.L. report, *ibid*, is applicable to wide deviation FSK.

V. PROPERTIES OF IMPULSE NOISE AND THE EFFECT OF IMPULSE NOISE
ON DIGITAL DATA COMMUNICATIONS SYSTEMS USING CLOSE-PACKED CODES

The presence of impulse noise is a major, and sometimes the primary, source of errors on some types of communications systems. The results of a brief literature search for information pertaining to impulse noise are reported in Appendix III(a). Impulse noise may have a wide variety of origins such as ignition noise, lightning discharges, static originating within the atmosphere and of extraterrestrial origin. The initial impulses which themselves may have random, nonuniform and nonstationary distribution in strength, time and space are modified by the characteristics of the medium prior to reception. It is not surprising, therefore, that efforts to describe impulse noise and to treat its effects analytically have had only very limited success. In order to obtain any results it is usually necessary to make assumptions which greatly restrict the applicability of the results obtained. This situation is, for instance, encountered in Appendix IV(c).

The form of impulse noise most adequately treated in the literature is Poisson Noise, which results from the linear superposition of the effects of elementary impulses which occur in a particular random fashion in time.* Assuming the wave forms produced at the receiver by the elementary impulses to be identical, it is possible to obtain an analytical representation of the first order statistics of Poisson noise.** The characteristics and the mathematical tractability of Poisson noise depend to a great extent upon the average density of the elementary pulses. At low pulse densities when there is little overlapping, there will be appreciable gaps between pulses. Consequently, zero amplitude is probable and amplitudes exceeding those of the elementary pulses are very improbable. On the other hand, as the average pulse density becomes very large, the precise form of the individual pulses becomes unimportant, the strength of the delta function at the origin goes to zero, and the Poisson noise goes over into Gaussian noise. Figure V-1 illustrates these effects for rectangular pulses, the amplitude of which are Gaussianly distributed.

* Laning I

** Rice I

Sections (b) and (c) of Appendix III determine the error probability of digital communications systems using close-packed codes when perturbed by impulse noise.* The model of impulse noise used in Appendix III(b) is that proposed by P. Mertz,** according to which,

1. Letter errors due to impulse noise occur in bursts. Within the time interval occupied by a burst, the probability of error occurrence is given by the Poisson approximation to the binomial (Bernoulli) distribution. Outside of this interval, the probability of error occurrence is zero.
2. Bursts of duration, ℓ , occur at random; the probability of burst occurrence in a given time interval being given by a Poisson approximation to the binomial distribution.
3. The probability of overlapping bursts is assumed negligible.

In Appendix III(c) assumptions 1 and 2 above were modified as follows. Letter errors within a burst are assumed to have a binomial rather than a Poisson distribution. The reason for this modification is that the Poisson distribution permits an unlimited number of errors to occur during a finite interval while, at most, all the letters of a word can be in error. The duration of bursts was assumed to be uniformly distributed over a finite range. This was felt to be a more realistic than the assumption of constant burst length.

Figure V-2 is a plot of error probability vs. expected number of letter errors per word (assuming the word to be completely covered by a burst), for various burst rates, using the original assumptions.

Figure V-3 is a similar plot which permits comparison of the error probabilities using the original and the modified assumptions. (Note that the average burst length is the same in both cases.) It is seen that over the range of variables plotted the two sets of assumptions lead to comparable error probabilities.

*Close-packed codes are defined in Appendix III(b).

**Mertz I

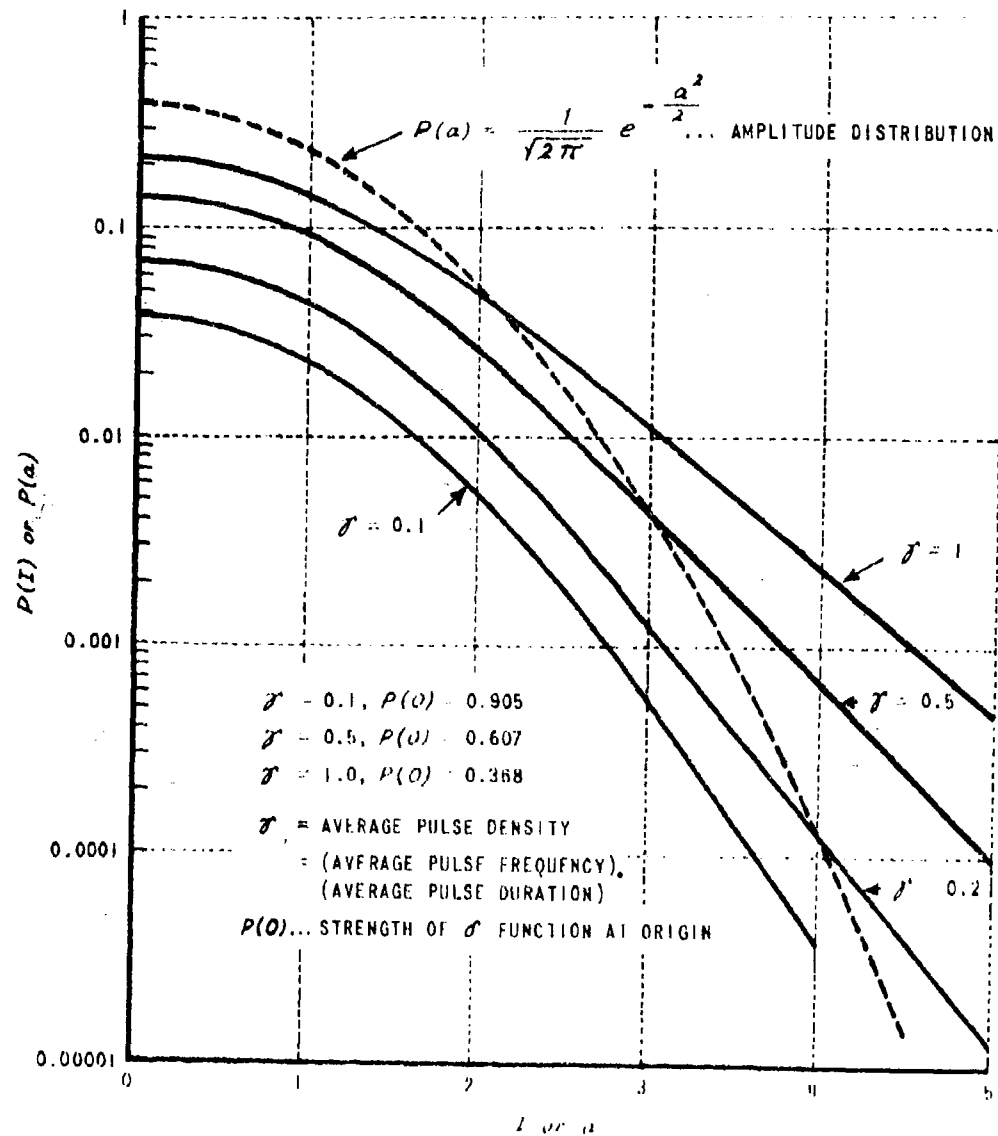


Figure VI-1 PROBABILITY DENSITY OF "RECTANGULAR" POISSON NOISE.

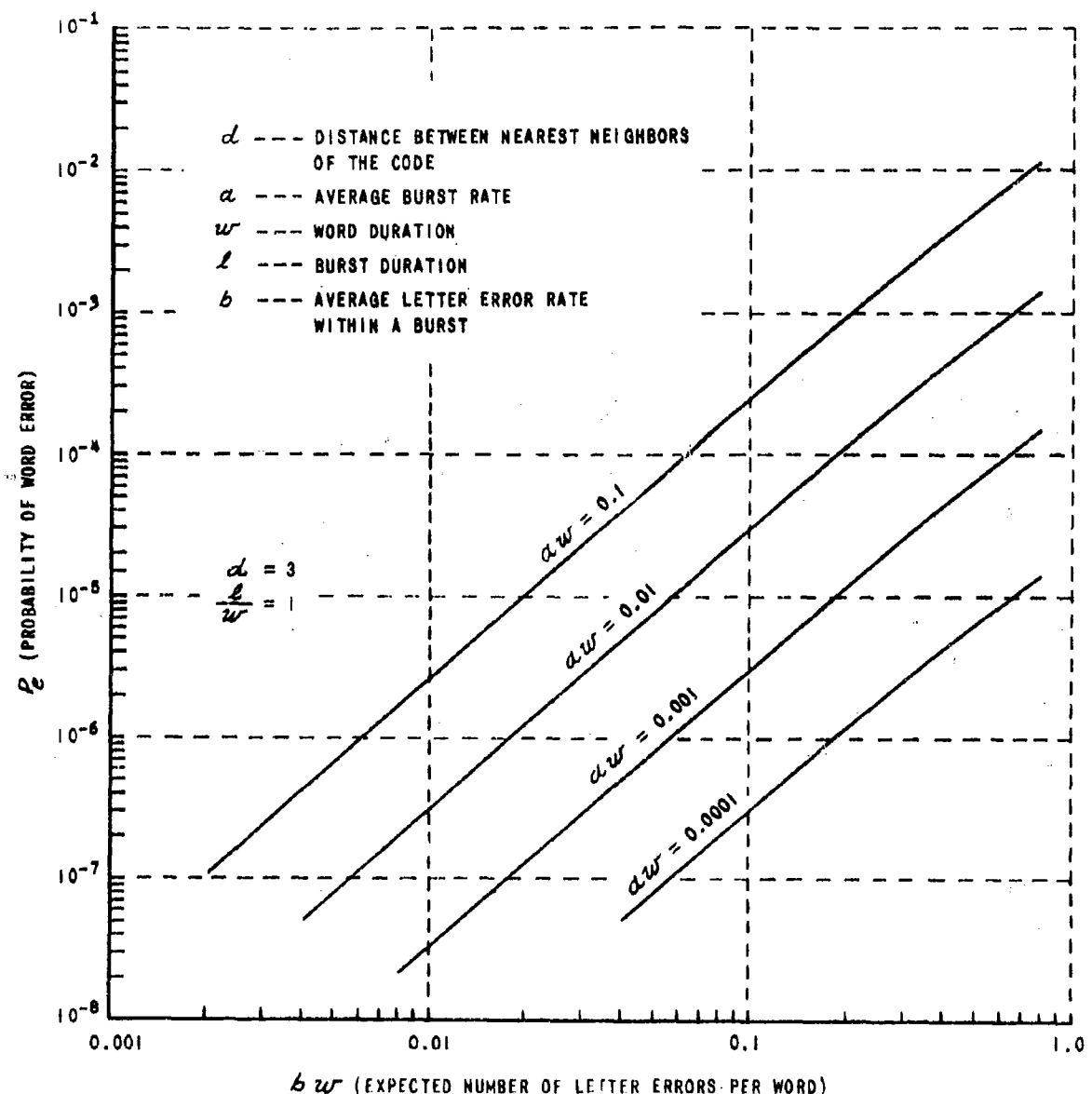


Figure I-2 WORD ERROR PROBABILITY vs. EXPECTED NUMBER OF LETTER ERRORS PER WORD (COMPLETELY OVERLAPPED BY A BURST).

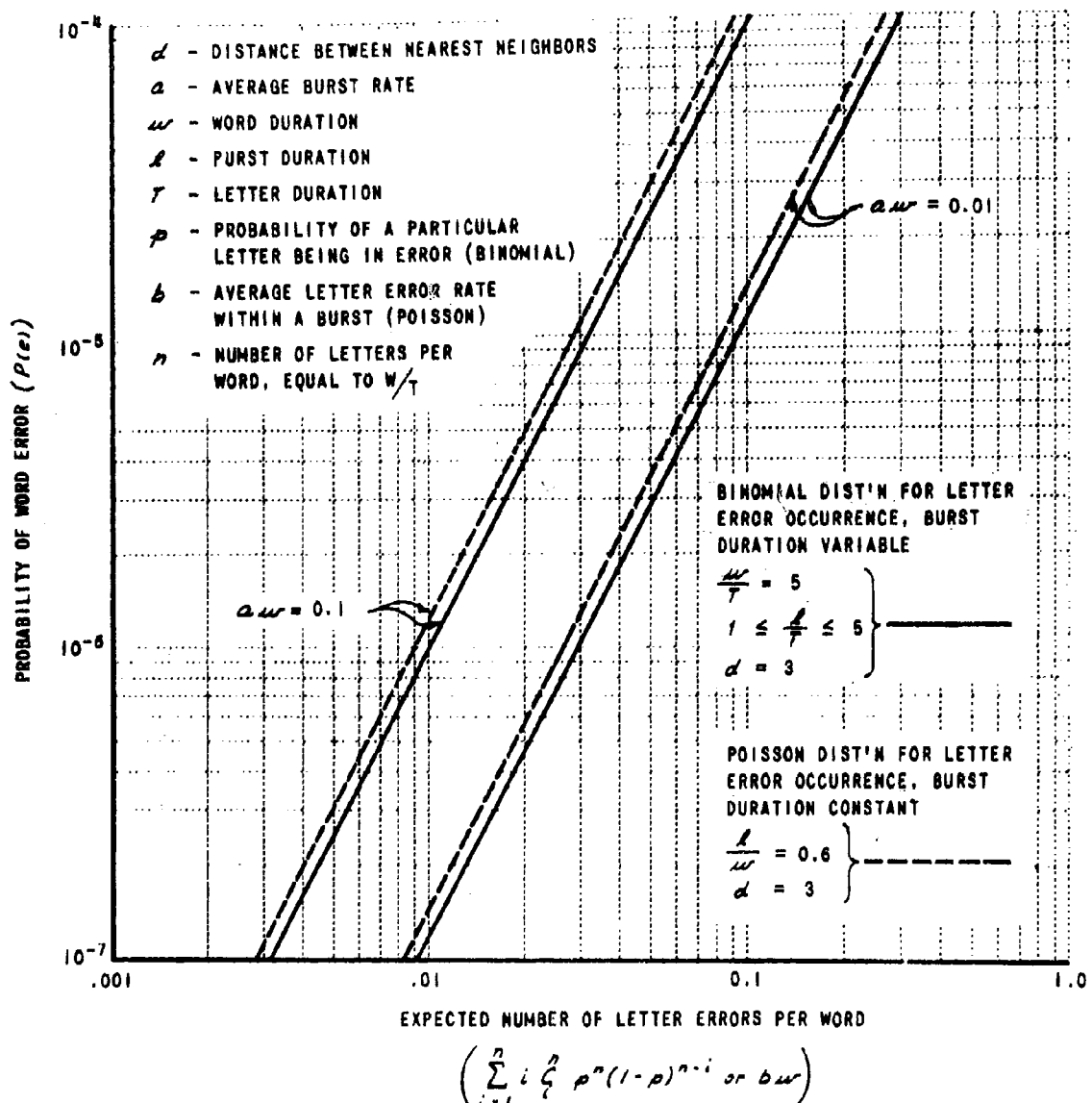


Figure II-3 COMPARISON OF WORD ERROR PROBABILITY WITH ORIGINAL AND MODIFIED ASSUMPTIONS

VI "MOMENT DETECTION"

The "Moment Detection" technique was originated at Rutgers University as part of the work performed under Contract DA-36-039-sc-15314 with the Signal Corps of the U. S. Army. In one of the references* to this work, the conception of "moment detection" is described thus: ".....the entire idea of a moment detector had its origin in the representation of pulses by a Gram-Charlier series." The work at Rutgers on "moment detection" represents, to a considerable extent, an ad hoc effort to utilize the Gram-Charlier series representation. In the Gram-Charlier representation of a waveform $v(t)$, the coefficients of the terms in the series are determined by the temporal moments, $m_k(T) = \int_0^T t^k v(t) dt$ of the waveform $v(t)$. The Gram-Charlier series is only one of many possible series representations which, under various restrictions**, converge to the functions which they represent. It is to be noted that "moment detection" was not conceived on the basis of satisfying some desirable criterion, e.g., a maximum likelihood receiver, or a receiver which minimizes the mean square error of its output.

Appendix IV reports in detail on the analytical and experimental investigations performed on "moment detection" under the current contract. Appendix IV(a) considers "Moment Detection in the Presence of White Gaussian Noise". It is shown that a linear filter having impulse response

$$h_k(t) = \begin{cases} (T-t)^k, & 0 \leq t \leq T \\ 0, & \text{elsewhere} \end{cases}$$

has an output equal to the k^{th} order moment of the input at time $t=T$. If the input signal has the form $v(t) = \begin{cases} t^k, & 0 \leq t \leq T \\ 0, & \text{elsewhere} \end{cases}$, then decisions based on the k^{th} order moment are equivalent to matched filter reception.

* Slade I

** The functions "of interest in practice" seemingly always fulfill these restrictions (primarily because they are of finite peak power, of finite duration and of finite bandwidth).

Reception of two pulse groups based on use of the 0^{th} and 1^{st} order moments are examined. It is shown that the effect of noise on the observed moments results in dependent deviations from the expected values. The optimum decision rules, i.e., those decision rules which will lead to the lowest possible error probability, are derived. While the optimum decision boundaries are known, it was not possible to derive a closed form expression for the resulting error probability; however, closed form expressions for rather tight upper and lower bounds to this probability are obtained. The effects of a simple low pass filter preceding the "moment detection" circuit and of overlapping of data pulses is examined.

Appendix IV(b), "Optimum Decision Based on Multiple Moment Detection", demonstrates how the optimum decision based on an arbitrary choice of moments is derived. Briefly, this involves a linear transformation to a space in which the noise which perturbs the moments has a 'n' dimensional normal spherical distribution. In this space, maximum likelihood decisions can, in principle, be readily performed. Thus, if all words are a priori, equally probable, the decision is in favor of that word whose expected coordinates are closest to the observed coordinates in this orthonormalized space.

Appendix IV(c), "Analysis of the Effect of Impulse Noise on Moment Detection", presents the results of an attempt to deal with the above topic analytically. It was clear at the outset that one could not expect to obtain results of completely general applicability. It was, therefore, assumed that the distribution of impulse strength has a symmetric hyperbolic distribution, as suggested by P. Mertz*, and that the distribution of the spacing λ of impulses was uniform over the range $\lambda_s \leq \lambda \leq \lambda_L$. The impulses were assumed to be true delta functions but these, as well as the data pulses, were passed through a simple low pass filter prior to the "moment detection" circuit. In order to derive numerical results, further restrictive assumptions had to be introduced.

* Mertz I

Appendix IV(d) describes the "Experimental Investigation of Moment Detection". This appendix gives a detailed description of the equipment which was developed and/or assembled and of the methods used in this task. It also includes a description of sources of errors and the shortcomings encountered.

The fairly extensive analytical and experimental investigations of "moment detection", reported in detail in Appendix IV, showed that this technique has serious difficulties of both a theoretical and practical nature. As a result, it is felt that "moment detection" does not, in theory, show advantages over other decision techniques under any of the circumstances considered and that the implementation of this technique poses excessive equipment requirements.

Having amassed sufficient evidence to draw the above conclusion, and in view of the basis on which "moment detection" was originally proposed, it did not appear warranted to attempt to investigate all of the characteristics of this technique. The major points bearing on the usefulness of "moment detection", or lack thereof, are described below.

(1) The dependence of the probability of error on the particular moments and the number of moments utilized in the decision remains unknown. It should be noted that it is not generally true that the error probability, computed on the assumption of optimum decision rules, decreases as more moments are used in arriving at a decision (although it is clear that the error probability cannot increase if additional moments are used to best advantage).

(2) It is easily demonstrated that any decisions based on "moment detection" processes can also be obtained through the use of linear filters. It is not, in general, possible to replace even very simple linear filters (viz., a simple bandpass filter) by decisions based on "moment detection". For instance, "moment detection" can be equivalent to matched filtering only if the signal has the form

$$r(t) = \begin{cases} t^k, & 0 \leq t \leq T \\ 0, & \text{elsewhere} \end{cases}$$

(3) The weighting functions used in "moment detection", viz., t^4 , have low-pass spectra, while most of the signals used in modern communication systems have bandpass spectra. Because of this spectral mismatch, it is virtually impossible to use "moment detection" with bandpass signals. For this reason, the "moment detection" technique was applied to the detected output of the FSK equipment during the experimental evaluation of this technique. (It is felt that it would be preferable to call the technique "moment decision" rather than "moment detection".)

(4) From a practical point of view, the equipment needed to implement "moment detection" is inordinately complicated, as can be appreciated from the following considerations.

The computation of the moments can be performed, in principle, by multiplying the waveform $v(t)$ by t^4 using a high speed precision analog multiplier and integration of the product thus obtained. As no multiplier having acceptable characteristics was available, the moments were computed by means of the "multiple definite integral method". With this method, $k+1$ integrations are performed in order to determine the k^{th} moment. The required moments are then obtained as the weighted sum and difference of these integrals. Since the resulting moment may be of much smaller magnitude than the various inputs of which it is composed, it is extremely sensitive to gain variations and drift of the equipment used (i.e., the small difference of two large numbers is very sensitive to small fractional changes of the large numbers).

The best decision rules* (i.e., those yielding the lowest probabilities of error) are too involved to be implemented with practical equipment. For this reason, the moments were computed in real time and transferred to magnetic tape for later analysis by a large digital computer. The computation of the theoretical error probability which results if the optimum decision rules are used has proven untractable; even for the simple cases considered in Appendix IV, closed form expressions could not be obtained.

* These rules have been formulated only for the case of additive white Gaussian noise.

(5) Because "moment detection" requires that decisions be based on absolute levels (as is also the case, for instance, with conventional ON-OFF keying) rather than on relative levels (as is the case, for instance, with conventional matched filter reception of FSK signals), this system is sensitive to gain variations. When "moment detection" is applied to code words extending over several pulse intervals, the decision boundaries are closely spaced and, consequently, the sensitivity to gain variations becomes very great. Under these conditions, the system also becomes very sensitive to small DC components such as may be generated by nonlinearities in the associated communications equipment. (A DC component due to noise was encountered in the experimental investigation of "moment detection". See Appendix IV(d).) The great sensitivity to DC is due to the DC being effective over the entire word duration and the t^4 weighting while the decision boundaries must be determined by the change in moments due to the presence or absence of a single, and in particular the first, pulse.

(6) In the experimental evaluation, the use of "moment detection" operating on the output of the FSK discriminator resulted in a much greater error probability than that obtained with a linear filter followed by a thresholding circuit.

BIBLIOGRAPHY

Abramson, N. M.:

I - A Class of Systematic Codes for Nonindependent Errors IRE Trans. on Info. Theory Vol. IT-5, 1959, pp. 150-157.

Banerji, R. B.:

I - A Systematic Method for the Construction of Error-correcting Group Codes May 21, 1960 p. 827.

Becker, H. D. and Lawton, J. G.:

I - Theoretical Comparison of Binary Data Transmission Systems Cornell Aeronautical Laboratory Report No. CA-1172-S-1 Contract AF-30(602)-1702 May 1958 RADC-TR-58-91 May 1958 AD-148803.

Bickel, H.:

I - The Coherent Memory Filter Proceedings Fourth Annual Radar Symposium February 4-6, 1958.

Brennan, D. G.:

I - Linear Diversity Combining Techniques Proc. IRE Vol. 47 June 1959, pp. 1075-1102.

Brilliant, M.:

I - Fading Loss in Diversity Systems Convention Record Fifth National Communications Symposium October 1959.

Cahn, C. R.:

I - Performance of Digital Phase Modulation Communication Systems IRE Transactions on Communications Systems Vol. CS-7, No. 1 May 1959.

II - Comparison of Coherent and Phase-Comparison Detection of a Four-Phase Digital Signal Correspondence Section Proceedings of the IRE Vol. 47, No. 9 September 1959.

Calabi, L. and Haefeli, H.:

I - A Class of Binary Systematic Codes Correcting Errors Occurring at Random and In Bursts Transactions of the 1959 International Symposium on Circuit and Information Theory Los Angeles, California June 16-18 1959 pp. 79-94 IRE Transactions on Information Theory Vol. IT-5 Special Supplement May 1959.

Campbell, G.:

I - Use of an Adaptive Servo to Obtain Optimum Airplane Responses Cornell Aeronautical Laboratory Report No. 84.

Clabaugh, R. G.:

I - Estimated AN/GSC-4 Characteristics on Truro Tropo Circuit Informal memo Collins Radio Company, Western Division A 27 December 1959

Collins Engineering:

I - Report No. CER-WF92 Performance of Predicted Wave Systems in the Presence of Additive, White, Gaussian Noise 29 January 1958.

Costas, J.:

I - Phase-shift Radio Teletype Proceedings of the IRE No. 1, pp. 16-20 January 1957.

Davenport, W. B. Jr. and Root, W. L.:

I - An Introduction to the Theory of Random Signals and Noise McGraw-Hill 1958.

Doelz, M. and Heald, E.:

I - A Predicted Wave Radio Teletype System Collins Radio Company Convention Record IRE National Convention Pt. 8 pp. 63-67 1954.

Enticknap, R. and Schuster, E.:

I - Space Data System Considerations, Communications and Electronics No. 40 pp. 821-832 January 1959.

Feinstein, A.:

I - Foundations of Information Theory McGraw-Hill Book Company New York
1958.

Fleck, J. T. and Trabka, E. A.:

I - Error Probabilities of Multiple-State Differentially Coherent Phase-Shift
Keyed Systems in the Presence of White, Gaussian Noise DETECT MEMO NO. 2
Cornell Aeronautical Laboratory 24 June 1960.

Gilbert, E. N.:

I - A Comparison of Signalling Alphabets BSTJ Vol. 31 pp. 504-22 May 1952.

Glenn, A.:

I - Comparison of PSK-AM vs. FSK-AM and PSK vs. FSK Binary Coded Transmission
Systems Proceedings Fifth National Communications Symposium
5 October 1959.

Hamming, R.:

I - Error Detecting and Error Correcting Codes The Bell System Technical
Journal, Volume 29 pp. 147-160 April 1950.

Harris, D. P.:

I - An Expanded Theory for Signal-to-Noise Performance of FM System Carrying
Frequency Division Multiplex IRE National Convention Record, Part 8
pp. 298-304 March 1958.

Hildebrand, F. B.:

I - Methods of Applied Mathematics Prentice-Hall, Inc. Article 1.13.

Holland, G. and Myrick, J.:

I - A 2500-Band Time-Sequential Transmission System for Voice-Frequency Wire
Line Transmission IRE Transactions on Communications Systems Vol. CS-7
No. 3 pp. 180-184 September 1959.

Kerlson, J. and Mermin, N.:

I - The Second-Order Distribution of Integrated Shot Noise IRE Transactions
on Information Theory Vol. IT-5 June 1959.

Hinchin, A.:

I - Mathematical Foundations of Information Theory (Translated by Silverman, R. and Friedman, M.) Dover Publications, Inc. New York 1957.

Kim, W. H. and Freiman, V.:

I - Multi-Error Correcting Codes for a Binary Asymmetric Channel IRE Transactions on Circuit Theory Vol. CT-6 Special Supplement pp. 71-78 May 1959.

Luning, J. H. and Battin, R. H.:

I - Random Processes in Automatic Control McGraw-Hill Book Company 1956.

Lawton, J. G.:

I - Comparison of Binary Data Transmission Systems Published in 1958 Conference Proceedings Presented at the Second National Convention on Military Electronics 16,17,18 June 1958.

II - Theoretical Error Rates of Differentially Coherent Binary and Kineplex Data Transmission Systems Published in the Proceedings of the IRE Vol. 47 No. 2 p. 333 February 1959.

Lee, C. Y.:

I - Some Properties of Nonbinary Error-correcting Codes IRE Transactions on Information Theory Vol. IT-4 pp. 77-82 1958.

Lerner, R.:

I - The Representation of Signals IRE Transactions on Information Theory Vol. IT-5 May 1959.

Lincoln Laboratory, MIT:

I - Quarterly Progress Report Division 3 Radio Physics 15 January 1959.

Marcum, J. L.:

I - A Statistical Theory of Target Detection by Pulsed Radar Mathematical Appendix RM-753 Rand Corporation 25 April 1952.

Mertz, P.:

I - Model of Impulsive Noise for Data Transmission Rand Corporation Report No. P-1761 27 July 1959.

Middleton, D.:

I - On the Theory of Random Noise Phenomenological Models I and II, and erratum Journal of Applied Physics 22 pp. 1143-1152, 1153-1163, 1326 1951.

II - An Introduction to Statistical Communication Theory McGraw-Hill Book Company, New York pp. 349, 490-498 1960.

III - Optimum Threshold FSK Communication with Decision Rejection AFCRC-TR-60-137 April 1960.

Middleton, D. and van Meter, D.:

I - On Optimum Multiple-Alternative Detection of Signals in Noise IRE Transactions on Information Theory Vol. IT-1 pp. 1-9 1955.

II - Detection and Extraction of Signals in Noise from the Point of View of Statistical Decision Theory Journal of the Society for Industrial and Applied Mathematics Vol. 3 pp. 192-253 1955; Vol. 4 pp. 86-119 1956.

Morita, M. and Ito, S.:

I - High Sensitivity Receiving System for Frequency Modulated Wave IRE International Convention Record, Part 5 pp. 228-237 March 1960.

Mosier, R.:

I - A Data Transmission System Using Pulse Phase Modulation Convention Record of First National Convention on Military Electronics Washington, D.C. 17-19 June 1957.

Mood, A. McF.:

I - Introduction to the Theory of Statistics McGraw-Hill Book Company, New York 1950.

Mullen, J. A. and Middleton, D.:

I - The Rectification of Non-Gaussian Noise Quarterly of Applied Mathematics
Vol. 15 pp. 395-419 1958.

Nuttall, A. H.:

I - Technical Note on Pulse Compression and Coded Waveform Techniques
Melpar, Inc. 15 March 1959 ASTIA Document No. AD-219116.

Peterson, W., Birdsall, T., Fox, W.:

I - The Theory of Signal Detectability IRE Transactions on Information Theory
Vol. PGIT-4 September 1954.

Price, R.:

I - The Search for Truth IRE Transactions on Information Theory Vol. IT-5
June 1959.

Reed, I.S.:

I - A Class of Multiple-Error-Correcting Codes and the Decoding Scheme
IRE Transactions on Information Theory Vol. PGIT-4 pp. 38-49 1954.

Reiger, S.:

I - Error Probabilities on Binary Data Transmission Systems in the Presence
of Random Noise, Part 8 Convention Record of the IRE 1953.

Rice, S. O.:

I - Statistical Properties of a Sine Wave Plus Random Noise BSTJ p. 109
27 January 1948.

II - Mathematical Analysis of Random Noise Selected Papers on Noise and
Stochastic Processes Dover Publications, Inc., New York p. 154,
Eq. (1.5-4) 1954.

Rosenblatt, F.:

I - Perceptron Simulation Experiments Project PARA Cornell Aeronautical
Laboratory Report No. VG-1196-G-3 June 1959.

Rutgers University:

I - Progress Report No. 8 Theoretical and Experimental Research in Communications Theory and Applications 15 July 1953.

Sanders, R. W.:

I - Digilock Communication System 1960 IRE WESCON Convention Record, Pt. 5 August 23-26, 1960.

Shannon, C. and Weaver, W.:

I - The Mathematical Theory of Communications University of Illinois Press Urbana, Illinois 1949.

Siebert, W. M.:

I - A Radar Detection Philosophy IRE Transactions on Information Theory Vol. IT-2 pp. 204-221 1956.

Siforov, V. I.:

I - On Noise Stability of a System with Error-Correcting Codes IRE Transactions on Information Theory Vol. IT-2 pp. 109-115 1956.

Skinner, F. J.:

I - Radio Transmission Systems - Theoretical Noise Performance Curves for Frequency Modulation Receivers Operating Below the Breaking Region BTL unpublished memo, file 36690-1 1 February 1954.

Slack, M.:

I - The Probability Distributions of Sinusoidal Oscillations Combined in Random Phase Journal of Institute of Electrical Engineers 93, Part 3 1946.

Slade, J. J., Jr., et al:

I - Detection of Information by Moments IRE Convention Record, Information Theory, Part 8 March 1953.

II - Moment Detection and Coding Transactions AIEE, Part I p. 275 July 1957.

Slepian, D.:

I - A Class of Binary Signalling Alphabets The Bell System Technical Journal Vol. 35 pp. 203-234 January 1956.

Sugar, G. R.:

I - Some Fading Characteristics of Regular UHF Ionospheric Propagation
Proceedings IRE pp. 1432 October 1955.

Sunde, E. D.:

I - Theoretical Fundamentals of Pulse Transmission Bell Telephone System
Monograph 2284.

II - Ideal Binary Pulse Transmission by AM and FM BSTJ pp. 1357-1426
November 1959.

Sylvania Electric Products, Inc.:

I - Anti-Jamming Techniques Study Final Report (SECRET Report)
(UNCLASSIFIED Title) October 30, 1957 AD-148671

Taber, John E.:

I - The Telebit System for Space Communication 1960 IRE WESCON Convention
Record, Pt. 5 August 23-26, 1960.

Trabka, E. A.:

I - Detectability of IFF Transmissions and Susceptibility of the System to
ECM (UNCLASSIFIED Title) CAL Memo (SECRET) July 8, 1958 NOT RE-
LEASABLE TO FOREIGN NATIONALS.

II - Detectability of IFF Transmissions by an Autocovariance Filter
(UNCLASSIFIED Title) CAL Memo for the Record (SECRET) November 13,
1958 NOT RELEASABLE TO FOREIGN NATIONALS.

III - Interception of Signals Having a Large Bandwidth-Time Product with an
Introduction to Pulse Compression Cornell Aeronautical Laboratory
Report No. UB-1207-S-2 6 October 1960.

Turin, G. L.:

I - Communication Through Noisy, Random-Multipath Channels Massachusetts
Inst. of Technology, Lincoln Laboratory Tech. Report No. 116
14 May 1956.

Turin, G. L.:

II - On the Estimation in the Presence of Noise of the Impulse Response
of a Random, Linear Filter IRE Transactions on Information Theory
Vol. IT-3 No. 1 pp. 5-10 March 1957.

III - Error Probabilities for Binary Symmetric Ideal Reception through
Nonselective Slow Fading and Noise Proceedings of the IRE, Vol. 46,
pp. 1603-1619 September 1958.

IV - The Asymptotic Behavior of Ideal M-ary Systems Proc. IRE Vol. 47,
January 1959 pp. 93-94.

V - An Introduction to Matched Filters IRE Transactions on Info. Theory
Vol. IT-6 No. 3 June 1960.

Ulrich, W.:

I - Nonbinary Error Correction Codes Bell System Tech. J., Vol. 36 1957
pp. 1341-1388.

Voelcker, H., Jr.:

I - Single Channel Radioteletype Communication Paper Presented at 1958
IRE National Convention March 27, 1958.

Walbesser, W. J.:

I - Error Correction Coding as a Statistical Game Cornell Aeronautical
Laboratory, Inc. Internal Memorandum dated 15 August 1960.

Watson, G. N.:

I - A Treatise on the Theory of Bessel Functions The MacMillan Company,
New York, 1945.

Whittaker, E. T. and Watson, G. N.:

I - A Course of Modern Analysis The MacMillan Company, New York 1946.

Weber, L.:

I - A Frequency-Modulation Digital Subset for Data Transmission over
Telephone Lines Communications and Electronics No. 40 January 1959
pp. 867-872.

Woodward, P.:

I - Probability and Information Theory with Applications to Radar
McGraw-Hill Book Company, Inc. New York 1955.

Wolfowitz, J.:

I - The Coding of Messages Subjected to Chance Errors The Illinois
Journal of Mathematics Volume 1 No. 4 pp. 591-606 December 1957.

Wozencraft, J.:

I - Active Filters U. S. Patent Applications and Signal Corps Patent
Agency Docket.

GLOSSARY

AM	Amplitude Modulation
BCPPSK	Binary Coherent Pulsed Phase Shift Keying
BDCPSK	Binary Differentially Coherent Phase Shift Keying
CPSK	Coherent Phase Shift Keying
DCPSK	Differentially Coherent Phase Shift Keying
E	Average Signal Energy per Signal Element
FM	Frequency Modulation
f	Frequency in Cycles per Second
GPSK	Gated Phase Shift Keying
HF	High Frequency
λ	Duration of Burst
MF	Matched Filter
N_o	Noise Power Density per Cycle per Second of One Sided Spectrum
$P()$	Probability of Quantity in Parenthesis
PPSK	Pulsed Phase Shift Keying
PSK	Phase Shift Keying
R_o	Mean Signal to Noise Ratio
T	Duration of One Signal Element
W	Signal to Noise Ratio

GREEK SYMBOLS

α	Δf
$\hat{\alpha}$	Phase Difference
ρ	Correlation Coefficient
ϕ	Phase
ω	Radian Frequency, Rad/Sec.

APPENDIX I

APPENDIX I

DERIVATION OF RESULTS USED IN CHAPTER II

- (a) DETECT MEMO NO. 5A - "Embodiments of the Maximum Likelihood Receiver for Detection of Coherent Phase Shift Keyed Signals" by Eugene A. Trabka.
- (b) DETECT MEMO NO. 12 - "Error Probability (in the presence of sampling time errors) of the Cross Correlation Embodiments of a Maximum Likelihood Receiver for Binary Coherent Gated Phase Shift Keyed Systems (BCGPSKS)" by Eugene A. Trabka.
- (c) DETECT MEMO NO. 15 - "Comments on m-State Coherent Digital Communications Systems" by Eugene A. Trabka.
- (d) DETECT MEMO NO. 7A - "Error Probabilities for Coherent Pulsed Phase-Shift Keyed Systems (CPPSKS) with Frequency and Sampling Time Errors" by Eugene A. Trabka.
- (e) DETECT MEMO NO. 8A - "Error Probability in a Binary Coherent Pulsed Phase Shift Keyed System (BCPPSKS) with Cross Talk from Adjacent Multiplexed Channels" by Eugene A. Trabka.
- (f) DETECT MEMO NO. 10(a) - "Double Bit Matched Filter (DBMF) Reception of Differentially Coherent Binary Phase Shift Keyed (DCBPSK) Signals"
 - (b) "The Equivalence of Integrate, Delay and Phase Comparison and DBMF Receivers for DCBPSK Systems" by John G. Lawton.

APPENDIX I (CONTD)

- (g) DETECT MEMO NO. 2A - "Error Probabilities of Multiple-State Differentially Coherent Phase Shift Keyed Systems in the Presence of White Gaussian Noise" by John T. Fleck and Eugene A. Trabka.
- (h) DETECT MEMO NO. 11 - "Error Probabilities of m-State Differentially Coherent Phase Shift Keyed Systems (DCPSKS) with a Frequency Offset of the Received Signals" by Eugene A. Trabka.

3 January 1961

I(a) DETECT MEMO* NO. 5A

Subject: "Embodiments of the Maximum Likelihood Receiver for Detection of Coherent Pulsed Phase Shift Keyed Signals in the Presence of Additive White Gaussian Noise"

By: Eugene A. Trabka

SUMMARY

Embodiments of the optimum (maximum likelihood) receiver for the detection of Coherent Phase Shift Keyed Signals in the presence of additive White Gaussian Noise are described (Figs. 1 and 2). A "practical" receiver (Fig. 4) is analyzed and the performance of this "practical" receiver is found to approach that of the maximum likelihood receiver as the number of cycles in the pulsed sinusoid increases.

INTRODUCTION

Consider a set of m signals consisting of pulsed sinusoids of a single angular frequency ω_0 , each having a rectangular envelope of duration T and amplitude A . The phases of the signals are taken to be uniformly spaced in the interval from 0 to 2π . Thus, one has for $i = 1, 2, \dots, m$

$$\begin{aligned} s_i(t) &= A \sin(\omega_0 t + \phi_i), \quad 0 \leq t \leq T \\ s_i(t) &= 0 \quad \quad \quad t < 0, t > T \\ \phi_i &= \frac{2\pi}{m} (i-1) \end{aligned}$$

(1)

*This is a revision of DETECT MEMO NO. 5 which was originally issued 29 August 1960.

3 January 1961
DETECT MEMO NO. 5A
AF 30(602)-2210

and it is assumed that $\omega_0 T \gg 1$ which implies narrow band signals having many cycles in the interval T . If $s_1(t)$ is transmitted, the received waveform is assumed to be given by

$$y(t) = s_i(t) + n(t) \quad (2)$$

where $n(t)$ is a member of an ensemble of white, gaussian noise with single sided power spectral density of N_0 watts/cps.

It has been shown⁽¹⁾ that a receiver which decides that the signal actually sent corresponds to the one having the greatest a posteriori probability (such a receiver is called a maximum likelihood receiver) minimizes its average error probability.* Moreover, a physical embodiment of a maximum likelihood receiver in terms of matched filters or correlation devices is well known.

A. Embodiments of the Optimum Receiver

The maximum likelihood receiver computes the quantities:

$$O_i(T) = \int_0^T y(t) s_i(t) dt \quad (3)$$

If the signals are all a priori equally likely, the receiver chooses the value of O_1 for which $O_1(T)$ is a maximum. The quantity $O_1(T)$ can be obtained as the output at time $t = T$ of a filter matched to $s_1(t)$, i.e., a filter with impulse response $s_1(T - t)$. The output of such a filter as a function of time is

*A different choice of $s_i(t)$ may yield a lower average error probability. The optimum choice of signals is not known for arbitrary m .

3 January 1961
DETECT MEMO NO. 5A
AF 30(602)-2210

is given by

$$O_i(t) = \int_0^t y(x) A_i(\tau-t+x) dx \quad (4)$$

and (3) is readily obtained by substituting $t = T$ in (4).

The receiver described above and sketched in Fig. 1, requires m different filters. This number may be reduced by noting that using (1), equation (3) may be written as

$$O_i(T) = O_a(T) \cos \phi_i + O_c(T) \sin \phi_i \quad (5)$$

where

$$\begin{aligned} O_a(T) &= \int_0^T y(t) A \sin \omega_0 t dt \\ O_c(T) &= \int_0^T y(t) A \cos \omega_0 t dt \end{aligned} \quad (6)$$

Thus, all $O_i(T)$ may be formed using the outputs of only two filters. Furthermore, by means of the transformation

$$\begin{aligned} O_a(T) &= V \cos \hat{\phi} \\ O_c(T) &= V \sin \hat{\phi} \end{aligned} \quad (7)$$

equation (5) may be written as

$$O_i(T) = V \cos (\phi_i - \hat{\phi}) \quad (8)$$

3 January 1961
 DETECT MEMO NO. 5A
 AF 30(602)-2210

where

$$\begin{aligned} \nu &= \sqrt{\sigma_s^2 + \sigma_e^2} \\ \hat{\phi} &= \arctan \frac{\sigma_e(T)}{\sigma_s(T)} \end{aligned} \quad (9)$$

If $\phi_1 - \hat{\phi}$ is reduced to the equivalent angle in the range from $-\pi$ to $+\pi$, then $\sigma_1(T)$ is a maximum when $|\phi_1 - \hat{\phi}|$ is a minimum. A maximum likelihood receiver based on the above considerations is sketched in Fig. 2. It is not difficult to show that the quantity $\hat{\phi}$ is a maximum likelihood estimate of the phase of a transmitted signal which is apriori uniformly and continuously distributed.

B. An Approximation to a Maximum Likelihood Receiver Using Unequal Sampling Times

The impulse responses of the m matched filters specified in A are identical except for phase. Consequently, it is interesting to examine the output of one filter, say the one matched to $s_1(t)$, when $s_j(t)$ is actually transmitted. Let the output of the filter matched to the i^{th} signal when the j^{th} signal is actually transmitted be denoted by $\sigma_{ij}(t)$. Using the fact that $\phi_1 = 0$, one has from (1), (2), and (4).

$$\begin{aligned} \sigma_{ij}(t) &= A^2 \int_0^t \sin(\omega_0 x + \phi_j) \sin(\omega_0 (\tau-t+x)) dx \\ &\quad + A \int_0^t n(x) \sin(\omega_0 (\tau-t+x)) dx \end{aligned} \quad (10)$$

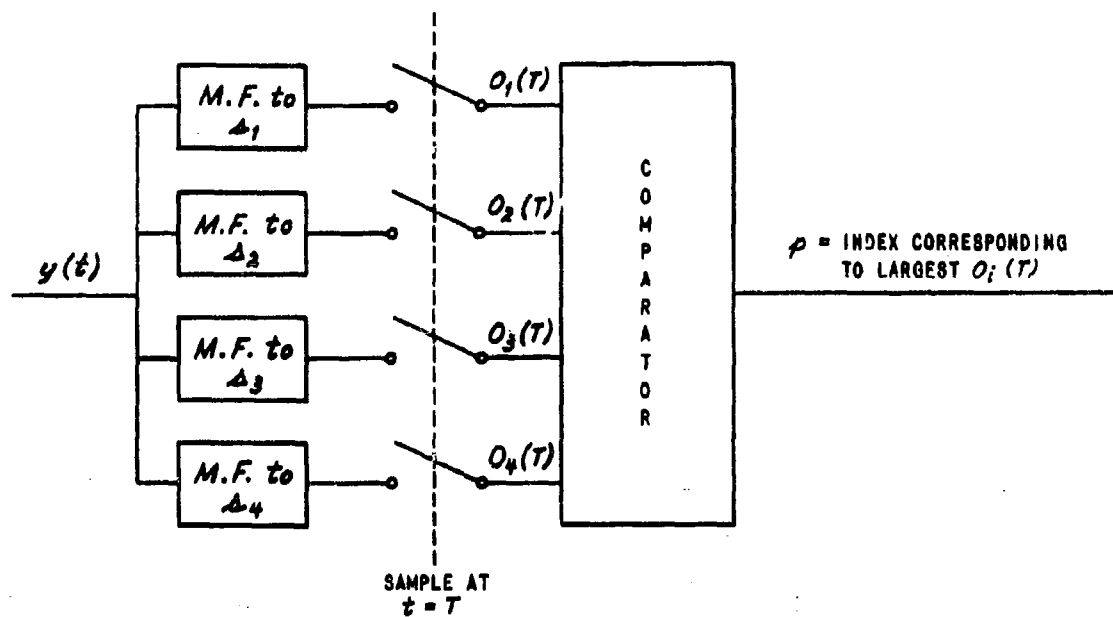


Figure 1 MATCHED FILTER EMBODIMENT OF MAXIMUM LIKELIHOOD RECEIVER

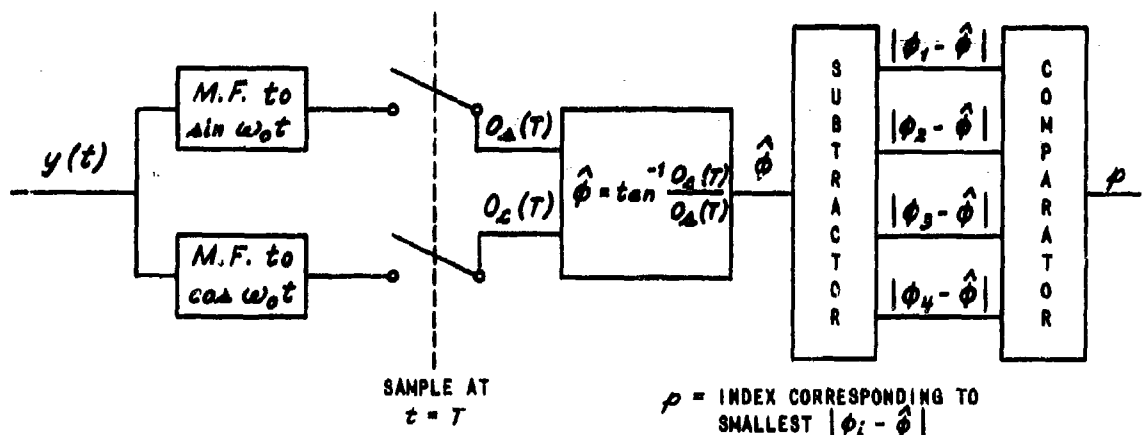


Figure 2 PHASE MEASURING EMBODIMENT OF MAXIMUM LIKELIHOOD RECEIVER

3 January 1961
 DETECT MEMO NO. 5A
 AF 30(602)-2210

Sampling $O_{1j}(t)$ at times $t_i = T - \frac{\phi_i}{\omega_0}$, one has from (10)

$$O_{1j}(t_i) = A^2 \int_0^{T - \frac{\phi_i}{\omega_0}} \sin(\omega_0 x + \phi_j) \sin(\omega_0 x + \phi) dx \quad (11)$$

$$= A \int_0^{T - \frac{\phi_i}{\omega_0}} n(x) \sin(\omega_0 x + \phi_i) dx$$

Now,

$$\frac{\phi_i}{\omega_0} \leq \frac{2\pi}{2\pi f_0} = \frac{1}{f_0} = P \quad (12)$$

where P is the period corresponding to f_0 . Consequently, if $P \ll T$, it is seen that the statistics of $O_{1j}(t_i)$ are very nearly the same as the statistics of $O_{1j}(T)$, which may be written symbolically as

$$O_{1j}(t_i) \rightarrow O_{1j}(T) \quad (13)$$

In the case when there are many cycles of $\sin \omega_0 t$ in the interval T , the performance of the receiver of Fig. 3 is nearly equivalent to that of the optimum receiver. The number of matched filters has been reduced to one, but the requirement of m distinct and precisely timed sampling instants may be unattractive.

3 January 1961
DETECT MEMO NO. 5A
AF 30(602)-2210

C. A "Practical" Receiver

Let the first term of (10), the component of the output due to signal be denoted by S_{ij} . Then, expanding the integrand, it is possible to write

$$S_{ij}(t) = \frac{A^2 t}{2} \cos(\omega_0 t + \phi_j - \omega_0 T) \quad (14)$$

$$- \frac{A^2}{2} \int_0^t \cos[2\omega_0 x + \phi_j + \omega_0(T-t)] dx$$

If there are many cycles of $\cos 2\omega_0 t$ in the interval T , it is permissible to neglect the second term of (14), so that for t near T , one has

$$S_{ij}(t) \approx - \frac{A^2 t}{2} \cos(\omega_0 t + \phi_j - \omega_0 T) \quad (15)$$

so that the phase of the component of the output due to signal in each case differs from the phase of the transmitted signal by $\omega_0 T$ which is independent of ϕ_j . The above argument suggests a receiver of the type shown in Fig. 4, which will be called a "practical" receiver (for want of a better name) since it requires only a single matched filter and a single sampling of phase at time $t \approx T$. It is similar to the receiver of Fig. 2 differing only in the manner in which estimates of phase are obtained. It remains to be determined whether or not it is equivalent to a maximum likelihood receiver.

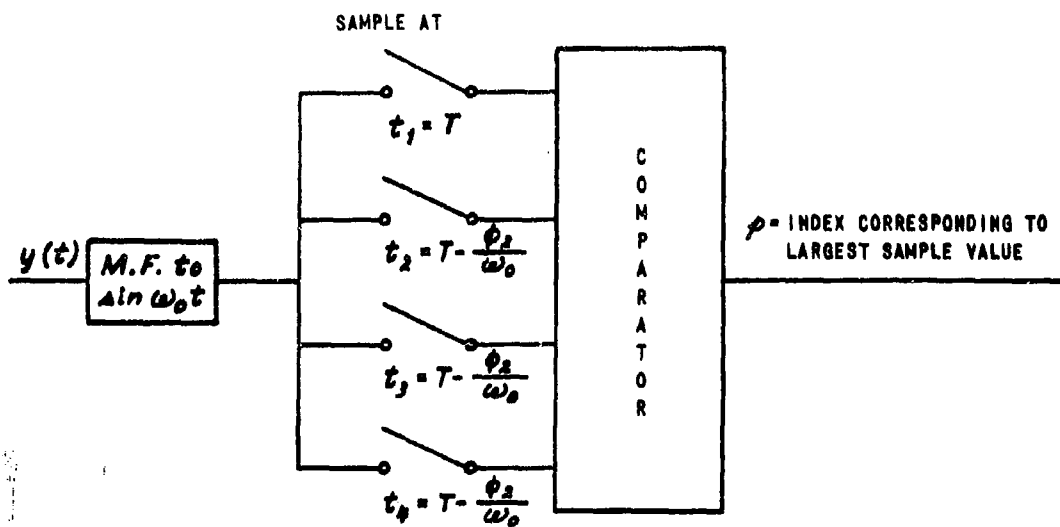


Figure 3 APPROXIMATION TO A MAXIMUM LIKELIHOOD RECEIVER USING UNEQUAL SAMPLING TIMES

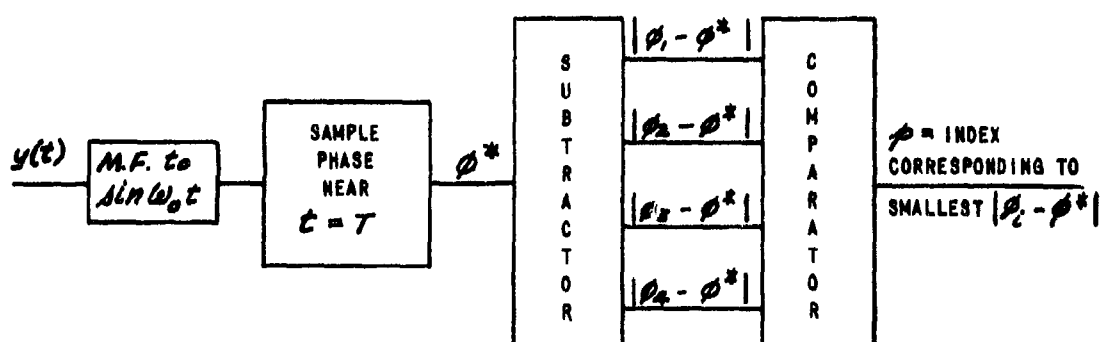


Figure 4 A "PRACTICAL" RECEIVER

3 January 1961
 DETECT MEMO NO. 5A
 AF 30(602)-2210

ANALYSIS OF "PRACTICAL" RECEIVER FOR $m = 2$ AND $m = 4$

Error probability curves for m -state CPSKS employing the practical receiver of Fig. 4 have been published by Cahn⁽²⁾. The output of the matched filter in Fig. 4 due to both signal and noise may be considered to be narrow-band when $\omega_0 T \ll 1$ and may be expressed in terms of envelope and phase as

$$O(t) = V(t) \cos [\omega_0 t + \phi(t)] \quad (16)$$

An ideal detector is usually assumed which operates on $O(t)$ to produce an output $\phi^* = \phi(T)$. In Ref. (3), it was shown that the probability density of ϕ^* (assuming without loss of generality that $\phi_1 = 0$ was sent) is given by

$$\rho(\phi^*) = \int_0^\infty \frac{\rho}{\pi} e^{-(\rho^2 - 2\rho s \cos \phi^* + s^2)} d\rho; \quad |\phi^*| \leq \pi \quad (17)$$

$$\rho(\phi^*) = 0; \quad |\phi^*| > \pi$$

where $s^2 = \frac{E}{N_0}$ (18)

is the ratio of signal energy per pulse to the noise power density (evaluated at input to receiver). The error probability of an m state CPSKS using the practical receiver of Fig. 4 is then given by

$$\rho(m) = 1 - 2 \int_0^{\pi/m} \rho(\phi^*) d\phi^* \quad (19)$$

3 January 1961
DETECT MEMO NO. 5A
AF 30(602)-2210

Substituting (17) into (19) and changing to rectangular coordinates according to

$$\begin{aligned} u &= \rho \cos \phi^* \\ v &= \rho \sin \phi^* \end{aligned} \quad (20)$$

one finds that

$$P(m) = 1 - \frac{2}{\pi c} \int_0^\infty \left[e^{-(u-s)^2} \int_0^u e^{-v^2} dv \right] du \quad (21)$$

The double integral for $P(m)$ is easily evaluated for $m = 2$ and yields

$$P(2) = \frac{1}{2} \left\{ 1 - \operatorname{erf} \sqrt{\frac{E'}{N_0}} \right\} \quad (22)$$

which is identical to the error probability obtainable with the optimum receiver of Fig. 1 as derived in Ref. 4.

For $m = 4$, $P(m)$ may be evaluated by taking the derivative of $P(m)$ with respect to s (as is shown in the Appendix to this report) and yields

$$P(4) = \frac{3}{4} - \frac{1}{2} \operatorname{erf} \sqrt{\frac{E'}{2N_0}} - \frac{1}{4} \operatorname{erf}^2 \sqrt{\frac{E'}{2N_0}} \quad (23)$$

It has not been possible to evaluate (21) in closed form for $m > 4$.

3 January 1961
DETECT MEMO NO. 5A
AF 30(602)-2210

ANALYSIS OF MATCHED FILTER EMBODIMENT OF
MAXIMUM LIKELIHOOD RECEIVER FOR $m = 4$

The following analysis of the maximum likelihood receiver of Fig. 1 for the special case when $m = 4$ was attempted in the hope that it might readily generalize for arbitrary m . Although this does not appear to be the case, and in spite of the fact that (23) may be directly obtained for the error probability of the optimum receiver for $m = 4$ by considering it to be composed of two independent binary channels, the following argument is of academic interest.

From (2) and (3) one can write

$$\begin{aligned} O_{ij} &= S_{ij} + N_i \\ S_{ij} &= \int_0^T s_j(t) s_i(t) dt \\ N_i &= \int_0^T n(t) s_i(t) dt \end{aligned} \tag{24}$$

Using (1), it can be shown that if $\omega_0 T \gg 1$,

$$S_{ij} \cong E \cos(\phi_j - \phi_i) \tag{25}$$

where the energy per pulse is given by $E = \frac{1}{2} A^2 T$. Moreover, the covariances of the noise components of the output are given by

$$\langle N_i N_k \rangle = \text{Expected Value} \left\{ N_i N_k \right\} = \sigma^2 \cos(\phi_i - \phi_k) \tag{26}$$

3 January 1961
DETECT MEAU 5A
AF 30(602)-221c

where $\sigma^2 = \frac{EN_0}{2}$. Assuming again without loss of generality that $s_1(t)$ was sent, the probability of error is given by

$$\begin{aligned} P(4) &= 1 - \text{Prob} \left\{ O_{21} < O_{11}; O_{31} < O_{11}; O_{41} < O_{11} \right\} \\ &= \int_{-\infty}^{+\infty} dO_{11} \int_{-\infty}^{O_{11}} dO_{21} \int_{-\infty}^{O_{11}} dO_{31} \int_{-\infty}^{O_{11}} dO_{41} p(O_{11}, O_{21}, O_{31}, O_{41}) \end{aligned} \quad (27)$$

and the probability density $p(O_{11}, O_{21}, O_{31}, O_{41})$ may be obtained from the joint probability density $f(N_1, N_2, N_3, N_4)$.

In a 4-state system $\phi_1 = 0$, $\phi_2 = \frac{\pi}{2}$, $\phi_3 = \pi$, $\phi_4 = \frac{3}{2}\pi$ so that from (26) one obtains

$$\begin{aligned} \langle N_i^2 \rangle &= \sigma^2 \quad i = 1, 2, 3, 4 \\ \langle N_1 N_2 \rangle &= \langle N_1 N_4 \rangle = \langle N_2 N_3 \rangle = \langle N_3 N_4 \rangle = 0 \\ \langle N_1 N_3 \rangle &= \langle N_2 N_4 \rangle = -\sigma^2 \end{aligned} \quad (28)$$

which indicates that N_1 and N_3 are independent of N_2 and N_4 . Therefore, one can write

$$f(N_1, N_2, N_3, N_4) = g(N_1, N_3) h(N_2, N_4) \quad (29)$$

and for (24)

$$\begin{aligned} N_3 &= -N_1 \\ N_4 &= -N_2 \end{aligned} \quad (30)$$

3 January 1961
 DETECT MEMO NO. 5A
 AF 30(602)-2210

Consider the density $g(N_1, N_3)$. The density of the variables N_1' and N_3'

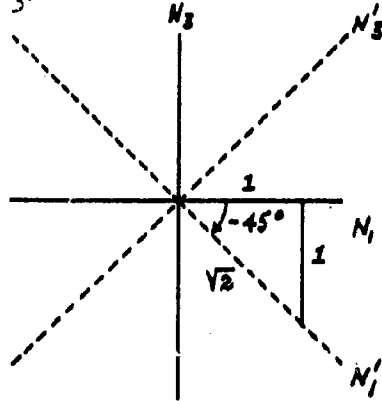


Figure 5

defined by Fig. 5 is given by

$$g'(N_1', N_3') = \frac{1}{\sqrt{2\pi}\sigma'^2} e^{-\frac{N_1'^2}{2\sigma'^2}} \delta(N_3') \quad (31)$$

where $\sigma'^2 = 2\sigma^2$. Since

$$\begin{aligned} N_1' &= \frac{N_1 - N_3}{\sqrt{2}} \\ N_3' &= \frac{N_1 + N_3}{\sqrt{2}} \end{aligned} \quad (32)$$

3 January 1961
DETECT MEMO NO. 5A
AF 30(602)-2210

one obtains

$$g(N_1, N_3) = \frac{1}{\sqrt{4\pi}\sigma^2} e^{-\frac{(N_1 - N_3)^2}{8\sigma^2}} \sigma\left(\frac{N_1 + N_3}{\sqrt{2}}\right) \quad (33)$$

and a similar expression for $h(N_2, N_4)$. Using (24) and (25) yields

$$\begin{aligned} P(O_{11}, O_{21}, O_{31}, O_{41}) &= \frac{1}{4\pi\sigma^2} e^{-\frac{(O_{11} - O_{31} - 2E)^2}{8\sigma^2}} \sigma\left(\frac{O_{11} + O_{31}}{\sqrt{2}}\right) \\ &\quad e^{-\frac{(O_{21} - O_{41})^2}{8\sigma^2}} \sigma\left(\frac{O_{21} + O_{41}}{\sqrt{2}}\right) \end{aligned} \quad (34)$$

Performing the integration indicated in (27) with respect to O_{21} and O_{41} by first changing to the variables $x = O_{21}/\sqrt{2}$ and $y = O_{41}/\sqrt{2}$, yields

3 January 1961
 DETECT MEMO NO. 5A
 AF 30(602)-2210

$$\int_{-\infty}^{0_{11}} dO_{21} \int_{-\infty}^{0_{11}} dO_{41} e^{-\frac{(O_{21}-O_{41})^2}{8\sigma^2}} \delta\left(\frac{O_{21}+O_{41}}{\sqrt{2}}\right) =$$

$$2 \int_{-\infty}^{\frac{0_{11}}{\sqrt{2}}} dx \int_{-\infty}^{\frac{0_{11}}{\sqrt{2}}} dy e^{-\frac{(x-y)^2}{4\sigma^2}} \delta(x+y) = \quad (35)$$

$$2 \int_{-\frac{0_{11}}{\sqrt{2}}}^{\frac{0_{11}}{\sqrt{2}}} e^{-\frac{x^2}{\sigma^2}} dx = 4 \int_0^{\frac{0_{11}}{\sqrt{2}}} e^{-\frac{x^2}{\sigma^2}} dx$$

Consequently, (27) reduces to

$$P(4) = 1 - \frac{1}{\pi\sigma^2} \int_{-\infty}^{+\infty} \left\{ \int_{-\infty}^{0_{11}} e^{-\frac{(O_{11}-O_{31}-2E)^2}{8\sigma^2}} \delta\left(\frac{O_{11}+O_{31}}{\sqrt{2}}\right) \left[\int_0^{\frac{O_{11}}{\sqrt{2}}} e^{-\frac{t^2}{\sigma^2}} dt \right] dO_{31} \right\} dO_{11} \quad (36)$$

and again letting $x = O_{11}/\sqrt{2}$, $y = O_{31}/\sqrt{2}$ gives

$$P(4) = 1 - \frac{2}{\pi\sigma^2} \int_{-\infty}^{+\infty} \left\{ \int_{-\infty}^{x/\sqrt{2}} e^{-\frac{(x-y-\frac{2E}{\sqrt{2}})^2}{4\sigma^2}} \delta(x+y) \left[\int_0^x e^{-\frac{t^2}{\sigma^2}} dt \right] dy \right\} dx \quad (37)$$

3 January 1961
 DETECT MEMO NO. 5A
 AF 30(602)-2210

which reduces to

$$P(4) = 1 - \frac{2}{\pi\sigma^2} \int_0^\infty \left\{ e^{-\frac{(x-\frac{z}{\sigma})^2}{\sigma^2}} \int_0^x e^{-\frac{t^2}{\sigma^2}} dt \right\} dx \quad (38)$$

and letting $v = t/\sigma$ and $u = x/\sigma$, one finally obtains

$$P(4) = 1 - \frac{2}{\pi} \int_0^\infty \left\{ e^{-(u-s)^2} \int_0^u e^{-v^2} dv \right\} du \quad (39)$$

where $S = \frac{E}{\sigma^2} = \sqrt{E/N_0}$ and (39) is seen to be identical to (21) for $m = 4$. This establishes the equivalence of the optimum and practical receiver for $m = 4$.

EQUIVALENCE OF "PRACTICAL RECEIVER" AND MAXIMUM LIKELIHOOD RECEIVER FOR ARBITRARY m

The "practical" receiver of Fig. 4 can, for arbitrary m be shown to be equivalent to a maximum likelihood receiver by showing that its performance is equivalent to that of the receiver of Fig. 2. As was pointed out previously, the receivers of Figs. 2 and 4 differ only in the manner in which the respective estimates $\hat{\phi}$ and $\hat{\phi}^*$ of phase are obtained. The probability density of $\hat{\phi}$ will be shown to be identical to that of $\hat{\phi}^*$.

Again, assuming that $s_1(t)$ was transmitted, it is possible from (6) to express equation (5) as

$$O_i = (E + N_1) \cos \phi_i + N_2 \sin \phi_i \quad (40)$$

3 January 1961
DETECT MEMO NO. 5A
AF 30(602)-2210

where the joint density of N_1 and N_2 is given by

$$P(N_1, N_2) = \frac{1}{2\pi\sigma^2} e^{-\frac{N_1^2 + N_2^2}{2\sigma^2}}. \quad (41)$$

and $\sigma^2 = \frac{E N_0}{2}$. The substitutions (7) become

$$E + N_1 = V \cos \hat{\phi}$$

$$N_2 = V \sin \hat{\phi}$$

and the probability density of $\hat{\phi}$ may be shown to be identical to $p(\phi^*)$ as given by equation (17) of this report in precisely the same manner that equation (13) of Ref. 3 was obtained from equation (7) of Ref. 3.

3 January 1961
DETECT MEMO NO. 5A
AF 30(602)-2210

REFERENCES

1. Davenport, W. B., Jr. and Root, W. L., An Introduction to the Theory of Random Signals and Noise McGraw-Hill 1958.
2. Cahn, C. R., Performance of Digital Phase-Modulation Communication Systems I.R.E. Transactions on Communications Systems Vol. CS-7, No. 1 May 1959.
3. Fleck, John T. and Trabka, Eugene A., Error Probabilities of Multiple-State Differentially Coherent Phase-Shift Keyed Systems in the Presence of White, Gaussian Noise DETECT MEMO NO. 2A Cornell Aeronautical Laboratory January 3, 1961.
4. Becker, H. D. and Lawton, J. G., Theoretical Comparison of Binary Data Transmission Systems Cornell Aeronautical Laboratory Report No. CA-1172-S-1 May 1958.

3 January 1961
 DETECT MEMO NO. 5A
 AF 30(602)-2210

APPENDIX
 Evaluation of $P(m)$ For $m = 4$

From equation (21), one may write

$$P(m, s) = 1 - \frac{2}{\pi} \int_0^\infty \left[e^{-(u-s)^2} \int_0^{u \tan \frac{\pi}{m}} e^{-v^2} dv \right] du$$

which upon letting $y = u - s$ becomes

$$P(m, s) = 1 - \frac{2}{\pi} \int_{-s}^\infty f(s, y) dy$$

where

$$f(s, y) = e^{-y^2} \int_0^{(y+s) \tan \frac{\pi}{m}} e^{-v^2} dv$$

so that using Leibniz' Rule, one has

$$\frac{\partial P}{\partial s} = -\frac{2}{\pi} \left\{ \int_{-s}^\infty \frac{\partial f}{\partial s} dy + f(-s, s) \right\}$$

where

$$\frac{\partial f}{\partial s} = e^{-y^2} \tan \frac{\pi}{m} e^{-(y+s)^2 \tan^2 \frac{\pi}{m}}$$

and hence,

$$\frac{\partial P}{\partial s} = -\frac{2}{\pi} \tan \frac{\pi}{m} \int_{-s}^\infty e^{-\left[y^2 \sec^2 \frac{\pi}{m} + 2ys \tan^2 \frac{\pi}{m} + s^2 \tan^2 \frac{\pi}{m} \right]} dy$$

3 January 1961
 DETECT MEMC NO. 5A
 AF 30(602)-2210

Completing the square in the exponent of the integrand yields

$$\frac{\partial P}{\partial S} = -\frac{2}{\pi} \tan \frac{\pi}{m} e^{-S^2 \sin^2 \frac{\pi}{m}} \int_{-S}^{\infty} e^{-\sec^2 \frac{\pi}{m} \left[y + S \sin^2 \frac{\pi}{m} \right]^2} dy$$

and making the substitution $x = \sec \frac{\pi}{m} \left[y + S \sin^2 \frac{\pi}{m} \right]$ gives

$$\begin{aligned} \frac{\partial P}{\partial S} &= -\frac{2}{\pi} \sin \frac{\pi}{m} e^{-S^2 \sin^2 \frac{\pi}{m}} \int_{-S \cos \frac{\pi}{m}}^{\infty} e^{-x^2} dx \\ &= -\frac{2}{\pi} \sin \frac{\pi}{m} e^{-S^2 \sin^2 \frac{\pi}{m}} \left\{ \frac{\sqrt{\pi}}{2} + \int_0^{S \cos \frac{\pi}{m}} e^{-x^2} dx \right\} \end{aligned}$$

If one now lets $m = 4$ so that $\sin \frac{\pi}{m} = \cos \frac{\pi}{m} = \frac{1}{\sqrt{2}}$ then it is found that

$$\sqrt{2} e^{-\frac{S^2}{2}} \int_0^{\frac{S}{\sqrt{2}}} e^{-x^2} dx = \frac{d}{dS} [v^2]$$

where

$$v = \int_0^{\frac{S}{\sqrt{2}}} e^{-x^2} dx$$

3 January 1961
DETECT MEMO NO. 5A
AF 30(602)-2210

and consequently,

$$P = C - \frac{1}{\sqrt{\pi}} \int_0^{\frac{s}{\sqrt{2}}} e^{-t^2} dt = \frac{1}{\pi} \left[\int_0^{\frac{s}{\sqrt{2}}} e^{-z^2} dz \right]^2$$

$$P = C - \frac{1}{2} \operatorname{erf} \frac{s}{\sqrt{2}} - \frac{1}{4} \operatorname{erf}^2 \frac{s}{\sqrt{2}}$$

where the constant C may be evaluated by considering the original expression for $P(m, S)$ at $S = 0$. This yields $C = 3/4$ and recalling that $\frac{s}{\sqrt{2}} = \sqrt{\frac{E}{2N_0}}$, one obtains

$$P = \frac{3}{4} - \frac{1}{2} \operatorname{erf} \sqrt{\frac{E}{2N_0}} - \frac{1}{4} \operatorname{erf}^2 \sqrt{\frac{E}{2N_0}}$$

3 January 1961

1(b) DETECT MEMO NO. 12

Subject: "Error Probability (in the Presence of Sampling Time Errors) of the Cross Correlation Embodiment of a Maximum Likelihood Receiver for Binary Coherent Gated Phase Shift Keyed Systems (BCGPSKs)"

By: Eugene A. Trabka

SUMMARY

The cross correlation embodiment of a maximum likelihood receiver for m -state coherent gated phase shift keyed systems is introduced. The error probability of such a binary receiver is obtained in the presence of sampling time errors.

INTRODUCTION

In Reference 1, several embodiments of the maximum likelihood receiver for the detection of m -state coherent pulsed phase shift keyed signals were investigated. The purpose of the investigation was to compare a "practical" embodiment, which required only one filter regardless of the number m of phase states, with a matched filter embodiment which requires m distinct filters*.

In order to complete the discussion of the embodiments of maximum likelihood receivers for CPSK systems, the present memo analyzes the performance of a cross-correlation embodiment. Moreover, since this embodiment is particularly suited for the detection of coherent gated phase shift keyed signals, this form of the coherent phase shift keyed signals will be used. Since, as is pointed out in Chapter II, it does not appear reasonable to consider gated operation with a frequency error, only errors in sampling time will be considered. Focusing attention on the particular signal interval from 0 to T ,

* In Chapter II, the difference between pulsed and gated PSK systems is discussed and it is pointed out that closely analogous embodiments of the respective receivers are possible.

3 January 1961
DETECT MEMO NO. 12
AF 30(602)-2210

it was assumed in Reference 1 that the m possible signals are of the form

$$s_i(t) = u\left(\frac{t}{T}\right) A \sin [\omega_0 t + \phi_i] \quad (1)$$

where $u(x) = 1$ for $0 \leq x \leq 1$ and $u(x) = 0$ elsewhere, and $\phi_i = \frac{2\pi i}{m}$ ($i = 1, 2, \dots, m$). Moreover, it was pointed out in Reference 1 that the maximum likelihood receiver requires the computation of the quantities

$$O_i(T) = \int_0^T y(t) s_i(t) dt \quad (2)$$

in which $y(t)$ is the input to the receiver assumed to be of the form

$$y(t) = s(t) + n(t) \quad (3)$$

where $s(t)$ is the actual transmitted signal and $n(t)$ is a sample of white Gaussian noise with single-sided power spectral density N_0 watts/cps. A block diagram of the cross-correlation receiver which computes the quantities $O_i(T)$ as given by (2) is shown in Figure 1. The box labeled "control" causes the comparator to determine at sampling times $t = kT$, where k is an integer, which ϕ_i produces the largest voltage at its input. Moreover, the control unit discharges the integrators at $t = kT^+$.

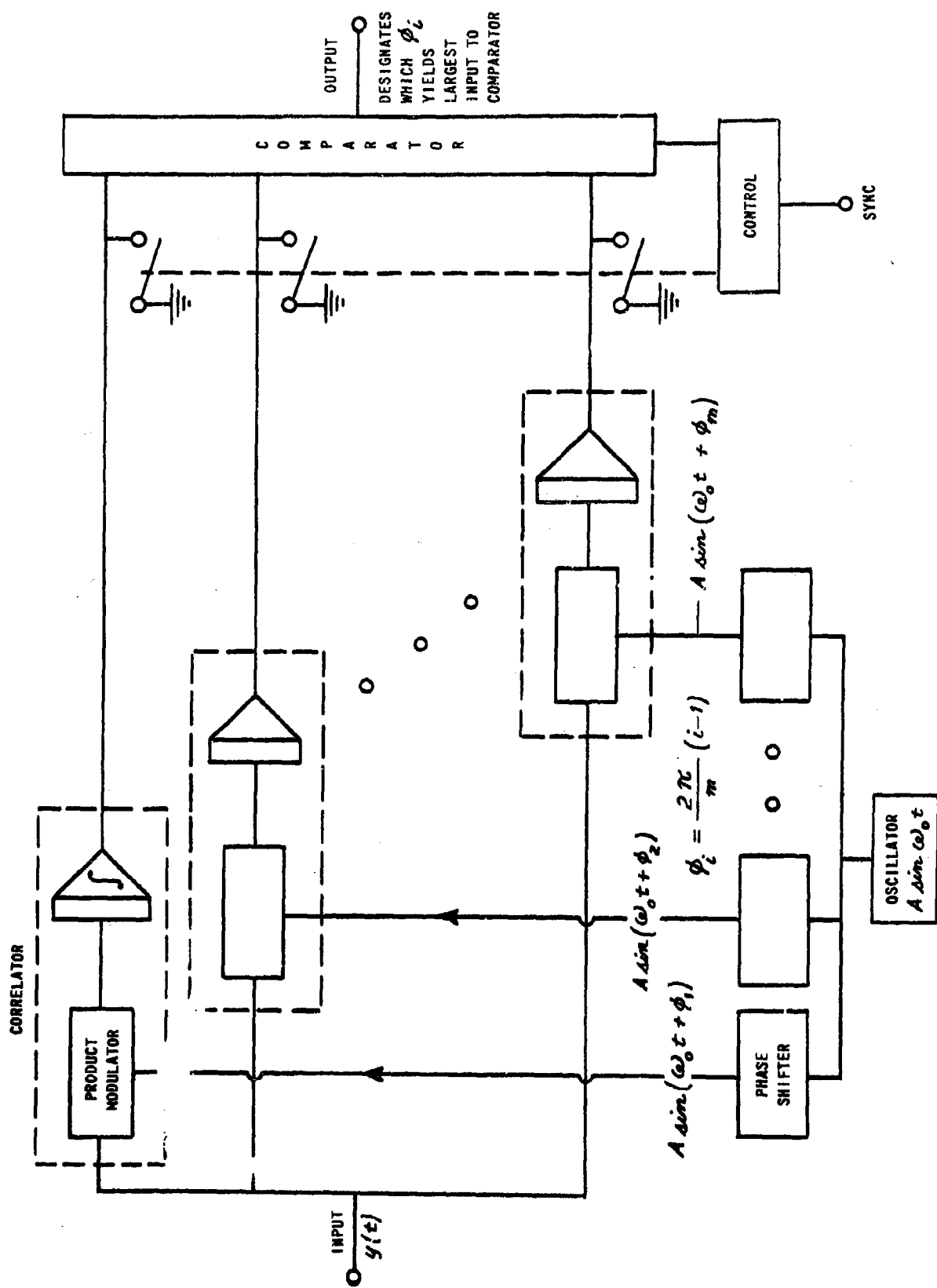


Figure 1 CROSS-CORRELATION EMBODIMENT OF MAXIMUM LIKELIHOOD RECEIVER

3 January 1961
DETECT MEMO NO. 12
AF 30(602)-2210

ERROR PROBABILITY IN THE PRESENCE OF SAMPLING TIME ERRORS

The transmitted coherent gated phase shift keyed signal is assumed to be of the form

$$s(t) = \sum_{k=-\infty}^{+\infty} u\left(\frac{t-kT}{T}\right) A \sin(\omega_0 t + \theta_k) \quad (4)$$

where the θ_k are independent random variables designating the transmitted phase in the k th interval. The θ_k all have identical discrete probability distributions, viz

$$\text{Prob. } \left\{ \theta_k = \phi_i \right\} = \frac{1}{m}; \quad i = 1, 2, \dots, m \quad (5)$$

If an error ΔT is made in the sampling time, then the comparator chooses the largest of the quantities

$$o_i(T + \Delta T) = \int_{AT}^{T + \Delta T} g(t) s_i(t) dt \quad (6)$$

instead of the quantities (2). Using (1), (3) and expanding (6), it is possible to write

$$o_i(T + \Delta T) = \mu_i + n_i \quad (7)$$

3 January 1961
DETECT MEMO NO. 12
AF 30(602)-2210

where

$$\mu_i = \int_{\Delta T}^{\tau + \Delta T} s(t) A \sin(\omega_0 t + \phi_i) dt \quad (8)$$

$$n_i = \int_{\Delta T}^{\tau + \Delta T} n(t) A \sin(\omega_0 t + \phi_i) dt$$

If $m=2$, then $\phi_1=0$ and $\phi_2=\pi$ and it is easily seen that $\mu_2 = -\mu_1$, and $n_2 = -n_1$, so that $O_2(\tau + \Delta T) = -O_1(\tau + \Delta T)$ and the error probability (assuming without loss of generality that the actual transmitted phase in the relevant interval is $\theta_0 = \phi_1 = 0$) as given by

$$P(2) = \text{Prob.} \left\{ O_1(\tau + \Delta T) < O_2(\tau + \Delta T) \right\} \quad (9)$$

reduces to

$$P(2) = \text{Prob.} \left\{ O_1(\tau + \Delta T) < 0 \right\} \quad (10)$$

It is easily ascertained that n_1 has a Gaussian distribution with zero mean and variance $\sigma^2 = \frac{EN_0}{2}$ where $E = \frac{1}{2}AT^2$ so that (10) becomes

$$P(2) = \frac{1}{2} \left(1 - \text{erf} \frac{\mu_1}{\sqrt{2\sigma^2}} \right) \quad (11)$$

3 January 1961
 DETECT MEMO NO. 12
 AF 30(602)-2210

Substituting (4) into (8) and assuming $0 \leq \Delta T \leq T$, it is found that

$$\mu_1 = \int_{\Delta T}^T A^2 \sin [\omega_0 t + \theta_0] \sin \omega_0 t dt \quad (12)$$

$$+ \int_T^{T+\Delta T} A^2 \sin [\omega_0 t + \theta_0] \sin \omega_0 t dt$$

which can be written as

$$\mu_1 = \frac{A^2}{2} \left\{ \int_{\Delta T}^T \cos \theta_0 dt - \int_{\Delta T}^T \cos (2\omega_0 t + \theta_0) dt \right. \quad (13)$$

$$+ \frac{A^2}{2} \left\{ \int_T^{T+\Delta T} \cos \theta_0 dt - \int_T^{T+\Delta T} \cos (2\omega_0 t + \theta_0) dt \right.$$

so that one finally obtains

$$\begin{aligned} \mu_1 = & E \left\{ \left(1 - \frac{\Delta T}{T} \right) \cos \theta_0 + \frac{\Delta T}{T} \cos \theta_0 \right. \\ & - \frac{1}{2(\omega_0 T)} \left[\sin (2\omega_0 T + \theta_0) - \sin (2\omega_0 T \frac{\Delta T}{T} + \theta_0) \right. \quad (14) \\ & \left. \left. + \sin \left(2\omega_0 T \left(1 + \frac{\Delta T}{T} \right) \right) - \sin (2\omega_0 T + \theta_0) \right] \right\} \end{aligned}$$

3 January 1961
DETECT MEMO NO. 12
AF 30(602)-2210

Considering μ_r from (14) as a function of $\frac{\Delta T}{T}$ with parameter $\omega_0 T$, it is easily shown that

$$\lim_{\omega_0 T \rightarrow \infty} \mu_r \left(\frac{\Delta T}{T}; \omega_0 T \right) = E \left\{ \left(1 - \frac{\Delta T}{T} \right) \cos \theta_0 + \frac{\Delta T}{T} \cos \theta_1 \right\} \quad (15)$$

and that the convergence is uniform. Recalling that it had been assumed that $\theta_0 = 0$, it is possible for large $\omega_0 T$ to approximate (14) by

$$\mu_r \approx E \left\{ \left(1 - \frac{\Delta T}{T} \right) + \frac{\Delta T}{T} \cos \theta_1 \right\} \quad (16)$$

and it is seen that μ_r depends on the transmitted phase θ_1 in the succeeding interval. Since $\theta_1 = 0$ or π each with probability 1/2, one obtains for the average error probability from (11) and (16)

$$P(2) = \frac{1}{4} \left\{ 1 - \operatorname{erf} \left[\sqrt{\frac{E}{N_0}} \right] \right\} + \frac{1}{4} \left\{ 1 - \operatorname{erf} \left[\left(1 - 2 \left| \frac{\Delta T}{T} \right| \right) \sqrt{\frac{E}{N_0}} \right] \right\} \quad (17)$$

where $\frac{\Delta T}{T}$ has been replaced by $\left| \frac{\Delta T}{T} \right|$ since it can be shown that (17) then holds for $-T \leq \Delta T \leq 0$ also. This result is identical to the error probability obtained for the "practical" receiver using coherent pulsed phase shift keyed signals, as can be seen from comparison with equation (21) of Reference 2.

3 January 1961
DETECT MEMO NO. 12
AF 30(602)-2210

REFERENCES

1. Trabka, Eugene A. Embodiments of the Maximum Likelihood Receiver for Detection of Coherent Pulsed Phase Shift Keyed Signals in the Presence of Additive White Gaussian Noise DETECT MEMO NO. 5A Cornell Aeronautical Laboratory, Inc. 3 January 1961.
2. Trabka, Eugene A. Error Probabilities for Coherent Pulsed Phase-Shift Keyed Systems (CPPSKS) With Frequency and Sampling Time Errors DETECT MEMO NO. 7A Cornell Aeronautical Laboratory, Inc. 3 January 1961.

3 January 1961

I(c) DETECT MEMO* NO. 15

SUBJECT: "Comments on M-State Coherent Digital Communications Systems"

BY: Eugene A. Trabka

Consider a communications system which can transmit any one of M signals, $S_i(t)$ $i = 1, \dots, M$, each of duration T . It has been shown⁽¹⁾ that for a given set of signals a receiver can minimize its average error probability by using a maximum likelihood detector, i.e., decide that the signal having the greatest a posteriori probability was sent. The input to the receiver $y(t)$ is usually assumed to consist of the transmitted signal plus white Gaussian noise with single-sided power spectral density N_0 watts/cps. From the identity

$$P(S_i/y) P(y) = P(y/S_i) P(S_i)$$

it is possible to express the a posteriori probability of S_i given the receiver input y as

$$P(S_i/y) = k_i P(S_i) P(y/S_i)$$

However, $y(t) - S_i(t) = n(t)$ and since it can be shown⁽²⁾ that

$$P(n) = k_n e^{-\frac{1}{N_0} \int_0^T n^2(t) dt}$$

one finds that

$$P(S_i/y) = k_i P(S_i) e^{-\frac{1}{N_0} \left\{ \int_0^T y(t) S_i(t) dt - \frac{E_i}{2} \right\}}$$

where

$$E_i = \int_0^T S_i^2(t) dt$$

is the energy of the i^{th} signal. Thus, in the case when all the signals are a priori equally likely, i.e., $P(S_i) = \frac{1}{M}$, a maximum likelihood detector will select as the transmitted signal, the $S_i(t)$ for which

* This material was originally published as Section C of the technical discussion of the "Technical Proposal for Extension of Detection Techniques for Digital Data Transmission", Contract AF 30(602)-2210, submitted by the Cornell Aeronautical Laboratory, 25 August 1960.

$$O_i = \int_0^T y(t) S_i(t) dt - \frac{E_i}{2}$$

is the greatest. Such a receiver may be realized with matched filters and is shown in Fig. 1 for $M = 4$. It should be noted that the above argument is

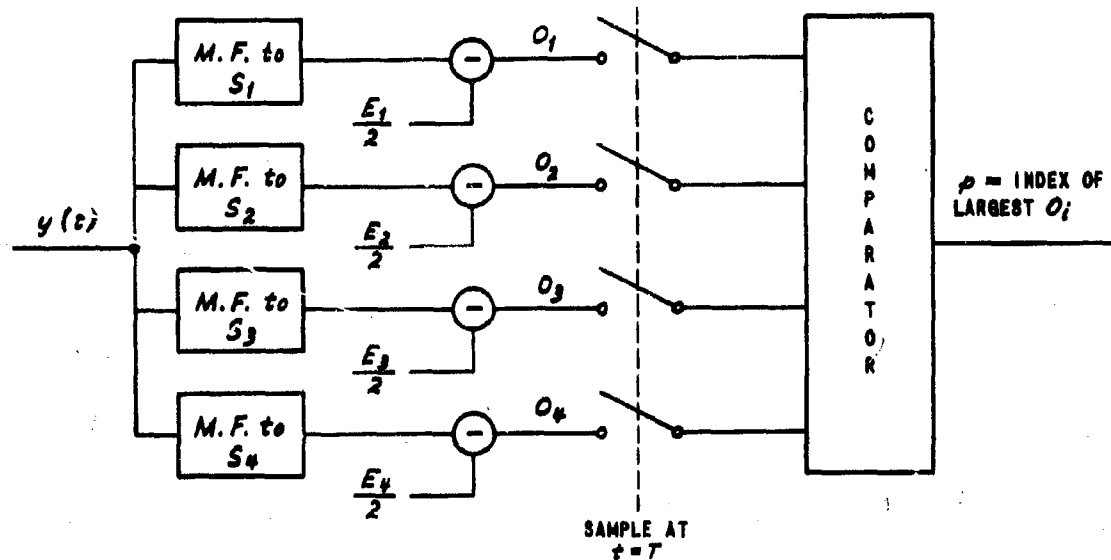


Figure 1 A MAXIMUM LIKELIHOOD RECEIVER

valid when the M possible signals are known completely to the receiver (the so-called coherent case without random parameters such as phase).

The average error probability depends on the choice of signal alphabet. Only in the binary case $M = 2$, is it known how to choose the signals so that

the average error probability is the minimum possible.* The probability of an error assuming S_j was sent is formally given by

$$P(\text{Error}/S_i) = 1 - P(\text{every } O_j < O_i) \quad j \neq i$$

and the average error probability is given by

$$P(\text{Error}) = \frac{1}{M} \sum_{i=1}^M P(\text{Error})$$

Even when the signals are specified, it is often difficult to evaluate the above expressions and much harder to visualize how the $S_i(t)$ should be chosen to minimize $P(E)$. In order to gain insight into this problem, the heuristic device of visualizing maximum likelihood detection geometrically in D-dimensional space is often used. This is possible through use of the sampling theorem which states that a signal, whose energy density spectrum is limited to a band W , is completely determined by samples spaced $\frac{1}{2W}$ seconds apart in time. Thus, in the interval T there are at most $D = 2TW$ numbers required to specify the signal and these numbers may be taken as the coordinates of a point in D-dimensional space. Thus, to each signal $S_i(t)$, there corresponds a point in D-dimensional space with coordinates:

$$\left\{ S_i\left(\frac{1}{2W}\right), S_i\left(\frac{2}{2W}\right), \dots, S_i\left(\frac{D}{2W}\right) \right\}$$

It is possible to show ⁽²⁾ that for two such waveforms, say $u(t)$ and $v(t)$ that

$$2W \int_0^T u(t) v(t) dt \approx \sum_{j=1}^D u\left(\frac{j}{2W}\right) v\left(\frac{j}{2W}\right)$$

*In this case, the signals should be the negative of one another.

so that if one lets $u = v = S_1$, it is seen that the square of the distance of a signal point from the origin is approximately $2WE_1$, since the preceding equation reduces to

$$2W \int_0^T S_i^2(t) dt \approx \sum_{j=1}^D S_i^2\left(\frac{j}{2W}\right),$$

Moreover, the receiver input $y(t)$ may be associated with a point in the same space as the possible transmitted signals. If one considers the distances between the point corresponding to $y(t)$ and each of the signal points, namely

$$\begin{aligned} d_i^2 &= \sum_j \left[y\left(\frac{j}{2W}\right) - S_i\left(\frac{j}{2W}\right) \right]^2 = \sum_j y^2\left(\frac{j}{2W}\right) - 2 \sum_j y\left(j/2W\right) S_i\left(j/2W\right) \\ &\quad + \sum_j S_i^2\left(j/2W\right) \end{aligned}$$

it is seen that

$$\begin{aligned} d_i^2 &\approx 2W \left\{ \int_0^T y^2(t) dt - 2 \left[\int_0^T y(t) S_i(t) dt \right. \right. \\ &\quad \left. \left. - \frac{E_i}{2} \right] \right\} = 2W \left\{ \int_0^T y^2(t) dt - 2O_i \right\} \end{aligned}$$

so that the maximum likelihood procedure of selecting that $S_1(t)$ which maximizes O_1 has the geometrical interpretation of selecting the signal point which is closest to the point corresponding to the receiver input $y(t)$.

Gilbert⁽³⁾, gives an approximate formula for the average error probability of a maximum likelihood detector in terms of the geometrical configuration of signals in signal space. It is interesting to apply Gilbert's Formula to M-state Coherent Phase Shift Keyed Systems (CPSKS). The signals of a CPSKS may be represented as points in a 2-dimensional space whose polar coordinates are the amplitude and phase of the carrier. This is

illustrated in Fig. 2 for M = 8.

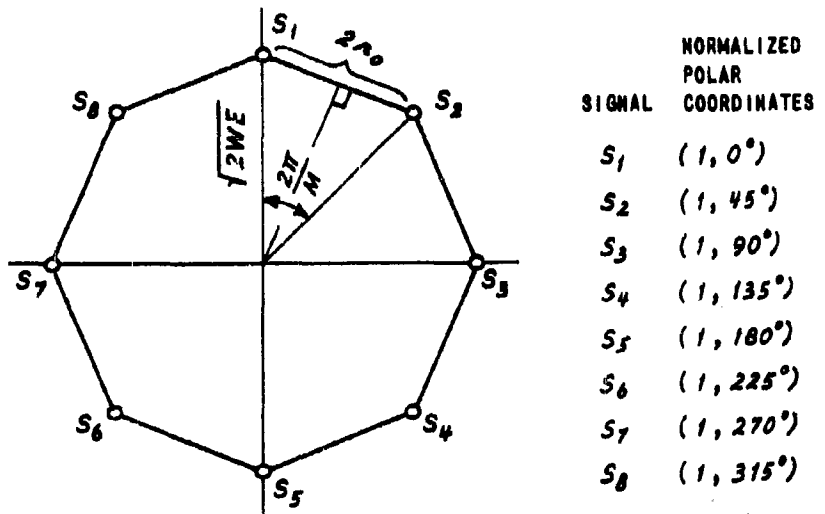


Figure 2 SIGNALS OF AN M = 8 CPSKS

According to Gilbert, the average error probability of a maximum likelihood detector is approximately given by

$$P(\text{Error}) = \frac{N}{\sqrt{2\pi}} \int_{\frac{r_0}{\sigma}}^{\infty} e^{-\frac{x^2}{2}} dx$$

$$\text{when } \frac{\sqrt{2WE}}{\sigma} = \frac{\sqrt{2WE}}{\sqrt{N_0 W}} = \sqrt{\frac{2E}{N_0}} \gg 1$$

where

$2r_0$ = the smallest of the $\frac{M(M-1)}{2}$ distances between pairs of signal points.

σ^2 = total power of input noise in bandwidth W

and N is determined as follows: for each signal $s_i(t)$ determine the number N_i of signals which are a distance $2r_0$ from it, then

$$N = \frac{1}{M} \sum_{i=1}^M N_i .$$

For M-state CPSKS, it is ascertained with the help of Fig. 2 that

$$r_0 = \sqrt{2EW} \sin \frac{\pi}{M}$$

$$\sigma = \sqrt{N_0 W}$$

and if $M > 2$

$$N = 2$$

and, therefore,

$$P(\text{Error}) = \frac{2}{\sqrt{2\pi}} \int_{\sqrt{\frac{2E}{N_0}} \sin \frac{\pi}{M}}^{\infty} e^{-\frac{x^2}{2}} dx = 1 - \text{erf} \left(\sqrt{\frac{E}{N_0}} \sin \frac{\pi}{M} \right)$$

For $M = 2$, $r_0 = \sqrt{2WE}$ and $N = 1$, in which case

$$P(\text{Error}) = \frac{1}{\sqrt{2\pi}} \int_{\sqrt{\frac{2E}{N_0}}}^{\infty} e^{-\frac{x^2}{2}} dx = \frac{1}{2} \left(1 - \text{erf} \sqrt{\frac{E}{N_0}} \right)$$

in agreement with the exact solution previously obtained.⁽⁴⁾

Error curves for M-state CPSKS have been obtained by Cahn⁽⁵⁾. The data summarized in the following table was computed from the approximate formula derived in this report. If these data are plotted on Fig. 3 of Ref. (5), good agreement with Cahn's result is obtained.*

$$P(\text{Error}) = 1 - \text{erf} \left\{ \sqrt{\frac{E}{N_0}} \ln \frac{\pi}{M} \right\}$$

M	$P(E) = 10^{-2}$	$P(E) = 10^{-3}$	$P(E) = 10^{-4}$
	E/N_0 (db)	E/N_0 (db)	E/N_0 (db)
4	8.2	10.3	11.8
8	13.6	15.7	17.1
16	19.4	21.5	23.0
32	25.4	27.5	29.0

Consideration of multiple signal alphabets sooner or later leads to the problem of how to compare signal alphabets. Gilbert⁽³⁾ does this in an interesting manner on the basis of efficiency in approaching theoretical channel capacity. Assume that the channel is to be used to transmit decimal numbers of L digits in length (e.g. map coordinates). If an alphabet of M symbols (letters) is used, let x denote the number of letters required to represent the L place decimal number. Since

$$10^L = M^x$$

*For $M = 4$, the approximate formula gives the first term of the exact expression, i.e., 2a is

$$P(\text{Error}) = 2a - a^2 \text{ where } a = \frac{1}{2} \left(1 - \text{erf} \sqrt{\frac{E}{2N_0}} \right)$$

is the probability of error in a subchannel. The exact expression may be derived by considering the 4-state case to consist of two independent binary subchannels in quadrature, each with energy $E/2$.

one has

$$x = \frac{L}{\log_{10} M}$$

If it is required that only one number in 10^4 be received incorrectly, then the average letter error probability must satisfy

$$1 - (1 - p)^x \approx xp = 10^{-4}$$

or

$$p = \frac{10^{-4} \log_{10} M}{L}$$

From the approximate formula for the average error probability per symbol

$$p = \frac{N}{\sqrt{2\pi}} \int_{-\infty}^{\infty} e^{-\frac{z^2}{2}} dz$$

the value of $\frac{r_0}{\sigma}$ may be determined once the signal alphabet has been specified. It is convenient to imagine at this point that distances have been scaled so that $2 r_0 = 1$ so that the latter calculation effectively determines σ . The average signal power is given by

$$P = \frac{\sum E_i}{TM} = \frac{1}{2TW} \sum_{i=1}^M d_i^2 = \frac{1}{DM} \sum_{i=1}^M d_i^2$$

where now d_i is the distance of the i^{th} signal point from the origin. The ratio

$$\gamma = \frac{P}{\sigma^2}$$

is the smallest signal-to-noise power ratio that meets the error requirements. Recalling that $D = 2 TW$ and since $\log_2 M$ bits of information are transmitted in an interval $T = D/2W$, one has for the rate at which information is received (since the error probability is low)

$$R \simeq \frac{\log_2 M}{D/2W} = \frac{2W \log_2 M}{D}$$

Consequently, a given signal alphabet may be plotted as a point (Y , R/W) and its distance above the theoretical curve

$$R/W = \log_2 (1 + Y)$$

may be taken as a measure of the efficiency with which the given signal alphabet utilizes channel capacity.

The results of the calculations indicated above for M -state CPSK with $p = 10^{-4}$ for a 10-digit decimal number are plotted in Fig. 3 and labeled (MCPSK). It is to be noted that 2-state CPSK is the most efficient. However, efficiency may not necessarily be the criterion by which the signal alphabet should be chosen. A less efficient alphabet yielding a higher information rate may be preferred in a particular situation. If this compromise is made, it is still disturbing to know that the minimum signal-to-noise power ratio required by the less efficient alphabet might be utilized more efficiently to obtain an even higher information rate. The search for efficient signal alphabets is, therefore, a problem of practical importance.

A more efficient set of signals for $M = 8$ than those of Fig. 2 is shown in Fig. 4. It plots as the point marked \square on the efficiency graph of Fig. 3.

It was previously pointed out that for a given $M > 2$, it is not known how to choose the signals so that the average error probability using a maximum likelihood detector is the minimum possible. Turin⁽⁶⁾ reports that "Dr. A. V. Balakrishnan has proved the following long-standing conjecture concerning the general case of M equiprobable signals. If the dimensionality of the signal space (roughly $2 TW$) is at least $M-1$, then the signals, envisaged as points in signal space, should be placed at the vertices

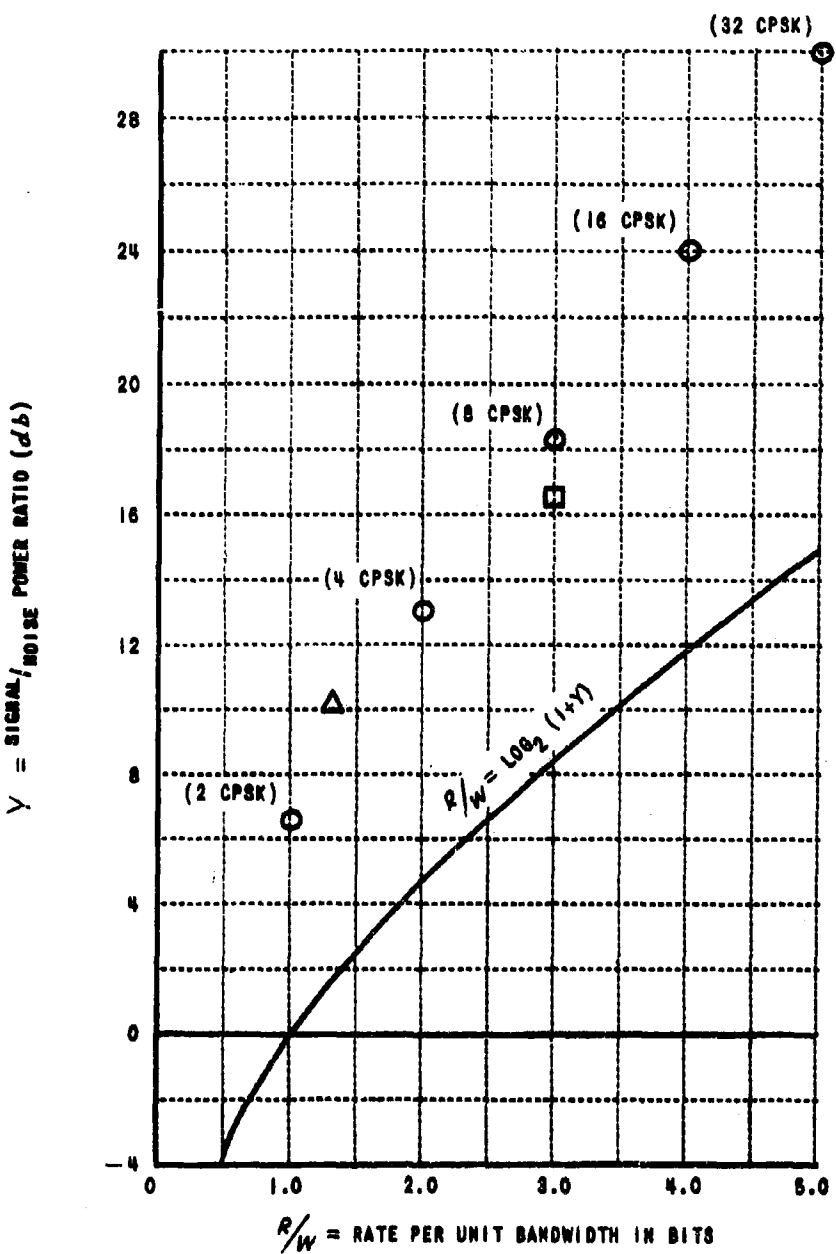


Figure 3 PROBABILITY IS 10^{-4} THAT AN ERROR IS MADE IN
A 10 DIGIT DECIMAL NUMBER

of an $(M-1)$ - dimensional regular simplex (i.e., a polyhedron, each vertex of which is equally distant from every other vertex)...." If one considers the case for $M = 4$, then there is no difficulty in picturing the optimum set of signals in 3-dimensional space. These were also considered by

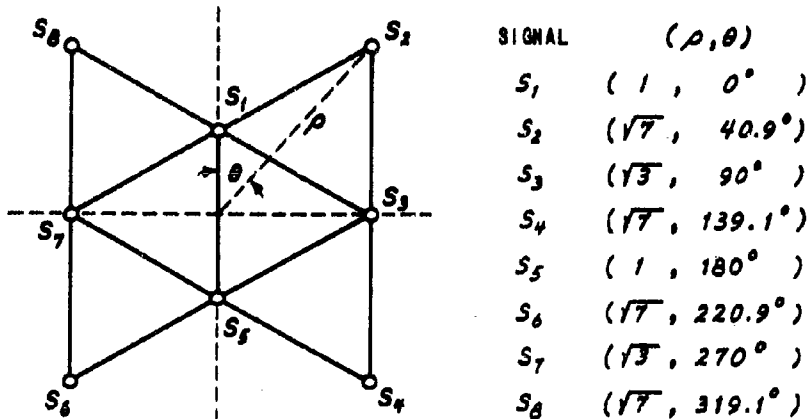


Figure 4 AN EFFICIENT SET OF 8 SIGNALS

Gilbert and are shown in Fig. 5 reproduced from Ref. 3. It is readily ascertained that $N = 3$, and since in the scale shown $2 r_o = 1$

$$\frac{1}{2r_o} = \frac{32\sqrt{6}}{\gamma 2WE}$$

and

$$\frac{r_o}{\sigma} = \frac{r_o}{\gamma N_o W} = \frac{2\sqrt{3}}{3} \sqrt{\frac{F}{N_o}}$$

consequently,

$$P(\text{Error}) = \frac{3}{\gamma 2\pi} \int_{\frac{4\sqrt{2}}{3}\sqrt{\frac{F}{N_o}}}^{\infty} e^{-\frac{x^2}{2}} dx = \frac{3}{2} \left(1 - \text{erf} \frac{2}{3} \sqrt{\frac{32}{N_o} \frac{E}{F}} \right)$$

An average per letter error probability of $.602 \times 10^{-5}$ is required for a 4-letter alphabet in order to achieve an error probability of 10^{-4} per

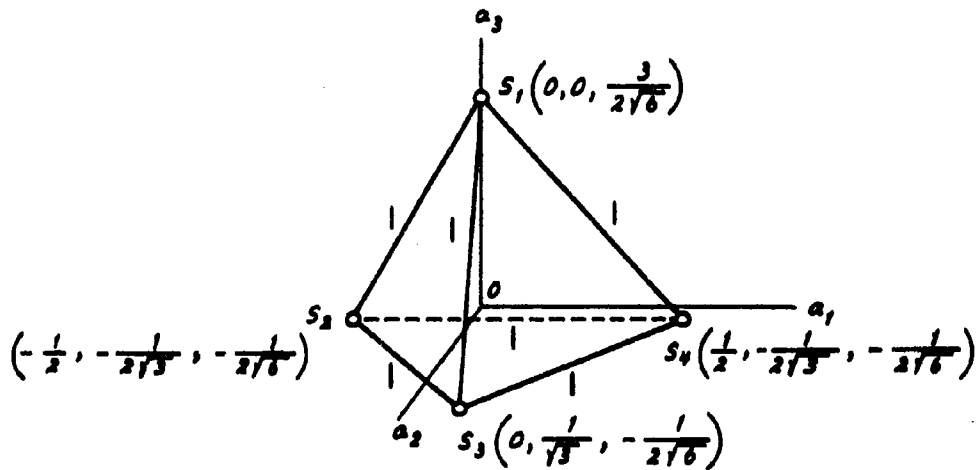


Figure 5 OPTIMUM SIGNALS IN THREE DIMENSIONAL SPACE FOR $M = 4$

ten-place decimal number. For 4-state CPSK, this is achieved at $\sqrt{\frac{E}{N_0}} = 4.611$. For this same value of $\sqrt{\frac{E}{N_0}}$, the average per letter error probability of the signals of Fig. 5 is $.052 \times 10^{-5}$, which is more than a factor of ten lower. The signals of Fig. 5 yield the point marked Δ on the efficiency graph of Fig. 3. It will be observed that, for the points plotted (i.e., an error probability $p = 10^{-4}$ per 10 digit decimal number) these signals are just about as efficient as the (4CSPSK). This observation is worthy of future investigation; in the meantime, it may be conjectured that as far as channel utilization is concerned, the lower error probability for a given E/N_0 is nearly balanced by the increase in dimensionality (i.e., bandwidth-time product) of these signals.

3 January 1961

REFERENCES

1. Davenport, W.B., Jr. and Root, W.L. An Introduction to the Theory of Random Signals and Noise Chapter 14 McGraw-Hill 1958
2. Woodward, P.M. Probability and Information Theory, with Applications to Radar McGraw-Hill 1953
3. Gilbert, E.N. A Comparison of Signalling Alphabets BSTJ, Vol. 31, pp. 504-22 May 1952
4. Becker, H.D. and Lawton, J.G. Theoretical Comparison of Binary Data Transmission Systems Cornell Aeronautical Laboratory Report No. CA-1172-S-1 May 1958
5. Cahn, C.R. Performance of Digital Phase-Modulation Communication Systems IRE Transactions on Communications Systems, Vol. CS-7, No. 1 May 1959
6. Turin, G.L. An Introduction to Matched Filters IRE Transactions on Information Theory, Vol. IT-6, No. 3 June 1960

3 January 1961

I(a) DETECT MEMO^{*} NO. 7A

Subject: "Error Probabilities for Coherent Pulsed Phase-shift Keyed Systems (CPPSKS) with Frequency and Sampling Time Errors."

By: Eugene A. Trabka

SUMMARY

The performance of two embodiments of the maximum likelihood receiver for CPPSK signals is investigated when the transmitted signals are subject to a frequency shift and the times at which the receiver outputs are sampled are in error. Expressions for the error probability are derived. It is found that in the presence of sampling time errors the "practical" receiver is to be preferred over the matched-filter receiver. It is shown how the "practical" receiver can be realized by so-called "integrate and dump" techniques.

INTRODUCTION

It was shown in Reference 1 that the "practical" receiver of Figure 1 was "equivalent" to the matched filter embodiment of the maximum likelihood receiver (Figure 2). This equivalence was established assuming that the physical components in each case were perfect and did not introduce errors. However, it is of interest to consider whether or not one of these receivers is superior in the respect that it is less sensitive to equipment errors. Two types of errors readily come to mind, viz., frequency errors and sampling time errors. (See Chapter II of this report for a discussion of the physical circumstances under which this analysis is applicable.)

The receiver input, $y(t)$, is assumed to consist of the sum of the signal, $s(t)$, and additive white Gaussian noise, $n(t)$, having a single-sided power spectral density of N_0 watts/cps, i.e.,

$$y(t) = s(t) + n(t) \quad (1)$$

* This is a revision of DETECT MEMO NO. 7 which was originally issued 21 November 1960.

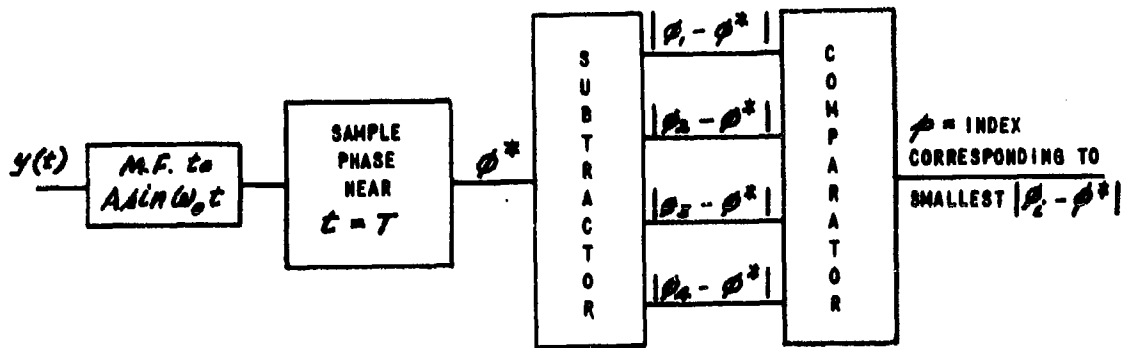


Figure 1 A "PRACTICAL" RECEIVER

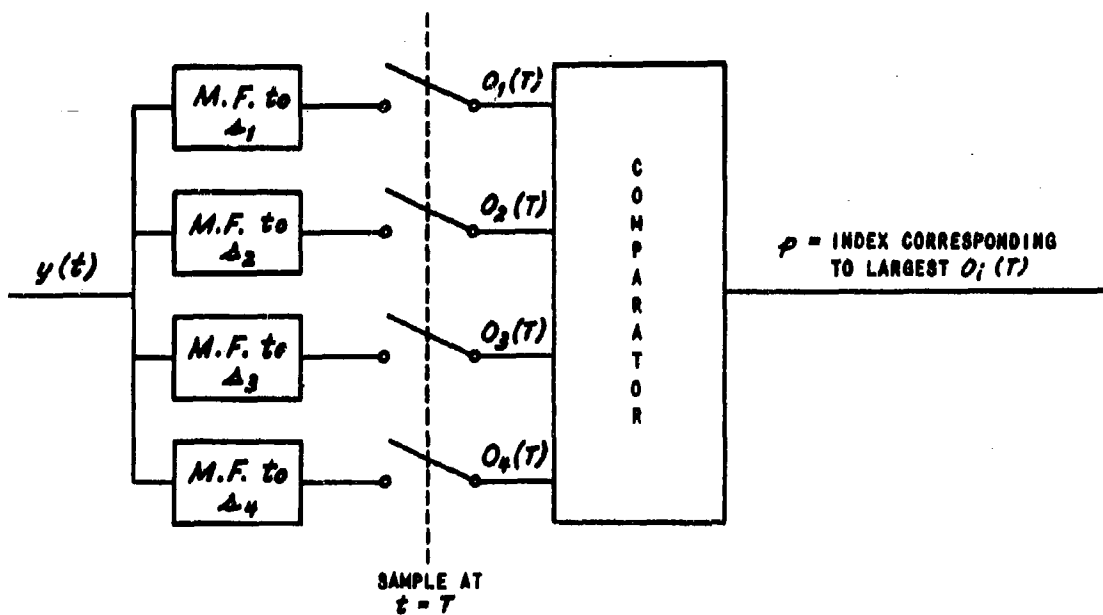


Figure 2 MATCHED FILTER EMBODIMENT OF MAXIMUM LIKELIHOOD RECEIVER

In order to describe the signal, $s(t)$, it is convenient to consider time to be divided into intervals having a duration T (duration of an elementary signal waveform). Introducing the unit rectangle function

$$u(t) = \begin{cases} 1 & ; 0 \leq t \leq T \\ 0 & ; t < 0, t > T \end{cases} \quad (2)$$

the received CPSK signal is assumed to be

$$s(t) = \sum_{k=-\infty}^{+\infty} u\left(\frac{t-kT}{T}\right) A \sin[(\omega_0 + \Delta\omega)(t-kT) + \phi_k] \quad (3)$$

where the transmitted information corresponds to the phase ϕ_k and the ϕ_k are assumed to be independently distributed from one interval to the next. During the k -th interval, ϕ_k may assume any one of the m values $* \frac{2\pi}{m}(i-1)$ where $i = 1, 2, \dots, m$ with probability $\frac{1}{m}$. The angular frequency error $\Delta\omega$ is assumed to be independent of k .

PRACTICAL RECEIVER

The filter in Figure 1 is assumed to be matched to zero transmitted phase ($i = 1$) at the frequency ω_0 so that its response to a unit impulse occurring at $t = 0$ is given by

$$h_i(t) = A u\left(\frac{t}{T}\right) \sin[\omega_0(T-t)] \quad (4)$$

and the filter output in response to $y(t)$ is given by

$$o_i(t) = \int_{-\infty}^{+\infty} y(\tau) h_i(t-\tau) d\tau \quad (5)$$

* The subscripts on ϕ in Figure 1 are used to note those m values that may be assumed during a particular baud interval. However, in the analysis to follow, ϕ_k is a random variable designating the transmitted phase in the k -th interval.

3 January 1961
DETECT MEMO NO. 7A
AF 30(602)-2210

which from (1) may be decomposed into

$$O_1(t) = g_1(t) + n_1(t) \quad (6)$$

where

$$\begin{aligned} g_1(t) &= \int_{-\infty}^{+\infty} a(\tau) h_1(t-\tau) d\tau \\ n_1(t) &= \int_{-\infty}^{+\infty} n(\tau) h_1(t-\tau) d\tau \end{aligned} \quad (7)$$

The variance σ^2 of $n_1(t)$ is readily shown to be

$$\sigma^2 = \frac{\pi N_0}{2} \quad (8)$$

and expressing $g_1(t)$ in the form

$$g_1(t) = R(t) \cos [\omega_0 t + \psi(t)] \quad (9)$$

the amplitude $R(t)$ and phase $\psi(t)$ are evaluated in Appendix B. From (6) and (9), one has

$$O_1(t) = R(t) \cos [\omega_0 t + \psi(t)] + n_1(t) \quad (10)$$

and (10) may be expressed in the form

$$O_1(t) = V(t) \cos [\omega_0 t + \phi^*(t)] \quad (11)$$

3 January 1961
DETECT MEMO NO. 7A
AF 30(602)-2210

It is recalled that for the case when $\psi(t) = 0$, it was shown in Reference 2 that the distribution of ϕ^* is given by

$$\rho(\phi^*) = \frac{1}{\pi} e^{-(\rho^2 - 2\rho\lambda \cos \phi^* + \lambda^2)} ; |\phi^*| \leq \pi \quad (12)$$
$$\rho(\phi^*) = 0 ; |\phi^*| > \pi$$

where

$$\lambda = \frac{R(t)}{\sqrt{2\sigma^2}} \quad (13)$$

The effect of $\psi(t) \neq 0$ is to shift the mean of the distribution of ϕ^* and writing

$$\psi(t) = \phi_0 + \epsilon(t) \quad (14)$$

the probability of error in an m -state system is given by

$$P(m) = 1 - \int_{-\frac{\pi}{m}}^{+\frac{\pi}{m}} \rho[\xi - \epsilon] d\xi \quad (15)$$

where the density $\rho[\cdot]$ is given by (12). (In Equation (15), the time dependence of $\epsilon(t)$ has been suppressed for convenience and the decision rule is apparent from the limits of integration.) Letting

$$\begin{aligned} u &= \rho \cos \xi \\ v &= \rho \sin \xi \end{aligned} \quad (16)$$

3 January 1961
 DETECT MEMO NO. 7A
 AF 30(602)-2210

one obtains

$$P(m) = 1 - \frac{1}{\pi} \int_0^{\infty} \left\{ \int_{-u \tan \frac{\pi}{m}}^{u \tan \frac{\pi}{m}} e^{-[u^2 + v^2 - 2\lambda(u \cos \epsilon + v \sin \epsilon + \lambda^2)]} dv \right\} du \quad (17)$$

For $m = 2$, (17) is readily evaluated by completing the square in the exponent and yields

$$P(2) = \frac{1}{2} [1 - \operatorname{erf}(\lambda \cos \epsilon)] \quad (18)$$

where λ and ϵ are to be evaluated at the sampling time $t = T + \Delta T$. In terms of the nondimensional parameters defined in Appendix B, viz.,

$$\begin{aligned} \alpha &= (\Delta f) T \\ \beta &= \frac{\Delta T}{T} \end{aligned} \quad (19)$$

and from (8), (13), (14), (18), (B13) or (B14) one obtains if $\beta = 0$ and $|\alpha| \leq \frac{1}{2}$

$$P(2) = \frac{1}{2} \left[1 - \operatorname{erf} \left\{ \frac{\sin 2\pi\alpha}{2\pi} \sqrt{\frac{\epsilon}{N_0}} \right\} \right] \quad (20)$$

and if $\alpha = 0$ and $|\beta| \leq \frac{1}{2}$

$$P(2) = \frac{1}{4} \left[1 - \operatorname{erf} \sqrt{\frac{\epsilon}{N_0}} \right] - \frac{1}{4} \left[1 - \operatorname{erf} \left\{ (1-2|\beta|) \sqrt{\frac{\epsilon}{N_0}} \right\} \right] \quad (21)$$

3 January 1961
DETECT MEMO NO. 7A
AF 30(602)-2210

where (21) is also obtained if only first order terms in the series expansion of $P(2)$ are retained for small $|\alpha|$ and $|\beta|$.

MATCHED FILTER RECEIVER ($m = 2$)

For $m = 2$ the matched filter receiver of Figure 2 utilizes two filters with impulse responses to a unit impulse occurring at $t = 0$ given by

$$\begin{aligned} h_1(t) &= A \pi \left(\frac{t}{T}\right) \sin [\omega_0(T-t)] \\ h_2(t) &= -h_1(t) \end{aligned} \quad (22)$$

Consequently, for their respective outputs in response to $y(t)$ one has

$$o_2(t) = -o_1(t) \quad (23)$$

where from (6)

$$o_1(t) = g_1(t) + n_1(t) \quad (24)$$

and assuming zero transmitted phase in the interval $0 \leq t \leq T$, the probability of error is given by

$$P(2) = Prob \{ o_1 < o_2 \} = Prob \{ o_1 < 0 \} \quad (25)$$

Since o_1 is Gaussian with mean q_1 given by (9) and σ^2 given by (8), it is easily shown that

$$P(2) = \frac{1}{2} \left(1 - e^{-\frac{q_1}{\sqrt{2\sigma^2}}} \right) \quad (26)$$

3 January 1961
 DETECT MEMO NO. 7A
 AF 30(602)-2210

where q_1 is to be evaluated at the sampling time $t = T + \Delta T$. Assuming that $\omega_0 T = 2\pi \cdot (\text{an integer})$, one obtains from (8), (9), (26), (B13) or (B14) if $\beta = 0$ and $|\alpha| \leq \frac{1}{2}$

$$P(2) = \frac{1}{2} \left[1 - \operatorname{erf} \left\{ \frac{\sin 2\pi\alpha}{2\pi\alpha} \sqrt{\frac{E}{N_0}} \right\} \right] \quad (27)$$

which is seen to be identical with the error probability (20) obtained for the "practical" receiver under these conditions. If $\alpha = 0$ and $|\beta| \leq \frac{1}{2}$

$$\begin{aligned} P(2) &= \frac{1}{4} \left[1 - \operatorname{erf} \eta_1 \sqrt{\frac{E}{N_0}} \right] + \frac{1}{4} \left[1 - \operatorname{erf} \eta_2 \sqrt{\frac{E}{N_0}} \right] \\ \eta_1 &= \cos 2\pi\gamma \\ \eta_2 &= (1 - 2|\beta|) \cos 2\pi\gamma \end{aligned} \quad (28)$$

where $\gamma = f_0(\Delta T)$ and f_0 is the frequency corresponding to ω_0 , so that (28) is seen to differ from the error probability (21) obtained for the "practical" receiver under these conditions.

If only first-order terms of the series expansion of (26) are retained for small $|\alpha|$ and $|\beta|$, one obtains

$$\begin{aligned} P(2) &= \frac{1}{4} \left[1 - \operatorname{erf} \eta_3 \sqrt{\frac{E}{N_0}} \right] + \frac{1}{4} \left[1 - \operatorname{erf} \eta_4 \sqrt{\frac{E}{N_0}} \right] \\ \eta_3 &= \cos(2\pi\gamma + \alpha\pi) \\ \eta_4 &= (1 - 2|\beta|) \cos(2\pi\gamma + \alpha\pi) \end{aligned} \quad (29)$$

which is also seen to differ from the error probability (21) obtained for the "practical" receiver.

PRACTICAL VS. MATCHED FILTER RECEIVER

Comparing (27) with (20), (28) with (21), and (29) with (21), it is found that the two receivers are equivalent if $\Delta T = 0$, but if $\Delta T \neq 0$, they are equivalent only for a set of measure zero, namely, those values of ΔT for which $f_0(\Delta T) = \gamma = \text{an integer}$. Because of the rapid variation of the error probability of the matched filter receiver in the presence of sampling time errors, the "practical receiver" is to be preferred. That the sensitivity of these receivers to timing errors differs is also apparent from a phasor diagram representation of their operation.

REALIZATION OF PRACTICAL RECEIVER

The "practical receiver" is easily realized by integrate and dump techniques which employ linear time-varying filters. The box labeled "M.F. to $A \sin \omega_0 t$ " in Figure 1 may be replaced by the lossless parallel L.C. circuit and switches of Figure 3. In this Figure, ρ and γ denote an initial current and an initial voltage respectively.

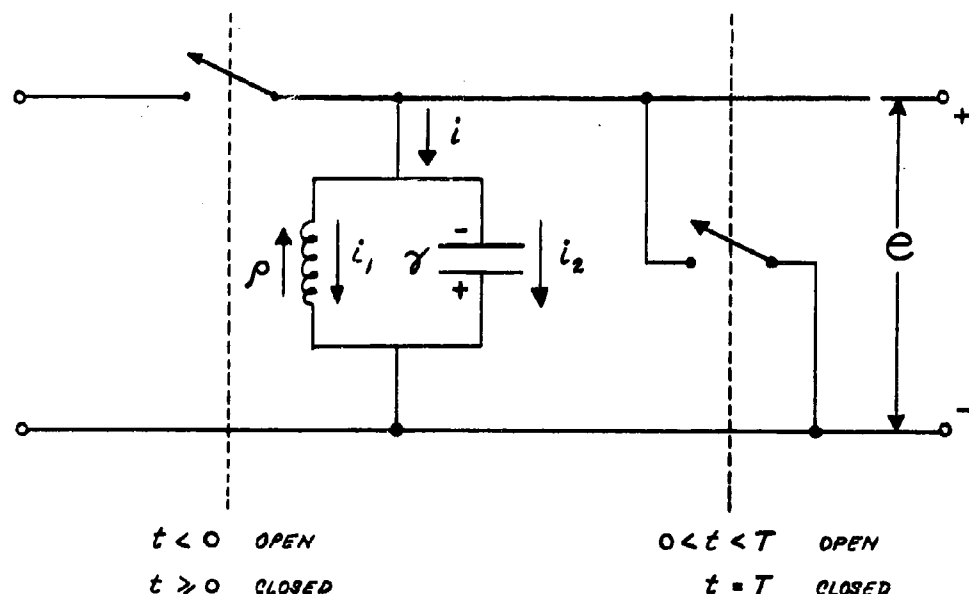


Figure 3
 Integrate and Dump Filter

3 January 1961
DETECT MEMO No. 7A
AF 30(602)-2210

The circuit equations are

$$\begin{aligned} i &= i_1 + i_2 \\ e &= L \frac{di}{dt} \\ e &= \frac{1}{C} \int i_2 dt \end{aligned} \tag{30}$$

which have Laplace transforms

$$\begin{aligned} \hat{i} &= \hat{i}_1 + \hat{i}_2 \\ \hat{e} &= L s \hat{i}_1 + L \rho \\ \hat{e} &= \frac{1}{C} \hat{i}_2 - \frac{\rho}{s} \end{aligned} \tag{31}$$

and solving for \hat{e} one obtains

$$\hat{e} = \frac{\frac{1}{C} s \hat{i}_2 - s \tau + \rho}{s^2 + \omega_0^2} \tag{32}$$

where LC is chosen such that $\omega_0^2 = \frac{1}{LC}$. If at $t = 0$, $\rho = \tau = 0$ then

$$\hat{e} = \frac{1}{C} \frac{s}{s^2 + \omega_0^2} \hat{i} \tag{33}$$

and the response to a unit impulse occurring at $t = 0$ (taking account of the operation of the switches in Figure 3) is

$$h(t) = u\left(\frac{t}{T}\right) A \cos \omega_0 t \tag{34}$$

3 January 1961
DETECT MEMO NO. 7A
AF 30(602)-2210

where C has been chosen such that $A = \frac{1}{C}$. Now, the filter matched to $A \sin \omega_0 t$ has impulse response

$$h_r(t) = u\left(\frac{t}{T}\right) A \sin \omega_0 (T-t) \quad (35)$$

so that (34) and (35) are identical if $\omega_0 T = \frac{\pi}{2} \pm k 2\pi$ where k is any integer. If this is not the case, the difference between (34) and (35) results only in a phase shift as will be shown. Using complex notation as in Appendix B (see B1), one finds for the respective complex modulation functions that

$$H(t) = H_r(t) e^{i(\omega_0 T - \frac{\pi}{2})} \quad (36)$$

so that the outputs differ only by a constant phase angle $\omega_0 T - \frac{\pi}{2}$ which may be biased out in the measurement process.

The measurement of the phase of the output of the matched filter of the receiver in Figure 3 is to be performed near $t = T$. If $\omega_0 T \gg 2\pi$ so that each signal interval contains many cycles, then a phase detector which performs a phase measurement during an interval not exceeding one cycle is satisfactory. Such a phase measurement may, for instance, be obtained from a measurement of the time delay between a positive zero crossing of a reference (zero phase) signal and the next positive zero crossing of the output of the matched filter.

3 January 1961
DETECT MEMO NO. 7A
AF 30(602)-2210

REFERENCES

1. Trabka, Eugene A., Embodiments of the Maximum Likelihood Receiver for Detection of Coherent Phase Shift Keyed Signals DETECT MEMO NO. 5A Cornell Aeronautical Laboratory January 3, 1961.
2. Fleck, John T. and Trabka, Eugene A., Error Probabilities of Multiple-State Differentially Coherent Phase Shift Keyed Systems in the Presence of White, Gaussian Noise DETECT MEMO NO. 2A Cornell Aeronautical Laboratory January 3, 1961.
3. Nuttall, Albert H., Technical Note on Pulse Compression and Coded Waveform Techniques Melpar, Inc. March 15, 1959 ASTIA Document No. AD 219116.

3 January 1961
DETECT MEMO NO. 7A
AF 30(602)-2210

APPENDIX A

Complex Notation for the Output of a Linear Filter

The purpose of this Appendix is to introduce the representation of real signals by complex functions of time. For a more detailed account, including proofs of the results which are here only stated, the interested reader is urged to consult the excellent Appendices of Reference 3.

Let $U(f)$ be the Fourier Transform (spectrum) of a real function $u(t)$. If one considers an operation which shifts the spectrum by an amount Δf yielding $U(f - \Delta f)$, then it is a simple exercise to show that the time function corresponding to the shifted spectrum is given by $u(t) e^{i 2\pi \Delta f t}$ which is a complex function of time. Thus, if one tries to exploit this simple transformation rule, one is ultimately led to consider complex signals. One may as well introduce complex signals at the outset. By writing

$$u(t) = \Re \{ u_c(t) \} \quad (A1)$$

where

$$u_c(t) = u(t) + i \hat{u}(t) \quad (A2)$$

and choosing the imaginary part $\hat{u}(t)$ to be the Hilbert Transform of $u(t)$, the spectrum of the complex signal is the same as that which would be obtained by suppressing the negative frequencies of $U(f)$ and doubling the magnitudes of the positive ones.

Now, if a real signal, $s(t)$, is the input to a linear filter with impulse response $h(t)$, then it is well known that the output of the filter, $q(t)$, is given by

$$q(t) = \int_{-\infty}^{+\infty} s(x) h(t-x) dx \quad (A3)$$

3 January 1961
 DETECT MEMO NO. 7A
 AF 30(602)-2210

It can be shown that in terms of the corresponding complex signals, the analogous relationship is

$$g(t) = \Re \{ g_c(t) \}$$

$$g_c(t) = \frac{1}{2} \int_{-\infty}^{+\infty} s_c(x) h_c(t-x) dx \quad (A4)$$

If $s(t)$ and $h(t)$ are narrow band time functions, it is customary to write*

$$s_c(t) = S(t) e^{i\omega_s t}$$

$$h_c(t) = H(t) e^{i\omega_h t} \quad (A5)$$

where $S(t)$ and $H(t)$ are low-pass modulation functions (not necessarily real) and ω_s is taken to be the carrier of $s(t)$ and ω_h , the center frequency of the filter. Substituting (A5) into (A4), it is possible to express $g_c(t)$ in the form

$$g_c(t) = Q(t) e^{i\omega_h t} \quad (A6)$$

where the modulation $Q(t)$ of the output is given by

$$Q(t) = \frac{1}{2} \int_{-\infty}^{+\infty} s(x) H(t-x) e^{i(\omega_s - \omega_h)x} dx \quad (A7)$$

*Recall that $e^{ix} = \cos x + i \sin x$ and it can be shown that the Hilbert Transform of $\cos x$ is $\sin x$.

3 January 1961
DETECT MEMO NO. 7A
AF 30(602)-2210

and the magnitude (amplitude) and argument (phase) of $Q(t)$ considered as a complex number are ordinarily the desired quantities.

A particular case of interest arises when $\omega_s = \omega_0 + \Delta\omega$ and $\omega_h = \omega_0$. Under these circumstances

$$Q(t) = \frac{1}{2} \int_{-\infty}^{+\infty} S(x) H(t-x) e^{i\Delta\omega x} dx \quad (A8)$$

APPENDIX B

Determination of the Amplitude and Phase of Filter Output

The amplitude $R(t)$ and phase $\psi(t)$ in (9) are respectively the magnitude and argument of the complex modulation function $Q_1(t)$ as described in Appendix A. Writing

$$h_1(t) = \Re \left\{ H_1(t) e^{i\omega_0 t} \right\}$$

$$s(t) = \Re \left\{ S(t) e^{i(\omega_0 + \Delta\omega)t} \right\} \quad (B1)$$

where

$$H_1(t) = u\left(\frac{t}{T}\right) A e^{i\left(\frac{\pi}{2} - \omega_0 T\right)} \quad (B2)$$

$$S(t) = \sum_{k=-\infty}^{+\infty} u\left(\frac{t-kT}{T}\right) A e^{i[\theta_k - kT(\omega_0 + \Delta\omega) - \frac{\pi}{2}]}$$

then from (A8) one has

$$Q_1(t) = \frac{A^2}{2} e^{-i\omega_0 T} \int_{t-T}^t e^{i\Delta\omega x} \sum_{k=-\infty}^{+\infty} u\left(\frac{x-kT}{T}\right) e^{i[\theta_k - kT(\omega_0 + \Delta\omega)]} dx \quad (B3)$$

Expanding (B3) at $t = T + \Delta T$ under the restriction that $|\Delta T| < T$, one

3 January 1961
 DETECT MEMO NO. 7A
 AF 30(602)-2210

obtains

$$Q_1(T+\Delta T) = \frac{A^2}{2} e^{i(\phi_0 - \omega_0 T)} \left\{ \int_0^{T+\Delta T} e^{i\Delta\omega x} dx + e^{i(\phi_1 - \phi_0)} e^{-i\tau(\omega_0 + \Delta\omega)} \int_{\Delta T}^{\infty} e^{i\Delta\omega x} dx \right\}; \quad \text{if } \Delta T \leq 0 \quad (\text{B4})$$

and

$$Q_1(T+\Delta T) = \frac{A^2}{2} e^{i(\phi_0 - \omega_0 T)} \left\{ \int_{\Delta T}^T e^{i\Delta\omega x} dx + e^{i(\phi_1 - \phi_0)} e^{-i\tau(\omega_0 + \Delta\omega)} \int_T^{T+\Delta T} e^{i\Delta\omega x} dx \right\}; \quad \text{if } \Delta T \geq 0 \quad (\text{B5})$$

In order to simplify the expressions (B4) and (B5), it is convenient to assume that $\omega_0 T = 2\pi f_0 T = 2\pi n$ where n is a positive integer. Letting $E = \frac{1}{2} A^2 T$ and

$$\frac{\Delta T}{T} = \beta$$

$$\Delta f = \frac{\alpha}{T} \quad (\text{B6})$$

where $\Delta\omega = 2\pi\Delta f$, then

$$Q_1(T+\Delta T) = E e^{i\phi_0} \left\{ \int_0^{\beta} e^{i2\pi\alpha y} dy + e^{i(\phi_1 - \phi_0)} e^{i2\pi\alpha} \int_{\beta}^{\infty} e^{i2\pi\alpha y} dy \right\}; \quad \text{if } \beta \leq 0 \quad (\text{B7})$$

3 January 1961
 DETECT MEMO NO. 7A
 AF 30(602)-2210

and

$$Q_1(\tau + \Delta\tau) = E e^{i\phi_0} \left\{ \int_{-\alpha}^{\beta} e^{i2\pi\alpha y} dy + e^{i(\phi_0 - \phi)} e^{-i2\pi\alpha} \int_{-\beta}^{1+\beta} e^{i2\pi\alpha y} dy \right\} \quad (B8)$$

if $\beta \geq 0$

where ΔT has been restricted so that $|\beta| < 1$. Performing the indicated integrations for binary systems ($\phi_k = 0$ or π), one finds

$$Q_1(\tau + \Delta\tau) = E \frac{\sin \alpha \pi}{\alpha \pi} Z(\alpha, \beta) e^{i(\phi_0 + \alpha \pi)} \quad (B9)$$

where $Z(\alpha, \beta)$ depends on whether or not there is a phase change between adjacent intervals. It is found that

$$Z(\alpha, \beta) = 1 \quad \text{no phase change}$$

$$Z(\alpha, \beta) = \frac{2e^{i2\pi\alpha(1+\beta)} - e^{i2\pi\alpha}}{e^{i2\pi\alpha} - 1} \quad (B10)$$

phase change and $\beta \leq 0$.

$$Z(\alpha, \beta) = \frac{1 + e^{i2\pi\alpha} - 2e^{i2\pi\alpha\beta}}{e^{i2\pi\alpha} - 1} \quad \text{phase change and } \beta \geq 0$$

For both α and β near zero, expansion of $Z(\alpha, \beta)$ by letting

$$e^{i\chi} \approx 1 + i\chi \quad (B11)$$

3 January 1961
 DETECT MEMO NO. 7A
 AF 30(602)-2210

yields in the case of a phase change

$$\Xi(\alpha, \beta) \approx 1 - 2|\beta| \quad (B12)$$

which is also an exact result when $\alpha = 0$ as may be ascertained directly from (B7) and (B8). Therefore, for α and β sufficiently small, retaining only first-order terms yields

$$\psi(\tau + \Delta\tau) = \phi_0 + \alpha \pi$$

$$R(\tau + \Delta\tau) = \begin{cases} \epsilon & \text{no phase change} \\ \epsilon(1 - 2|\beta|) & \text{phase change} \end{cases} \quad (B13)$$

The above expressions are exact when $\alpha = 0$ and $|\beta| \leq \frac{1}{2}$. When $\beta = 0$ and $|\alpha| \leq \frac{1}{2}$ the exact expressions are

$$\psi(\tau + \Delta\tau) = \phi_0 + \alpha \pi \quad (B14)$$

$$R(\tau + \Delta\tau) = \epsilon \frac{\sin \alpha \pi}{\alpha \pi}$$

3 January 1961

I(e) DETECT MEMO NO. 8A

Subject: "Error Probability in a Binary Coherent Pulsed Phase Shift Keyed System (BCPPSKS) with Crosstalk from Adjacent Multiplexed Channels"

By: Eugene A. Trabka

SUMMARY

The error probability in a BCPPSKS channel is derived in the presence of crosstalk from adjacent frequency multiplexed channels. The crosstalk is considered to arise from a frequency error of the received signals. Error probability curves are plotted in Figure 2 for various values of frequency error.

INTRODUCTION

Assume that in a BCPPSKS the signals that it is desired to transmit are given by

$$s_o(t) = u\left(\frac{t}{T}\right) A \sin [\omega_0 t + \phi_0] \quad (1)$$

where ϕ_0 is equal to 0 or π each with probability $\frac{1}{2}$ and $u\left(\frac{t}{T}\right)$ is the unit rectangle function defined to be 1 for $0 \leq t \leq T$, and zero elsewhere. Let the decision as to which signal was actually transmitted be made by the practical embodiment of the maximum likelihood receiver as shown in Figure 1. (The conditions under which the performance of this receiver is equivalent to the matched filter embodiment of the maximum likelihood receiver were analyzed in References 1 and 2.) It is well known that several such channels may be frequency-multiplexed without impairing the theoretical performance of the individual unmultiplexed channels provided that the separation of their carrier frequencies is an integral multiple of $\frac{1}{T}$. This result follows

*This is a revision of DETECT MEMO NO. 8 which was originally issued 30 November 1960.

3 January 1961
 DETECT MEMO NO. 8A
 AF 30(602)-2210

from the fact that the crosstalk (component of the filter output in a particular channel due to the signal in another channel) is zero at the proper sampling time. The purpose of the present analysis is to determine the effect on a particular channel of the crosstalk at the proper sampling time caused by a frequency error in the incoming signal.

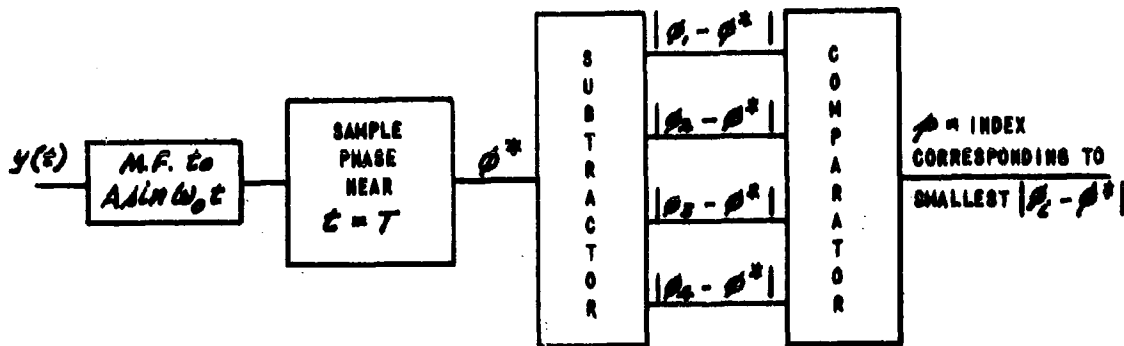


Figure 1 A "PRACTICAL" RECEIVER

Three channels indexed by k are considered so that the input to the receiver, $y(t)$, during one signal interval is given by

$$y(t) = s(t) + n(t)$$

$$s(t) = \sum_{k=-1}^{+1} u\left(\frac{t}{T}\right) A \sin [(\omega_k + \Delta \omega)t + \phi_k] \quad (2)$$

where $n(t)$ is a member of an ensemble of white Gaussian noise with spectral density N_0 watts/cps. It will further be assumed that

$$\begin{aligned} \omega_{-1} &= \omega_0 - \frac{2\pi}{T} \\ \omega_{+1} &= \omega_0 + \frac{2\pi}{T} \end{aligned} \quad (3)$$

3 January 1961
 DETECT MEMO NO. 8A
 AF 30(602)-2210

and letting $\Delta\omega = 2\pi\Delta f$, the frequency error Δf is measured in fractions of $\frac{1}{T}$, viz.

$$\Delta f = \frac{\alpha}{T} ; |\alpha| \leq \frac{1}{2} \quad (4)$$

The transmitted phases ϕ_k are assumed to be independent random variables.* The error probability of the zeroth channel whose receiving filter has impulse response

$$h_0(t) = u(\frac{t}{T}) A \sin \omega_0(T-t) \quad (5)$$

will be derived.

CROSSTALK DETERMINATION

Decomposing the output of the filter defined by (5) into a signal and noise component one has

$$o(t) = g_0(t) + n_0(t)$$

$$g_0(t) = \int_{-\infty}^{+\infty} s(x) h_0(t-x) dx \quad (6)$$

$$n_0(t) = \int_{-\infty}^{+\infty} n_0(x) h_0(t-x) dx$$

and writing

$$g_0(t) = R(t) \cos(\omega_0 t + \psi(t)) \quad (7)$$

* The subscripts on ϕ in Figure 1 are used to note those permissible values of phase that may be assumed in a particular channel during a given baud interval. However, in the analysis which follows ϕ_k is a random variable designating the transmitted phase in the k-th channel.

3 January 1961
 DETECT MEMO NO. 8A
 AF 30(602)-2210

the amplitude $R(T)$ and phase $\psi(T)$ at $t = T$ may be determined (as shown in Appendix A of Reference 2) as respectively the magnitude and argument of

$$Q(t) = \frac{1}{2} \int_{-\infty}^{+\infty} S(\chi) H(T-\chi) e^{i\Delta\omega\chi} d\chi \quad (8)$$

where

$$\begin{aligned} S(t) &= \Re \left\{ s(t) e^{i(\omega_0 + \Delta\omega)t} \right\} \\ H(t) &= \Re \left\{ H(t) e^{i\omega_0 t} \right\} \end{aligned} \quad (9)$$

and from (2), (3), and (5) it can be determined that

$$\begin{aligned} S(t) &= A u\left(\frac{t}{T}\right) e^{i[\phi_0 - \frac{\pi}{2}]} \left\{ 1 + e^{i[\phi_0 - \phi_0 - \frac{2\pi}{T}t]} + e^{i[\phi_0 - \phi_0 + \frac{2\pi}{T}t]} \right\} \\ H(t) &= A u\left(\frac{t}{T}\right) e^{i\left[\frac{\pi}{2} - \omega_0 T\right]} \end{aligned} \quad (10)$$

Substituting (10) into (8), changing the variable of integration according to $\chi = Ty$, and letting $E = \frac{1}{2} A^2 T$ yields

$$\begin{aligned} Q(T) &= E e^{i[\phi_0 - \omega_0 T]} \int_0^1 e^{i2\pi\alpha y} \left\{ 1 + e^{i(\Delta\phi_0 - 2\pi y)} \right. \\ &\quad \left. + e^{i(\Delta\phi_0 + 2\pi y)} \right\} dy \end{aligned} \quad (11)$$

3 January 1961
 DETECT MEMO NO. 8A
 AF 30(602)-2210

where $\Delta\phi_{-1} = \phi_{-1} - \phi_0$ and $\Delta\phi_1 = \phi_1 - \phi_0$. Performing the integration indicated in (11) one obtains

$$Q(\tau) = E \frac{\sin \pi \alpha}{\pi \alpha} e^{i[\phi_0 + \pi \alpha - \omega_0 \tau]} \left\{ 1 + \right. \quad (12)$$

$$\left. \frac{e^{i\Delta\phi_{-1}(1+\frac{1}{\alpha})} + e^{i\Delta\phi_1(1-\frac{1}{\alpha})}}{1-(\frac{1}{\alpha})^2} \right\}$$

Since the only permissible values of $\Delta\phi_{-1}$ and $\Delta\phi_1$ are 0, $+\pi$, and $-\pi$, the second term in $\{ \}$ is real so that

$$\psi(\tau) = \phi_0 + \pi \alpha - \omega_0 \tau \quad (13)$$

and

$$R(\tau) = E \left[1 + \frac{\eta_k}{1-(\frac{1}{\alpha})^2} \right] \frac{\sin \pi \alpha}{\pi \alpha} \quad (k=1,2,3,4) \quad (14)$$

where η_k assumes the values, each with probability $\frac{1}{4}$,

$$\eta_1 = +2; \quad \eta_2 = -2; \quad \eta_3 = \frac{2}{\alpha}; \quad \eta_4 = -\frac{2}{\alpha} \quad (15)$$

Examining (13) it is found that the effect of the frequency error is to introduce an error

$$\epsilon = \alpha \pi \tau \quad (16)$$

3 January 1961
DETECT MEMO NO. 8A
AF 30(602)-2210

into the phase measurement (the term $\omega_0 T$ being a constant independent of transmitted phase may be biased out). Under these circumstances it was shown in Reference 2 that the probability of error is given by

$$P\{\text{error}/R(T)\} = \frac{1}{2} [1 - \text{erf}(\lambda \cos \theta)] \quad (17)$$

where

$$\lambda = \frac{R(T)}{\sqrt{2\sigma^2}} \quad (18)$$

and σ^2 , the variance of $n_o(t)$ as given by (6) is

$$\sigma^2 = \frac{EN_0}{2} \quad (19)$$

Consequently, the total error probability is given by

$$P(2) = \frac{1}{4} \sum_{k=1}^4 \frac{1}{2} \left[1 - \text{erf} \left\{ \sqrt{\frac{E}{N_0}} \left(1 + \frac{\eta_k}{1 - (\frac{1}{\alpha})^2} \right) \frac{\sin 2\pi\alpha}{2\pi\alpha} \right\} \right] \quad (20)$$

where the η_k are given by (15).

RESULTS

The error probabilities considered as functions of E/N_0 are plotted as the solid curves in Figure 2 for $\alpha = 0, .1, .2, .3, .4$ and $.5$. The dashed curves are the error probabilities that would result from corresponding frequency errors in the absence of the two adjacent multiplexed channels and were plotted from Equation (27) of Reference 2.

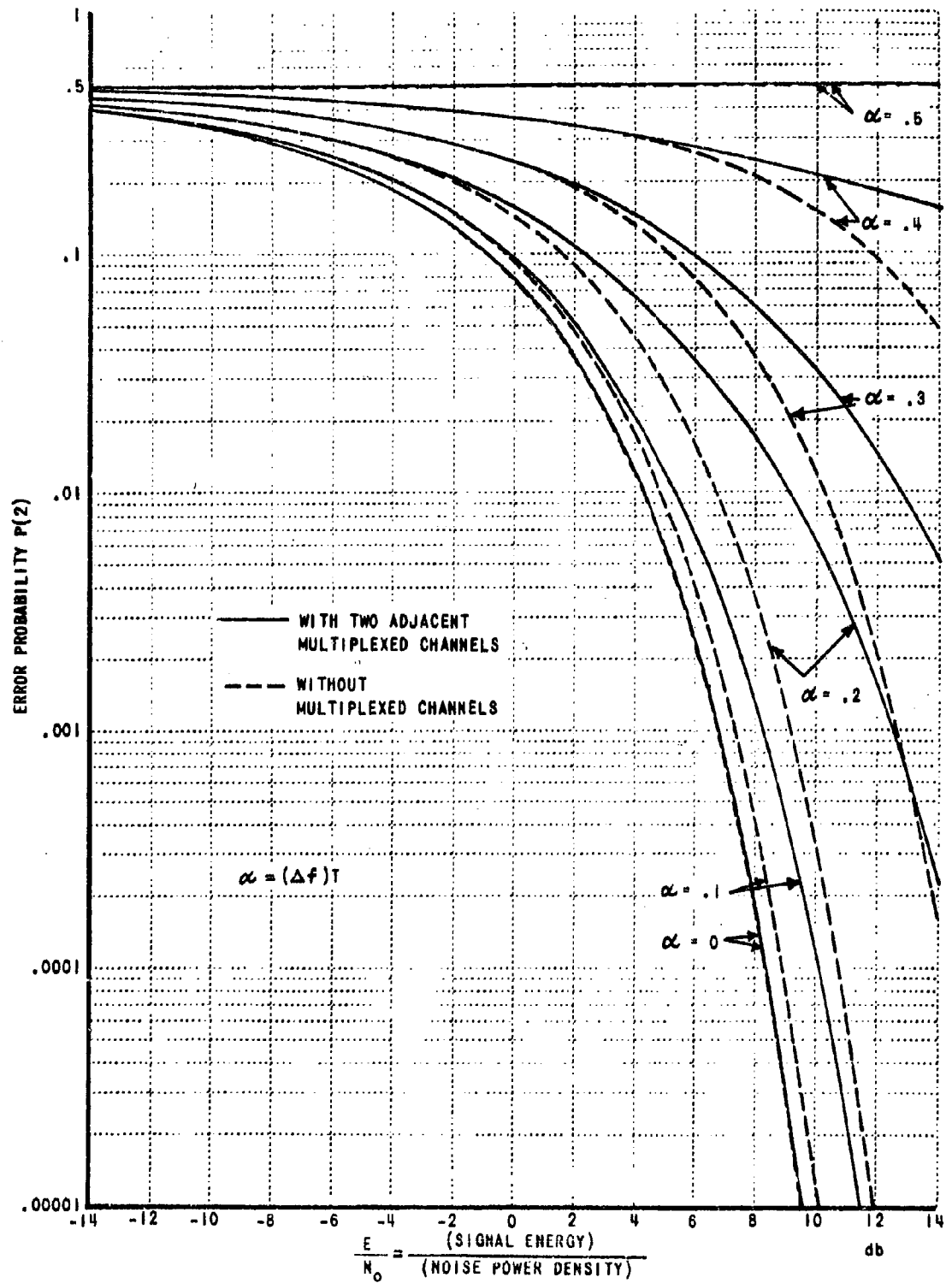


Figure 2 ERROR PROBABILITY OF A BCPPSKS WITH FREQUENCY ERROR

3 January 1961
DETECT MEMO NO. 8A
AF 30(602)-2210

REFERENCES

1. Trabka, Eugene A., Embodiments of the Maximum Likelihood Receiver for Detection of Coherent Phase Shift Keyed Signals DETECT MEMO NO. 5A Cornell Aeronautical Laboratory January 3, 1961.
2. Trabka, Eugene A. Error Probabilities for Coherent Phase Shift Keyed Systems (CPSKS) with Frequency and Sampling Time Errors DETECT MEMO NO. 7A Cornell Aeronautical Laboratory January 3, 1961.

7 December 1960

I(f) DETECT MEMO NO. 10

Subject: (a) "Double Bit Matched Filter (DBMF) Reception of Differentially Coherent Binary Phase Shift Keyed (DCBPSK) Signals."
(b) "The Equivalence of Integrate, Delay and Phase Comparison and DBMF Receivers for DCBPSK Systems."

By: John G. Lawton

SUMMARY

A new receiver concept for the reception of Differentially Coherent Binary Phase Shift Keyed signals is described. The operation of this receiver, called a Double Bit Matched Filter (DBMF) receiver, is compared with that of the Integrate, Delay and Phase Comparison receiver, which has been previously analyzed.⁽¹⁾ It is shown that the theoretical operation of both receivers is described by the same mathematical expression. It follows that these receivers will theoretically make identical decisions for all inputs and synchronization errors. The question as to which receiver is to be preferred in practice cannot be decided on theoretical grounds. Some of the sources for differences in performance between the above ideal receivers and practical receivers of the Integrate, Hold and Dump variety are pointed out.

DISCUSSION

The probability of error of a DCBPSK system operating in the presence of additive white Gaussian noise is given in Ref. (1) as

$$P_{e_{DCBPSK}} = \frac{1}{2} e^{-E/N_0}$$

(1a)

while that of a noncoherent binary FSK system is given as

$$P_e_{FSK} = \frac{1}{2} e^{-\frac{E}{2N_0}} \quad (1b)$$

where E ... Signal energy per received bit,
 No... Noise power density per cycle/sec. of one-sided spectrum.

Examination of the derivation of Equation (1b) in Reference (1) shows that while the analysis was performed with noncoherent FSK signals in mind, the analysis is not restricted to that particular form of modulation. The analysis can, in fact, be easily extended to include all noncoherent binary systems which use orthogonal ($\rho=0$) signals of equal energy. The question then arose whether the similarity of Equations (1a) and (1b) could be explained on this basis. This was found to be the case and a new receiver embodiment, which we will call a Double Bit Matched Filter (DBMF) receiver, naturally suggested itself.

The purposes of this memo are:

- 1) To describe the operation of the DBMF receiver.
- 2) To explain the connection between Equations (1a) and (1b).
- 3) To demonstrate the equivalence of the DBMF receiver, the Integrate, Delay and Phase Comparison receiver (which is based directly on the theory of DCPSK systems), and the commonly used Integrate, Hold and Dump receivers.

DBMF RECEIVER

Consider the waveforms transmitted during an interval of two-bit duration by a DCBPSK system. There are two sets of signals; in one, the phase of the second bit is the same as that of the first bit, and in the other there is a phase reversal. The different signals within each set can be differentiated only on the basis of absolute phase, which is assumed not available to the receiver. The receiver must decide at the end of every bit interval to which set the signal received during the previous two-bit intervals belongs.

It will be noted that adjacent decisions, which are made at the bit rate, are not independent since the two signals (each of two-bit interval duration) on which they are based are identical over a one-bit interval.

The four possible transmitted signals are described as

$$\left. \begin{array}{l} S_1(t) = \begin{cases} \sin \omega_0 t, & 0 < t < 2T \\ 0, & \text{elsewhere} \end{cases} \\ S_1'(t) = \begin{cases} -\sin \omega_0 t, & 0 < t < 2T \\ 0, & \text{elsewhere} \end{cases} \end{array} \right\} \text{Mark set} \quad (2)$$

$$\left. \begin{array}{l} S_2(t) = \begin{cases} \sin \omega_0 t, & 0 < t < T \\ -\sin \omega_0 t, & T \leq t < 2T \\ 0, & \text{elsewhere} \end{cases} \\ S_2'(t) = \begin{cases} -\sin \omega_0 t, & 0 < t < T \\ \sin \omega_0 t, & T \leq t < 2T \\ 0, & \text{elsewhere} \end{cases} \end{array} \right\} \text{Space set}$$

$$\omega_0 t = 2\pi n \quad \text{where } n \text{ is an integer.}$$

It will be noted that all signals contain equal energy and that the correlation coefficient of any signal in the Mark set with any signal in the Space set is zero.

In Differentially Coherent systems it is assumed that the possible received signals are known completely at the receiver except for phase; the phase is assumed a priori to be uniformly distributed, but to remain

fixed over adjacent bits. Under these assumptions,* the received signals may be described by

$$S_M(t) = \begin{cases} \sin(\omega_0 t + \psi), & 0 < t < 2T \\ 0, & \text{elsewhere} \end{cases}$$

$$S_S(t) = \begin{cases} \sin(\omega_0 t + \psi), & 0 < t < T \\ -\sin(\omega_0 t + \psi), & T \leq t < 2T \\ 0, & \text{elsewhere} \end{cases} \quad (3)$$

where ψ represents the unknown phase. Now $S_M(t)$ and $S_S(t)$ have all the properties required by the derivation of Equation (1b) carried out in Reference (1). Those properties are:

- (a) Correlation coefficient $\rho = 0$
- (b) Equal energy
- (c) Unknown phase assumed distributed uniformly

The analysis in Reference (1) shows that a receiver (sketched in Figure 1) consisting of two matched filters, envelope detectors, a comparator and synchronization circuitry, will perform in accordance with Equation (1b) in the presence of additive white Gaussian noise, where the energy E must now be taken as the signal energy during a two-bit interval as is discussed in the next paragraph.

* Although it is not the purpose of the current memo to investigate the validity of these assumptions, we point out that there are arguments to justify these assumptions in cases of practical interest. Also note that no claim is made that any of the receivers described are the best receivers to use under these assumptions. (For instance, the assumption that the phase remains constant over adjacent bits clearly implies that it remains constant for all time. In DCPSK operation, advantage is taken only of the invariance of phase over adjacent bits. It has not been shown that these receivers are optimum. However, in cases where the phase varies slowly, the approximation of constant phase over adjacent bits may be reasonable, while the assumption of constant phase is not.)

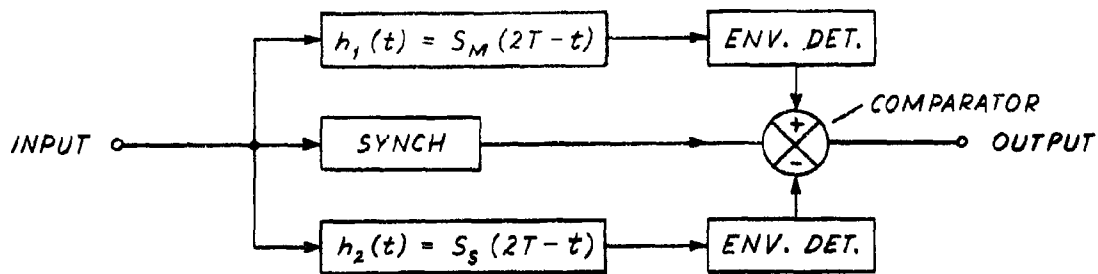


Figure 1

Block Diagram of DBMF Receiver

THE RELATION OF EQUATION (1a) TO EQUATION (1b)

In the derivation of Equations (1a) and (1b) carried through in Reference (1), E represents the signal energy per received bit. As has already been mentioned, Equation (1b) which was derived for noncoherent (wide band) FSK holds for all binary systems in which

- (a) the correlation coefficient between the two (sets of) signals is zero, $\rho = 0$
- (b) the signals have equal energy,
- (c) the phase of the received signal is unknown and (assumed) distributed uniformly,

provided that E is interpreted as the energy per received signal. In the case of wide band FSK, it happens that the energy per bit is equal to the energy per orthogonal signal element. In the case of DCBPSK, however, two-bit decisions are made per orthogonal signal element of duration $2T$. The energy per bit, E_b , is therefore one-half of the energy per signal E_s .

$E_s = 2E_b$ from which the relationship of Eqn. (1a) to Eqn. (1b) follows.

Thus

$$P_e = \frac{1}{2} e^{-\frac{E_s}{2N_0}} = \frac{1}{2} e^{-\frac{E_b}{N_0}} \quad (4)$$

THE EQUIVALENCE OF DBMF AND INTEGRATE,DELAY AND PHASE COMPARISON RECEIVERS

We will now show that the DBMF receiver and the Integrate,Delay and Phase Comparison receiver perform in formally equivalent ways.

The impulse response $h_1(t)$ of the filter in Figure 1, matched to the Mark set of signals is given by

$$h_1(t) = \begin{cases} \sin \omega_0 t, & 0 < t < 2T \\ 0, & \text{elsewhere} \end{cases} \quad (5a)$$

and the impulse response $h_2(t)$ of the filter matched to the Space set of signals is given by

$$h_2(t) = \begin{cases} +\sin \omega_0 t, & 0 < t < T \\ -\sin \omega_0 t, & T \leq t < 2T \\ 0, & \text{elsewhere} \end{cases} \quad (5b)$$

We now define a function $f(t)$ in terms of which both $h_1(t)$ and $h_2(t)$ may be conveniently expressed.

Let

$$f(t) = \begin{cases} \sin \omega_0 t, & 0 < t < T \\ 0, & \text{elsewhere} \end{cases} \quad (6)$$

then

$$h_1(t) = f(t) + f(t-T) \quad (7)$$

$$h_2(t) = f(t) - f(t-T)$$

The outputs of the two filters in response to an arbitrary input $i(t)$ are given by

$$\begin{aligned} \theta_1(t) &= \int_{-\infty}^{+\infty} i(\tau) h_1(t-\tau) d\tau \\ &= \int_{-\infty}^{+\infty} i(\tau) [f(t-\tau) + f(t-T-\tau)] d\tau \end{aligned} \quad (8a)$$

and

$$\begin{aligned}\theta_2(t) &= \int_{-\infty}^{+\infty} i(\tau) h_2(t-\tau) d\tau \\ &= \int_{-\infty}^{+\infty} i(\tau) [f(t-\tau) - f(t-\tau-\tau)] d\tau\end{aligned}\quad (8b)$$

It is always possible to find functions $A_1(t)$, $A_2(t)$, $\phi_1(t)$, $\phi_2(t)$, with $A_1(t), A_2(t) \geq 0$ such that

$$\int_{-\infty}^{+\infty} i(\tau) f(t-\tau) d\tau = A_1(t) \cos [\omega_0 t + \phi_1(t)] \quad (9a)$$

$$\int_{-\infty}^{+\infty} i(\tau) f(t-\tau-\tau) d\tau = A_2(t) \cos [\omega_0 t + \phi_2(t)] \quad (9b)$$

The functions $A_1(t)$, $A_2(t)$, $\phi_1(t)$, $\phi_2(t)$ are not uniquely defined by the left-hand side of (9a) and (9b). If the process is narrow band,^{*} as it will be in practice, then $A_1(t)$, $A_2(t)$ and $\phi_1(t)$, $\phi_2(t)$ can be so chosen that they may reasonably be described as the envelope and phase of these processes. We assume that this is the case.

The envelope detectors, Figure 1, produce the envelopes $E_1(t)$, $E_2(t)$ of the filter outputs $\theta_1(t)$ and $\theta_2(t)$.

$$E_1(t) = \left\{ A_1^2(t) + A_2^2(t) + 2A_1(t) A_2(t) \cos [\phi_1(t) - \phi_2(t)] \right\}^{1/2} \quad (10a)$$

$$E_2(t) = \left\{ A_1^2(t) + A_2^2(t) - 2A_1(t) A_2(t) \cos [\phi_1(t) - \phi_2(t)] \right\}^{1/2} \quad (10b)$$

* Note that narrow-bandedness is not a requisite for the formal argument.

The decision as to whether a signal from the Mark or Space set has been transmitted is made by comparing $E_1(2T)$ with $E_2(2T)$. If $E_1(2T) > E_2(2T)$, then it is decided that a Mark has been sent and vice versa. Since $A_1(t) \geq 0$, it is apparent from (10a) and (10b) that $E_1(2T) > E_2(2T)$ if and only if $|\phi_1(2T) - \phi_2(2T)| < \frac{\pi}{2}$.

We will now show that the Integrate, Delay and Phase Comparison receiver decides that a signal from the Mark set has been received when $|\phi_1(2T) - \phi_2(2T)| < \frac{\pi}{2}$ and otherwise decides that a signal from the space set has been received. It is seen that the DBMF and the Integrate, Delay and Phase Comparison receivers will make identical decisions for all inputs $i(t)$. Note that since these receivers make identical decisions for all inputs $i(t)$ their sensitivity to crosstalk due to frequency offset or synchronization errors is also identical.

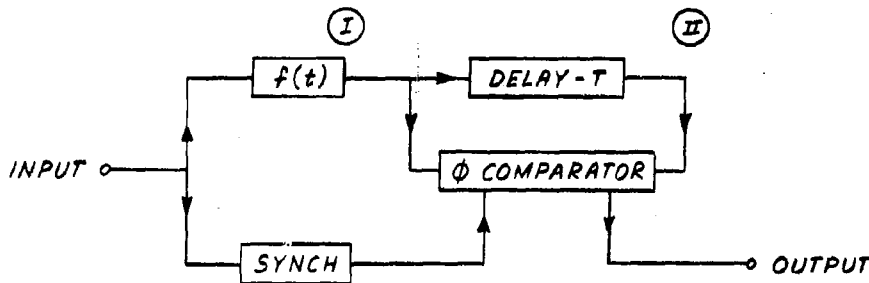


Figure 2
Block Diagram of Integrate, Delay and Phase Comparison Receiver

Figure 2 is a block diagram of the Integrate, Delay and Phase Comparison Receiver. The receiver contains one filter having impulse response

$$f(t) = \begin{cases} \sin \omega_0 t, & 0 < t < T \\ 0, & \text{elsewhere} \end{cases} \quad (11)$$

matched to the signal transmitted during one bit interval. The output of

this filter at point I is applied to one input of a phase comparator and to a delay circuit having a delay of one-bit duration T. The output of the delay circuit point II is applied to the other input of the phase comparator. The comparator makes decisions at intervals of T seconds, as controlled by the synchronization circuit. The decisions are based on whether the phase difference at the two inputs to the comparator exceed $\frac{\pi}{2}$ radians in absolute magnitude.

The output of the filter at point I in response to input $i(t)$

$$I(t) = \int_{-\infty}^{+\infty} i(\tau) f(t-\tau) d\tau \\ = A_1(t) \cos [\omega_0 t + \phi_1(t)] \quad (12)$$

and the output of the delay circuit at point II is

$$II(t) = \int_{-\infty}^{+\infty} i(\tau) f(t-T-\tau) d\tau \\ = A_2(t) \cos [\omega_0 t + \phi_2(t)] \quad (13)$$

The decisions are made on the basis of whether or not $|\phi_1(2T) - \phi_2(2T)|$ is greater than $\frac{\pi}{2}$ which was shown to be the criterion for the DBMF also.

It follows that if the performance of the synchronization circuits of the DBMF and the Integrate, Delay and Phase Comparison receivers are identical the two receivers will make identical decisions for all inputs.

The receivers actually used for the reception of differentially coherent signals at present are often of the Integrate, Hold and Dump type.⁽²⁾ These receivers use very simple filters, ideally a single lossless resonant circuit, the impulse response of which is

$$h(t) = \begin{cases} \sin \omega_0 t, & 0 < t \\ 0, & \text{elsewhere} \end{cases} \quad (14)$$

The required impulse response (11) is, in effect, obtained through the operation of properly synchronized switches to terminate $h(t)$ as given by (11). The delaying function is obtained by disconnecting the input and letting the resonant circuit ring at its natural frequency. A pair of such filters are needed, so that alternately one filter can be connected to the input (integrating) while the other delays (holds) the accumulated phase of the previous bit interval. The stored energy which is used to "remember" the previous phase must be discharged (dumped) before the signal may be connected to the filter.

From an analytic point of view, the major difference between the practical Integrate, Hold and Dump (IHAD) receiver and the theoretical DBMF and the Integrate, Delay and Phase Comparison receivers is that the latter two require only one input from the synchronization circuits, i.e., when to compare, whereas the former requires several, i.e., when to connect and disconnect the signal to the input of the filters, when to compare, and when to dump. From a practical point of view, it is clear that none of these operations can be performed in zero time.

REFERENCES

1. Becker, H. D., Lawton, J. G. Theoretical Comparison of Binary Data Transmission Systems Cornell Aeronautical Laboratory Report No. CA-11172-S-1 May 1958.
2. Mosier, R. A Data Transmission System Using Pulse Phase Modulation Convention Record of First National Convention on Military Electronics Washington, D. C. June 17-19, 1957.

3 January 1961

I(g) DETECT MEMO* NO. 2A

Subject: "Error Probabilities of Multiple-State Differentially Coherent Phase-shift Keyed Systems in the Presence of White, Gaussian Noise."

By: John T. Fleck and Eugene A. Trabka

SUMMARY

The character error probability in an m-state differentially coherent phase-shift keyed system (DCPSKS) is derived and plotted for various values of m in Figure 6. The subchannel error probability in a 4-state differentially coherent phase-shift keyed system is plotted in Figure 9. The analysis from which these curves were obtained includes formulae of more general interest relating to two vectors independently perturbed by Gaussian noise, viz., (a) an approximate formula for the probability that their phase difference (about the mean) exceeds a specified value as given by Equation (80) and (b) a tractable integral expression for the probability that their dot product is negative as given by Equation (137).

* This is a revision of DETECT MEMO NO. 2 which was originally issued 24 June 1960.

TABLE OF CONTENTS

	<u>PAGE NO.</u>
I. INTRODUCTION.	3
II. MULTIPLE-STATE DIFFERENTIALLY COHERENT PHASE-SHIFT KEYED SYSTEMS (DCPSKS)	
A. Mathematical Formulation	4
B. Distribution (About the Mean) of the Phase Difference Between Two Vectors of Equal Length Independently Perturbed by Gaussian Noise . . .	6
C. Error Probability in a Binary DCPSKS	13
D. Error Probabilities in a m-State DCPSKS.	15
E. An Approximate Formula for the Error Probabilities when $m > 2$	17
III. SUBCHANNEL ERROR PROBABILITY IN A 4-STATE DCPSKS	
A. Mathematical Formulation	24
B. Probability of a Negative Dot Product for Two Vectors Independently Perturbed by Gaussian Noise.	26
C. Calculation of Error Probability	37
IV. REFERENCES.	41
APPENDIX A Some Relationships Concerning the Special Functions Used in Analysis.	42
APPENDIX B Tables of $P_c(m)$ as Computed From Approximate Formula.	45
APPENDIX C Tables of $P_c(m)$ as Computed From Exact Formula	48

I. INTRODUCTION

A digital communications system in which the signal alphabet consists of m narrow band signals which differ only in the phases of the carrier is called an m -state phase-shift keyed system (PSK). At least two modes of operating phase-shift keyed systems have been considered; these are the coherent and the differentially coherent modes. With coherent phase-shift keying the information to be transmitted determines the phase of the transmitted signal carrier relative to an absolute reference; it follows that the receiver must also have access to an absolute phase reference in order to interpret the received signals. In a differentially coherent phase-shift keyed system (DCPSKS) the phase of the previously transmitted signal is used as the reference for the succeeding signal; the receiver uses the phase of the last received signal as a reference in interpreting the current signal. Although the error rates of coherent PSK systems are theoretically lower than those of differentially coherent PSK systems, the requirement for absolute phase references (i.e. phase lock between the transmitter and receiver references) is a serious disadvantage in practice. The error probabilities of binary ($m = 2$) DCPSKS in the presence of white Gaussian noise were obtained in Ref. 1. The present memo extends that analysis for arbitrary m . The coherent PSK mode for arbitrary m has been analysed by C. Gahn in Ref. (2).

II. MULTIPLE-STATE DIFFERENTIALLY COHERENT PHASE-SHIFT KEYED SYSTEMS (DCPSKS)

A. Mathematical Formulation

The signals (characters) of an m -state DCPSKS are shown represented vectorially in Fig. 1 for the case $m = 8$. The reference (preceding) signal is shown pointing vertically upward and the dotted lines represent decision thresholds for the detector.

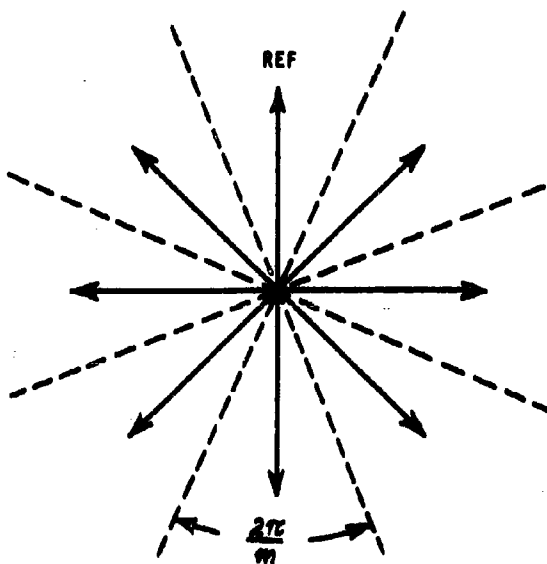


Figure 1

A block diagram which illustrates the operation of the receiving terminal of a DCPSKS to be analyzed is shown in Figure 2. The input to the matched filter consists of a sequence of non-overlapping pulsed signals, each of duration T , and the accompanying noise. It is assumed that the noise is white, Gaussian and has a single-sided power spectral density of

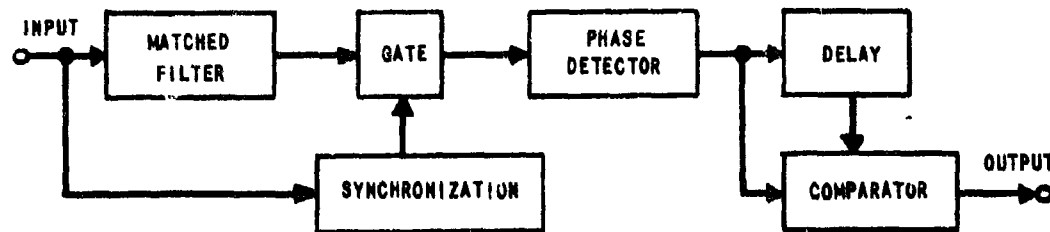


Figure 2

N_0 watts/cps over the pass band of the filter matched to the signal. It is well known, e.g. Ref. 1, that under the above conditions a matched filter* maximizes the ratio at its output of instantaneous signal power to average noise power and that the maximum value of this ratio is given by

$$\text{Max} \left\{ \frac{\text{instantaneous signal power}}{\text{average noise power}} \right\}_{\text{Output}} = \frac{2E}{N_0} \quad (1)$$

where E is the energy of the input signal. The synchronizing circuit passes the output of the matched filter to a phase detector at the instant when the ratio (1) attains its maximum. Let ϕ_i denote the transmitted phase of the i th signal and $\hat{\phi}_i$ the measured phase corresponding to ϕ_i . The measured phase $\hat{\phi}_i$ is applied to one input of the comparator and to a delay circuit. The other input to the comparator is the measured phase $\hat{\phi}_{i-1}$ of the previous signal pulse. The output of the comparator is the difference $\hat{\phi}_i - \hat{\phi}_{i-1}$. After a delay equal to a pulse period, $\hat{\phi}_i$, becomes available from the delay circuit for use as a reference for comparison with $\hat{\phi}_{i+1}$. The probability of error $P_e(m)$ is then the probability that the measured phase difference $\hat{\phi}_i - \hat{\phi}_{i-1}$, differs by more than π/m in absolute value from the phase difference of the transmitted signals $\phi_i - \phi_{i-1}$.

*A matched filter has an impulse response which is the time reversal of the signal. The entire June 1960 issue of the IRE TRANSACTIONS OF THE PGIT is devoted to a discussion of the properties and applications of matched filters.

Let $h(\alpha)$ denote the probability density about the mean of the measured phase difference between two successive received signals where $-7\pi \leq \alpha \leq +7\pi$. If one defines

$$H(\theta) = 1 - \int_{-\theta}^{+\theta} h(\alpha) d\alpha = 2 \int_{\theta}^{\pi} h(\alpha) d\alpha \quad (2)$$

then* the probability of a character error is given by

$$P_c(m) = H\left(\frac{\pi}{m}\right). \quad (3)$$

B. Distribution (About the Mean) of the Phase Difference Between Two Vectors of Equal Length Independently Perturbed by Gaussian Noise

The output of the matched filter in Figure 2, due to a particular input signal, may be represented by

$$y(t) = A(t) \cos \omega_0 t + n(t) \quad (4)$$

where the time origin has been chosen such that the transmitted signal has zero phase, $A(t)$ is the envelope of the response due to the signal component of the input, ω_0 the angular frequency of the transmitted signal, and $n(t)$ is a member of an ensemble of band-limited Gaussian noise with zero mean and total average power σ^2 . Substituting into (4), the band-limited representation

$$n(t) = n_c \cos \omega_0 t - n_s \sin \omega_0 t \quad (5)$$

where n_c, n_s are uncorrelated Gaussian random variables whose joint distribution is given by

$$p(n_c, n_s) = \frac{1}{2\pi\sigma^2} e^{-\frac{n_c^2 + n_s^2}{2\sigma^2}} \quad (6)$$

*The intermediate function H of the continuous variable θ is introduced to emphasize that $P_c(m)$ is a special case of a more general problem to which the analysis given in this report also applies.

one obtains

$$y(t) = (A + n_c) \cos \omega_0 t - n_s \sin \omega_0 t \quad (7)$$

Equation (7) may also be written in the form

$$y(t) = V \cos(\omega_0 t + \phi) \quad (8)$$

where V , ϕ are respectively the envelope and phase of the matched filter output. This is accomplished by means of the substitution

$$\begin{aligned} V \cos \phi &= A + n_c & 0 \leq V < \infty \\ V \sin \phi &= n_s & -\pi \leq \phi \leq +\pi \end{aligned} \quad (9)$$

From (6), taking into account the Jacobian of the transformation (9), one obtains the joint probability density of V and ϕ , viz.

$$p_2(V, \phi) = \frac{V}{2\pi\sigma^2} e^{-\frac{V^2}{2\sigma^2} [V^2 \sin^2 \phi + (V \cos \phi - A)^2]} \quad (10)$$

Transforming the variable V and parameter A according to

$$\begin{aligned} V &= \rho \sqrt{2\sigma^2} \\ A &= S \sqrt{2\sigma^2} \end{aligned} \quad (11)$$

there obtains the joint probability density

$$p_3(\rho, \phi) = \frac{\rho}{\pi} e^{-(\rho^2 - 2\rho s \cos \phi + s^2)} \quad (12)$$

and the probability density of ϕ may be obtained by integrating over ρ , i.e.

$$p_4(\phi) = \int_0^\infty p_3(\rho, \phi) d\rho ; \quad |\phi| \leq \pi .$$

$$p_4(\phi) = 0 ; \quad |\phi| > \pi$$

Consider the phase difference α defined by

$$\alpha = \phi_1 - \phi_2 \quad (14)$$

where ϕ_1 and ϕ_2 are the phases of successive received signals, and may be considered to be independent, each with a probability density given by (12). The probability density of α is given by the convolution

$$p_s(\alpha) = \int_{-\infty}^{+\infty} p_s(\phi) p_s(\phi + \alpha) d\phi \quad (15)$$

and taking into account the range of values where the integral in (15) is zero, one finds

$$p_s(\alpha) = \begin{cases} p_s(\phi) p_s(\phi + \alpha) d\phi & ; |\alpha| \leq 2\pi \\ 0 & ; |\alpha| > 2\pi \end{cases} \quad (16)$$

$$p_s(\alpha) = 0 ; \quad |\alpha| > 2\pi$$

Since α and $\alpha + 2\pi$ are effectively the same angle, it is convenient to introduce the density $h(\alpha)$ where

$$h(\alpha) = p_s(\alpha) + p_s(\alpha + 2\pi) ; \begin{cases} - \text{for } 0 \leq \alpha \leq \pi \\ + \text{for } -\pi \leq \alpha < 0 \end{cases} \quad (17)$$

$$h(\alpha) = 0 ; \quad |\alpha| > \pi$$

Now, considering only the case** when $0 \leq \alpha \leq \pi$, one has

$$p_s(\alpha) = \int_{-\pi}^{\pi} p_s(\phi) p_s(\phi + \alpha) d\phi \quad (18)$$

* It is assumed without loss of generality that zero phase change has been transmitted.

** The argument is similar for $-\pi \leq \alpha < 0$

and

$$p_s(\alpha - 2\pi) = \int_{\pi - \alpha}^{\pi} p_+(\phi) p_+(\phi + \alpha - 2\pi) d\phi \quad (19)$$

and for $0 \leq \alpha \leq \pi$ one may write

$$h(\alpha) = \int_{-\pi}^{\pi - \alpha} p_+(\phi) p_+(\phi + \alpha) d\phi + \int_{\pi - \alpha}^{\pi} p_+(\phi) p_+(\phi + \alpha - 2\pi) d\phi \quad (20)$$

In Figure 3, the heavier sections of the curves shown represent the densities $p_+(\phi)$ and $p_+(\phi + \alpha)$ as functions of ϕ for the case of a positive α . The lighter sections of these curves represent the periodic extensions of the respective densities. Reflecting upon Figure 3, one finds that if

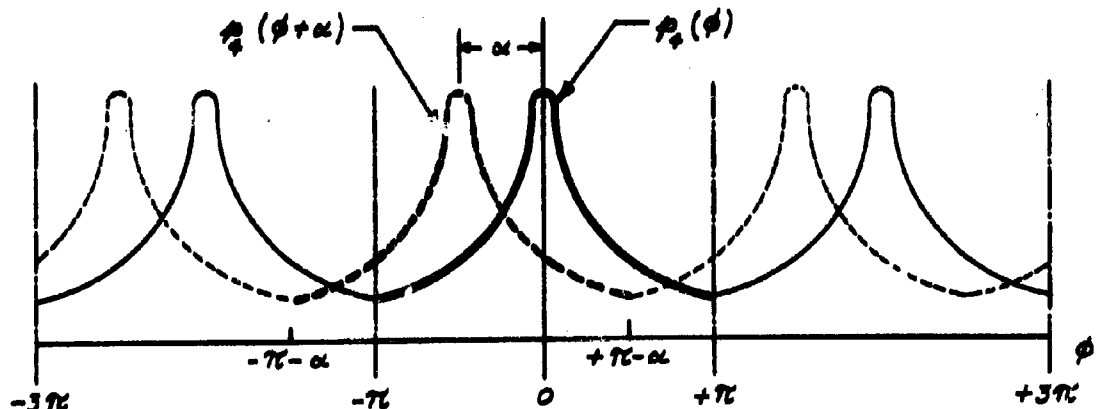


Figure 3

instead of (13), $p'_4(\phi)$ is defined as

$$p'_4(\phi) = \int_0^\infty p_4(r, \phi) dr \text{ for all } \phi \quad (21)$$

then, it is possible to express $h(\alpha)$ as given by (20) as

$$h(\alpha) = \int_{-\pi}^{\pi} p'_4(\phi) p'_4(\phi + \alpha) d\phi; |\alpha| \leq \pi \quad (22)$$

The expressions (22) and (21) are as yet purely formal. Using (22), (21) and (12) gives

$$h(\alpha) = \frac{1}{\pi^2} \int_{-\pi}^{\pi} d\phi \int_0^\infty dr \int_0^\infty r e^{-[\rho^2 - 2\rho s \cos \phi + s^2 + r^2 - 2rs \cos(\phi + \alpha) + \epsilon^2]} \quad (23)$$

and the integration with respect to ϕ is readily performed yielding

$$h(\alpha) = \frac{2}{\pi} \int_0^\infty dr \int_0^\infty r e^{-[\rho^2 + r^2 + 2s^2]} I_0(2s\sqrt{\rho^2 + r^2 + 2rs \cos \alpha}) \quad (24)$$

where $I_0(x)$ is the Bessel function of order zero and imaginary argument. (See Appendix A). Making the substitutions

$$\begin{aligned} \rho &= u \cos \beta \\ r &= u \sin \beta \end{aligned}; I_0(x) = \sum_{k=0}^{\infty} \frac{(x/2)^{2k}}{k! k!} \quad (25)$$

yields

$$\begin{aligned} h(\alpha) &= \frac{2}{\pi} \int_0^{\pi/2} d\beta \int_0^\infty du u^3 \sin \beta \cos \beta e^{-[u^2 + 2s^2]} \\ &\quad \sum_{k=0}^{\infty} \frac{s^{2k} u^{2k} (1 + \cos \alpha \sin 2\beta)^k}{k! k!} \end{aligned} \quad (26)$$

and since

$$\int_0^\infty u^{2k+3} e^{-u^2} du = \frac{(k+1)!}{2} \quad (27)$$

one obtains on performing the integration indicated in (26) with respect to u

$$h(\alpha) = \frac{1}{2\pi} \int_0^{\pi/2} d\beta \sin 2\beta e^{-S^2} \sum_{k=0}^{\infty} \frac{S^k (1 + \cos \alpha \sin 2\beta)^k (k+1)!}{k!} \quad (28)$$

Now, it is easily seen that

$$\sum_{k=0}^{\infty} \frac{(k+1)x^k}{k!} = \frac{d}{dx} (xe^x) = (1+x)e^x \quad (29)$$

so that (28) may be written as

$$h(\alpha) = \frac{1}{2\pi} \int_0^{\pi/2} \sin 2\beta \cdot [1 + S^2(1 + \cos \alpha \sin 2\beta)] e^{-S^2(1 - \cos \alpha \sin 2\beta)} d\beta \quad (30)$$

or letting

$$\begin{aligned} \psi &= 2\beta \\ R &= S^2 \end{aligned} \quad (31)$$

one finally obtains from the symmetry of $\sin \psi$ with respect to $\pi/2$

$$h(\alpha) = \frac{1}{2\pi} \int_0^{\pi/2} \sin \psi [1 + R(1 + \cos \alpha \sin \psi)] e^{-R(1 - \cos \alpha \sin \psi)} d\psi \quad (32)$$

where from (31), (11) and (1)

$$R = \frac{1}{2} \left(\frac{A^2}{\sigma^2} \right) = \frac{1}{2} \left(\frac{2E}{N_0} \right) = \frac{E}{N_0} \quad (33)$$

so that the parameter R in (32) is just the ratio of signal energy per pulse to the input noise power density.

From (32), it is obvious that

$$h(-\alpha) = h(\alpha) \quad (34)$$

which was anticipated intuitatively and used to simplify (2). Moreover, since $h(\alpha)$ is a probability density, it must satisfy

$$\int_{-\pi}^{\pi} h(\alpha) d\alpha = 1 \quad (35)$$

This relationship may be verified by using (32) in (35) and expanding (35) as the sum of two integrals

$$\int_{-\pi}^{\pi} h(\alpha) d\alpha = e^{-R}(1+R)I + e^{-R}RII \quad (36)$$

where

$$I = \frac{1}{2\pi} \int_{-\pi}^{\pi} d\alpha \int_0^{\pi/2} d\psi \sin \psi e^{R \cos \alpha \sin \psi} \quad (37)$$

and

$$II = \frac{1}{2\pi} \int_{-\pi}^{\pi} d\alpha \int_0^{\pi/2} d\psi \sin^2 \psi \cos \alpha e^{R \cos \alpha \sin \psi} \quad (38)$$

Performing the integration with respect to α first in (37) gives

$$I = \int_0^{\pi/2} \sin \psi I_0(R \sin \psi) d\psi \quad (39)$$

and using again the series representation of $I_n(x)$ given in (25) yields upon interchanging the order of summation and integration

$$I = \sum_{r=0}^{\infty} \frac{\left(\frac{R}{2}\right)^{2r}}{(r!)^2} \int_0^{\pi/2} \sin^{2r+1} \psi d\psi \quad (40)$$

and since

$$\int_0^{\pi/2} \sin^m \psi d\psi = \int_0^{\pi/2} \cos^m \psi d\psi = \frac{\sqrt{\pi}}{2} \cdot \frac{(\frac{m-1}{2})!}{(\frac{m}{2})!} \quad (41)$$

and

$$\left(r + \frac{1}{2}\right)! = \sqrt{\pi} \cdot \frac{(2r+1)!}{r! 2^{2r+1}} \quad (42)$$

finally,

$$I = \sum_{r=0}^{\infty} \frac{R^{2r}}{(2r+1)!} = \frac{1}{R} \sum_{r=0}^{\infty} \frac{R^{2r+1}}{(2r+1)!} = \frac{\sinh R}{R} \quad (43)$$

From inspection of (37) and (38), it is seen that

$$\frac{\partial I}{\partial R} = \Pi \quad (44)$$

hence, using (36), (43) and (44)

$$\int_{-\pi}^{+\pi} h(\alpha) d\alpha = e^{-R}(1+R) \frac{\sinh R}{R} + e^{-R} R \left(\frac{R \cosh R - \sinh R}{R^2} \right) = 1 \quad (45)$$

which shows that $h(\alpha)$ satisfies Eq. (35).

C. Error Probability in a Binary DCPSKS

The probability of error in a binary DCPSKS ($m=2$) is given by (3) and (2) as

$$P_e(2) = 1 - \int_{-\pi/2}^{+\pi/2} h(\alpha) d\alpha \quad (46)$$

Now, again using (32) in (46) and expanding the integral in (46) as the sum of two integrals, one obtains an expression similar to (36), viz.

$$\int_{-\pi/2}^{+\pi/2} h(\alpha) d\alpha = e^{-R^2} (1+R) III + e^{-R^2} R IV \quad (47)$$

where

$$III = \frac{1}{2\pi} \int_{-\pi/2}^{+\pi/2} d\alpha \int_0^{\pi/2} d\psi \sin \psi e^{R \cos \alpha \sin \psi} \quad (48)$$

and

$$IV = \frac{1}{2\pi} \int_{-\pi/2}^{+\pi/2} d\alpha \int_0^{\pi/2} d\psi \sin^2 \psi \cos \alpha e^{R \cos \alpha \sin \psi} \quad (49)$$

Performing the integration in (48) with respect to ψ first this time by expanding the exponential in the integrand in a power series and using (41) yields

$$III = \frac{1}{2\pi} \int_{-\pi/2}^{+\pi/2} \sum_{r=0}^{\infty} \frac{R^r \cos^r \alpha}{r!} \frac{\sqrt{\pi}}{2} - \frac{\left(\frac{r}{2}\right)!}{\left(\frac{r+1}{2}\right)!} d\alpha \quad (50)$$

and now integrating with respect to α and using (41) again gives

$$III = \frac{1}{2R} \sum_{n=0}^{\infty} \frac{R^{n+1}}{(n+1)!} = \frac{1}{2R} (e^R - 1). \quad (51)$$

and since also

$$\frac{\partial III}{\partial R} = IV \quad (52)$$

so that (47) reduces to

$$\int_{-\pi/2}^{+\pi/2} h(\alpha) d\alpha = e^{-R} (1+R) \frac{1}{2R} (e^R - 1) + e^{-R} R \left(\frac{Re^R - e^R + 1}{2R^2} \right) \quad (53)$$

$$= 1 - \frac{1}{2} e^{-R}$$

Substituting (53) into (46) and recalling (33), one obtains finally

$$P_c(2) = \frac{1}{2} e^{-\frac{E}{N_0}} \quad (54)$$

which is identical to the expression obtained previously by other means in References (1) and (2).

D. Error Probabilities in a m-State DCPSKS

The density $h(\alpha)$ as given by (32) was evaluated on the IBM 704 computer for values of $R = \frac{E}{N_0}$ from 0 to 30 db in steps of 2 db (including also +7, -7, -14 db). The numerical integration was performed using Simpson's Rule and gave $h(\alpha)$ every 5° for $90^\circ \leq \alpha \leq 180^\circ$ and every 1 for $0^\circ \leq \alpha \leq 90^\circ$. Some plots of $h(\alpha)$ are shown in Figure 4. The cumulative probability $H(\theta)$ as given by (2) was expressed as

$$H(\theta) = 2 \int_{\theta}^{\pi/2} h(\alpha) d\alpha + 2 \int_{\pi/2}^{\pi} h(\alpha) d\alpha \quad (55)$$

where the second integral in (55) may be evaluated using (35) and (53) to give

$$H(\theta) = 2 \int_{\theta}^{\pi/2} h(\alpha) d\alpha + \frac{1}{2} e^{-R} \quad (56)$$

*The value of $h(\alpha)$ at $\alpha = \frac{\pi}{2}$ is readily shown from (29) to be $h\left(\frac{\pi}{2}\right) = \frac{1+R}{2\pi} e^{-R}$

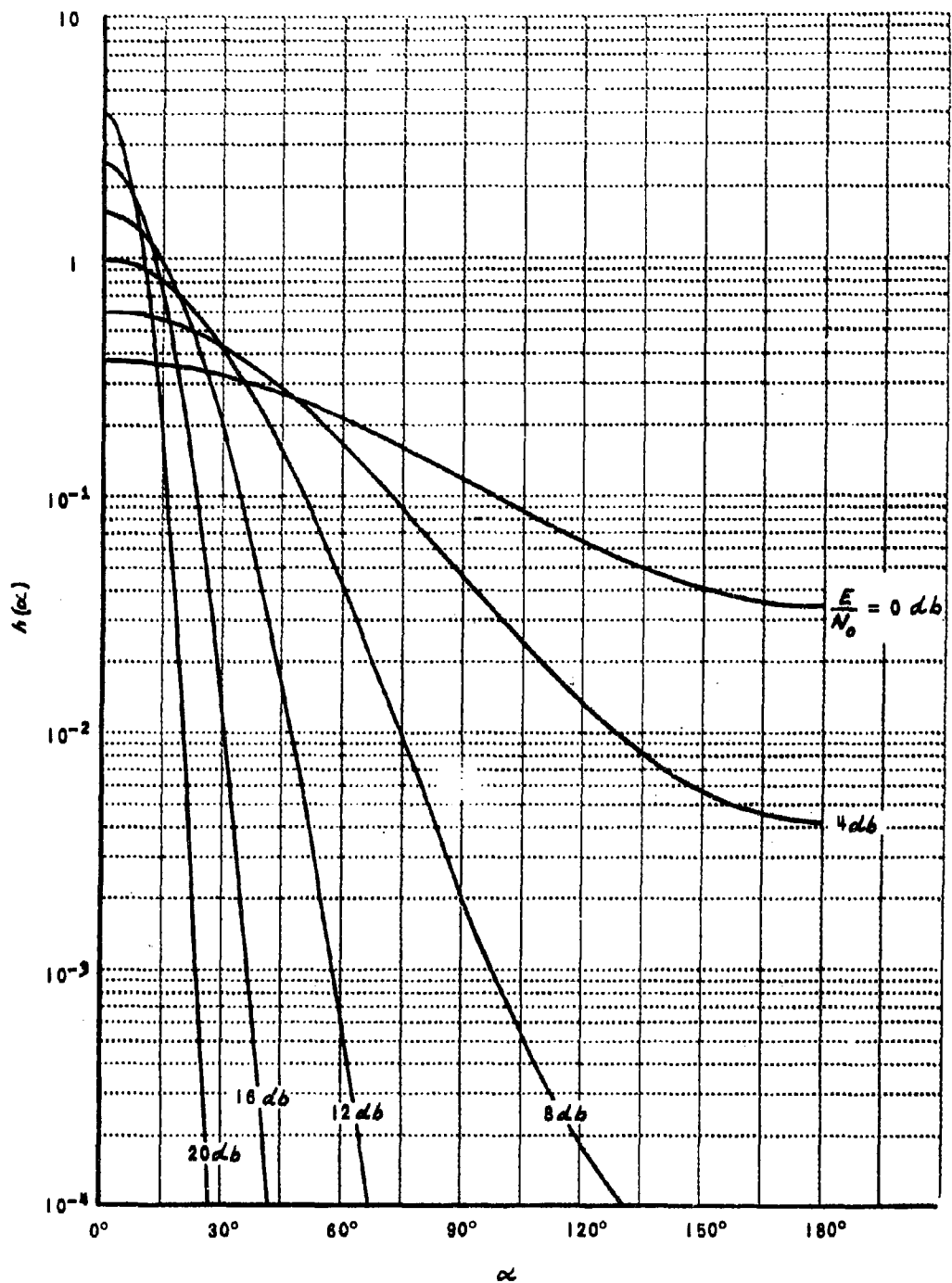


Figure 4 PROBABILITY DENSITY OF PHASE DIFFERENCE

Using the values of $h(\alpha)$ obtained in one degree steps as described above, a second numerical integration again using Simpson's Rule was performed by accumulating (θ) in 2° steps starting from $\theta = \frac{\pi}{2}$ until the value 1 was attained at $\theta = 0$. Thus for a fixed $R = \frac{E}{N_0}$, tables of $H(\theta)$ were generated at 2° intervals from 0° to 90° .

Since the probability of a character in an m -state DCPSKS is given by (3) viz.

$$P_c(m) = H\left(\frac{\pi}{m}\right) \quad (57)$$

Crossplots of $P_c(m)$ vs. $\frac{E}{N_0}$ in db were readily obtained from the tables of $H(\theta)$ for $m = 2, 15, 30$ corresponding respectively to $\theta = \frac{\pi}{m}$ of $90^\circ, 12^\circ, 6^\circ$. Error curves for $m = 4, 8$ corresponding respectively to $\theta = \frac{\pi}{m}$ of 45° and 22.5° were obtained by interpolation. The resulting curves are plotted in Figure 5.

For $m = 4$ and $\frac{E}{N_0} = 10.8$ db, $P_c(4) = .0089$ which is fairly good agreement with the single point calculated previously by Cain (3) who obtained .0083.

E. An Approximate Formula For the Error Probabilities When $m > 2$

Some relationships between $h(\alpha)$ and some special functions of mathematical analysis are

$$h(\alpha) - h(\pi - \alpha) = \frac{1}{2} R e^{-R} [I_1(R \cos \alpha) + \cos \alpha I_0(R \cos \alpha)] \quad (58)$$

$$h(\alpha) + h(\pi - \alpha) = 2h\left(\frac{\pi}{2}\right) + \frac{1}{2} R e^{-R} [L_1(R \cos \alpha) + \cos \alpha L_0(R \cos \alpha)] \quad (59)$$

$$h(\alpha) + h(\pi - \alpha) = \frac{1}{\pi} e^{-R} + \frac{1}{2} R e^{-R} [E_1(iR \cos \alpha) + i \cos \alpha E_0(iR \cos \alpha)] \quad (60)$$

where I_j , L_j , and E_j ($j = 1, 2$) are defined in APPENDIX A. For example, (58) may be obtained from (32) by writing

$$h(\alpha) - h(\pi - \alpha) = \frac{(1+R)}{2} e^{-R} \left\{ I - II \right\} + \frac{R e^{-R}}{2} \frac{\partial}{\partial R} \left\{ I - II \right\} \quad (61)$$

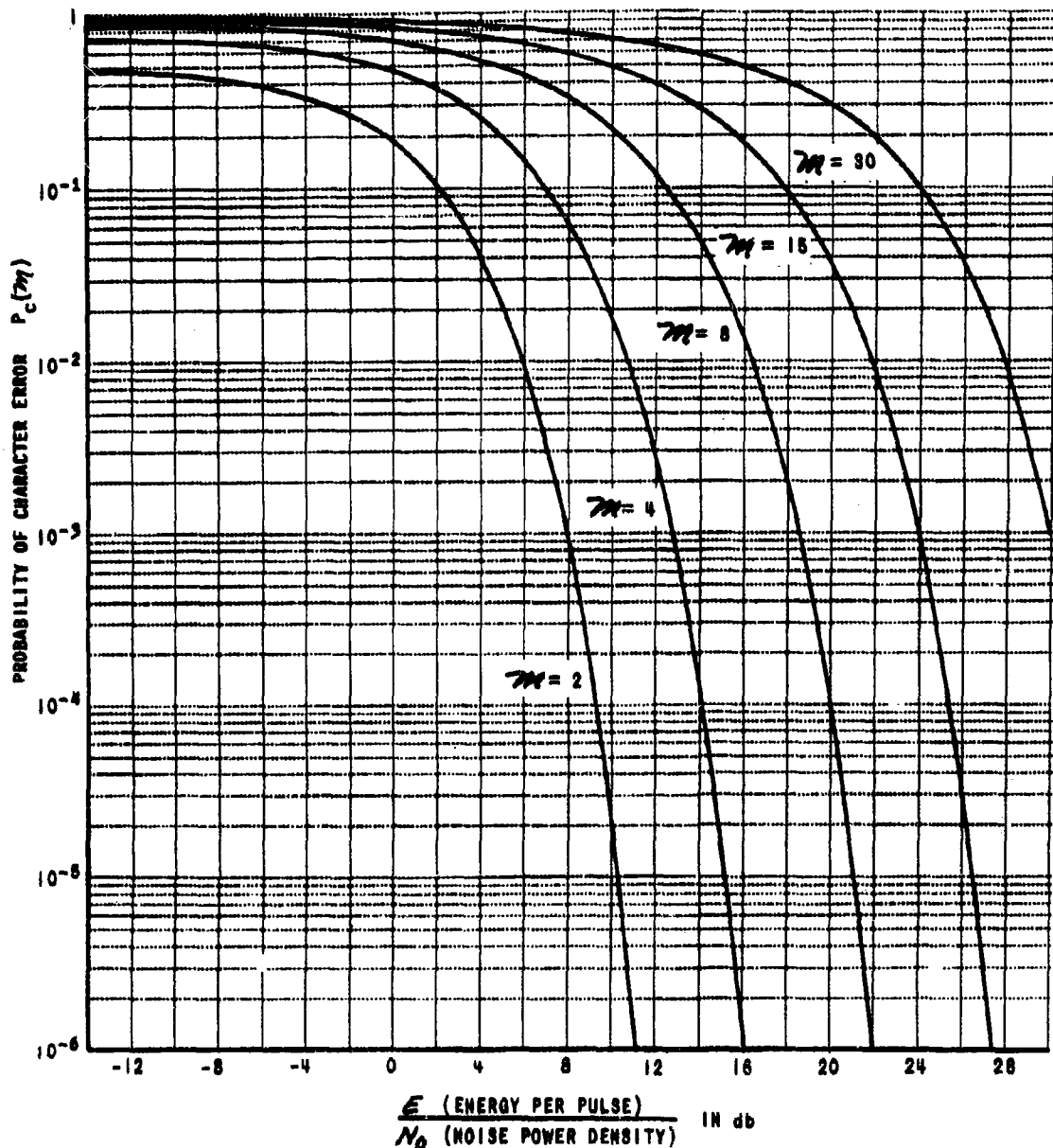


Figure 5 PROBABILITY OF CHARACTER ERROR IN m -STATE DCPSKs
(Computed as described in Section III-D)

where

$$I = \frac{1}{\pi} \int_0^{\pi/2} \sin \psi e^{R \cos \alpha \sin \psi} d\psi \quad (62)$$

and

$$II = \frac{1}{\pi} \int_0^{\pi/2} \sin \psi e^{-R \cos \alpha \sin \psi} d\psi \quad (63)$$

Using the power series representation of the exponential in the integral, interchanging the order of integration and summation, and performing the integration with respect to ψ with the help of (41), one obtains

$$I = \frac{1}{2\sqrt{\pi}} \sum_{r=0}^{\infty} \frac{(R \cos \alpha)^r}{r!} \frac{\left(\frac{r}{2}\right)!}{\left(\frac{r+1}{2}\right)!} \quad (64)$$

and

$$II = \frac{1}{2\sqrt{\pi}} \sum_{r=0}^{\infty} \frac{(-1)^r (R \cos \alpha)^r}{r!} \frac{\left(\frac{r}{2}\right)!}{\left(\frac{r+1}{2}\right)!} \quad (65)$$

Now, in the difference I-II, the even powers of $R \cos \alpha$ cancel so that

$$I - II = \frac{1}{\sqrt{\pi}} \sum_{k=0}^{\infty} \frac{(R \cos \alpha)^{2k+1}}{(2k+1)!} \frac{(k+1/2)!}{(k+1)!} \quad (66)$$

and using (42)

$$I - II = \sum_{k=0}^{\infty} \frac{\left(\frac{R \cos \alpha}{2}\right)^{2k+1}}{k!(k+1)!} \quad (67)$$

Substituting (67) into (61), a little regrouping yields (58). Similar procedures may be used to obtain (59) and (60).

Subtracting (58) from (60) and using (A13) and (A14) from APPENDIX A, one obtains

$$h(\pi - \alpha) = \frac{1}{2\pi} e^{-R} + \frac{1}{4} R e^{-R} q(\alpha) \quad (68)$$

where

$$g(\alpha) = \frac{2}{\pi} \int_0^{\pi/2} e^{-R \cos \alpha \cos \theta} (\cos \theta - \cos \alpha) d\theta \quad (69)$$

and (65) into (55) gives

$$\begin{aligned} h(\alpha) &= \frac{1}{2} R e^{-R} \left[I_1(R \cos \alpha) + \cos \alpha I_0(R \cos \alpha) \right] \\ &\quad + \frac{e^{-R}}{2\pi} + \frac{1}{4} R e^{-R} g(\alpha) \end{aligned} \quad (70)$$

Equation (70) may be used to obtain an approximate expression for $H(\theta)$ as given by (2), namely

$$H(\theta) = 1 - 2 \int_0^\theta h(\alpha) d\alpha \quad (71)$$

The second term in (70) tends to zero for large R as does the third term for $\alpha < \pi/2$, so that they may be ignored in (71) if an asymptotic expression is sought. Retaining the first two terms of the asymptotic expansions of I_0 and I_1 given in APPENDIX A, one may write

$$H(\theta) = 1 - \int_0^\theta \sqrt{\frac{R}{2\pi \cos \alpha}} e^{-R(1-\cos \alpha)} \left\{ \cos \alpha + \left(1 + \frac{1}{8R}\right) - \frac{3}{8R \cos \alpha} \right\} d\alpha \quad (72)$$

Let

$$u^2 = R(1 - \cos \alpha) = 2R \sin^2 \frac{\alpha}{2} \quad (73)$$

$$Q = \sqrt{2R} \sin \frac{\theta}{2}$$

then

$$H(\theta) = 1 - \frac{1}{\sqrt{\pi}} \int_0^Q \frac{e^{-u^2}}{\sqrt{1 - \frac{u^2}{2R}}} \left\{ \sqrt{1 - \frac{u^2}{R}} + \left(1 + \frac{1}{8R}\right) \frac{1}{\sqrt{1 - \frac{u^2}{R}}} - \frac{3}{8R} \frac{1}{(1 - \frac{u^2}{R})^{3/2}} \right\} du \quad (74)$$

which for $\frac{u^2}{R} \ll 1$ may be approximated by

$$H(\Theta) = 1 - \frac{1}{\sqrt{\pi R}} \int_0^Q e^{-u^2} \left(1 + \frac{u^2}{4R} \right) \left[\left(1 - \frac{u^2}{2R} \right) + \left(1 + \frac{1}{8R} \right) \left(1 + \frac{u^2}{2R} \right) - \frac{3}{8R} \left(1 + \frac{3}{2} \frac{u^2}{R} \right) \right] du \quad (75)$$

If in the third factor of the integrand of (75), only terms of the order of $1/R$ are retained, one obtains

$$H(\Theta) = 1 - \frac{2}{\sqrt{\pi R}} \int_0^Q e^{-u^2} \left(1 + \frac{u^2}{4R} \right) \left(1 - \frac{1}{8R} \right) du. \quad (76)$$

Now, for large R ,

$$1 - \frac{1}{8R} \approx \frac{1}{1 + \frac{1}{8R}} \quad (77)$$

and it does not matter much whether the left or right hand side of (77) is used. Note, however, that for small R the right hand side of (77) is to be preferred (for example, for $R = 1/8$ the left hand side is zero). In the hope that (76) will also be a valid approximation for moderately small values of R , one can write

$$H(\Theta) = 1 - \frac{2}{\sqrt{\pi R}} \int_0^Q e^{-u^2} \frac{\left(1 + \frac{u^2}{4R} \right)}{\left(1 + \frac{1}{8R} \right)} du \quad (78)$$

and direct evaluation of (78) gives

$$H(\Theta) = 1 - \frac{2}{\sqrt{\pi R}} \int_0^Q e^{-u^2} du + \frac{Q e^{-Q^2}}{4\sqrt{\pi R} \left(R + \frac{1}{8} \right)} \quad (79)$$

Summarizing the analysis, an approximate expression for the probability of a character error in an m -state ($m > 2$) DCPSKS is given by

$$P_c(m) = H\left(\theta = \frac{\pi}{m}\right) \quad (m > 2)$$

$$H(\theta) = \operatorname{erfc} Q + \frac{Q e^{-Q^2}}{4\sqrt{\pi} \left(R + \frac{1}{8}\right)} \quad (80)$$

$$Q = \sqrt{2R} \sin \frac{\theta}{2}$$

$$R = \frac{E}{N_0}$$

Since (80) is relatively easy to compute, extensive tables were calculated on the 704 and the results are tabulated in APPENDIX B.

In order to check the error with which (80) approximates $P_c(m)$, a special program was written for the 704. This program computes $H(\theta)$ by numerical integration of $h(\alpha)$ as given by

$$h(\alpha) = h\left(\frac{\pi}{2}\right) + \frac{1}{4} R e^{-R^2} \left\{ I_1(R \cos \alpha) + L_1(R \cos \alpha) + \cos \alpha [I_0(R \cos \alpha) + L_0(R \cos \alpha)] \right\} \quad (81)$$

which may be obtained by adding (58) and (59). Subroutines were written which calculated the special functions from their series representations given in APPENDIX A and the program was especially designed to give $P_c(m)$ directly without the necessity for interpolating $H(\theta)$. Tables of $P_c(m)$ for $m = 4, 8, 16, 32, 64$ as calculated from this exact expression are given in APPENDIX C for comparison with the approximate values given in APPENDIX B. It is found that the approximate formula gives $P_c(m)$ accurate to within a few percent over the range of $\frac{E}{N_0}$ from 0 to 30 db.

Since a set of curves describing $P_c(m)$ as m increases by powers of 2 may be desired, the probabilities computed from the exact expression which are tabulated in APPENDIX C are plotted in Figure 6.

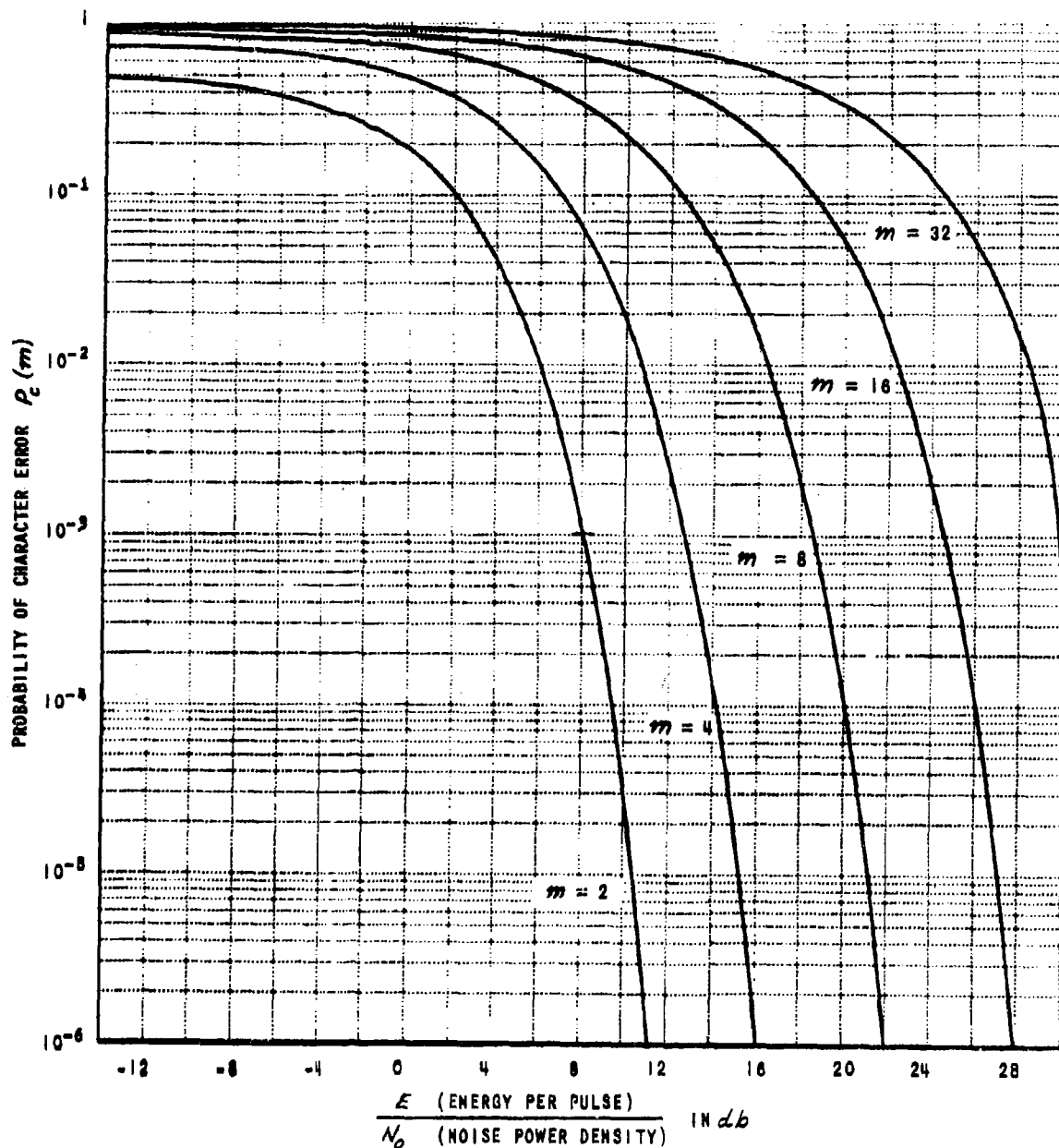


Figure 6 PROBABILITY OF CHARACTER ERROR IN m - STATE DCPSKS
(Computed using Equation 81)

III. SUBCHANNEL ERROR PROBABILITY IN A 4-STATE DCPSKS

A. Mathematical Formulation

A 4-state DCPSKS may be considered as being composed of two subchannels in quadrature as illustrated in Figure 7.

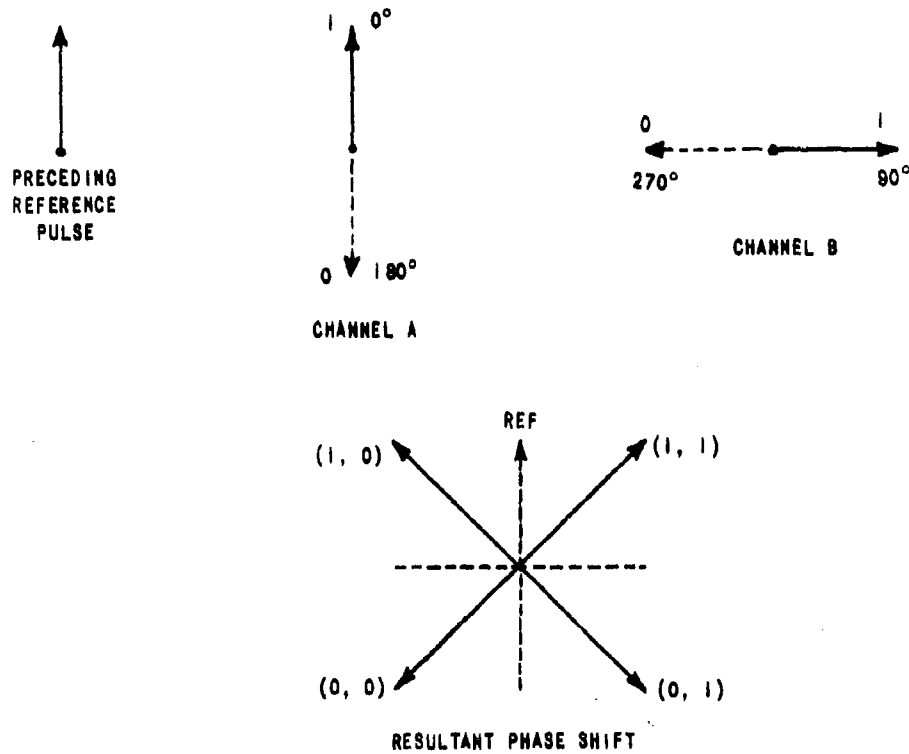


Figure 7

conceptually, the detector may be considered to consist of quadrature dot product detectors. Let

$x =$ dot product of received signal vector with preceding received signal vector.

$y =$ dot product of received signal vector with preceding received signal vector shifted 90° clockwise.

then the detector decision matrix is given by

		x	> 0	< 0
		y		
y	> 0	(1, 1)	(0, 1)	
	< 0	(1, 0)	(0, 0)	

Let P_A = probability of an error in Channel A. Assuming 1 and 0 to be transmitted independently with probability 1/2 on both channels and that the channels are independent, it is possible to express P_A as the sum of conditional probabilities

$$P_A = \frac{1}{4} \text{Prob.}(x < 0 / (1, 1)) + \frac{1}{4} \text{Prob.}(x > 0 / (0, 1)) \\ + \frac{1}{4} \text{Prob.}(x < 0 / (1, 0)) + \frac{1}{4} \text{Prob.}(x > 0 / (0, 0)) \quad (82)$$

It is not difficult to show that the above conditional probabilities are all equal, and that the subchannel error probability $P_{SUB}(4)$ of a 4-state DCPSKS is given by

$$P_{SUB}(4) = P_A = P_B = \text{Prob.}(x < 0 / (1, 1)) \quad (83)$$

Let A denote the peak signal amplitude at the output of a filter matched to the transmitted sinusoid. If 2 successive and independent samples of the output noise are represented by their in-phase and quadrature components,

then it can be inferred from Figure 8 that the dot product χ , assuming that a $(1, 1)$ was transmitted, is given by

$$\chi = (A + n_1) \left(\frac{A}{\sqrt{2}} + n_2 \right) + n_3 \left(\frac{A}{\sqrt{2}} + n_4 \right) \quad (84)$$

where n_1, n_2, n_3, n_4 are independent Gaussian variables with zero mean and variances σ^2 and it is well known as was stated in (1) that

$$\frac{A^2}{\sigma^2} = \frac{2E}{N_0} \quad (85)$$

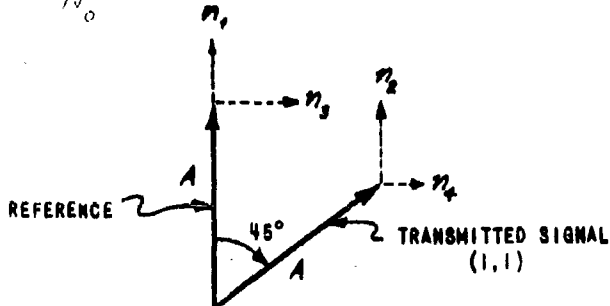


FIGURE 8

If the probability density of χ is denoted by $g(\chi)$ then from (83), one has

$$P_{SUB}(4) = \int_{-\infty}^{\infty} g(\chi) d\chi \quad (86)$$

3. The PDF of a Negative Dot Product for Two Vectors Independently Perturbed by Gaussian Noise

The expression (84) is a special case of

$$\chi = (\tau_1 + u_1) (\tau_2 + u_2) + (\tau_3 + u_3) (\tau_4 + u_4) \quad (87)$$

Consider the first term of (87), namely

$$\tau_1 + u_1 (\tau_2 + u_2) (\tau_4 + u_4) \quad (88)$$

where the joint density of n_1 and n_2 is given by

$$p(n_1, n_2) = \frac{1}{2\pi\sigma^2} e^{-\frac{n_1^2 + n_2^2}{2\sigma^2}} \quad (89)$$

from which the density of x , may be shown to be given by (6)

$$p(x_1) = \frac{1}{2\pi\sigma^2} \int_{-\infty}^{+\infty} \frac{e^{-\frac{(u+\mu_1)^2 + (\frac{x_1}{u} + \mu_2)^2}{2\sigma^2}}}{|u|} du \quad (90)$$

The second term of (87), namely

$$x_2 = (n_3 + \mu_3)(n_4 + \mu_4) \quad (91)$$

is also distributed according to (90), and since

$$x = x_1 + x_2 \quad (92)$$

one has for the density of x , the convolution

$$g(x) = \int_{-\infty}^{+\infty} p(x_1) p(x-x_1) dx_1, \quad (93)$$

Using (90), (93) may be expressed as the triple integral

$$g(x) = \frac{1}{(2\pi\sigma^2)^2} \int_{-\infty}^{+\infty} \frac{du}{|u|} \int_{-\infty}^{+\infty} \frac{dv}{|v|} \int_{-\infty}^{+\infty} e^{-\frac{1}{2\sigma^2} \left\{ (u+\mu_1)^2 + (\frac{x_1}{u} + \mu_3)^2 + (v+\mu_2)^2 + (\frac{x-x_1}{v} + \mu_4)^2 \right\}} \quad (94)$$

Integrating with respect to x_1 gives

(95)

$$g(x) = \frac{1}{(2\pi\sigma^2)^{3/2}} \int_{-\infty}^{+\infty} \frac{du}{|u|} \int_{-\infty}^{+\infty} \frac{dv}{|v|} \sqrt{\frac{1}{u^2} + \frac{1}{v^2}} e^{-\frac{1}{2\sigma^2} \left\{ (u+\mu_1)^2 + (v+\mu_3)^2 + \frac{(\frac{x}{u} + \frac{\mu_2}{v} + \frac{\mu_4}{u})^2}{\frac{1}{u^2} + \frac{1}{v^2}} \right\}} \quad (95)$$

Letting

$$\begin{aligned} u &= r \cos \theta \\ v &= r \sin \theta \end{aligned} \quad (96)$$

gives

$$g(x) = \frac{1}{(2\pi\sigma^2)^{3/2}} \int_0^{2\pi} d\theta \int_0^\infty dr e^{-\frac{1}{2\sigma^2} \left\{ (r \cos \theta + u_1)^2 + (r \sin \theta + u_2)^2 + \left(\frac{x}{r} + u_3 \cos \theta + u_4 \sin \theta\right)^2 \right\}} \quad (97)$$

and the substitutions

$$\begin{aligned} u_1 &= \sqrt{2\sigma^2} \alpha \cos \xi & u_2 &= \sqrt{2\sigma^2} \beta \cos \eta \\ u_3 &= \sqrt{2\sigma^2} \alpha \sin \xi & u_4 &= \sqrt{2\sigma^2} \beta \sin \eta \end{aligned} \quad (98)$$

$$r = \sqrt{2\sigma^2} \rho$$

$$x = \sqrt{2\sigma^2} z$$

yield the density of

$$f(z) = \frac{1}{\pi^{3/2}} \int_0^{2\pi} d\theta \int_0^\infty d\rho e^{-\left[\rho^2 + 2\rho \alpha \cos(\theta - \xi) + \alpha^2 + \left(\frac{z}{\rho} + \beta \cos(\theta - \eta)\right)^2\right]} \quad (99)$$

Since the integrand of (99) is periodic in θ and is integrated over a complete period, one may write

$$f(z) = \frac{1}{\pi^{3/2}} \int_0^{2\pi} d\theta \int_0^\infty d\rho e^{-\left[\rho^2 + 2\rho \alpha \cos(\theta + \phi) + \alpha^2 + \left(\frac{z}{\rho} + \beta \cos \theta\right)^2\right]} \quad (100)$$

where

$$\phi = \eta - \xi \quad (101)$$

Thus, there are three significant parameter α , β and ϕ .

Because of the relationship between x and z given by (98), one has

$$P = \int_{-\infty}^{\infty} g(x) dx = \int_{-\infty}^0 f(z) dz = \int_0^{\infty} f(-z) dz \quad (102)$$

and from (100)

$$P = \frac{1}{\pi^{3/2}} \int_0^{2\pi} d\theta \int_0^{\infty} d\rho \int_0^{\infty} d\bar{z} e^{-[\rho^2 + 2\rho \alpha \cos(\theta + \phi) + \alpha^2 + (\beta \cos \theta - z/\rho)^2]} \quad (103)$$

Letting $\bar{z} = \rho w$ gives

$$P = \frac{1}{\pi^{3/2}} \int_0^{2\pi} d\theta \int_0^{\infty} \rho d\rho \int_0^{\infty} dw e^{-[\rho^2 + 2\rho \alpha \cos(\theta + \phi) + \alpha^2 + (w - \beta \cos \theta)^2]} \quad (104)$$

Since

$$\int_0^{\infty} e^{-(w - \beta \cos \theta)^2} dw = \int_{-\beta \cos \theta}^{\infty} e^{-y^2} dy = \frac{\sqrt{\pi}}{2} + \int_0^{\beta \cos \theta} e^{-y^2} dy \quad (105)$$

and because any 2π range may be used for the integration with respect to θ in (104), if one splits the θ integration into

$$\int_{-\frac{\pi}{2}}^{\frac{\pi}{2}} d\theta + \int_{\frac{\pi}{2}}^{\frac{3\pi}{2}} d\theta' \quad (106)$$

and lets $\theta' = \theta + \pi$ in the second range, (104) reduces to

$$P = \frac{1}{\pi^{3/2}} \int_0^\infty \rho d\rho \left\{ \int_{-\frac{\pi}{2}}^{\frac{\pi}{2}} d\theta e^{-(\rho^2 + 2\rho \alpha \cos(\theta + \phi) + \alpha^2)} \left[\frac{\sqrt{\pi}}{2} + \int_0^{\beta \cos \theta} e^{-y^2} dy \right] \right. \\ \left. (107) \right.$$

$$\left. + \int_{-\frac{\pi}{2}}^{\frac{\pi}{2}} d\theta e^{-(\rho^2 - 2\rho \alpha \cos(\theta + \phi) + \alpha^2)} \left[\frac{\sqrt{\pi}}{2} - \int_0^{\beta \cos \theta} e^{-y^2} dy \right] \right\}$$

or, equivalently

$$F = \frac{1}{2\pi} \int_0^\infty \rho d\rho \int_0^{2\pi} d\theta e^{-(\rho^2 + 2\rho \alpha \cos(\theta + \phi) + \alpha^2)} \\ (108)$$

$$+ \frac{1}{\pi^{3/2}} \int_0^\infty \rho d\rho \int_{-\frac{\pi}{2}}^{\frac{\pi}{2}} d\theta \int_0^{\beta \cos \theta} e^{-y^2} \left[e^{-(\rho^2 + 2\rho \alpha \cos(\theta + \phi) + \alpha^2)} - e^{-(\rho^2 - 2\rho \alpha \cos(\theta + \phi) + \alpha^2)} \right]$$

but

$$\frac{1}{2\pi} \int_0^\infty \rho d\rho \int_0^{2\pi} d\theta e^{-(\rho^2 + 2\rho \alpha \cos(\theta + \phi) + \alpha^2)} = \int_0^\infty \rho e^{-(\rho^2 + \alpha^2)} I_0(2\rho \alpha) d\rho = \frac{1}{2} \\ (109)$$

Evaluation of the integral of Eqn. (109) follows upon recalling ⁽¹⁾ that the probability density, $w(\rho)$, of the envelope of a sinusoidal signal of amplitude α plus Gaussian noise of power σ^2 is given by

$$w(\rho) = \frac{1}{\sigma^2} e^{-\left(\frac{\alpha^2 + \rho^2}{2\sigma^2}\right)} I_0\left(\frac{\alpha \rho}{\sigma^2}\right) \\ (110)$$

and that

$$\int_0^\infty w(\rho) d\rho = 1 \quad (111)$$

for all values of σ^2 . If $\sigma^2 = 1/2$, (109) is obtained. Moreover, completing the square in ρ and letting $r = \rho + \alpha \cos(\theta + \phi)$, one finds that

$$\begin{aligned} \int_0^\infty \rho e^{-\frac{(\rho^2 + 2\rho\alpha \cos(\theta + \phi) + \alpha^2)}{\alpha \cos(\theta + \phi)}} d\rho &= \int_0^\infty (r - \alpha \cos(\theta + \phi)) e^{-\frac{r^2 - \alpha^2 \sin^2(\theta + \phi)}{\alpha \cos(\theta + \phi)}} dr \\ &= \frac{e^{-\alpha^2}}{2} - \alpha \cos(\theta + \phi) e^{-\frac{\alpha^2 \sin^2(\theta + \phi)}{\alpha \cos(\theta + \phi)}} \left[\frac{\sqrt{\pi}}{2} - \int_0^{\alpha \cos(\theta + \phi)} e^{-r^2} dr \right] \end{aligned} \quad (112)$$

and similarly,

$$\begin{aligned} \int_0^\infty \rho e^{-\frac{(\rho^2 - 2\rho\alpha \cos(\theta + \phi) + \alpha^2)}{\alpha \cos(\theta + \phi)}} d\rho &= e^{-\frac{\alpha^2}{2}} + \\ &\alpha \cos(\theta + \phi) e^{-\frac{\alpha^2 \sin^2(\theta + \phi)}{\alpha \cos(\theta + \phi)}} \left[\frac{\sqrt{\pi}}{2} + \int_0^{\alpha \cos(\theta + \phi)} e^{-r^2} dr \right] \end{aligned} \quad (113)$$

Substituting (109), (112) and (113) in (108), yields

$$P = \frac{1}{2} - \frac{\alpha}{\pi} \int_{-\frac{\pi}{2}}^{\frac{\pi}{2}} d\theta \cos(\theta + \phi) e^{-\frac{\alpha^2 \sin^2(\theta + \phi)}{\alpha \cos(\theta + \phi)}} \int_0^{\alpha \cos \theta} e^{-y^2} dy \quad (114)$$

and letting

$$\begin{aligned} u &= y \\ v &= \alpha \sin(\theta + \phi) \end{aligned} \quad (115)$$

the probability that the dot product (87) is negative as given by (114) becomes

$$P = \frac{1}{2} - \frac{1}{\pi} \int_{-\alpha \cos \phi}^{\alpha \cos \phi} dv \int_0^{\beta \cos(\sin^{-1} v/\alpha - \phi)} du e^{-(u^2 + v^2)} \quad (116)$$

The double integral appearing in (116) has an interesting geometrical interpretation which may be obtained by working with the upper limit

$$u = \beta \cos(\sin^{-1} v/\alpha - \phi) \quad (117)$$

Expanding the right hand side of (117) and then squaring both sides, one obtains after rearranging terms

$$\alpha^2 u^2 + \beta^2 v^2 - 2uv\alpha\beta \sin\phi = \alpha^2\beta^2 \cos^2\phi \quad (118)$$

which is the equation of an ellipse centered at the origin and contained within the lines $u = \pm\beta$ and $v = \pm\alpha$. Hence, the integral

$$I = \frac{1}{\pi} \int_{-\alpha \cos \phi}^{\alpha \cos \phi} dv \int_0^{\beta \cos(\sin^{-1} v/\alpha - \phi)} du e^{-(u^2 + v^2)} \quad (119)$$

is just the integral of the function $1/\pi e^{-(u^2 + v^2)}$ over the shaded area in the right half plane shown in Figure 9.

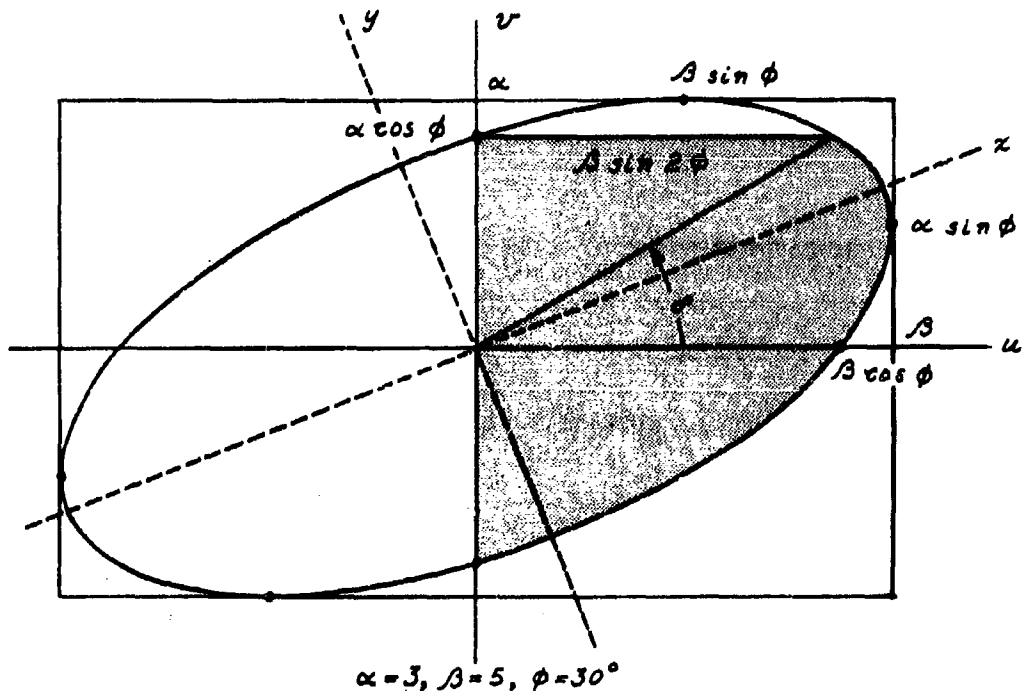


Figure 9

Changing to polar coordinates by letting $u = r \cos \theta$ and $v = r \sin \theta$, one gets

$$I = \frac{1}{\pi} \int_{-\frac{\pi}{2}}^{\frac{\pi}{2}} d\theta \int_0^{\infty} dr r^2 e^{-r^2} + \frac{1}{\pi} \int_{\frac{\pi}{2}}^{\frac{3\pi}{2}} d\theta \int_0^{\infty} dr r^2 e^{-r^2} \quad (120)$$

where ρ_0 is on the ellipse (118) so that

$$\rho_0^2 = \frac{\alpha^2 \beta^2 \cos^2 \phi}{\alpha^2 \cos^2 \theta + \beta^2 \sin^2 \theta - 2\alpha\beta \sin \phi \sin \theta \cos \theta} \quad (121)$$

and it is seen from Figure 9 that

$$\tan \sigma' = \frac{\alpha \cos \phi}{\beta \sin 2\phi} = \frac{\alpha}{2\beta \sin \phi} \quad (122)$$

Performing the integration with respect to ρ in (120), and from (116) and (119), one finds that

$$P = IN_1 + IN_2 \quad (123)$$

where

$$IN_1 = \frac{1}{2\pi} \int_{-\frac{\pi}{2}}^{\frac{\pi}{2}} e^{-\alpha^2 \cos^2 \phi \csc^2 \theta} d\theta \quad (124)$$

and

$$IN_2 = \frac{1}{2\pi} \int_{-\pi/2}^{\sigma} e^{-\rho_0^2} d\theta \quad (125)$$

Letting $\theta = -\theta' + \pi/2$ in (124) yields

$$IN_1 = \frac{1}{2\pi} \int_0^{\pi/2 - \sigma'} e^{-\alpha^2 \cos^2 \phi \sec^2 \theta'} d\theta' \quad (126)$$

The expression (121) for ρ_0^2 in IN_2 may be simplified by letting

$$\begin{aligned} \alpha &= r \cos \pi/2 \\ \beta &= r \sin \pi/2 \end{aligned} \quad (127)$$

so that

$$r^2 = \alpha^2 + \beta^2 \quad (128)$$

and using the half angle formulas

$$\begin{aligned} \sin^2 \pi/2 &= 1/2 (1 - \cos \pi) \\ \cos^2 \pi/2 &= 1/2 (1 + \cos \pi) \end{aligned} \quad (129)$$

(121) becomes

$$\rho_0^2 = \frac{r^2/2 \sin^2 \pi \cos^2 \phi}{1 + \cos 2\theta \cos \pi - \sin 2\theta \sin \pi \sin \phi} \quad (130)$$

Defining an angle τ such that

$$\sin \tau = \frac{\sin \pi \sin \phi}{\sqrt{1 - \sin^2 \pi \cos^2 \phi}} ; \cos \tau = \frac{\cos \pi}{\sqrt{1 - \sin^2 \pi \cos^2 \phi}} \quad (131)$$

(130) reduces to

$$\rho_0^2 = \frac{r^2/2 \sin^2 \pi \cos^2 \phi}{1 + \sqrt{1 - \sin^2 \pi \cos^2 \phi} \cos(2\theta + \tau)} \quad (132)$$

and letting

$$\cos \epsilon = \sin \pi \cos \phi \quad (133)$$

IN_2 as given by (119) becomes

$$IN_2 = \frac{1}{2\pi} \int_{-\frac{\pi}{2}}^{\frac{\sigma}{2}} e^{-\frac{r^2}{2}} \frac{e^{\frac{r^2 \epsilon^2}{2} \cos(2\theta + \tau)}}{1 + \sin \epsilon \frac{r^2 \epsilon^2}{2} \cos(2\theta + \tau)} d\theta \quad (134)$$

which upon letting $\psi = 2\theta + \tau'$ reduces to

$$IN_2 = \frac{1}{4\pi} \int_{-\pi/2+\tau'}^{2\sigma+\tau'} e^{-\frac{r^2}{2}} \frac{\cos^2 \epsilon}{1 + \sin \epsilon \cos \psi} d\psi \quad (135)$$

and finally setting $\psi = \theta + \frac{\pi}{2}$, one has

$$IN_2 = \frac{1}{4\pi} \int_{-3/2\pi+\tau'}^{2\sigma+\tau'-\pi/2} e^{-\frac{r^2}{2}} \frac{\cos^2 \epsilon}{1 - \sin \epsilon \sin \theta} d\theta \quad (136)$$

Summarizing the results obtained in this section, one finds that

$$P = \text{Prob } (\chi < 0)$$

$$\chi = (n_1 + \mu_1)(n_2 + \mu_2) + (n_3 + \mu_3)(n_4 + \mu_4)$$

$\mu_1, \mu_2, \mu_3, \mu_4$ arbitrary parameters

n_1, n_2, n_3, n_4 independent Gaussian variables with zero means and variance σ^2

$$\begin{aligned} P &= \frac{1}{2\pi} \int_0^{\frac{\pi}{2}-\sigma} e^{-\alpha^2 \cos^2 \phi \sec^2 \theta} d\theta \\ &+ \frac{1}{4\pi} \int_{-3/2\pi+\tau'}^{2\sigma+\tau'-\pi/2} e^{-\frac{r^2}{2}} \frac{\cos^2 \epsilon}{1 - \sin \epsilon \sin \theta} d\theta \end{aligned} \quad (137)$$

$$\phi = \eta - \xi$$

$$\mu_1 = \sqrt{2G^2} \alpha \cos \xi \quad \mu_2 = \sqrt{2G^2} \beta \cos \eta$$

$$\mu_3 = \sqrt{2G^2} \alpha \sin \xi \quad \mu_4 = \sqrt{2G^2} \beta \sin \eta$$

$$\delta = \tan^{-1} \frac{\alpha}{2\beta \sin \phi}$$

$$\sin \frac{\pi}{2} = \frac{\beta}{r}$$

$$\cos \frac{\pi}{2} = \frac{\alpha}{r} \quad r^2 = \alpha^2 + \beta^2$$

$$\cos \epsilon = \sin \pi \cos \phi; \quad \sin \epsilon = \sqrt{1 - \cos^2 \epsilon}$$

$$\sin \tau = \frac{\sin \pi \cos \phi}{\sqrt{1 - \sin^2 \pi \cos^2 \phi}}; \quad \cos \tau = \frac{\cos \pi}{\sqrt{1 - \sin^2 \pi \cos^2 \phi}}$$

C. Calculation of Error Probability

It is interesting to note that the known expression (54) for the probability of error $P_e(2)$ in a binary DCPSKS may be obtained from the set of equations (137). Assuming without loss of generality that a zero phase change was transmitted in a binary DCPSKS, the dot product of the two succeeding received signal vectors as shown in Figure 10 is given by

$$x = (A + n_1)(A + n_2) + n_3 n_4 \quad (138)$$

and

$$P_e(2) = \text{Prob}(x < 0) \quad (139)$$

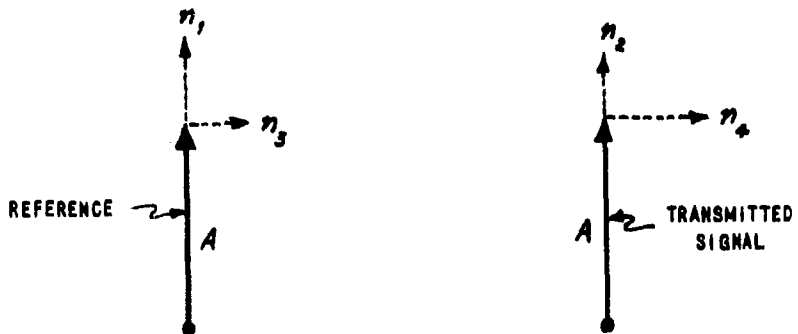


Figure 10

Now, one has

$$\begin{aligned} \mu_1 = \mu_2 = A; \quad \mu_3 = \mu_4 = 0; \quad \theta = \eta = \phi = 0; \quad \alpha^2 = \beta^2 = \frac{4\pi^2}{2\sigma^2} \\ \sigma^2 = \frac{\pi^2}{2}; \quad r^2 = \frac{A^2}{\sigma^2}; \quad \theta_1 = \frac{\pi}{2}; \quad \epsilon = \frac{\pi}{2}; \quad N = 0 \end{aligned} \quad (140)$$

so that

$$P_e(z) = 0 + \frac{1}{4\pi} \int_{-\pi/2}^{\pi/2} e^{-\frac{A^2}{2\sigma^2}} d\theta \quad (141)$$

and recalling from (33) that $\frac{A^2}{2\sigma^2} = \frac{E}{N_0}$, one obtains finally

$$P_e(z) = \frac{1}{z} e^{-\frac{E}{N_0}} \quad (142)$$

which was obtained by other means in References (1) and (2) and also in Section IIC of this report.

In order to evaluate $P_{SUB}(4)$, a comparison of (84) and (87) yields

$$\begin{aligned} \mu_1 &= A; \quad \mu_2 = \mu_4 = \frac{A}{\sqrt{2}}; \quad \mu_3 = 0; \quad \xi = 0; \quad \eta = \frac{\pi}{4}; \quad \phi = \frac{\pi}{4} \\ \alpha^2 = \beta^2 &= \frac{A^2}{2G^2} = \frac{E}{N_0}; \quad \sigma = \tan^{-1} \frac{1}{\sqrt{2}}; \quad r^2 = \frac{A^2}{G^2} \quad (143) \\ \tau &= \frac{\pi}{2}; \quad \epsilon = \frac{\pi}{4}; \quad \tau = \frac{\pi}{2} \end{aligned}$$

and since

$$\frac{\pi}{2} - \tan^{-1} \frac{1}{\sqrt{2}} = \tan^{-1} \sqrt{2} \quad (144)$$

one finally obtains from (137)

$$P_{SUB}(4) = \frac{1}{2\pi} \int_0^{\tan^{-1} \sqrt{2}} e^{-\frac{1}{2} \frac{E}{N_0} \sec^2 \theta} d\theta + \frac{1}{4\pi} \int_{-\pi}^{\tan^{-1} 2\sqrt{2}} e^{-\frac{1}{2} \frac{E}{N_0} \frac{1}{1 - \frac{\sin \theta}{\sqrt{2}}}} d\theta \quad (145)$$

where E is again the total energy per pulse.

The expression (145) was evaluated on the IBM 704 computer and is plotted as the solid curve of Figure 11. The character error rate $P_c(4)$ of a four-state DCPSKS is bounded by

$$P_{SUB}(4) < P_c(4) < 2P_{SUB}(4) \quad (146)$$

and $2P_{SUB}(4)$ is plotted also in Figure 11 as the dashed curve. The circles correspond to the values of $P_c(4)$ as computed according to the description given in Section II of this report. For large E/N_0 , it is seen that

$$P_c(4) \sim 2P_{SUB}(4) \quad (147)$$

as is expected intuitively. This serves to check the calculation of $P_c(4)$ described in Section II. Moreover, in cases when it is desirable to feed independent signals into the 2 subchannels of a 4-state DCPSKS, $P_{SUB}(4)$ is of direct interest.

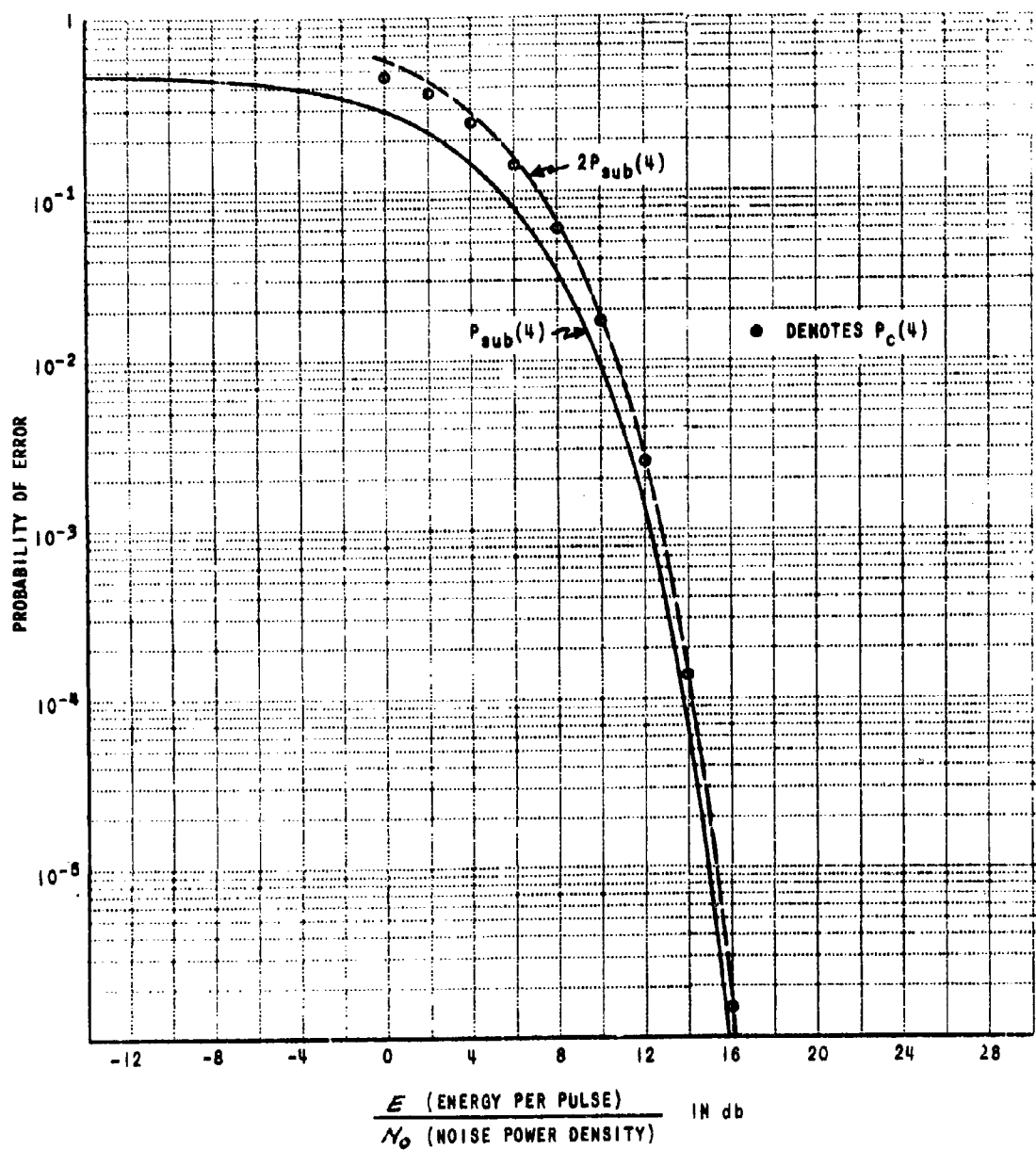


Figure 11 SUB-CHANNEL ERROR PROBABILITY IN AN $M = 4$ DCPSKS

IV. REFERENCES

1. Becker, H. D. and Lawton, J. G. Theoretical Comparison of Binary Data Transmission Systems Cornell Aeronautical Laboratory Report No. CA-1172-S-1 May 1958.
2. Cahn, C. R. Performance of Digital Phase - Modulation Communication Systems IRE Transactions on Communications Systems Vol. CS-7, No. 1 May 1959.
3. Cahn, C. R. Comparison of Coherent and Phase-Comparison Detection of a Four-Phase Digital Signal Correspondence Section Proceedings of the IRE Vol. 47, No. 9 September 1959.
4. Whittaker, E. T. and Watson, G. N. A Course of Modern Analysis The MacMillan Company, New York 1946.
5. Watson, G. N. A Treatise on the Theory of Bessel Functions The MacMillan Company, New York 1945.
6. Mood, Alexander McF., Introduction to the Theory of Statistics McGraw-Hill Book Company, New York 1950.

APPENDIX A - Some Relationships Concerning the
Special Functions Used in Analysis

For convenience the various properties of the special functions used in the analysis in this report are presented in this Appendix as obtained from References (4) and (5).

Bessel's Function of a complex variable and integral order $n \geq 0$ is given by

$$J_n(z) = \frac{1}{2\pi} \int_{-\pi}^{\pi} e^{-n\theta + iz \sin \theta} d\theta \quad (A1)$$

If z is taken to be pure imaginary, i.e., $z = ix$ where x is real

$$I_n(x) = J_n(ix) = \frac{1}{2\pi} \int_{-\pi}^{\pi} e^{-ni\theta - x \sin \theta} d\theta \quad (A2)$$

In particular for $n = 0$, one obtains Bessel's Function of zero order and pure imaginary argument, namely,

$$I_0(x) = \frac{1}{2\pi} \int_{-\pi}^{\pi} e^{-x \sin \theta} d\theta \quad (A3)$$

from which it is obvious that

$$I_0(-x) = I_0(x) \quad (A4)$$

hence,

$$I_0(x) = \frac{1}{2\pi} \int_{-\pi}^{\pi} e^{x \sin \theta} d\theta \quad (A5)$$

Moreover, since the integrand in (A4) is periodic in θ and the integral is taken over a period, 2π , one has

$$I_0(x) = \frac{1}{2\pi} \int_{-\pi}^{\pi} e^{x \sin(\theta + \phi)} d\theta \quad (A6)$$

and letting $\phi = \pi/2$

$$I_0(x) = \frac{1}{2\pi} \int_{-\pi}^{\pi} e^{x \cos \theta} d\theta \quad (A7)$$

The series representation of $I_n(x)$ is given by

$$I_n(x) = \sum_{n=0}^{\infty} \frac{(x/2)^{2n+n}}{n!(n+n)!} \quad (A8)$$

An analogous function

$$L_n(x) = \sum_{n=0}^{\infty} \frac{(x/2)^{2(n+1/2)+n}}{(n+1/2)! (n+1/2+n)!} \quad (A9)$$

bears the same relationship to Struve's function as $I_n(x)$ bears to $J_n(z)$ (see Reference 5, pg. 329). Weber's function of pure imaginary argument has the series representations (Reference 5, Chapter X)

$$i E_0(ix) = \sum_{n=0}^{\infty} \frac{(x/2)^{2n+1}}{(n+1/2)!(n+1/2)!} \quad (A10)$$

and

$$E_i(ix) = \sum_{n=0}^{\infty} \frac{(x/2)^{2n}}{(n-1/2)!(n+1/2)!} \quad (A11)$$

so that

$$L_o(x) = i E_o(ix) \quad (A12)$$

Moreover,

$$I_o(x) - i E_o(ix) = I_o(x) - L_o(x) = \frac{1}{\pi} \int_{-\pi/2}^{+\pi/2} e^{-x \cos \theta} d\theta \quad (A13)$$

and

$$I_o(x) - E_o(ix) = - \frac{1}{\pi} \int_{-\pi/2}^{+\pi/2} e^{-x \cos \theta} \cos \theta d\theta \quad (A14)$$

The identity (A13) may be obtained by expanding the integrand of the left-hand side in a power series, performing the integration with respect to θ term by term, and breaking up the resultant series into two series, one of even powers, the other of odd powers of x . If in the series of odd powers $r!$ is replaced by the expression obtained by solving (42) for $r!$, the series so obtained is readily recognized as $I_o(x)$. If in the series of even powers $(r - \frac{1}{2})!$ is rewritten as

$$\left(r - \frac{1}{2}\right)! = \frac{(r + 1/2)!}{r + 1/2} \quad (A15)$$

and $(r + \frac{1}{2})!$ is replaced by (42), the series so obtained is readily recognized as $L_o(x)$. A similar procedure may be used to obtain (A14).

Finally, $I_o(x)$ and $I_1(x)$ have asymptotic expansions

$$I_o(x) \sim \frac{e^x}{\sqrt{2\pi x}} \left\{ 1 + \frac{1^2}{1!(8x)} + \frac{1^2 3^2}{2!(8x)^2} + \frac{1^2 3^2 5^2}{3!(8x)^3} + \dots \right\} \quad (A15)$$

and

$$I_1(x) \sim \frac{e^x}{\sqrt{2\pi x}} \left\{ 1 - \frac{3}{1!(8x)} - \frac{3 \cdot 5}{2!(8x)^2} - \frac{3 \cdot 5 \cdot 21}{3!(8x)^3} \dots \right\} \quad (A16)$$

APPENDIX B

Tables of $P_c(m)$ as Computed From Approximate Formula

PROBABILITY OF ERROR (APPROXIMATE FORMULA)

E/N ⁰	(DB)	P (4) C	P (6) C	P (8) C	P (10) C	P (12) C	P (14) C	P (16) C	P (20) C
0	0.4947E-00	0.6448E 00	0.7285E 00	0.7808E 00	0.8164E 00	0.8422E 00	0.8616E 00	0.8891E 00	0.9166E 00
1	0.4333E-00	0.5967E 00	0.6902E 00	0.7493E 00	0.7898E 00	0.8192E 00	0.8414E 00	0.8727E 00	0.8877E 00
2	0.3706E-00	0.5454E 00	0.6487E 00	0.7149E 00	0.7606E 00	0.7938E 00	0.8190E 00	0.8547E 00	0.8854E 00
3	0.3080E-00	0.4910E-00	0.6028E 00	0.6774E 00	0.7285E 00	0.7659E 00	0.7944E 00	0.8348E 00	0.8734E 00
4	0.2471E-00	0.4342E-00	0.5556E 00	0.6366E 00	0.6934E 00	0.7353E 00	0.7672E 00	0.8127E 00	0.8612E 00
5	0.1899E-00	0.3756E-00	0.5043E 00	0.5924E 00	0.6551E 00	0.7016E 00	0.7373E 00	0.7884E 00	0.8384E 00
6	0.1383E-00	0.3164E-00	0.4502E-00	0.5449E 00	0.6135E 00	0.6648E 00	0.7045E 00	0.7615E 00	0.8165E 00
7	0.9480E-01	0.2580E-00	0.3940E-00	0.4943E-00	0.5685E 00	0.6247E 00	0.6685E 00	0.7318E 00	0.7818E 00
8	0.5924E-01	0.2022E-00	0.3364E-00	0.4409E-00	0.5202E 00	0.5812E 00	0.6292E 00	0.6991E 00	0.7591E 00
9	0.3360E-01	0.1508E-00	0.2789E-00	0.3853E-00	0.4688E-00	0.5344E 00	0.5865E 00	0.6633E 00	0.7233E 00
10	0.1678E-01	0.1059E-00	0.2229E-00	0.3285E-00	0.4149E-00	0.4843E-00	0.5404E 00	0.6241E 00	0.6941E 00
11	0.7148E-02	0.6893E-01	0.1704E-00	0.2717E-00	0.3590E-00	0.4314E-00	0.4910E-00	0.5814E 00	0.6581E 00
12	0.2495E-02	0.4087E-01	0.1232E-00	0.2165E-00	0.3025E-00	0.3764E-00	0.4387E-00	0.5354E 00	0.6234E 00
13	0.6784E-03	0.2156E-01	0.8325E-01	0.1649E-00	0.2465E-00	0.3202E-00	0.3842E-00	0.4861E-00	0.5861E-00
14	0.1350E-03	0.9831E-02	0.5166E-01	0.1187E-00	0.1929E-00	0.2641E-00	0.3282E-00	0.4339E-00	0.5339E-00
15	0.1806E-04	0.3736E-02	0.2885E-01	0.7969E-01	0.1437E-00	0.2097E-00	0.2722E-00	0.3794E-00	0.4794E-00
16	0.1475E-05	0.1130E-02	0.1412E-01	0.4908E-01	0.1006E-00	0.1590E-00	0.2176E-00	0.3236E-00	0.4236E-00
17	0.6468E-07	0.2568E-03	0.5861E-02	0.2714E-01	0.6525E-01	0.1138E-00	0.1662E-00	0.2678E-00	0.3678E-00
18	0.1296E-08	0.4086E-04	0.1980E-02	0.1313E-01	0.3850E-01	0.7386E-01	0.1202E-00	0.2135E-00	0.3135E-00
19	0.9693E-11	0.4099E-05	0.5166E-03	0.5368E-02	0.2018E-01	0.4630E-01	0.8109E-01	0.1626E-00	0.2626E-00
20	0.2098E-13	0.2341E-06	0.9765E-04	0.1779E-02	0.9126E-02	0.2532E-01	0.5024E-01	0.1171E-00	0.2171E-00
21	0.9542E-17	0.6540E-08	0.1222E-04	0.4534E-03	0.3432E-02	0.1207E-01	0.2799E-01	0.7859E-01	0.1299E-01
22	0.6086E-21	0.7434E-10	0.9190E-06	0.8320E-04	0.1024E-02	0.4849E-02	0.1366E-01	0.4839E-01	0.6839E-01
23	0.3275E-26	0.2725E-12	0.3629E-07	0.1003E-04	0.2288E-03	0.1572E-02	0.5652E-02	0.2675E-01	0.4675E-01
24	0.7841E-33	0.2404E-15	0.6374E-09	0.7190E-06	0.3564E-04	0.3895E-03	0.1900E-02	0.1293E-01	0.2933E-01
25	0.	0.3531E-19	0.4040E-11	0.2675E-07	0.3478E-05	0.6901E-04	0.4929E-03	0.5281E-02	0.6281E-02
26	0.	0.5429E-24	0.7099E-14	0.4359E-09	0.1919E-06	0.7950E-05	0.9248E-04	0.1748E-02	0.2748E-02
27	0.	0.4874E-30	0.2482E-17	0.2514E-11	0.5134E-08	0.5390E-06	0.1147E-04	0.4448E-03	0.6448E-03
28	0.	0.	0.1137E-21	0.3923E-14	0.5525E-10	0.1869E-07	0.8515E-06	0.8145E-04	0.9788E-05
29	0.	0.	0.4036E-27	0.1181E-17	0.1891E-12	0.2787E-09	0.3311E-07	0.5705E-09	0.9788E-05
30	0.	0.	0.5720E-34	0.4484E-22	0.1530E-15	0.1438E-11	0.5705E-09	0.6993E-06	0.9993E-06

PROBABILITY OF ERROR (APPROXIMATE FORMULA)

E/N_0	P (24) C_C	P (28) C_C	P (32) C_C	P (40) C_C	P (48) C_C	P (56) C_C	P (64) C_C
0	0.9074E 00	0.9206E 00	0.9305E 00	0.9444E 00	0.9536E 00	0.9602E 00	0.9652E 00
1	0.8938E 00	0.9089E 00	0.9202E 00	0.9361E 00	0.9467E 00	0.9543E 00	0.9600E 00
2	0.8787E 00	0.8959E 00	0.9088E 00	0.9270E 00	0.9391E 00	0.9478E 00	0.9543E 00
3	0.8620E 00	0.8815E 00	0.8962E 00	0.9169E 00	0.9307E 00	0.9406E 00	0.9480E 00
4	0.8434E 00	0.8656E 00	0.8822E 00	0.9056E 00	0.9213E 00	0.9325E 00	0.9409E 00
5	0.8229E 00	0.8479E 00	0.8667E 00	0.8931E 00	0.9109E 00	0.9236E 00	0.9331E 00
6	0.8002E 00	0.8283E 00	0.8494E 00	0.8793E 00	0.8993E 00	0.9136E 00	0.9244E 00
7	0.7751E 00	0.8065E 00	0.8303E 00	0.8638E 00	0.8863E 00	0.9025E 00	0.9146E 00
8	0.7473E 00	0.7824E 00	0.8050E 00	0.8466E 00	0.8720E 00	0.8901E 00	0.9038E 00
9	0.7166E 00	0.7557E 00	0.7854E 00	0.8275E 00	0.8559E 00	0.8763E 00	0.8917E 00
10	0.6829E 00	0.7262E 00	0.7592E 00	0.8063E 00	0.8381E 00	0.8609E 00	0.8782E 00
11	0.6458E 00	0.6936E 00	0.7303E 00	0.7827E 00	0.8182E 00	0.8438E 00	0.8631E 00
12	0.6054E 00	0.6578E 00	0.6983E 00	0.7564E 00	0.7960E 00	0.8247E 00	0.8463E 00
13	0.5615E 00	0.6186E 00	0.6631E 00	0.7274E 00	0.7714E 00	0.8034E 00	0.8275E 00
14	0.5142E 00	0.5760E 00	0.6246E 00	0.6954E 00	0.7442E 00	0.7797E 00	0.8066E 00
15	0.4638E-00	0.5299E 00	0.5825E 00	0.6601E 00	0.7140E 00	0.7534E 00	0.7834E 00
16	0.4106E-00	0.4806E-00	0.5371E 00	0.6214E 00	0.6806E 00	0.7242E 00	0.7575E 00
17	0.3556E-00	0.4284E-00	0.4883E-00	0.5792E 00	0.6440E 00	0.6920E 00	0.7299E 00
18	0.2997E-00	0.3740E-00	0.4366E-00	0.5336E 00	0.6039E 00	0.6566E 00	0.6972E 00
19	0.2444E-00	0.3183E-00	0.3825E-00	0.4847E-00	0.5604E 00	0.6177E 00	0.6623E 00
20	0.1914E-00	0.2627E-00	0.3270E-00	0.4329E-00	0.5134E 00	0.5753E 00	0.6240E 00
21	0.1426E-00	0.2088E-00	0.2713E-00	0.3788E-00	0.4633E-00	0.5295E 00	0.5822E 00
22	0.9988E-01	0.1583E-00	0.2170E-00	0.3233E-00	0.4104E-00	0.4804E-00	0.5370E 00
23	0.6482E-01	0.1134E-00	0.1660E-00	0.2677E-00	0.3556E-00	0.4285E-00	0.4894E-00
24	0.3826E-01	0.7566E-01	0.1200E-00	0.2136E-00	0.2999E-00	0.3742E-00	0.4369E-00
25	0.2006E-01	0.4622E-01	0.8108E-01	0.1628E-00	0.2447E-00	0.3187E-00	0.3829E-00
26	0.9078E-02	0.2530E-01	0.5030E-01	0.1173E-00	0.1918E-00	0.2632E-00	0.3276E-00
27	0.3415E-02	0.1208E-01	0.2806E-01	0.7885E-01	0.1430E-00	0.2093E-00	0.2720E-00
28	0.1020E-02	0.4858E-02	0.1372E-01	0.4862E-01	0.1003E-00	0.1589E-00	0.2177E-00
29	0.2280E-03	0.1577E-02	0.5685E-02	0.2692E-01	0.6518E-01	0.1140E-00	0.1666E-00
30	0.3555E-04	0.3917E-03	0.1916E-02	0.1304E-01	0.3854E-01	0.7613E-01	0.1207E-00

APPENDIX C

Tables of $P_c^{(m)}$ As Computed From Exact Formula

PROBABILITY OF ERROR (EXACT FORMULA)

E/N^0	$P(2)$	$P(4)$	$P(8)$	$P(16)$	$P(32)$	$P(64)$
(dB)	C_C	C_C	C_C	C_C	C_C	C_C
-14	0.4805E-00	0.7361E-00	0.8674E-00	0.9336E-00	0.9668E-00	0.9834E-00
-7	0.4096E-00	0.6832E-00	0.8383E-00	0.9187E-00	0.9593E-00	0.9797E-00
0	0.1839E-00	0.4762E-00	0.7163E-00	0.8551E-00	0.9272E-00	0.9635E-00
1	0.1420E-00	0.4255E-00	0.6836E-00	0.8376E-00	0.9183E-00	0.9591E-00
2	0.1025E-00	0.3703E-00	0.6462E-00	0.8173E-00	0.9079E-00	0.9539E-00
3	0.6799E-01	0.3120E-00	0.6039E-00	0.7940E-00	0.8960E-00	0.9479E-00
4	0.4056E-01	0.2529E-00	0.5571E-00	0.7676E-00	0.8824E-00	0.9410E-00
5	0.2116E-01	0.1956E-00	0.5063E-00	0.7380E-00	0.8670E-00	0.9332E-00
6	0.9333E-02	0.1429E-00	0.4522E-00	0.7052E-00	0.8497E-00	0.9245E-00
7	0.3329E-02	0.9754E-01	0.3956E-00	0.6691E-00	0.8305E-00	0.9148E-00
8	0.9094E-03	0.6123E-01	0.3377E-00	0.6297E-00	0.8092E-00	0.9039E-00
9	0.1775E-03	0.3468E-01	0.2798E-00	0.5868E-00	0.7855E-00	0.8917E-00
10	0.2270E-04	0.1730E-01	0.2235E-00	0.5406E-00	0.7593E-00	0.8782E-00
11	0.1704E-05	0.7357E-02	0.1708E-00	0.4912E-00	0.7303E-00	0.8631E-00
12	0.6544E-07	0.2565E-02	0.1235E-00	0.4389E-00	0.6983E-00	0.8463E-00
13	0.1081E-08	0.6967E-03	0.8342E-01	0.3843E-00	0.6631E-00	0.8275E-00
14	0.6166E-11	0.1383E-03	0.5176E-01	0.3283E-00	0.6246E-00	0.8066E-00
15	0.9234E-14	0.1853E-04	0.2890E-01	0.2722E-00	0.5826E-00	0.7834E-00
16	0.2567E-17	0.1513E-05	0.1414E-01	0.2176E-00	0.5371E-00	0.7575E-00
17	0.8564E-22	0.6630E-07	0.5870E-02	0.1663E-00	0.4883E-00	0.7289E-00
18	0.1981E-27	0.1328E-08	0.1983E-02	0.1202E-00	0.4366E-00	0.6972E-00
19	0.1591E-34	0.9932E-11	0.5172E-03	0.8110E-01	0.3825E-00	0.6623E-00
20	0*	0.2150E-13	0.9754E-04	0.5029E-01	0.3270E-00	0.6240E-00
21	0*	0*	0.1224E-04	0.2800E-01	0.2713E-00	0.5822E-00
22	0*	0*	0.9203E-06	0.1367E-01	0.2170E-00	0.5370E-00
23	0*	0*	0.3635E-07	0.5652E-02	0.1660E-00	0.4884E-00
24	0*	0*	0.6387E-09	0.1901E-02	0.1201E-00	0.4369E-00
25	0*	0*	0.4051E-11	0.4928E-03	0.8108E-01	0.3829E-00
26	0*	0*	0.7135E-14	0.9226E-04	0.5030E-01	0.3276E-00
27	0*	0*	0*	0.1147E-04	0.2806E-01	0.2720E-00
28	0*	0*	0*	0.8529E-06	0.1372E-01	0.2177E-00
29	0*	0*	0*	0.3324E-07	0.5687E-02	0.1666E-00
30	0*	0*	0*	0.5759E-09	0.1917E-02	0.1207E-00

3 January 1961

I(h) DETECT MEMO NO. 11

SUBJECT: "Error Probabilities of m-state Differentially Coherent Phase Shift Keyed Systems (DCPSKS) with a Frequency Offset of the Received Signals"

BY: Eugene A. Trabka

SUMMARY

Expressions are obtained for the subject error probabilities which were then evaluated on the IBM 704 computer. The results are presented graphically in Figure 3 and also in tabular form in Appendix A.

INTRODUCTION

The operation of m-state DCPSKS was described in Reference 1 at which time error probability curves representing their performance were given. It is the intent of the present analysis to obtain error probabilities in the case when the received signals are subject to a frequency offset, such as may be caused by frequency errors of heterodyne oscillators used for spectrum shifting.

The receiver input, $y(t)$, is again assumed to consist of signal, $s(t)$, plus white Gaussian noise, $n(t)$, with single-sided power spectral density N_0 watts/cps, viz

$$y(t) = s(t) + n(t) \quad (1)$$

The signal component of the receiver input may be written as

$$s(t) = \sum_{k=0}^m u\left(\frac{(k-1)T}{T}\right) A \sin \left[(\omega_b + \Delta\omega) t + \theta + \phi_k \right] \quad (2)$$

3 January 1961
DETECT MEMO NO. 11
AF 30(602)-2210

where $\epsilon(X)$ is the unit rectangle function defined to be one for $0 \leq X \leq 1$ and zero elsewhere, T is the duration of an elementary signal, ω_0 is the carrier angular frequency, $\Delta\omega$ is the frequency offset and θ is an arbitrary unknown phase. The ϕ_i are random variables determined by the transmitted information. The ϕ_i associated with the k -th interval, as shown in Figure 1, are determined at the transmitter as follows: ϕ_0 is an arbitrary starting phase and in an m -state system ϕ_i is chosen such that $\phi_i - \phi_{i-1}$ has one of the m equal spaced phases $\frac{2\pi}{m}(i-1)$ where $i = 1, 2, \dots, m$.

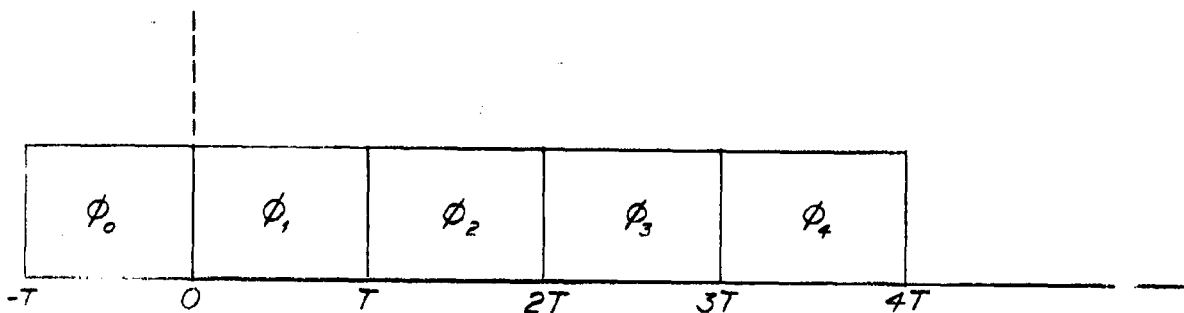


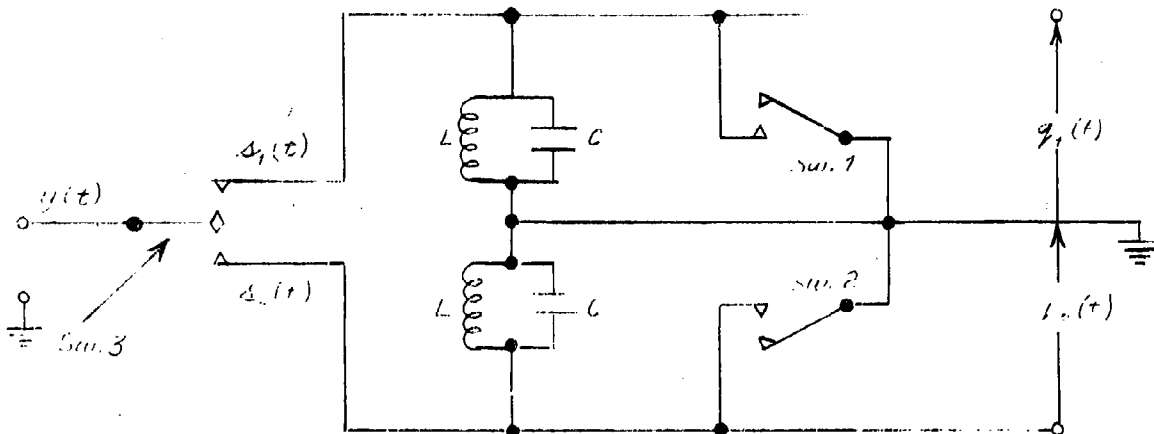
FIGURE 1

INTEGRATE, HOLD AND DUMP FILTERS

The receiving filters are assumed to be of the "integrate, hold and dump" variety as indicated in Figure 2, and described in Reference 2. The lumped parameters L and C are chosen such that $1/C = A$ and $1/LC = \omega_0^2$. The operation of the switches in Figure 2 is as follows: SW1 and SW2 are open for all t except that SW1 is closed for $t = kT$ where k is even

3 January 1961
DETECT MEMO NO. 11
AF 30(602)-2210

and SW2 is closed for $t = kT$ where k is odd; SW3 is up for $(k-1)T < t < kT$ where k is odd and down for $(k-1)T < t < kT$ where k is even. Consequently, one filter is allowed to ring while the other is "integrating".



INTEGRATE, HOLD AND DUMP FILTER
FIGURE 2

DECISION PROCESS

The phase difference between the filter outputs, $q_1(t)$ and $q_2(t)$ is sampled just prior to $t = kT$ (i.e., at $t = kT^-$) and the value of $\frac{2\pi}{m} (i-1)$ for $i = 1, 2, m$ closest to this phase difference is considered to have been the transmitted phase difference. If k is even, the difference in phase of the keyed filter pair is taken in the order 2 minus 1;

3 January 1961
 DETECT MEMO NO. 11.
 AF 30(602)-2210

and 1 minus 2 if ϵ is odd. It will be sufficient in determining the error probability to consider the statistics at one sampling time, say $t = 2T$

KEYED FILTER PAIR OUTPUTS

Formal expressions for the signal components of the keyed filter pair outputs, $q_i(t)$, in terms of their respective inputs, $s_i(t)$, are

$$q_i(t) = \int_{-\infty}^{+\infty} s_i(\tau) w_i(t, \tau) d\tau; \quad i=1, 2 \quad (3)$$

where $w_i(t, \tau)$ is the response at time t of the i th filter to a unit current impulse applied at time τ . It is not difficult to show that the voltage response of the upper section in Figure 1 to a unit current impulse applied at time $t = \tau$ where $0 < \tau < T$ is given by

$$w_1(t, \tau) = A u\left(\frac{t-\tau}{2T-\tau}\right) \cos \omega_o(t-\tau) = h_1(t-\tau) \quad (4)$$

and the voltage response of the lower section to a unit current impulse applied at $t = \tau$ where $T < \tau < 2T$ is given by

$$w_2(t, \tau) = A u\left(\frac{t-\tau}{3T-\tau}\right) \cos \omega_o(t-\tau) = h_2(t-\tau) \quad (5)$$

From equation (2) and taking account of the operation of the switches in Figure 2, one has for the respective inputs

$$s_1(t) = u\left(\frac{t}{T}\right) A \sin \left[(\omega_o + \Delta \omega) t + \theta + \phi_1 \right] \quad (6)$$

3 January 1961
 DETECT MEMO NO. 7.1
 AF 30(602)-2210

for $0 < t < T$ and

$$s_e(t) = u \left(\frac{t-T}{T} \right) A \sin \left[(\omega_0 + \Delta\omega)t + \theta + \phi_e \right] \quad (7)$$

for $T < t < 2T$. Introducing complex notation by letting

$$h_i(t) = \operatorname{Re} \left\{ H_i(t) e^{i\omega_0 t} \right\}; \quad i = 1, 2 \quad (8)$$

where

$$H_1(t) = Au \left(\frac{t}{2T-t} \right) \quad (9)$$

$$H_2(t) = Au \left(\frac{t}{3T-t} \right)$$

and

$$s_i(t) = \operatorname{Re} \left\{ S_i(t) e^{i(\omega_0 + \Delta\omega)t} \right\}; \quad i = 1, 2 \quad (10)$$

where

$$S_1(t) = Au \left(\frac{t}{T} \right) e^{i[\theta + \phi_1 - \pi/2]} \quad (11)$$

$$S_2(t) = Au \left(\frac{t-T}{T} \right) e^{i[\theta + \phi_2 - \pi/2]}$$

then

$$q_i(t) = \operatorname{Re} \left\{ Q_i(t) e^{i\omega_0 t} \right\} \quad (12)$$

where*

$$Q_i(t) = \frac{1}{2} \int_{-\infty}^{+\infty} S_i(\tau) H_i(t-\tau) e^{-i\Delta\omega\tau} d\tau \quad (13)$$

and it is the arguments at $t = 2T^-$ of $Q_i(t)$ (complex numbers) which are the desired phases. Using (9) and (11), one obtains

$$Q_1(2T^-) = \frac{A^2}{2} e^{i[\theta + \phi_1 - \pi/2]} \int_0^T e^{i\Delta\omega\tau} d\tau \quad (14)$$

$$Q_2(2T^-) = \frac{A^2}{2} e^{i[\theta + \phi_2 - \pi/2]} \int_T^{2T} e^{i\Delta\omega\tau} d\tau$$

Letting $\Delta\omega = 2\pi\Delta f$, $\Delta f = \alpha/T$, $E = \frac{1}{2} A^2 T$ and performing the indicated integrations in (14) yields

* See Appendix A of Reference 2

3 January 1965
 DETECT MEMO NO. 11
 AF 30(602)-2210

$$Q_1(2T) = E \frac{\sin \alpha \pi}{\alpha \pi} e^{i[\theta + \phi_1 - \frac{\pi}{2} + \alpha \pi]} \quad (15)$$

$$Q_2(2T) = E \frac{\sin \alpha \pi}{\alpha \pi} e^{i[\theta + \phi_2 - \frac{\pi}{2} + 3\alpha \pi]}$$

If the phase of $Q_2(2T)$ minus the phase of $Q_1(2T)$ is denoted by $\Delta\phi$, then

$$\Delta\phi = \phi_2 - \phi_1 + \epsilon$$

where

$$\epsilon = 2\alpha \pi \quad (17)$$

so that the effect of the unknown frequency offset has been to introduce an unknown bias, ϵ , in the phase difference measurement.

ERROR PROBABILITY

Upon consulting Reference 1, it is easily seen that the formal expression for the character error probability in an m -state DCPSKS with frequency offset of the received signals is

$$P_e(m) = 1 - \int_{-\frac{\pi}{m}}^{\frac{\pi}{m}} h(x - \epsilon) dx \quad (18)$$

3 January 1961
DETECT MEMO NO. 11
AF 30(602)-2210

where $\alpha(\chi)$ is given by equation (81) of Reference 1 and the parameter R of this equation must be taken to be

$$R = \frac{E}{N_0} \left(\frac{\sin \alpha \pi}{\alpha \pi} \right)^2 \quad (19)$$

and if (18) is to be valid for integer values of m greater than one, it is required that $|\epsilon| \leq \frac{\pi}{2}$ or $|\alpha| \leq \frac{1}{4}$.

RESULTS

The expression (18) was evaluated on the IBM 704 computer using a modification of the program used to obtain the results for $\alpha = 0$ reported in Reference 1. The results are presented graphically in Figure 3 and tabulated in Appendix A. The tendency of the curves representing systems with $m > 2$ to approach 1 for large α with increasing E/N_0 is due to the fact that if the bias ϵ is larger than the decision threshold π/m then in the absence of noise, wrong decisions are rendered with certainty. While Figure 3 illustrates the analytical results for a large range of α it is well to bear in mind that in many practical cases values of α of the order of 10^{-3} or less will be of interest.

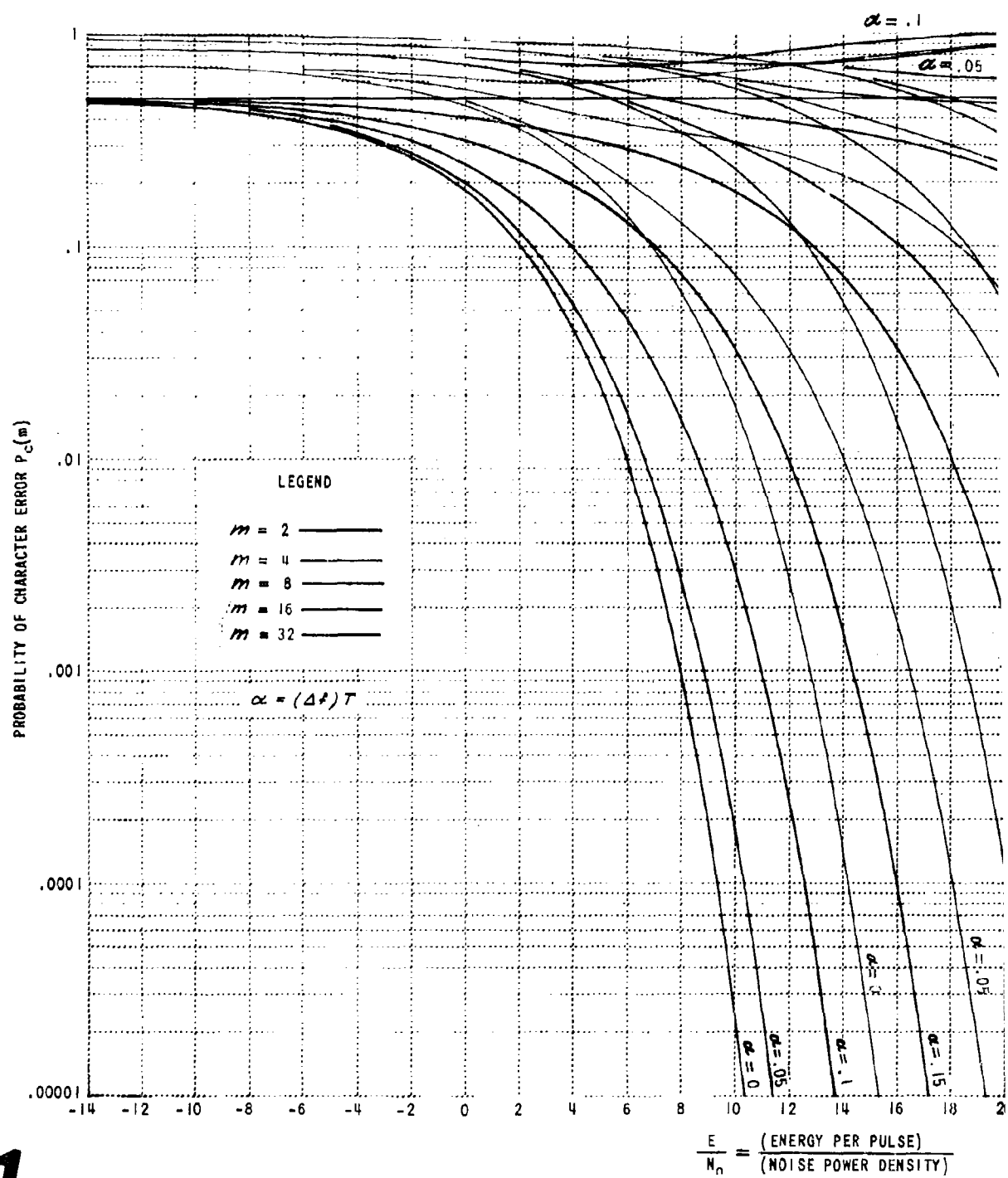


Figure 3 ERROR PROBABILITY OF m -STATE DCPSKS WITH

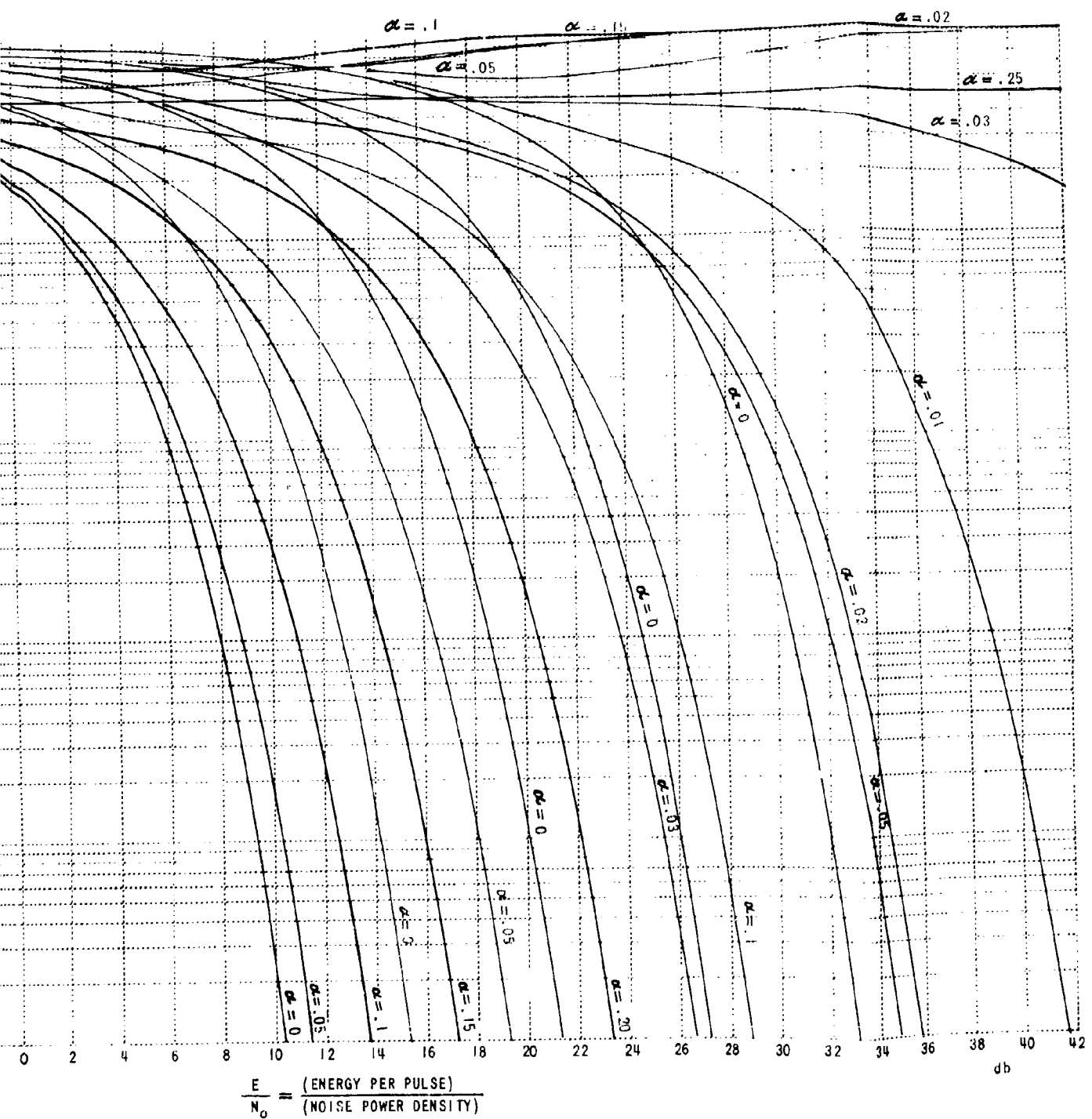


Figure 3 ERROR PROBABILITY OF m -STATE DCPSKS WITH FREQUENCY ERROR

3 January 1961
DETECT MEMO NO. 11
AF 30(602)-2210

REFERENCES

1. Fleck, John T. and Trabka, Eugene A. Error Probabilities of Multiple-State Differentially Coherent Phase Shift Keyed Systems in the Presence of White, Gaussian Noise DETECT MEMO NO. 2A Cornell Aeronautical Laboratory, Inc. 3 January 1961.
2. Trabka, Eugene A. Error Probabilities for Coherent Pulsed Phase-Shift Keyed Systems (CPPSKS) with Frequency and Sampling Time Errors DETECT MEMO NO. 7A Cornell Aeronautical Laboratory, Inc. 3 January 1961.

APPENDIX A - TABLES OF $P_c(m)$

E/N_G	(DE)	CHARACTER ERROR PROBABILITY P_c (2)	$\alpha = 0.05$	$\alpha = 0.10$	$\alpha = 0.15$	$\alpha = 0.20$
-14	0.4805E-00	0.4816E-00	0.4847E-00	0.4893E-00	0.4947E-00	0.4993E-00
-1C	0.4524E-00	0.4551E-00	0.4627E-00	0.4739E-00	0.4870E-00	0.4870E-00
-5	0.3644E-00	0.3719E-00	0.3931E-00	0.4249E-00	0.4624E-00	0.4624E-00
C	0.1839E-00	0.1991E-00	0.2440E-00	0.3157E-00	0.4057E-00	0.4057E-00
1	0.1420E-00	0.1579E-00	0.2063E-00	0.2862E-00	0.3896E-00	0.3896E-00
2	0.1025E-00	0.1184E-00	0.1685E-00	0.2551E-00	0.3720E-00	0.3720E-00
3	0.6799E-01	0.8291E-01	0.1320E-00	0.2230E-00	0.3530E-00	0.3530E-00
4	0.4056E-01	0.5336E-01	0.9860E-01	0.1906E-00	0.3326E-00	0.3326E-00
5	0.2116E-01	0.3101E-01	0.6951E-01	0.1586E-00	0.3108E-00	0.3108E-00
6	0.9333E-02	0.1592E-01	0.4569E-01	0.1277E-00	0.2875E-00	0.2875E-00
7	0.3329E-02	0.7020E-02	0.2755E-01	0.9877E-01	0.2628E-00	0.2628E-00
8	0.9094E-03	0.2571E-02	0.1492E-01	0.7261E-01	0.2366E-00	0.2366E-00
9	0.1775E-03	0.7472E-03	0.7049E-02	0.5012E-01	0.2093E-00	0.2093E-00
10	0.2270E-04	0.1627E-03	0.2809E-02	0.3198E-01	0.1810E-00	0.1810E-00
11	0.1704E-05	0.2461E-04	0.9036E-03	0.1851E-01	0.1524E-00	0.1524E-00
12	0.6544E-07	0.2354E-05	0.22220E-03	0.9476E-02	0.1242E-00	0.1242E-00
13	0.	0.1263E-06	0.3889E-04	0.4165E-02	0.9722E-01	0.9722E-01
14	0.	0.	0.4452E-05	0.1512E-02	0.7240E-01	0.7240E-01
15	0.	0.	0.2986E-06	0.4320E-03	0.5070E-01	0.5070E-01
16	0.	0.	0.	0.9134E-04	0.3290E-01	0.3290E-01
17	0.	0.	0.	0.1324E-04	0.1942E-01	0.1942E-01
18	0.	0.	0.	0.1194E-05	0.1019E-01	0.1019E-01
19	0.	0.	0.	0.5929E-07	0.4613E-02	0.4613E-02
20	0.	0.	0.	0.	0.1738E-02	0.1738E-02
21	0.	0.	0.	0.	0.5200E-03	0.5200E-03
22	0.	0.	0.	0.	0.1167E-03	0.1167E-03
23	0.	0.	0.	0.	0.1830E-04	0.1830E-04
24	0.	0.	0.	0.	0.1836E-05	0.1836E-05
25	0.	0.	0.	0.	0.1058E-06	0.1058E-06
26	0.	0.	0.	0.	0.	0.
27	0.	0.	0.	0.	0.	0.
28	0.	0.	0.	0.	0.	0.
29	0.	0.	0.	0.	0.	0.
30	0.	0.	0.	0.	0.	0.

E/N _c (DB)	CHARACTER ERROR PROBABILITY P _c (4)		
	$\alpha = 0.$	$\alpha = 0.05$	$\alpha = 0.10$
-14	0.7361E 00	0.7369E 00	0.7392E 00
-15	0.7156E 00	0.7176E 00	0.7234E 00
-16	0.6473E 00	0.6540E 00	0.6726E 00
-17	0.4762E-00	0.4986E-00	0.5583E 00
-18	0.4255E-00	0.4536E-00	0.5282E 00
-19	0.3703E-00	0.4053E-00	0.4975E-00
-20	0.3120E-00	0.3549E-00	0.4694E-00
-21	0.2529E-00	0.3043E-00	0.4393E-00
-22	0.1956E-00	0.2554E-00	0.4141E-00
-23	0.1429E-00	0.2098E-00	0.3918E-00
-24	0.9754E-01	0.1688E-00	0.3720E-00
-25	0.6123E-01	0.1326E-00	0.3534E-00
-26	0.3468E-01	0.1012E-00	0.3347E-00
-27	0.1730E-01	0.7421E-01	0.3151E-00
-28	0.7357E-02	0.5154E-01	0.2940E-00
-29	0.2565E-02	0.3324E-01	0.2711E-00
-30	0.6967E-03	0.1958E-01	0.2467E-00
-31	0.1383E-03	0.1024E-01	0.2208E-00
-32	0.1853E-04	0.4616E-02	0.1937E-00
-33	0.1513E-05	0.1730E-02	0.1659E-00
-34	0.6630E-07	0.5141E-03	0.1379E-00
-35	0.	0.1142E-03	0.1106E-00
-36	0.	0.1760E-04	0.8482E-01
-37	0.	0.1714E-05	0.6160E-01
-38	0.	0.9373E-07	0.4181E-01
-39	0.	0.	0.2610E-01
-40	0.	0.	0.1467E-01
-41	0.	0.	0.7244E-02
-42	0.	0.	0.3040E-02
-43	0.	0.	0.1041E-02
-44	0.	0.	0.2766E-03
-45	0.	0.	0.5351E-04
-46	0.	0.	0.6972E-05
-47	0.	0.	0.5558E-06

E/N _c	(dB)	$\alpha = 0.$	$\alpha = 0.03$	$\alpha = 0.05$	$\alpha = 0.10$
-14	0.8674E 00	0.8676E 00	0.8679E 00	0.8691E 00	0.8691E 00
-10	0.8563E 00	0.8567E 00	0.8574E 00	0.8606E 00	0.8606E 00
-5	0.8182E 00	0.8196E 00	0.8221E 00	0.8329E 00	0.8329E 00
0	0.7163E 00	0.7219E 00	0.7314E 00	0.7704E 00	0.7704E 00
1	0.6836E 00	0.6911E 00	0.7037E 00	0.7543E 00	0.7543E 00
2	0.6462E 00	0.6561E 00	0.6729E 00	0.7386E 00	0.7386E 00
3	0.6039E 00	0.6172E 00	0.6394E 00	0.7244E 00	0.7244E 00
4	0.5571E 00	0.5748E 00	0.6042E 00	0.7133E 00	0.7133E 00
5	0.5063E 00	0.5298E 00	0.5684E 00	0.7067E 00	0.7067E 00
6	0.4522E-00	0.4830E-00	0.5332E 00	0.7061E 00	0.7061E 00
7	0.3956E-00	0.4355E-00	0.4998E-00	0.7122E 00	0.7122E 00
8	0.3377E-00	0.3885E-00	0.4694E-00	0.7249E 00	0.7249E 00
9	0.2798E-00	0.3430E-00	0.4426E-00	0.7433E 00	0.7433E 00
10	0.2235E-00	0.2999E-00	0.4195E-00	0.7661E 00	0.7661E 00
11	0.1708E-00	0.2598E-00	0.3997E-00	0.7919E 00	0.7919E 00
12	0.1235E-00	0.2228E-00	0.3820E-00	0.8194E 00	0.8194E 00
13	0.8342E-01	0.1888E-00	0.3654E-00	0.8476E 00	0.8476E 00
14	0.5176E-01	0.1572E-00	0.3486E-00	0.8755E 00	0.8755E 00
15	0.2890E-01	0.1278E-00	0.3308E-00	0.9023E 00	0.9023E 00
16	0.1414E-01	0.1004E-00	0.3114E-00	0.9270E 00	0.9270E 00
17	0.5870E-02	0.7534E-01	0.2904E-00	0.9487E 00	0.9487E 00
18	0.1983E-02	0.5332E-01	0.2677E-00	0.9666E 00	0.9666E 00
19	0.5172E-03	0.3506E-01	0.2433E-00	0.9802E 00	0.9802E 00
20	0.9754E-04	0.2103E-01	0.2174E-00	0.9895E 00	0.9895E 00
21	0.1224E-04	0.1126E-01	0.1904E-00	0.9952E 00	0.9952E 00
22	0.9203E-06	0.5227E-02	0.1626E-00	0.9982E 00	0.9982E 00
23	0.	0.2031E-02	0.1348E-00	0.9995E 00	0.9995E 00
24	0.	0.6313E-03	0.1077E-00	0.9999E 00	0.9999E 00
25	0.	0.1483E-03	0.8226E-01	0.1000E 01	0.1000E 01
26	0.	0.2454E-04	0.5941E-01	0.	0.
27	0.	0.2611E-05	0.4004E-01	0.	0.
28	0.	0.1596E-06	0.2478E-01	0.	0.
29	0.	0.	0.1378E-01	0.	0.
30	0.	0.6710E-02	0.	0.	0.

E/N_0	CHARACTER ERROR PROBABILITY $P_C(8)$		
(dB)	$\alpha = 0.$	$\alpha = 0.03$	$\alpha = 0.05$
31	0.	0.	$0.2768E-02$
32	0.	0.	$0.9279E-03$
33	0.	0.	$0.2400E-03$
34	0.	0.	$0.4490E-04$
35	0.	0.	$0.5613E-05$

E/N_0	(DB)	$\alpha = 0.$	CHARACTER ERROR PROBABILITY $P_c(16)$	$\alpha = 0.02$	$\alpha = 0.03$	$\alpha = 0.05$
-14	0.9336E 00	0.9337E 00	0.9337E 00	0.9337E 00	0.9339E 00	0.9339E 00
-10	0.9279E 00	0.9280E 00	0.9280E 00	0.9281E 00	0.9285E 00	0.9285E 00
-5	0.9084E 00	0.9087E 00	0.9087E 00	0.9091E 00	0.9104E 00	0.9104E 00
0	0.8551E 00	0.8564E 00	0.8564E 00	0.8581E 00	0.8633E 00	0.8633E 00
1	0.8376E 00	0.8395E 00	0.8395E 00	0.8417E 00	0.8486E 00	0.8486E 00
2	0.8173E 00	0.8198E 00	0.8198E 00	0.8229E 00	0.8322E 00	0.8322E 00
3	0.7940E 00	0.7975E 00	0.7975E 00	0.8016E 00	0.8143E 00	0.8143E 00
4	0.7676E 00	0.7723E 00	0.7723E 00	0.7781E 00	0.7952E 00	0.7952E 00
5	0.7380E 00	0.7445E 00	0.7445E 00	0.7524E 00	0.7756E 00	0.7756E 00
6	0.7052E 00	0.7141E 00	0.7141E 00	0.7249E 00	0.7562E 00	0.7562E 00
7	0.6691E 00	0.6814E 00	0.6814E 00	0.6960E 00	0.7380E 00	0.7380E 00
8	0.6297E 00	0.6465E 00	0.6465E 00	0.6663E 00	0.7220E 00	0.7220E 00
9	0.5868E 00	0.6097E 00	0.6097E 00	0.6364E 00	0.7094E 00	0.7094E 00
10	0.5406E 00	0.5715E 00	0.5715E 00	0.6070E 00	0.7013E 00	0.7013E 00
11	0.4912E-00	0.5324E 00	0.5324E 00	0.5790E 00	0.6986E 00	0.6986E 00
12	0.4389E-00	0.4931E-00	0.4931E-00	0.5535E 00	0.7019E 00	0.7019E 00
13	0.3843E-00	0.4545E-00	0.4545E-00	0.5312E 00	0.7115E 00	0.7115E 00
14	0.3283E-00	0.4174E-00	0.4174E-00	0.5129E 00	0.7267E 00	0.7267E 00
15	0.2722E-00	0.3826E-00	0.3826E-00	0.4987E-00	0.7468E 00	0.7468E 00
16	0.2176E-00	0.3504E-00	0.3504E-00	0.4885E-00	0.7704E 00	0.7704E 00
17	0.1663E-00	0.3208E-00	0.3208E-00	0.4814E-00	0.7964E 00	0.7964E 00
18	0.1202E-00	0.2933E-00	0.2933E-00	0.4764E-00	0.8237E 00	0.8237E 00
19	0.8110E-01	0.2670E-00	0.2670E-00	0.4725E-00	0.8516E 00	0.8516E 00
20	0.5025E-01	0.2410E-00	0.2410E-00	0.4689E-00	0.8792E 00	0.8792E 00
21	0.2800E-01	0.2145E-00	0.2145E-00	0.4650E-00	0.9056E 00	0.9056E 00
22	0.1357E-01	0.1872E-00	0.1872E-00	0.4607E-00	0.9299E 00	0.9299E 00
23	0.5652E-02	0.1594E-00	0.1594E-00	0.4559E-00	0.9511E 00	0.9511E 00
24	0.1901E-02	0.1316E-00	0.1316E-00	0.4506E-00	0.9684E 00	0.9684E 00
25	0.4928E-03	0.1047E-00	0.1047E-00	0.4446E-00	0.9814E 00	0.9814E 00
26	0.9226E-04	0.7947E-01	0.7947E-01	0.4378E-00	0.9903E 00	0.9903E 00
27	0.1147E-04	0.5698E-01	0.5698E-01	0.4303E-00	0.9957E 00	0.9957E 00
28	0.8529E-06	0.3806E-01	0.3806E-01	0.4219E-00	0.9984E 00	0.9984E 00
29	0.	0.2329E-01	0.2329E-01	0.4125E-00	0.9995E 00	0.9995E 00
30	0.	0.1277E-01	0.1277E-01	0.4021E-00	0.9999E 00	0.9999E 00

E/N_0	$\alpha = 0.$	$\alpha = 0.02$	$\alpha = 0.03$	$\alpha = 0.05$
(dB)				
31	0.	0.6112E-02	0.3904E-00	0.
32	0.	0.2466E-02	0.3774E-00	0.
33	0.	0.8040E-03	0.3631E-00	0.
34	0.	0.2005E-03	0.3471E-00	0.
35	0.	0.3575E-04	0.3296E-00	0.
36	0.	0.	0.3104E-00	0.
37	0.	0.	0.2894E-00	0.
38	0.	0.	0.2666E-00	0.
39	0.	0.	0.2423E-00	0.
40	0.	0.	0.2164E-00	0.
41	0.	0.	0.1894E-00	0.
42	0.	0.	0.1616E-00	0.

E/N _C	CHARACTER ERROR PROBABILITY P _C (32)		
	(Df)	$\alpha = 0.$	$\alpha = 0.01$
-10	0.9668E 00	0.9668E 00	0.9668E 00
-5	0.9639E 00	0.9639E 00	0.9640E 00
0	0.9541E 00	0.9541E 00	0.9543E 00
1	0.9272E 00	0.9273E 00	0.9278E 00
2	0.9183E 00	0.9185E 00	0.9192E 00
3	0.9079E 00	0.9082E 00	0.9092E 00
4	0.8960E 00	0.8964E 00	0.8978E 00
5	0.8824E 00	0.8830E 00	0.8848E 00
6	0.8670E 00	0.8678E 00	0.8704E 00
7	0.8497E 00	0.8510E 00	0.8545E 00
8	0.8305E 00	0.8322E 00	0.8372E 00
9	0.8092E 00	0.8116E 00	0.8184E 00
10	0.7593E 00	0.7639E 00	0.7772E 00
11	0.7303E 00	0.7367E 00	0.7550E 00
12	0.6983E 00	0.7072E 00	0.7322E 00
13	0.6631E 00	0.6754E 00	0.7094E 00
14	0.6246E 00	0.6414E 00	0.6873E 00
15	0.5826E 00	0.6054E 00	0.6668E 00
16	0.5371E 00	0.5680E 00	0.6488E 00
17	0.4883E-00	0.5295E 00	0.6344E 00
18	0.4366E-00	0.4909E-00	0.6246E 00
19	0.3825E-00	0.4528E-00	0.6201E 00
20	0.3270E-00	0.4162E-00	0.6210E 00
21	0.2713E-00	0.3817E-00	0.6271E 00
22	0.2170E-00	0.3498E-00	0.6377E 00
23	0.1660E-00	0.3205E-00	0.6518E 00
24	0.1201E-00	0.2932E-00	0.6685E 00
25	0.8108E-01	0.2671E-00	0.6874E 00
26	0.5030E-01	0.2413E-00	0.7081E 00
27	0.2806E-01	0.2151E-00	0.7307E 00
28	0.1372E-01	0.1880E-00	0.7549E 00
29	0.5687E-02	0.1602E-00	0.7806E 00
30	0.1917E-02	0.1323E-00	0.8075E 00

E/N_0	CHARACTER ERROR PROBABILITY $P_c(32)$	
(DF)	$\alpha = 0.$	$\alpha = 0.01$
21	0.4984E-03	0.1052E-00
32	0.9355E-04	0.7983E-01
33	0.1170E-04	0.5726E-01
34	0.	0.3829E-01
35	0.	0.2346E-01
36	0.	0.1289E-01
37	0.	0.6184E-02
38	0.	0.2502E-02
39	0.	0.8186E-03
40	0.	0.2051E-03
41	0.	0.3677E-04
42	0.	0.4330E-05

APPENDIX II

APPENDIX II

DERIVATION OF RESULTS USED IN CHAPTER III

- (a) DETECT MEMO NO. 13 - "Analysis of a Differentially Coherent Phase Shift Keyed (DCPSK) Digital Data Systems Operating Over a Fading FM Tropospheric Scatter Circuit" by Harold A. Becker.

CORNELL AERONAUTICAL LABORATORY, INC.
Buffalo 21, New York

17 January 1961

II(a) DETECT MEMO NO. 13

SUBJECT: "Analysis of DPSK Digital Data Systems Operating over a Fading FM Tropospheric Scatter Circuit."

BY: Harold D. Becker

SUMMARY

The theoretical performance of several phase modulation systems employed for the transmission of digital data over Rayleigh fading FM tropospheric scatter circuits is analyzed. The probabilities of error of two, four and eight-state differentially coherent PSK systems are computed and compared. A typical FM tropospheric scatter link with short-term Rayleigh amplitude fading characteristics is assumed. The relative importance of several of the transmission system parameters in determining the resultant error rate performance is then discussed. In particular, consideration is given to the effects of:

- a) different orders of diversity,
- b) a lowered FM receiver threshold,
- c) various median signal levels,
- d) operation on different frequency division multiplex channels.

INTRODUCTION

Considerable effort has been expended recently in the development of phase-shift keyed techniques as a method of transmitting digital data. This interest has developed, principally, because of: (1) recent developments in practical matched filters for demodulating this type of transmission, (2) the decreased bandwidth requirements of PSK systems, and (3) the superior theoretical performance of PSK systems with respect to other binary systems in the presence of white Gaussian noise.

The theoretical error rate performance of a binary differentially coherent PSK (DCPSK) system operating in the presence of additive, white Gaussian noise was derived in Reference 1. This work has been extended to include the analysis of m-state DCPSK systems as reported in DETECT Memo No. 2A. The results of these analyses are now applied to the investigation of the performance of DCPSK data link systems when utilizing a Rayleigh fading FM tropospheric scatter link.

The differentially coherent phase-shift keyed technique has been brought to an advanced state of development in the Collins' Kineplex equipment. One of these equipments designated as the GSC-4 is designed to transmit six frequency-division multiplexed subchannels of differentially coherent PSK signals via a 4 kc/s channel. The use of a DCPSK system of this type for the transmission of digital data over a typical FM tropospheric scatter circuit is shown in Figure 1. The DCPSK data link is assigned one subchannel of the frequency division multiplex system.

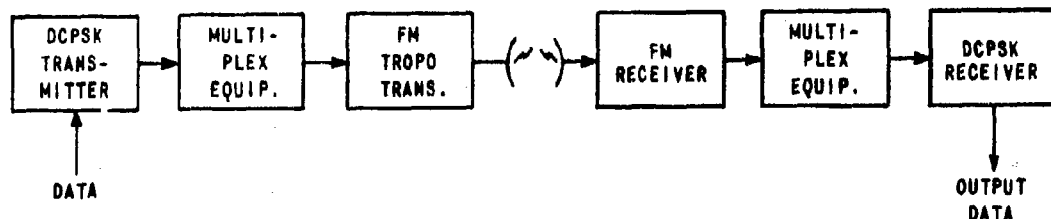


Figure 1 BLOCK DIAGRAM OF TROPO SYSTEM

The DCPSK system is assumed to consist of six subchannel tones on which the data is encoded as differential phase shifts between adjacent signals. The duration of each signal element is 1/300 seconds and the six tones are spaced 300 cps apart so that, theoretically, crosstalk between the six subchannels is eliminated.

The receiving system is shown in Figure 2. (The symbols used to denote signal-to-noise ratios at various points in the receiver are explained below.)

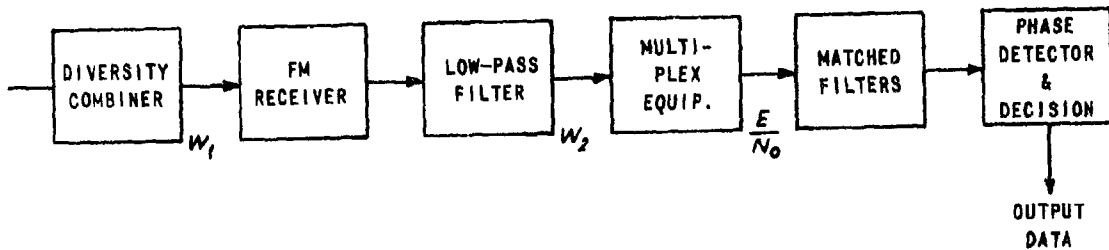


Figure 2 BLOCK DIAGRAM OF RECEIVING SYSTEM

Tropospheric scatter systems are characterized by rapid variations in the received signal level which may be assumed to be Rayleigh distributed as well as long-term variations due to slow changes in the characteristics of the troposphere, such as variations in the index of refraction. In this analysis, long-term fading was not considered except that computations for different median signal levels were made. A diversity receiving system using ideal predetection combining is postulated. In this system the received signals, which are assumed to have independent Rayleigh amplitude distributions, are optimally weighted in proportion to the square root of the signal-to-noise ratio of each signal and then combined coherently. Brilliant⁽²⁾ has derived the probability density function of the output signal-to-noise ratio, W_1 , of this type of combiner.

The theoretical performance of an FM receiver is then used to obtain the relationship of the receiver output signal-to-noise ratio (W_2) to the input signal-to-noise ratio (W_1). The signal energy-to-noise power density ratio, E/N_0 , at the input to the DCPSK matched filters is then calculated with respect to W_2 . Then the relationship between E/N_0 and W_1 is used with the expression for the probability density function of W_1 to derive the probability density function of E/N_0 at the input to the matched filters. The probability of

error of various differentially coherent PSK systems are derived in DETECT Memo No. 2A. as a function of E/N_0 , assuming that a maximum likelihood receiver (matched filter receiver or its equivalent) is used. Assuming that the fading is sufficiently slow so that these results may be applied, the average probability of error is computed by integrating the product of the probability density function of E/N_0 at the matched filter input and the conditional probability of error for a given E/N_0 , $P(e|E/N_0)$, over all values of E/N_0 .

$$P_e = \int_0^{\infty} P(e|E/N_0) f(E/N_0) d(E/N_0) \quad (3)$$

DETAILED ANALYSIS

If two or more signals are available, the fading characteristics of which are not completely correlated, diversity techniques may be utilized to obtain performance superior to that available from any one of the signals alone. If it can be assumed that the signals fade independently and all have the same Rayleigh distribution, the analysis becomes tractable. It has been shown⁽²⁾ that the probability density function, (w_1) , of the signal-to-noise ratio at the output of an ideal coherent diversity combiner is given by

$$p(w_1) = \frac{w_1^{m-1} e^{-\frac{w_1}{R_o}}}{(m-1)! R_o^m} \quad (4)$$

where m is the order of diversity and R_o is the mean signal-to-noise ratio in each channel. The mean signal level can be expected to vary hourly, daily, monthly, etc., as the conditions of the troposphere change; however, short-term fading, which is characterized by fading rates of the order of 1 to 10 cycles per second is found to follow the Rayleigh distribution very closely.

The actual distribution may depart somewhat from the Rayleigh distribution due to components of a reasonably constant level caused by diffraction or specular reflection.

In order to proceed with the analysis on a quantitative basis, the following characteristics taken from a typical FM tropospheric scatter system⁽³⁾ will be used.

a. Minimum yearly received Median signal	- 80 dbm
b. Design target received Median signal	- 60 dbm
c. I.F. bandwidth	4 mc/s
d. Receiver noise figure	5 db
e. Equivalent receiver Input noise level	- 103 dbm
f. Maximum deviation	240 kc/s
g. Base bandwidth (77 channels)	320 kc/s
h. Pre-emphasis at 320 kc/s	26 db
i. System voice-channel Load factor (77 channels)	18.5 db

The permissible deviation on each of the 77 frequency division multiplexed channels was determined in accordance with generally accepted channel assignment procedure.⁽⁴⁾ Pre-emphasis is employed to equalize the S/N on each of the 77 channels by compensating for the variation in the noise power density over the various channels during above threshold operation. For the assigned pre-emphasis, the deviation is modified with modulation frequency according to the relationship

$$\text{DEVIATION} \propto \sqrt{f_F(\omega_m T)^{\prime\prime}} \quad (5)$$

where $T = 10 \times 10^{-6}$ and ω_m is the channel radian frequency. Using this relationship, the relative deviation (Scale Factor) on each of the 77 channels was computed. See Table I.

TABLE I

Channel No.	Channel Center Frequency	Deviation Scale Factor	Computed Deviation
1	6 kc/s	1.1	2.7 kc/s
2	10 kc/s	1.2	3.0 kc/s
.	.	.	.
.	.	.	.
.	.	.	.
45	186 kc/s	11.7	29 kc/s
46	190 kc/s	12.0	30 kc/s
.	.	.	.
.	.	.	.
.	.	.	.
76	314 kc/s	19.8	49 kc/s
77	318 kc/s	20.0	50 kc/s

Because of the random phase addition of the subcarriers and the nature of the information transmitted, it is permissible for the sum of the deviations of each channel to exceed the prescribed maximum carrier deviation. The statistical nature of voice signal variations and channel utilization have been used (1) to obtain a loading factor curve. This curve shows that for a 77-channel system, the loading factor $F_{(db)}$ is approximately 18.5 db. This means that if the ratio of the specified carrier peak deviation to the deviation allotted to each channel in the absence of pre-emphasis is 18.5 db, the specified carrier deviation will not be exceeded more than one percent of the time. The loading factor is given by

$$F_{(db)} = 20 \log \frac{\Delta f}{f_d} \quad (6)$$

where Δf is the peak carrier deviation, and f_d is the deviation per channel. When re-emphasis is employed, the deviation in each channel is not constant and the deviation, f_d , is established on a channel near the mean frequency of the multiplex range. The mean subcarrier frequency in the assumed system is approximately 185 kc/s (channel 45) and therefore with the specified loading factor of 18.5 db, the deviation f_d of channel 45 is established as follows:

$$20 \log \frac{240 \text{ kc/s}}{f_d} = 18.5$$

$$\frac{240 \text{ kc/s}}{f_d} = 8.4$$

$$f_d = \frac{240}{8.4} = 29 \text{ kc/s}.$$

The deviation of each of the other channels is scaled according to the deviation scale factor as given in Table I. In practice, the deviations assigned to the lowest frequency channels are usually increased from the values obtained above in order to combat the residual noise level due to circuit hum, etc.

The performance of the data link utilizing channel 77 will now be computed. The modulation index for this channel is

$$\text{Mod. Index} = \frac{f_d}{f_m} = \frac{50}{318} = 0.16$$

Using this modulation index, the relationship between the input and output S/N of the FM receiving system may be used to relate W_1 and W_2 . The expressions commonly used in the analysis of FM receiver performance are valid only when the signal level exceeds the threshold. The theoretical noise performance curves for a frequency modulation receiver operating below the improvement threshold have been computed by F. J. Skinner⁽⁵⁾ and the curve corresponding to the FM system postulated for this analysis is plotted in Figure 3.

$$W_2(\text{db}) = \frac{E}{N_0} (\text{db}) - 22.5 \text{db}$$

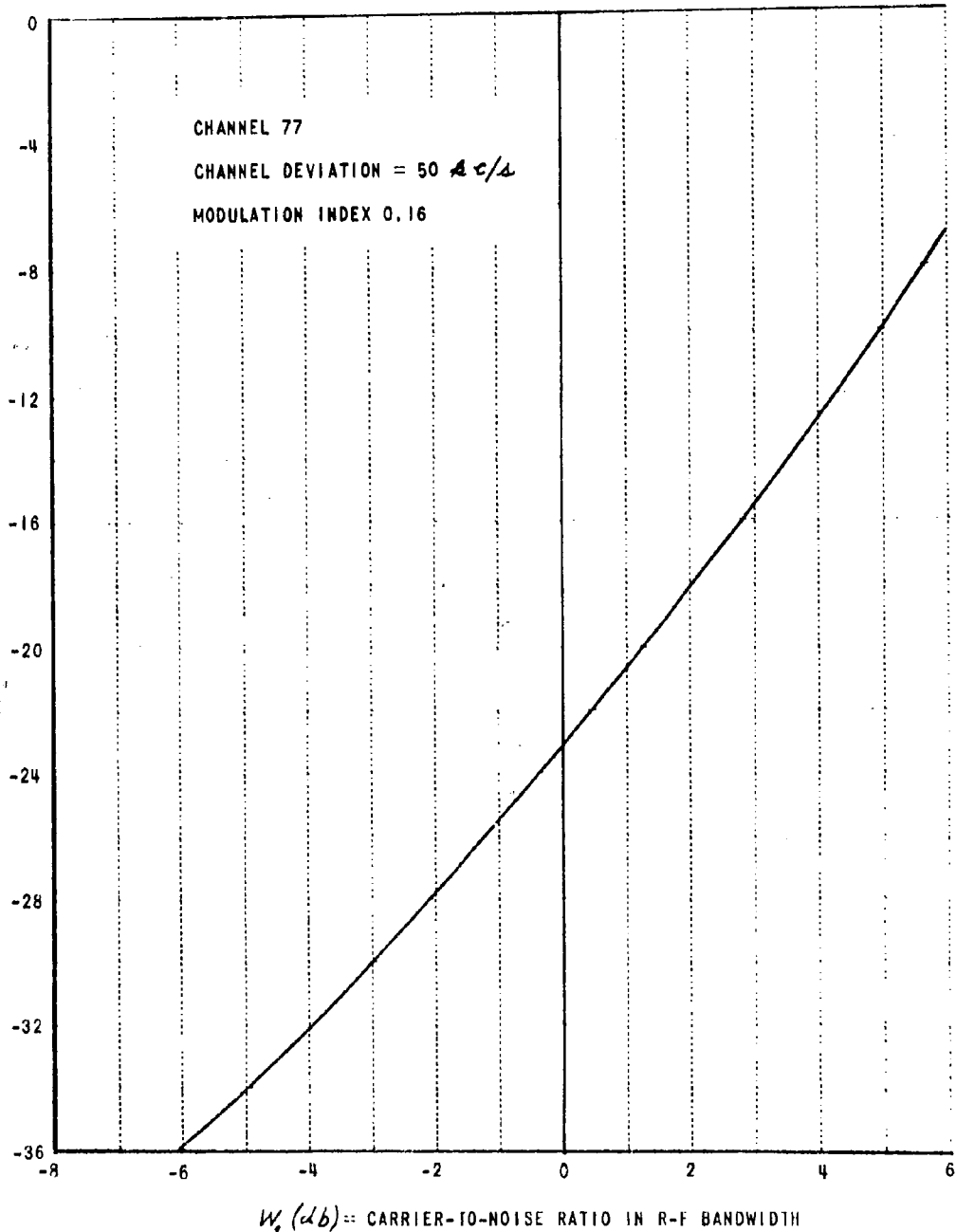


Figure 3 FM RECEIVING CHARACTERISTIC

Above threshold, the noise power density $N(f)$ at the output of the discriminator is generally assumed to be proportional to the square of the frequency. However, when the signals are well below the threshold, the curves in Skinner's memo show that $N(f)$ is reasonably constant with frequency. Therefore, well below threshold, the noise power (P_N) in the 320 kc/s bandwidth at the output of the FM receiver is

$$P_N = \int_0^{320 \text{ kc/s}} N(f) df = N_0 320 \text{ kc/s} = \frac{S}{W_2} \quad (7)$$

where S is the signal power in the 6 subchannel tones.

Therefore,

$$N_0 = \frac{S}{W_2 \times 3.2 \times 10^5} \quad (8)$$

Now, let S_c equal the signal power in each of the 6 tones.

Then

$$\frac{S_c}{N_0} = \frac{SW_2 \times 3.2 \times 10^5}{6S} \quad (9)$$

Hence,

$$\frac{E}{N_0} = \frac{S_c T}{N_0} = \frac{W_2 \times 3.2 \times 10^5}{6 \times 300}$$

$$\frac{E}{N_0} (\text{db}) = W_2 (\text{db}) + 22.5 \text{ db} \quad (10)$$

For every value of E/N_0 , the corresponding value of W_1 is obtained through the use of Equation (10) and the FM receiver characteristic curve which is plotted in Figure 3.

The probability density function of W_1 is given by⁽²⁾

$$P(W_1) = \frac{W_1^{m-1} e^{-\frac{W_1}{R_o}}}{(m-1)! R_o^m} \quad (11)$$

The probability density function, $q(E/N_0)$ of E/N_0 may be obtained in the following manner. Let W_1 , expressed as a function of E/N_0 , be

$$W_1 = f(E/N_0)$$

then

$$q(E/N_0) = p[f(E/N_0)] f'(E/N_0) = p[f(E/N_0)] \frac{d W_1}{d E/N_0} \quad (12)$$

The value of $d W_1 / d E/N_0$ is obtained graphically at each value of E/N_0 from the slope of straight lines tangent to the actual curve in Figure 3. The equation of these tangents may be written in the form $y = A x + b$ where A is the slope of the curve at the point of tangency.

Thus,

$$10 \log E/N_0 = A 10 \log W_1 + b \quad (13)$$

and using the relationship

$$\frac{d}{dx} \left[\log u \right] = \lim_{x \rightarrow 0} \frac{1}{u} \cdot \frac{du}{dx}$$

and differentiating both sides of Equation (13) with respect to E/N_0 results in

$$\log e \frac{1}{E/N_0} = A \log e \frac{1}{W_1} \frac{d W_1}{d E/N_0}$$

$$\frac{d W_1}{d E/N_0} = -\frac{W_1}{E/N_0} \frac{1}{A}$$

The error probability is computed by evaluating the integral

$$P_e = \int_0^\infty P(e | E/N_0) p[f(E/N_0)] \frac{d W_1}{d E/N_0} d(E/N_0) \quad (14)$$

For each value of E/N_0 , the value of the integrand of Equation (14) is computed as shown in the sample calculation in Table II. The integrand was plotted as a function of E/N_0 and the probability of error, which is equal to the area under the curve, was determined by graphical means. The resulting probabilities of error were computed in this manner for several combinations of DCPSK systems, orders of diversity, m , and mean signal levels, and are tabulated in Table III. A four-state DCPSK system may be obtained by combining two binary DCPSK subchannels in quadrature, as discussed in DETECT Memo No. 2A. The error probability of these DCPSK subchannels is indicated in column 5 of Table III.

In all cases which were examined, it was found that virtually all errors occurred when the signal level faded below the threshold level. Therefore, this analysis has been based on the theoretical signal-to-noise ratio performance of FM receivers operating below the FM threshold which has been investigated by F. J. Skinner. Although Skinner's analysis was derived for single frequency modulation, one finds that, below threshold, the noise output of FM receivers is independent of the modulation frequency and Skinner's curves may be applied to the multiplex case. It is believed that the performance predicted by these curves is approached closely by conventional FM receivers.

BDCPSK SYSTEM
 DUAL DIVERSITY
 $R_o = 43d/6 = 2 \times 10^4$

E/N_o (POWER)	W_t (POWER)	$\rho \left[f \left(E/N_o \right) \right] \cong \frac{W_t}{R_o^2}$	$\frac{d W_t}{d E/N_o} = \frac{W_t}{E/N_o} \cdot \frac{1}{A}$	$\rho \left(e E/N_o \right)$	INTEGRAND
4	1.82	0.455×10^{-8}	.175	9.2×10^{-3}	0.73×10^{-11}
3	1.64	0.410×10^{-8}	.21	2.5×10^{-2}	2.15×10^{-11}
2	1.39	0.348×10^{-8}	.27	6.8×10^{-2}	6.4×10^{-11}

$$*\rho \left[f \left(E/N_o \right) \right] = \rho \left(\omega_t \right) = \frac{W_t^{m-1} e^{-\frac{W_t}{R_o}}}{(m-1)! R_o^m}$$

$$\approx \frac{W_t^{m-1}}{(m-1)! R_o^m} \quad \text{if} \quad \frac{W_t}{R_o} \ll 1$$

$$\text{For } m = 2 \quad \rho(\omega) \approx \frac{W_t}{R_o^2}$$

TABLE II SAMPLE COMPUTATION

TABLE III COMPUTED ERROR PROBABILITIES

BINARY DCPSK SYSTEM			BINARY SUB-CHANNEL OF 4-STATE DCPSKS	4-STATE DCPSKS $P_e(4)$	8-STATE DCPSKS $P_e(8)$
ρ_o	m	NO. DIVERSITY	DUAL DIVERSITY	DUAL DIVERSITY	DUAL DIVERSITY
23 dB	2.2×10^{-3}	6.2×10^{-6}	2.2×10^{-11}	1.1×10^{-5}	1.8×10^{-5}
33 dB	2.2×10^{-4}	6.2×10^{-8}	2.2×10^{-15}	1.1×10^{-7}	1.8×10^{-7}
43 dB	2.2×10^{-5}	6.2×10^{-10}	2.2×10^{-19}	1.1×10^{-9}	1.8×10^{-9}

The results obtained in Table III assumed data link operation over the highest frequency multiplex channel and the performance over other channels could be computed in a similar manner. However, the range of the system parameters considered by Skinner does not permit the evaluation of the performance of the very low frequency channels. In another analysis⁽⁷⁾ by D. P. Harris, a convenient set of curves is presented from which the signal-to-noise ratio performance in any channel of a frequency division multiplex system may be determined. Figure 4 has been derived from Harris' article and illustrates the relationship between E/N_0 at the input to the matched filters as a function of carrier-to-noise ratio with channel frequency deviation, f_d , as a parameter. If operation is assumed on channel 77 ($f_d = 50$ kc/s), the resulting curve in Figure 4 is found to be in reasonable agreement with the corresponding curve taken from Skinner's work.

The effect of channel assignment on the performance of a given data link is easily obtained from Figure 4. For example, if operation on channel 77 ($f_d = 50$ kc/s) is to be compared with operation on channel 15 ($f_d = 10$ kc/s), the factor $20 \log 2^{f_d/B}$ would change by

$$\frac{20 \log 2(f_d = 50 \text{ kc/s})}{B} - \frac{20 \log 2(f_d = 10 \text{ kc/s})}{B} = 20 \log \frac{50}{10} = 14 \text{ db.}$$

From the slope of the curve in Figure 4, it is seen that a 14 db change in the value of the ordinate corresponds approximately to a 7 db change in the carrier-to-noise ratio, W_1 .

Referring to Table II, it is seen that if the value of W_1 required to obtain a given E/N_0 is increased by 7 db (power ratio of 5), both $p[f(E/N_0)]$ and $dW_1/dE/N_0$ will be increased by a factor of 5. Thus, in the case of dual diversity, the value of the integrand and, hence, the integral will be increased by a factor of 25. Therefore, the error probability of channel 15 is 25 times as great at the error probability of channel 77.

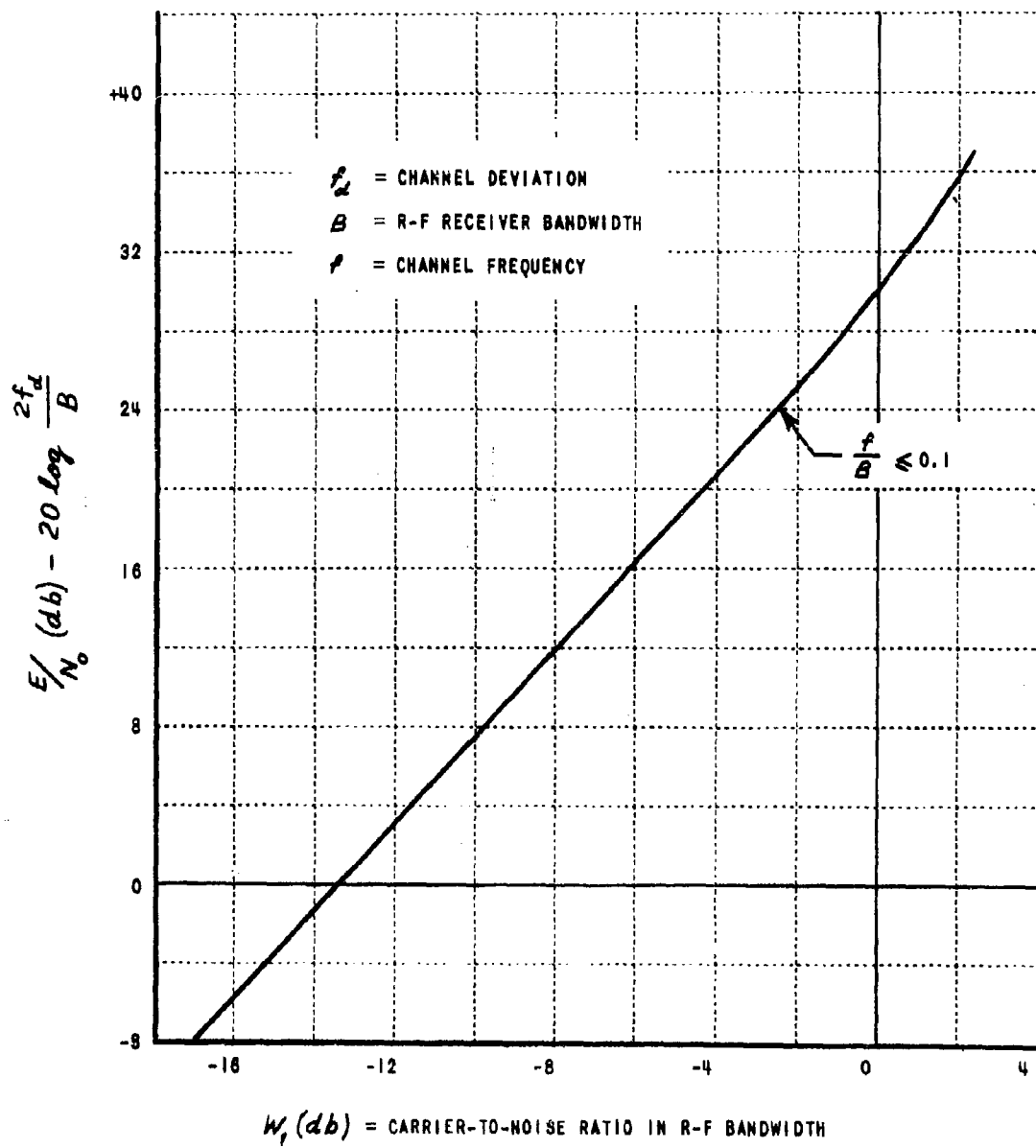


Figure 4 FM RECEIVING CHARACTERISTIC

In the case of quadruple diversity,

$$P\left[f\left(\frac{E}{N_0}\right)\right] \frac{dW_1}{d\left(\frac{E}{N_0}\right)} \approx \frac{W_1^3}{6R_o^2} \times \frac{W_1}{E/N_0 \cdot A} = \frac{W_1^4}{6R_o^2(E/N_0)A}$$

and the probability of error would be increased by a factor of 625 if operation were shifted from channel 77 to channel 15 of the assumed system.

New FM receiver designs⁽⁸⁾ have recently been developed which attempt to improve FM receiver threshold performance. These efforts have included the application of negative feedback at the modulation frequency (FMFB) and carrier insertion techniques of reception in conjunction with the FMFB technique. The theory of operation below threshold of these receivers has not been adequately covered in the available literature. If it may be assumed that the performance of these FM receivers will be characterized only by shifting the curve of Figure 4 to the left, the effect on the performance of data link systems can be easily ascertained. From the general equation for the M-fold diversity combiner, Equation (11) and the sample calculation of the probability of error in Table II, it is observed that a 3 db shift in the threshold is equivalent to a 3 db increase in R_o for all orders of diversity. For example, if the FM threshold is moved 3 db to the left, the required value of W_1 will be decreased by a factor of 2 at each value of E/N_0 . Therefore, the resulting error rate will be decreased by a factor of 4 in the case of dual diversity and by a factor of 16 in the case of quadruple diversity, as would be the case if the transmitter power and, hence, R_o were increased by 3 db.

CONCLUSIONS

This analysis shows that the performance of digital data systems operating over FM tropospheric scatter links is dependent to a great extent on the effectiveness of the diversity system. The analysis assumed an optimum, predetection, coherent combiner; however, contemporary tropospheric scatter systems commonly employ post-detection combiners which can be expected to be less effective in FM systems than the ideal predetection combiner.⁽⁶⁾ Multiple diversity systems often employ a combination of spatial and polarization diversity. That is, each receiving antenna may contain a horizontally and a

vertically polarized feed. It has been found that the amplitudes of the horizontally and vertically polarized signals arriving at the same antenna show a greater correlation than two signals of the same polarization which are received at separated antennas. Hence, the system performance computed in this memo can be expected to be optimistic for the degree of diversity assumed if polarization diversity is employed.

This analysis also indicates that the error rate performance of a prescribed data link, transmitted over the assumed FM tropospheric scatter link employing pre-emphasis, is strongly dependent upon the assigned multiplex channel. This results from the fact that nearly all the errors occur during the small fraction of the time when the fading signal is below threshold. In this subthreshold region, the FM receiver output noise power density is found to be very nearly independent of frequency, and equivalent performance on each channel would be achieved if the same deviation were used on all channels. The channel deviations in FM scatter systems are commonly established on the basis of performance above the threshold where the noise power density is found to increase as the square of frequency. That is, pre-emphasis is employed whereby the channel deviation is increased with channel frequency. This is logical for use with voice transmissions which would be judged on the performance during the large fraction of the time when the signal is above the threshold level. Hence, there is a conflict between the requirements for optimum voice and optimum digital data transmission if equivalent performance on all channels is desired. If both voice and digital data are to be transmitted over an FM tropospheric scatter link which employs pre-emphasis, it would be advantageous to assign the channels having the higher deviation (the higher frequency channels) to the data systems and assign the lower frequency channels to voice circuits.

In order to optimize the performance of scatter circuits for use with digital data systems, the threshold performance of each system component must be considered, such as the diversity-combining technique and the detection technique.

It should be emphasized that this analysis has considered only the effects of amplitude fading. It will be necessary to extend this analysis to include the effects of phase perturbations of the received signal, particularly when PSK data systems are being considered.

REFERENCES

1. Becker, H. D. and Lawton, J. G.:
Theoretical Comparison of Binary Data Transmission Systems Cornell
Aeronautical Laboratory Report No. CA-1172-S-1 RADC Technical Report
No. 58-91 May 1958.
2. Brilliant, M.:
Fading Loss in Diversity Systems Convention Record Fifth National
Communications Symposium October 1959.
3. Clabaugh, R. G.:
Estimated AN/GSC-4 Characteristics on Truro Tropo Circuit Informal
Memo Collins Radio Company Western Division A 27 December 1959.
4. U. S. Army Electronic Proving Ground, Fort Huachuca, Arizona:
Tropospheric Scatter - Principles and Applications Instruction Manual
Report No. 960-67 (AD 240280) March 1960.
5. Skinner, F. J.:
Radio Transmission Systems .. Theoretical Noise Performance Curves for
Frequency Modulation Receivers Operating below the Breaking Region
BTL Unpublished Memo File 36690-1 February 1, 1954.
6. Brennan, D. G.:
Linear Diversity Combining Techniques Proc. IRE Vol. 47 June 1959
pp. 1075-1102.
7. Harris, D. P.:
An Expanded Theory for Signal-to-Noise Performance of FM Systems
Carrying Frequency Division Multiplex IRE National Convention
Record, Part 8 March 1958, pp. 298-304.
8. Morita, M. and Ito, S.:
High Sensitivity Receiving System for Frequency Modulated Wave
IRE International Convention Record, Part 5 March 1960
pp. 228-237.

APPENDIX III

APPENDIX III

DERIVATION OF RESULTS USED IN CHAPTER V

- (a) DETECT MEMO NO.6A - "Some Properties of Impulse Noise" by Richard E. Cleary.
- (b) DETECT MEMO NO. 3A - "Error Probability of a System Using Close Packed Codes in the Presence of Impulse Noise" by Richard E. Cleary.
- (c) ADDENDUM TO DETECT MEMO NO. 3 - "Error Probability of a System Using Close Packed Codes in the Presence of Impulse Noise" by Richard E. Cleary and Peter Crimi.

3 January 1961

TII(a) DETECT MEMO^{*} NO. 6A

Subject: "Some Properties of Impulse Noise"

By: Richard E. Cleary

SUMMARY

The results of a search of the C.A.I. Library literature for information pertaining to impulse noise have been received and examined. Of the many (approximately 15-20) articles reviewed, those listed below were considered the most pertinent and material extracted from these is reported herein.

1. Middleton, D. An Introduction to Statistical Communication Theory pp. 349, 490-498 McGraw-Hill Book Co., Inc., New York 1960.
2. Middleton, D. On the Theory of Random Noise Phenomenological Models I and II, and erratum. Journal of Applied Physics 22, 1143-1152, 1153-1163, 1326. 1951.
3. Mullen, J. A. and Middleton, D. The Rectification of Non-Gaussian Noise, Quart. Appl. Math., 15, 395-419 (1958).
4. Rice, S. O. Mathematical Analysis of Random Noise from Noise and Stochastic Processes New York Dover Publication, Inc. 1954.
5. Slack, M. The Probability Distributions of Sinusoidal Oscillations Combined in Random Phase, Journal Inst. Elec. Eng. 93 Pt. 3, (1946).

* This is a revision of DETECT MEMO NO. 6 which was originally issued 21 September 1960.

3 January 1961
DETECT MEMO NO. 6A
AF 30(602)-2210

INTRODUCTION

A substantial body of literature is available concerning stochastic variables which belong to the normal random process. There is, however, a considerable amount of noise present in a communication link which may have a noticeably different statistical character from the normal random process. A characterizing feature of this noise is its impulsive nature. The elementary disturbances consist of sequences of pulses of varying duration, intensity, phase, and shape and with random occurrence in time. Such noise is, in the literature, usually termed impulse noise. In contrast to the body of literature available concerning the normal random process, that concerning impulse noise is quite meager. A foundation does appear to have been laid, however, upon which further investigations might be based.

Middleton (2) defines three impulse noise* models; (1) periodic, non-overlapping impulse noise, (2) nonperiodic, non-overlapping impulse noise, and (3) Poisson noise. Of the three, Poisson noise appears to be of greatest general use and the most mathematically tractable. It is the concern of almost the whole of the literature on the subject of impulse noise. We, therefore, restrict our attention herein to this process.

*Due to a lack of sufficient and consistent data, it remains to be established that the disturbance encountered in a communication link which is commonly termed impulse noise is actually represented by any of the three models.

3 January 1961
DETECT MEMO NO. 6A
AF 30(602)-2210

Poisson Noise

Poisson noise, results from the linear superposition of the effects of elementary independent impulses which occur at random in time. In practice, the effect of each elementary impulse is given by a particular waveform governed by the frequency response of the circuits or the selective properties of the medium in which the disturbance is evolved. Middleton (2) gives the following descriptive summary of Poisson Noise:

"The distinctive feature of this model is the completely random occurrence of the elementary impulses; overlapping is common and characteristic. Familiar physical examples are atmospheric and solar "static," precipitation noise, ignition and lightning discharges, the interference effects of randomly oriented scatterers in the medium of propagation, etc. Unlike fluctuation noise or Brownian motion, where the density (in time) of the individual effects is so great that overlapping is extremely frequent, this latter type of disturbance is characterized by relatively few impulse per unit time, with a weak overlapping of individual effects, and so does not belong to a normal random process. Only in the limit of a high impulse density does the Poisson noise (so named because of its statistical structure) exhibit gaussian properties."

An analytical representation of the first order statistics of generalized stationary Poisson noise has been obtained by Rice (4). In this, the waveforms of the elementary pulses are assumed identical and denoted by $F(t)$. The first order characteristic function of the random wave of Poisson noise

3 January 1961
 DETECT MEMO NO. 6 A
 AF 30(602)-2210

is then given by

$$g_1(u) = e^{-\nu \int_{-\infty}^{\infty} [e^{iuF(t)} - 1] dt} \quad (1)$$

where ν is the average number of pulses per unit time. This is easily extended to the case in which the amplitude (a) and duration (r) of the waveform of the elementary pulses are stochastic and independently distributed according to $A(a)$ and $R(r)$. In this case,

$$g_1(u) = e^{-\nu \int_0^{\infty} R(r) \int_{-\infty}^{\infty} A(a) \int_{-\infty}^{\infty} [e^{iuF(t; a, r)} - 1] dt da dr} \quad (2)$$

Using the method of Rice (2), Middleton (1) and (2) has obtained a generalized representation of the multiple-order characteristic function for nonstationary Poisson noise. This is of a form similar to Eq. 2 above, but considerably more complex and will not be discussed in detail here.

Some insight into the nature of the Poisson noise process may be obtained by examination of one of the few examples where explicit results have been obtained. This is the case of a train of independent overlapping rectangular pulses of mean duration \bar{r} . In this case, Eq. 2 becomes

$$g_1(u) = e^{-\nu + \int_{-\infty}^{\infty} A(a) [e^{iuu} - 1] da} = e^{-\nu + J g_a(u)} \quad (3)$$

3 January 1961
DETECT MEMO NO. 6A
AF 30(602)-2210

where

$\tau = \nu \bar{r}$ is the average pulse "density", i.e., the average number of pulses per second multiplied by the average duration of a pulse.

$g_a(u)$ is the characteristic function of the distribution of amplitudes. The probability density distribution is given by

$$\left. \begin{aligned} P(t) &= \frac{1}{2\pi} \int_{-\infty}^{\infty} g_a(u) e^{-itu} du = \frac{e^{-\tau}}{2\pi} \int_{-\infty}^{\infty} e^{itg_a(u) - itu} du \\ &= e^{-\tau} \int_{-\infty}^{\infty} \frac{\tau^k [g_a(u)]^k}{k!} e^{-itu} \frac{du}{2\pi} \\ &= e^{-\tau} \left\{ \delta(t) + \sum_{k=1}^{\infty} \frac{\tau^k}{k!} \int_{-\infty}^{\infty} [g_a(u)]^k e^{-itu} \frac{du}{2\pi} \right\} \end{aligned} \right\} \quad (4)$$

With the Poisson noise process, there is at any given time, a finite probability of having no noise at all, and this is represented by the δ -function of strength $e^{-\tau}$ at the origin.

For a Gaussian distribution of amplitudes

$$A(a) = \frac{1}{\sqrt{2\pi}\sigma} e^{-\frac{(a-\bar{a})^2}{2\sigma^2}} \quad (5)$$

3 January 1961
DETECT MEMO NO. 6A
AF 30(602)-2210

the characteristic function is given by

$$g_a(u) = \langle e^{iu\alpha} \rangle = e^{-\frac{\sigma^2 u^2}{2} + iu\bar{\alpha}} \quad (6)$$

and the probability density distribution of Poisson noise becomes

$$P(r) = e^{-r} \left\{ \delta(r) + \sum_{k=1}^{\infty} \frac{r^k}{k!} \cdot \frac{1}{\sqrt{2\pi} (\sqrt{k}\sigma)} e^{-(r-k\bar{\alpha})^2/2(\sqrt{k}\sigma)^2} \right\} \quad (7)$$

The probability density distribution defined by Eq. (7) is shown in Fig. 1 for several values of average pulse density r . The cumulative probability distribution given by the integral of Eq. 7 is shown in Fig. 2. This figure is a plot of probability that the abscissa will be exceeded in absolute value. In each case, the appropriate gaussian probability distribution or cumulative probability of the amplitudes of the elementary pulses is also shown. The effect of increased overlapping of the elementary pulses as the average pulse density increases is apparent from either figure. At low pulse densities when there is little overlapping, there will be appreciable gaps (in time) between successive pulses. Accordingly, small or zero amplitudes are the most likely to occur and only rarely will the intensity of the Poisson noise wave be found comparable to that of the elementary pulses. On the other hand, as the average pulse density increases and overlapping becomes more common, two effects begin to show up. First, the Poisson noise wave is less likely to be found with zero amplitude and secondly, there is an increased probability that the Poisson noise wave will exceed the intensity of the elementary pulses.

3 January 1961
DETECT MEMO NO. 6A
AF 30(602)-2210

In addition to the above effect, the magnitude of the average pulse density has a substantial bearing on the mathematical tractability of the problem of obtaining explicit results in any case. In the limiting case in which the pulse density becomes very large and substantial overlapping exists, it is expected that the precise form of the elementary pulses becomes relatively less important since their individuality is lost in the combined effect. This case is discussed to some degree by Middleton (2) and by Mullen and Middleton (3). On the other hand, in the limiting case in which the pulse density becomes very small and overlapping is negligible, the statistics of the Poisson process will be just those of the elementary pulses. However, in the region between these limiting cases, the shape and statistical properties of the elementary pulses are critical in determining the statistics of the Poisson noise process. It is this fact which makes a general evaluation of the statistical properties of Poisson noise so difficult.

The relatively simple result of Eq. 7 on page 6 occurs only because of the idealization of pulse shape which allowed the characteristic function to be derived by the use of the sum of k-fold products of identical elements. For pulses whose amplitude changes with duration, this procedure breaks down and it is apparently no longer possible to obtain explicit results for all values of γ .

Mullen and Middleton (3) discuss an approximate representation of the characteristic function of Poisson noise which is valid when the pulse density is small. Using this, together with work of Slack (5) curves of the first order probability distribution of Poisson noise derived from rectangular

3 January 1961
DETECT MEMO NO. 6A
AF 30(602)-2210

c-w pulses are given. A short tabulation and discussion of the physical situations to which Poisson noise applies is given by Middleton (2). In this, the order of magnitude of σ associated with a number of sources of Poisson noise, together with the character of the distributions of the process are presented and discussed.

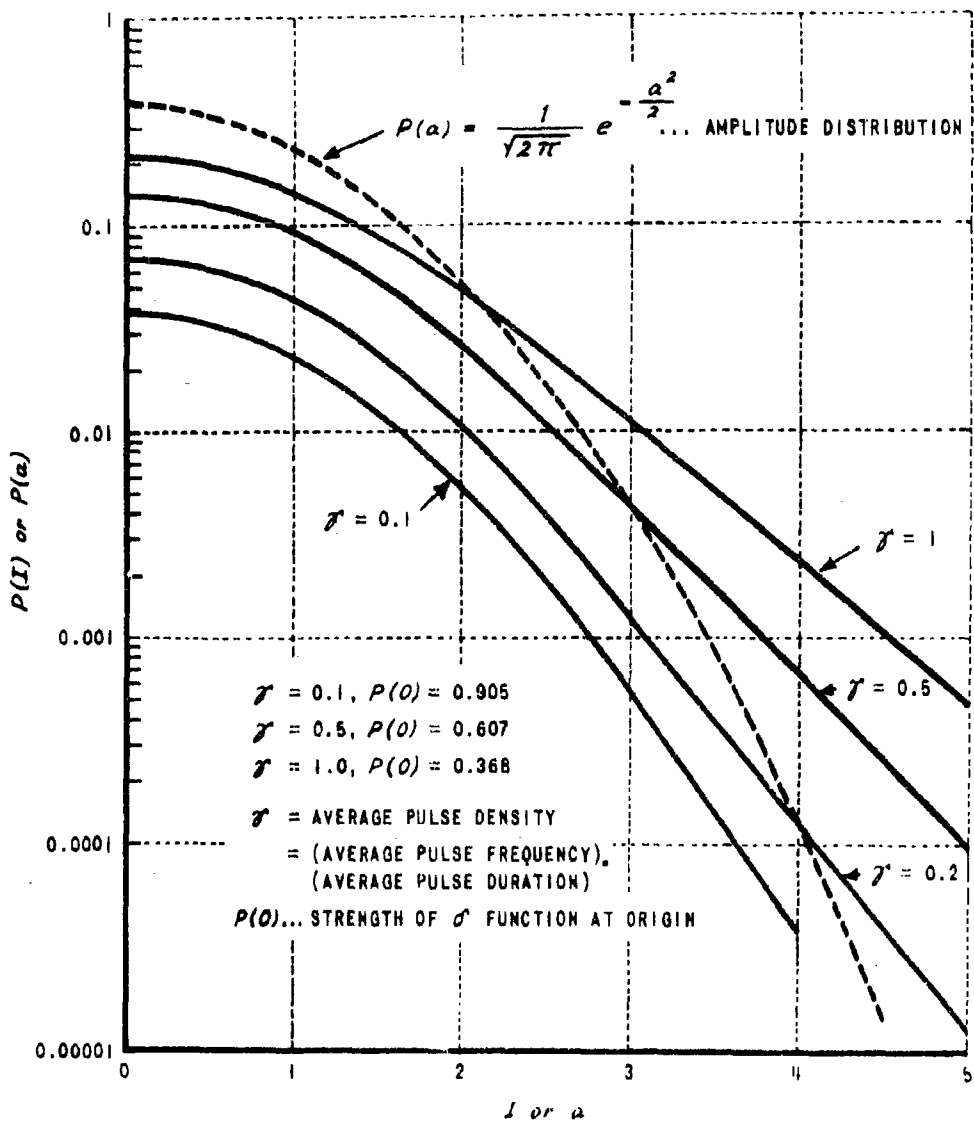


Figure 1 PROBABILITY DENSITY OF "RECTANGULAR" POISSON NOISE

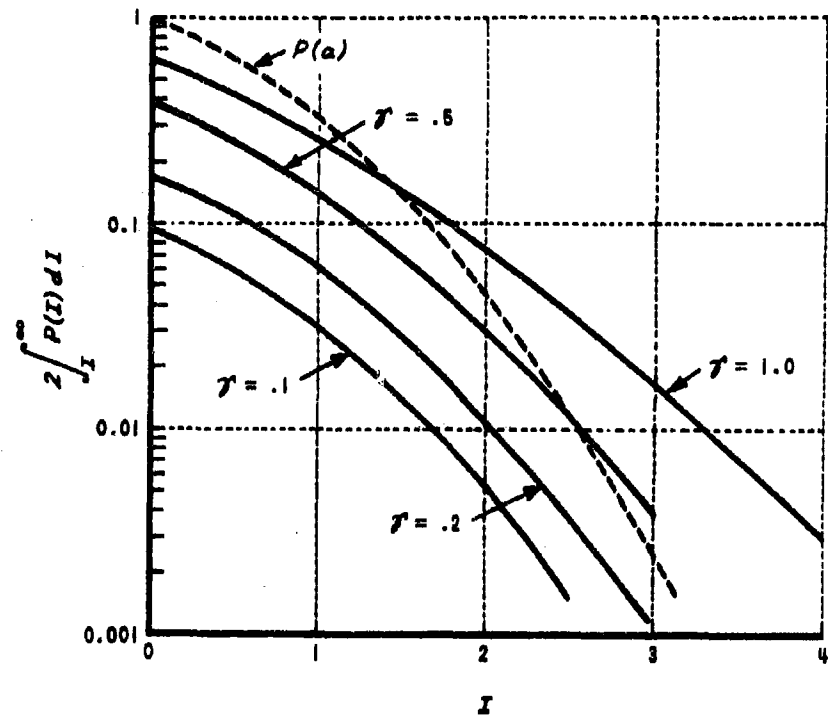


Figure 2 POISSON PROBABILITY DISTRIBUTION
 (PROBABILITY THAT ABSCISSA WILL BE
 EXCEEDED IN ABSOLUTE VALUE)

3 January 1961

III(b) DETRCT MEMO* No. 3A

Subject: "Error Probability of a System Using Close-Packed Codes in the Presence of Impulse Noise"

- References:
- (1) Mertz, P. Model of Impulse Noise for Data Transmission Rand Report P-1761 July 27, 1959.
 - (2) Hamming, R.W. Error Detecting and Error Correcting Codes Bell System Technical Journal Vol. 29 April 1950.
 - (3) Ulrich, W. Non-Binary Error Correcting Codes Bell System Technical Journal November 1957.
 - (4) Lee, C.Y. Some Properties of Non-Binary Error Correcting Codes I.R.E. Transactions on Information Theory June 1958.

By: Richard Cleary

SUMMARY

The contamination of the signals of digital data transmission systems by noise of an impulsive nature is recognized as a serious limitation on the information transfer ability of such systems. This memo investigates the word error probability of a system using close-packed codes when perturbed according to a mathematical model of impulse noise proposed by Mertz¹.

Curves showing word error probability vs. long term average letter error rate are included for several combinations of system parameters. These curves will allow comparison with the performance of other systems currently under study.

Two proposed extensions of the present analysis are described.

* This is a revision of DETRCT MEMO NO. 3 which was originally issued 30 June 1960.

3 January 1961

INTRODUCTION

In the processes of detection and decision involving digital data, some of the most serious difficulties encountered over certain communication links are due to the presence of impulse noise. It is desirable, therefore, to devise a system which will offer substantial resistance to this type of disturbance. The first approach to this problem has been the examination of the performance of certain promising data transmission systems when the signals are perturbed according to a mathematical model of impulsive disturbances.

The minimum effective duration of a received impulse is determined by the channel bandwidth and is equal to or greater than the reciprocal of the bandwidth. If we postulate that during the presence of an impulse, the channel output is independent of signal input, then at least two methods of combating impulse noise are available to us. One is to make each symbol (pulse) long compared to the reciprocal bandwidth and another is to encode groups of symbols into messages which contain sufficient redundancy to permit error correction. We are here concerned with the latter approach.

Analysis

We identify each transmitted pulse with a letter so that the number of letters in the system alphabet is equal to the number of different pulses employed. The mathematical model of impulse noise which is employed is due to P. Mertz¹. His model defines the probability of letter error occurrence in the following way:

3 January 1961

In the data transmission system considered herein, each word consists of a sequence of n letters, each identified by one of k possible states.* The k^n different sequences (words) which may be thus formed are collectively denoted as the set $S_k(n)$. The transmitted signals are chosen from this set and form a subset C (C for code) of $S_k(n)$. We wish to examine the susceptibility of the system to impulse noise as a function of the minimum "distance between words of the code". The distance between two words has for the present purposes been taken as the number of letters (in corresponding positions in the words) by which the two words differ. Symbolically, each word of $S_k(n)$ represents a point in the n dimensional space of k^n points.** A single letter error will carry a given point in C across a unit distance into another point of the set $S_k(n)$, two errors across a distance of two, etc. If the points (words) of the subset C are chosen such that the minimum distance between words in C is d , then $\frac{d-1}{2}$ *** or fewer letter errors will result in a received point nearer the correct (transmitted) point than any other point of the subset C .

-
- * If the k states or letters are identified by distinct frequencies, a k -ary FSK system results in which the bandwidth-time product required per word is approximately kn .
 - ** In binary systems all words are located at vertices of an n dimensional cube.
 - *** The symbol $[]$ is read as "the greatest integer in", for example $\left[\frac{3}{2} \right] = 1$.

3 January 1961

We restrict our attention to "close-packed codes". A close-packed code has the property that every point in $S_k(n)$ is at a distance equal to or less than $\left[\frac{d}{2}\right]$ from some point in C .* If upon reception of a word w_i of $S_k(n)$, that word w_j of C which is at the smallest distance d_{ij} to w_i is designated as the transmitted word, then a word error occurs if and only if the number of letter errors exceeds $\left[\frac{d}{2}\right]$. Some of the properties of error correcting codes have been discussed in the literature by Hamming², Ulrich³ and Lee⁴.

We seek to determine the error probability of a system using a close-packed code C of distance d when the signals are perturbed by impulse noise in accordance with the mathematical model of Reference (1). All words of the code contain exactly n letters chosen from a k state alphabet.

The conditional probability $P(e/\text{burst})$ of word error in the presence of a burst is given by

$$P(e/\text{burst}) = \sum_{i=0}^n P(e/i) P(i/\text{burst}) \quad (1)$$

where

$P(e/i)$ is the conditional probability of a word error given i letter errors

$P(i/\text{burst})$ is the conditional probability of i letter errors given a burst.

If the decision rule is to designate that word in C which is at the smallest distance from the received word, then

$$\begin{aligned} P(e/i) &= 0, \quad i = 0, 1, 2, \dots, \left[\frac{d}{2}\right] \\ &= 1, \quad i = \left[\frac{d}{2}\right] + 1, \dots, n \end{aligned} \quad (2)$$

*In the case of close-packed codes, d is always odd.

3 January 1961

whereby (1) becomes

$$P(e/burst) = \sum_{l= \left[\frac{d}{2} \right] + 1}^n P(i/burst) = 1 - \sum_{i=0}^{\left[\frac{d}{2} \right]} P(i/burst) \quad (3)$$

Two cases may be distinguished according to whether the ratio of burst duration, ℓ , to word duration, w , is greater or less than unity. (It will be recalled that the burst duration is assumed fixed.) In either case, we assign a time origin at the onset of the word and denote the interval between this and the termination of the burst by the parameter u , which is assumed distributed according to

$$p(u) = \frac{1}{\ell + w}, \quad 0 \leq u \leq \ell + w \quad (4)$$

With the aid of Figure 1, the case in which $\frac{\ell}{w} \geq 1$ will be examined first.

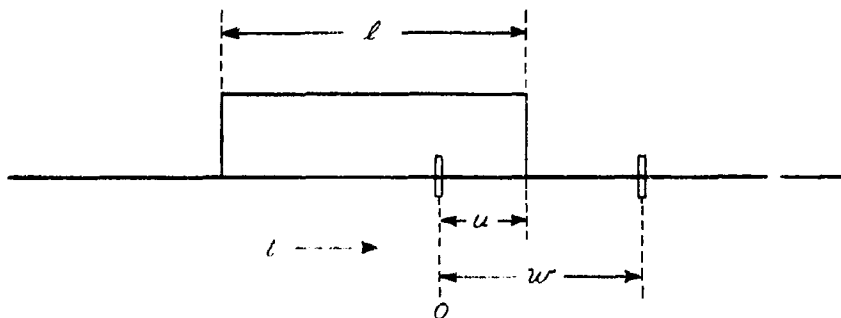


Figure 1.

3 January 1961

The conditional Poisson probability of i letter errors, given the time interval u , may be written*.

$$P(0/u) = e^{-bu},$$

$$0 \leq u \leq w$$

$$= e^{-bw},$$

$$w \leq u \leq l$$

$$= e^{-b[w-(u-l)]},$$

$$l \leq u \leq w+l$$

$$P(i/u) = 0,$$

$$0 \leq u \leq (i-1)T, i \geq 1$$

$$= \frac{(bu)^i}{i!} e^{-bu},$$

$$(i-1)T < u \leq w, i \geq 1$$

$$= \frac{(bw)^i}{i!} e^{-bw},$$

$$w \leq u \leq l, i \geq 1$$

$$= \frac{[b[w-(u-l)]]^i}{i!} e^{-b[w-(u-l)]}, l \leq u \leq w+l-(i-1)T, i \geq 1$$

$$= 0,$$

$$u \geq w+l-(i-1)T, i \geq 1$$

where b is the average error rate within a burst and T is the letter duration, i.e. $nT = w$.

*The discontinuities of $P(i/u)$ are a result of the particular mathematical model used. In practice, $P(i)$ is a more significant parameter than $P(i/u)$; in fact, considerable difficulty in determining u may be anticipated.

3 January 1961

With the aid of (4) and (5)

$$\begin{aligned}
 P(i/\text{burst}) &= \int_{-\infty}^{\infty} p(u) P(i/u) du \\
 &= \frac{1}{w+\ell} \left\{ \frac{2}{b} (1 - e^{-bw}) + (\ell - w) e^{-bw} \right\}, \quad i = 0 \\
 &= \frac{1}{w+\ell} \left\{ (\ell - w) \frac{(bw)^i}{i!} e^{-bw} + \frac{2}{b} \left[e^{-(i-1)bT} - e^{-bw} \right] \right. \\
 &\quad \left. + \frac{2}{b} \sum_{j=1}^i \left[\frac{[(i-1)bT]^j}{j!} e^{-(i-1)bT} - \frac{(bw)^j}{j!} e^{-bw} \right] \right\}, \quad i \geq 1
 \end{aligned} \tag{6}$$

The case in which $\frac{\ell}{w} \leq 1$ may be examined with the aid of Figure 2.

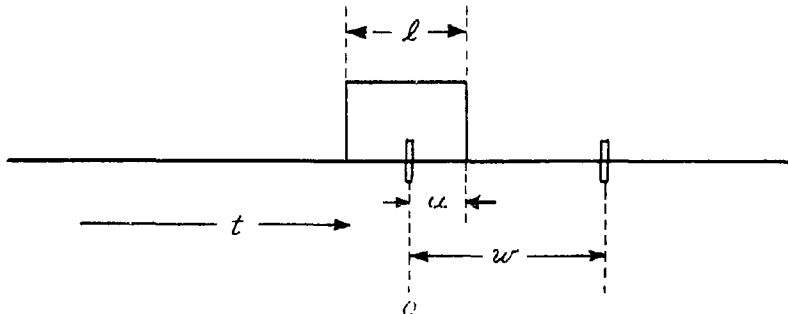


Figure 2.

3 January 1961

In this case, the conditional Poisson probability of i letter errors, given the time interval u , may be written

$$P(0/u) = e^{-bu},$$

$$0 \leq u \leq \ell$$

$$= e^{-b\ell},$$

$$\ell \leq u \leq w$$

$$= e^{-b[w-(u-\ell)]},$$

$$w \leq u \leq w+\ell$$

$$P(i/u) = 0,$$

$$u \leq (i-1)T, i \geq 1$$

$$= \frac{(bu)^i}{i!} e^{-bu},$$

$$(i-1)T < u \leq \ell, i \geq 1$$

$$= \frac{(b\ell)^i}{i!} e^{-b\ell},$$

$$\ell \leq u \leq w, i \geq 1$$

$$= \frac{\{b[w-(u-\ell)]\}^i}{i!} e^{-b[w-(u-\ell)]}, w \leq u \leq w+\ell-(i-1)T, i \geq 1$$

$$= 0,$$

$$u \geq w+\ell-(i-1)T, i \geq 1$$

It is worthwhile at this point to note that (7) may be obtained from (5) by a simple interchange of word length and burst length. We may then immediately write the equivalent of (6) for the case $\frac{\ell}{w} \leq 1$.

3 January 1961

Returning to equation (3), we may write

$$\begin{aligned} P_e &= \left[P(e/burst) \right] P(burst) \\ &= \left[1 - \sum_{i=0}^{\left[\frac{d}{2}\right]} P(i/burst) \right] P(burst) \end{aligned} \quad (8)$$

which, upon substitution of the Poisson probability of a burst in the time interval $w+\ell$, becomes

$$P(e) = \left[1 - \sum_{i=0}^{\left[\frac{d}{2}\right]} P(i/burst) \right] a(w+\ell) e^{-a(w+\ell)} \quad (9)$$

where 'a' is the average burst rate.

Finally, with the aid of (6) and (9)

$$\begin{aligned} P_e &= \left\{ 1 - \frac{1}{w+\ell} \left[\frac{2}{b} (1 - e^{-bw}) + (\ell - w) e^{-bw} \right] - \frac{1}{w+\ell} \sum_{i=1}^{\left[\frac{d}{2}\right]} \left[(\ell - w) \frac{(bw)^i}{i!} e^{-bw} \right. \right. \\ &\quad \left. \left. + \frac{2}{b} \left\{ e^{-(i-1)bT} - e^{-bw} \right\} + \frac{2}{b} \sum_{j=1}^i \left\{ \frac{[(i-1)bT]^j}{j!} e^{-(i-1)bT} \right. \right. \right. \\ &\quad \left. \left. \left. - \frac{(bw)^j}{j!} e^{-bw} \right\} \right] \right\} a(w+\ell) e^{-a(w+\ell)}, \quad \frac{\ell}{w} \geq 1 \end{aligned} \quad (10)$$

The probability of word error for the case $\frac{\ell}{w} \leq 1$ may be obtained from (10) by interchanging ℓ and w .

3 January 1961

Curves of word error probability vs. average number of errors per word are given in Figures 3, 4 & 5 for several combinations of the parameters ℓ (burst length) and a (average burst rate).

Validity of the Assumptions

It would appear worthwhile now to examine the conditions under which the Poisson approximation is, for practical purposes, an adequate representation of the binomial distribution. If we denote the former by $P(x;\bar{x})$ and the latter by $B(x;n, p)$, these conditions may be written

$$x \ll n \quad (11)$$

$$\bar{x} \ll n$$

which, for the case in question becomes

$$\left[\frac{d}{2} \right] \ll n \quad (12)$$

$$bw \ll n$$

Further analyses which are proposed below are expected to reveal the severity of the restrictions imposed by these inequalities.

Finally, it appears desirable to examine the restriction upon the average burst rate in order that the probability of multiple burst occurrence in a time interval Δt be negligibly small.

Let $P(i;a, \Delta t)$ designate the probability of i bursts during an interval of duration Δt if the average rate of burst occurrence is ' a ' bursts per unit time.

$$P(0;a,\Delta t) = e^{-a\Delta t}$$

$$P(1;a,\Delta t) = a\Delta t e^{-a\Delta t}$$

3 January 1961

Probability of no overlap =

$$\begin{aligned}
 &= P(0, a, \Delta t) + P(1, a, \Delta t) = (1 + a\Delta t)e^{-a\Delta t} \\
 &= (1 + a\Delta t) \left[1 - a\Delta t + \frac{(a\Delta t)^2}{2!} + \dots \right] \quad (13) \\
 &= 1 - \frac{1}{2}(a\Delta t)^2 + \dots \\
 &\approx 1 \text{ if } a\Delta t \ll 1
 \end{aligned}$$

For the case in question

$$\Delta t = w + \ell$$

and (13) requires

$$a(w + \ell) = aw(1 + \frac{\ell}{w}) \ll 1 \quad (14)$$

Most cases of practical interest are believed to satisfy this inequality.

Proposed Further Effort

The applicability to a practical system of some of the assumptions about impulse noise as used herein is open to some questions. Principal among these assumptions are the following:

1. Within the time interval occupied by a burst, the probability of letter error occurrence has a Poisson distribution.
2. For a given transmission, the time interval occupied by a burst is fixed.

The principal objection to the first of these is that the maximum number of errors permitted by the Poisson distribution within a finite time interval is unbounded, while in practice, at most all of the letters of a word can be in error.

3 January 1961

Sufficient data upon which to judge the validity of assumption (2) above is not yet available. However, it may be argued intuitively that burst length should be represented as a stochastic process defined by a probability density distribution function.

To overcome the above difficulties, it would be desirable to replace (1) and (2) from page 11 with corresponding observations which are based upon a substantial body of evidence. Although there was some doubt that such a body of evidence existed, a literature search on the subject of impulse noise was undertaken, the results of this literature search are reported in Appendix III(a). It was proposed that (1) and (2) from page 11 be replaced with the following (intuitively more reasonable) assumptions.

1. Within the time interval occupied by a burst, the probability of letter error occurrence has a binomial distribution.
2. Burst duration is represented by a stochastic process and has a uniform distribution.

The first of these satisfies the requirement that the number of errors per word cannot exceed the number of letters per word, while retaining the idea of random error occurrence within a burst. The uniform probability distribution of burst duration (assumption 2) expresses the feeling that, with the data available, no preference for a particular duration can be stated. Analysis using these assumptions has been carried out in Appendix III(c).

3 January 1961

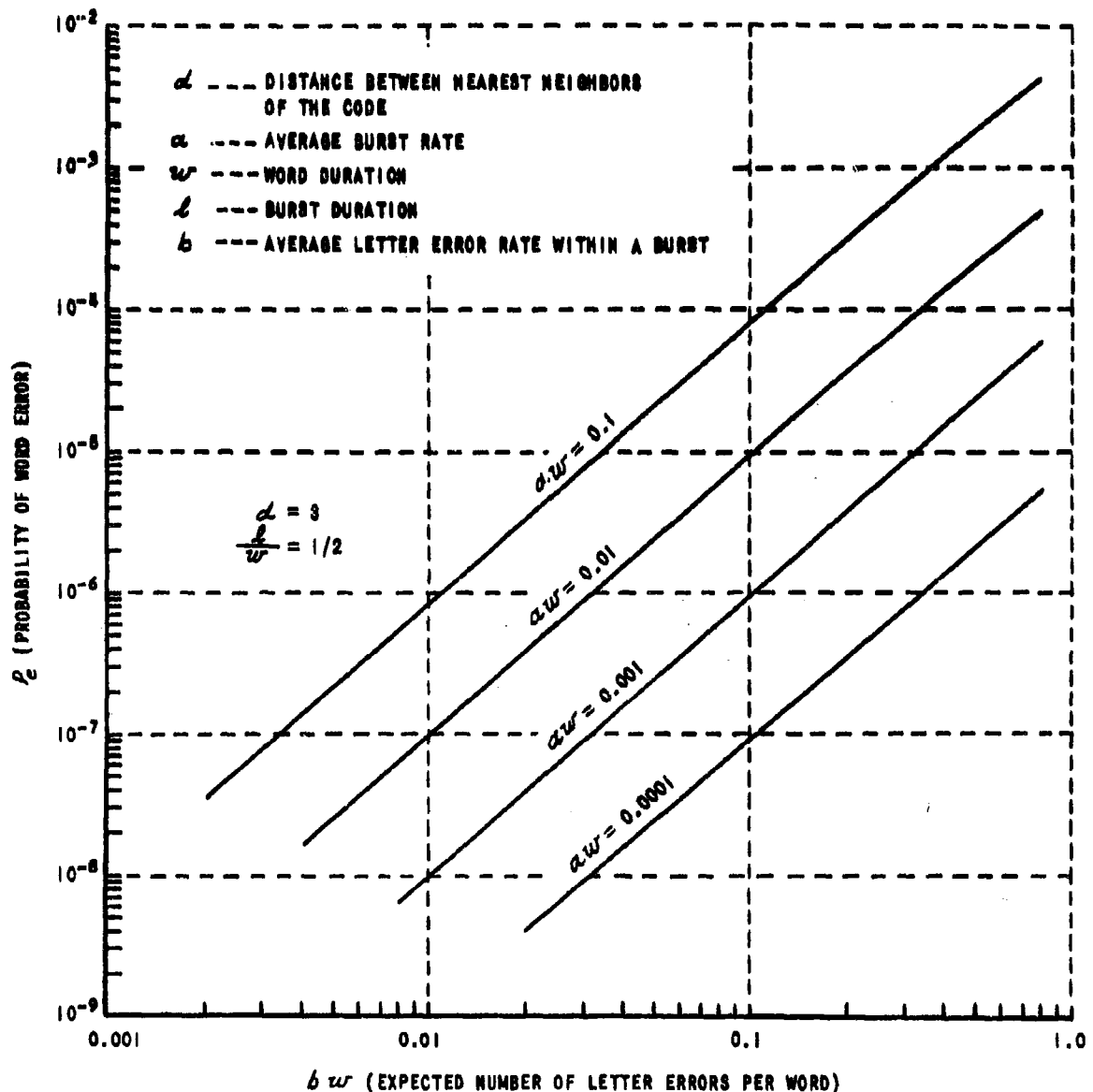


Figure 3

3 January 1961

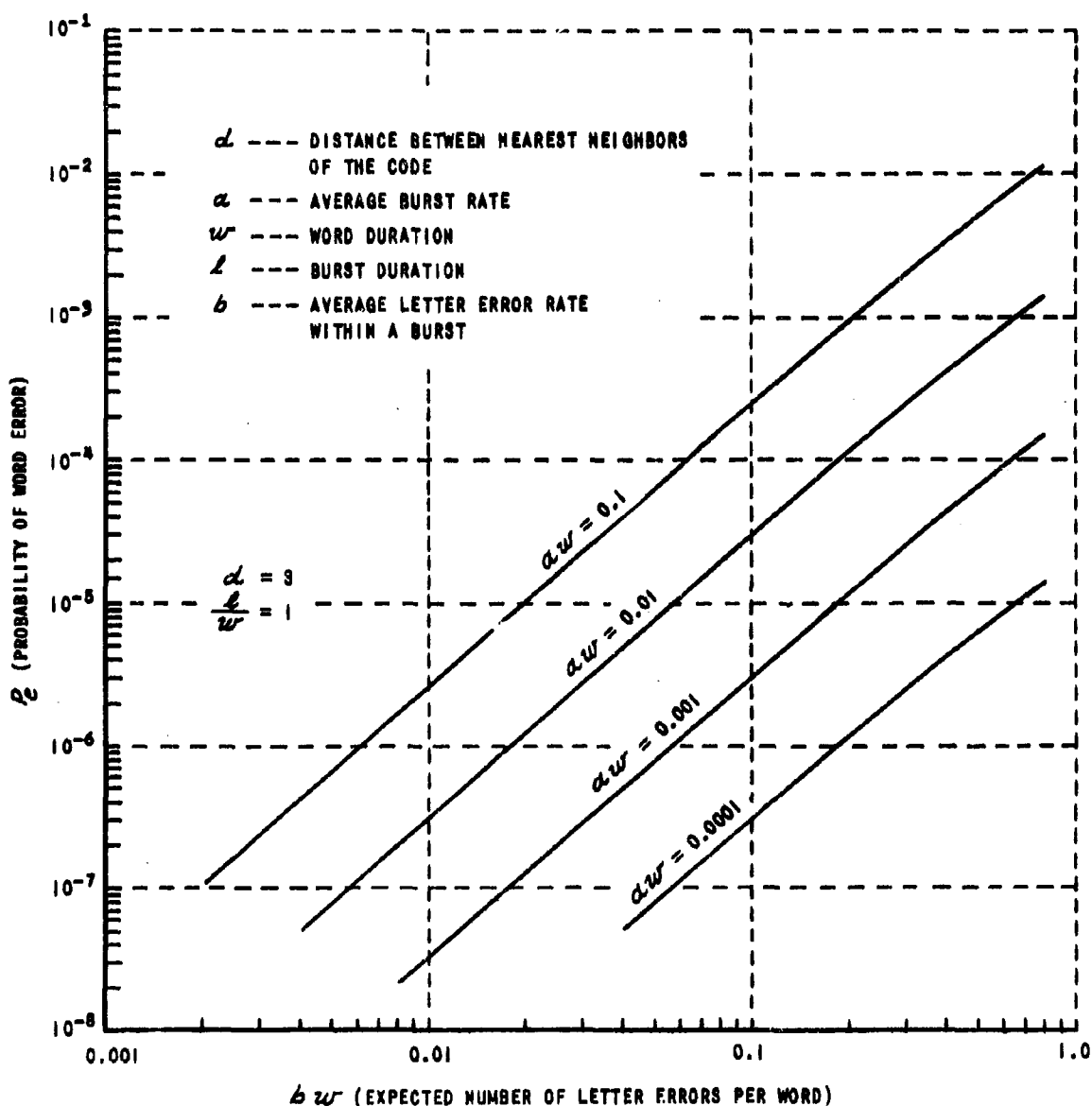


Figure 4

3 January 1961

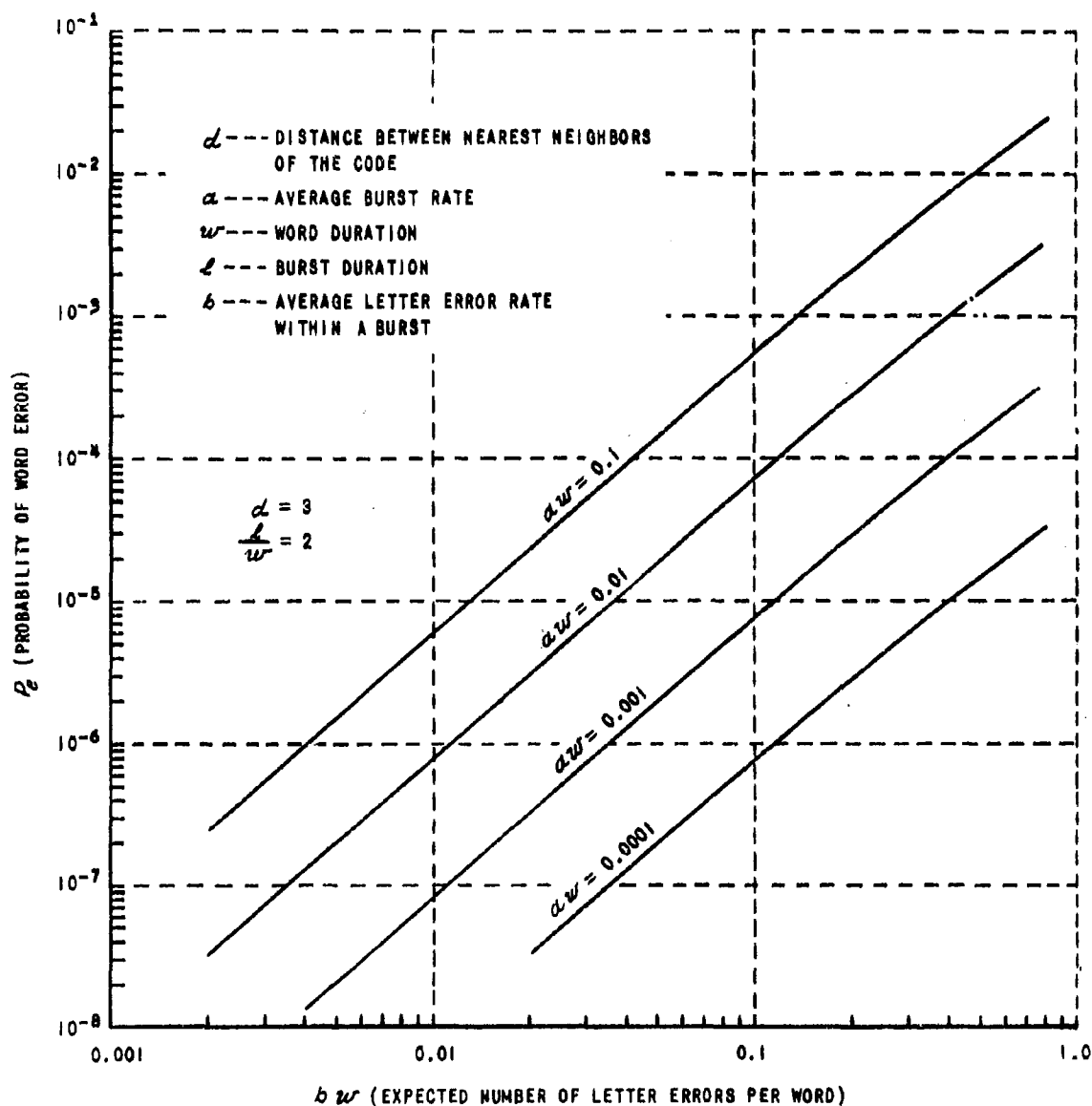


Figure 5

14 October 1960

III(c) Addendum to DETECT MEMO NO. 3

Subject: "Error Probability of a System Using Close-packed Codes
in the Presence of Impulse Noise"

By: R. E. Cleary and P. Crimi

References: (1) Mertz, P. Model of Impulse Noise for Data
Transmission Rand Report P-1761 27 July 1959.
(2) Cleary, R. Error Probability of a System Using
Close-packed Codes in the Presence of Impulse Noise
CAL DETECT MEMO NO. 3 30 June 1960.

SUMMARY

This memo represents an extension of DETECT MEMO NO. 3. An analysis is presented of the word error probability of a system using K-ary, close-packed, error-correcting codes when perturbed according to a mathematical model of impulse noise. The impulse noise model employed is that due to P. Mertz, with the modifications proposed in the final section of DETECT MEMO NO. 3.

INTRODUCTION

Reference (2) analyzed the word error probability of communications systems using K-ary, close-packed codes when perturbed according to a mathematical model of impulse noise proposed by Mertz in Reference (1). It was proposed that two of Mertz's assumptions be replaced with the modified assumptions shown on the following page.

	<u>Mertz's Assumption</u>	<u>Modified Assumption</u>
1. Distribution of the probability of letter errors within a burst of impulse noise.	Poisson	Binomial
2. Distribution of the length of bursts of impulse noise	All bursts of equal length	Uniform

This addendum presents an analysis of the word error probability of a system using close-packed error correcting codes when perturbed according to the modified model of impulse noise. While the assumption of a Poisson distribution of burst occurrence has been retained as far as the computation of the probability of a burst overlapping a word is concerned, the following assumption has been made for reasons of analytic convenience: a burst of noise overlaps a word by a period of duration equal to that of an integral number of letters. Aside from the changes specifically noted here, the data transmission system and impulse noise model, as well as the notation, are as described in Reference (2).

Analysis

We seek to determine the error probability of a system using a close-packed code C of distance d when the signals are perturbed according to the modified model of impulse noise. All words of the code contain exactly n letters each of duration T and each chosen from one of k possible states.

We assume that the decision rule is to designate as the transmitted word that word in C which is at the smallest distance from the received word. Then the conditional probability of word error given an overlapping burst of duration μT is given by

$$P(e; n, p, d/o, \mu) = 1 - \sum_{i=0}^{\lfloor \frac{d}{2} \rfloor^*} P(i; n, p/o, \mu) \quad (1)$$

* The symbol $\lfloor \cdot \rfloor$ is, as in Reference (2), read as "the greatest integer in"; for example, $\lfloor 3/2 \rfloor = 1$.

where $P(i; n, p/o, \mu)$ is the conditional probability of exactly i letter errors in a word containing n letters which is overlapped by a burst of duration μ when the probability that any one letter overlapped by a burst is in error is p . In the sequel, the parametric dependence of the various probabilities on n , p , and d is implied, even though it is not written explicitly.

As in the analysis of Reference (2), two cases may be distinguished according to whether the ratio of burst duration $\ell = \mu T$ to word duration $w = nT$ is greater or less than unity. In either case, we assign a time origin at the onset of the word and denote the interval between this and the termination of the burst by mT^* , where m is assumed distributed

$$P(m) = \frac{1}{n + \mu - 1} \quad (2)$$

With the aid of Figure 1, the case in which $\frac{\ell}{w} = \frac{\mu}{n} \geq 1$ will be examined first.

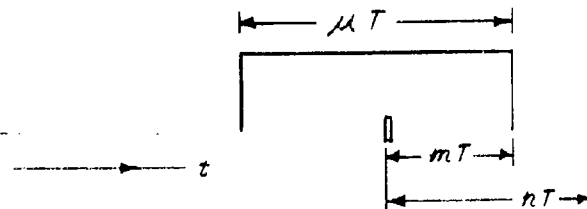


Figure 1

* Note that, in view of our assumption, the parameter m takes on only integral values.

The conditional probability of i letter errors is given by

$$\begin{aligned}
 P(i|m, o, \mu) &= 0, & m < i, \\
 &= \sum_{i}^m p^i (1-p)^{m-i}, & i \leq m \leq n, \\
 &= \sum_{i}^n p^i (1-p)^{n-i}, & n \leq m \leq \mu, \\
 &= \sum_{i=n+1}^{n+\mu-m} p^i (1-p)^{n+\mu-m-i} & \mu \leq m \leq n+\mu-i, \\
 &= 0, & m > n+\mu-i.
 \end{aligned} \tag{3}$$

The case in which $\frac{\ell}{w} = \frac{\mu}{n} < 1$ may be examined with the aid of Figure 2.

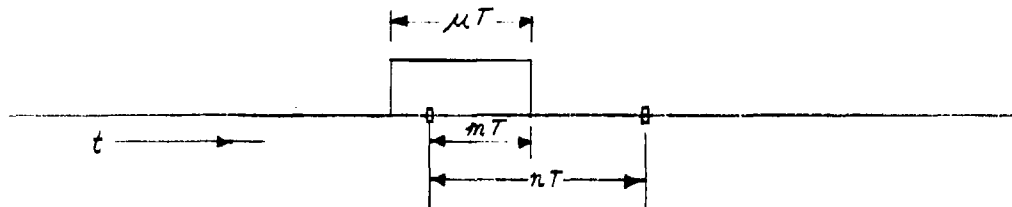


Figure 2

In this case, the conditional probability of i letter errors is given by

$$\left. \begin{aligned} P(i|m, o, \mu) &= 0, & m < i, \\ &= \sum_{l=0}^m p^i (1-p)^{m-i}, & i \leq m \leq \mu, \\ &= \sum_{l=0}^{\mu} p^i (1-p)^{\mu-i}, & \mu \leq m \leq n, \\ &= \sum_{l=0}^{n-\mu-m} p^i (1-p)^{n+\mu-m-i} & n \leq m \leq n+\mu-i, \\ &= 0 & m > n+\mu-i \end{aligned} \right\} \quad (4)$$

We may now write that

$$P(i/o, \mu) = \sum_m P(i|m, o, \mu) P(m) \quad (5)$$

Utilizing Equation (1), the expression for the probability of a word error is:

$$P(e) = \sum_{\mu} \left[1 - \sum_{i=0}^{[\frac{n}{2}]} P(i/o, \mu) \right] P(o, \mu) \quad (6)$$

where o stands for overlapping burst and $P(o, \mu)$ is the probability that a word will be overlapped by a burst of duration $\ell = \mu T$. As in the analysis of Reference (2), the burst occurrence is assumed to be specified by a Poisson distribution, while μ is assumed uniformly distributed over $\ell \leq \mu \leq \mu_{max}$, so that

$$\begin{aligned} P(o, \mu) &= \frac{\alpha}{\mu_{max}} (\omega + \ell) e^{-\alpha(\omega + \ell)} \\ &= \frac{\alpha \omega}{\mu_{max}} \left(1 + \frac{\mu}{\omega} \right) e^{-\alpha \omega \left(1 + \frac{\mu}{\omega} \right)} \end{aligned} \quad (7)$$

where α is the average burst rate. Note that this is the probability of a single burst occurring in the time interval $w + \ell$ (the whole interval is used since it is assumed that, if a burst overlaps even part of a letter, it may be regarded as overlapping the whole letter). The word error probability thus does not include the contribution due to the occurrence of more than one burst overlapping the word. However, it may be shown (Reference 2) that the probability of two or more bursts overlapping the same word is very small in most cases of practical interest.

Substituting Equation (7) into Equation (6), one obtains

$$P(e) = \frac{1}{\mu_{\max}} \sum_{\mu=1}^{\mu_{\max}} \left\{ 1 - \sum_{i=0}^{[\frac{w}{\ell}]} P(i/\ell, \mu) \right\} \alpha w \left(1 + \frac{\mu}{n} \right) e^{-\alpha w \left(1 + \frac{\mu}{n} \right)} \quad (8)$$

The probability of a word error, as given by Equation (8) above, is plotted in Figure 3 as a function of the expected number of letter errors per word (the latter being equal to $\sum_i i \zeta^i p^i (1-p)^{n-i}$) for two selected values of αw . For purposes of comparison, the word error probabilities using the original assumptions (i.e., (1) the occurrence of letter errors is governed by a Poisson distribution; (2) μ is assumed constant and equal to the mean value $\bar{\mu}$ of μ for the corresponding case with μ variable) are also plotted in Figure 3.

CONCLUSIONS

As may be seen from Figure 3, over the range of variables plotted, the probability of a word error in a close-packed error correcting code as computed under the more realistic assumptions of a binomial distribution for letter errors and variable burst duration does not differ drastically from the probability as computed under the simpler assumptions of Reference (2). It may be concluded, then, that reasonably accurate word error probabilities may be computed by assuming constant burst duration and a letter error occurrence governed by the Poisson approximation to the binomial distribution.

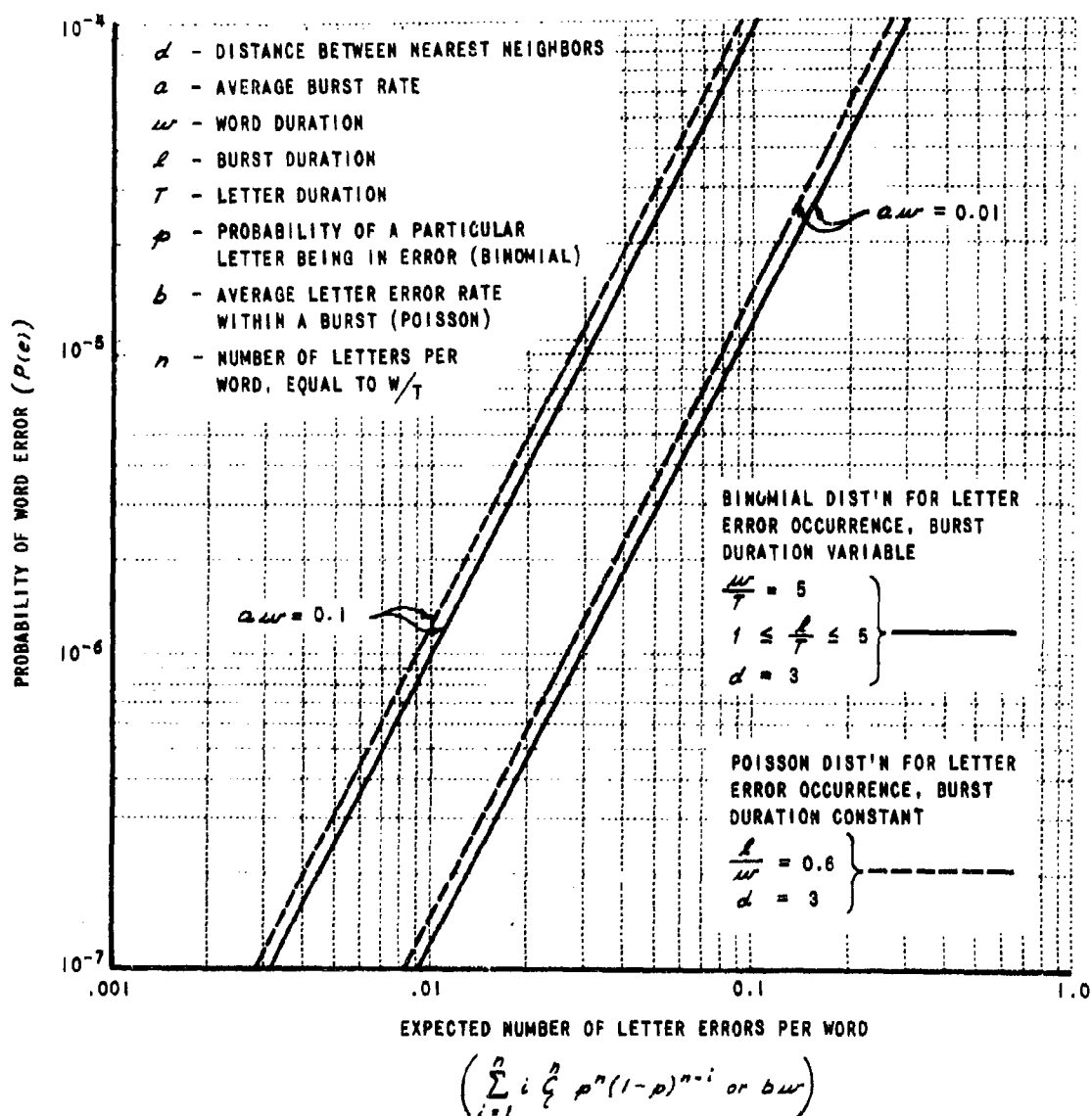


Figure 3

APPENDIX IV

APPENDIX IV

DERIVATION OF RESULTS USED IN CHAPTER VI

- (a) DETECT MEMO NO. 1A - "Moment Detection in the Presence of White Gaussian Noise" by T. T. Chang.
- (b) DETECT MEMO NO. 4 - "Optimum Decision Based on Multiple Moment Detection" by T. T. Chang.
- (c) DETECT MEMO NO. 9 - "Analysis of the Effects of Impulse Noise on Moment Detection" by T. T. Chang.
- (d) DETECT MEMO NO. 14 - "Experimental Investigation of Moment Detection" by Ned B. Smith.

3 January 1961

IV(a) DETECT MEMO NO. 1A

Subject: "Moment Detection in the Presence of White Gaussian Noise"

By: T. T. Chang

SUMMARY

The performance of moment detection in the presence of additive white gaussian noise is analyzed. The functional dependence of the probability of error on the ratio of average transmitted energy (per symbol) to noise power spectral density E/N_0 is determined. Where this functional relationship could not be stated in closed form, closed form expressions for upper and lower bounds have been obtained.

It is shown that all moment detection processes can be replaced by the use of linear filters having appropriate impulse responses. The converse is, however, not true; that is, linear filter detection cannot, in general, be replaced by moment detection.

The organization of this memorandum follows that of the original work at Rutgers University (Reference 1). However, the treatment has been extended to include certain effects not previously considered. The material is presented in four sections, as follows:

1. Moment detection of a single pulse
2. Moment detection of multiple-pulse groups
3. Effect of a filter preceding the moment detector
4. Effect of pulse overlap (intersymbol interference)

^{*}This is a revision of DETECT MEMO NO. 1 which was originally issued 24 May 1960.

INTRODUCTION

In 1957, a decision method for the decoding of pulse coded signals was described by a group at Rutgers University College of Engineering (Reference 1). The method was called moment detection. This memorandum investigates the theoretical performance of moment detection in the presence of additive white gaussian noise.

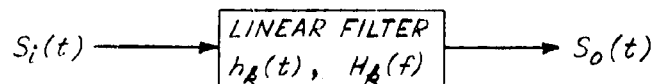
The basic idea of moment detection is that by determining a sufficient number of the temporal moments, $M_k(T, s(t)) = \int_0^T t^k s(t) dt$, of a time limited signal $s(t)$, that signal can be specified to any prescribed degree of accuracy. Discrete pulse-coded signals may be uniquely identified by specifying one or more of the temporal moments. The integer k designates the order of the moment; thus, M_0 is the zeroth-order moment, which happens to be the area under $s(t)$, M_1 is the first-order moment, etc.

It is convenient to call the set of possible transmitted signals a code, C , and to call each possible transmitted signal a word. We are concerned with binary codes in which each word consists of a sequence of identical pulses. The pulses in each word can occur only at prescribed uniform intervals. All words in the code have the same number of pulse positions and the words differ only by the number and location (in time) of the pulse positions which are occupied. It is found that there (usually) exists some k such that each word in the code results in a unique value of M_k for each word in the code C (there may exist some pathological pulse shapes for which this statement is not true). Although the use of such a value of k results in a very simple decision doctrine, the probability of error in the presence of noise may be greater than with other schemes to be described below. The reason for this is that the larger value of k required in order to obtain unique M_k results in smaller percentage differences between the various M_k and a larger variance due to noise. It is found that lower probability of error results when the decision is based on the measured values of several low order moments rather than on a single higher order moment.

1. Moment Detection of a Single Pulse

The k th temporal moment $M_k(T, S(t))$ of a signal $S(t)$ on the interval $[0, T]$ is defined by $M_k(T, S(t)) = \int_0^T t^k S(t) dt$. We can easily show that the moments $M_k(T, S(t))$ can be obtained by linear filtering. Thus, consider a linear filter having impulse response.

$$h_k(t) = \begin{cases} (T-t)^k, & 0 \leq t \leq T \\ 0, & \text{elsewhere} \end{cases} \quad (1.1)$$



The output $S_o(t)$ of this filter in response to an input signal $S_i(t)$ is then given by the convolution of $S_i(t)$ and $h_k(t)$,

$$\begin{aligned} S_o(t) &= \int_{-\infty}^{+\infty} S_i(\tau) h_k(t-\tau) d\tau \\ &= \int_{t-T}^t S_i(\tau) (T-t+\tau)^k d\tau. \end{aligned}$$

The output at time $t = T$ is then

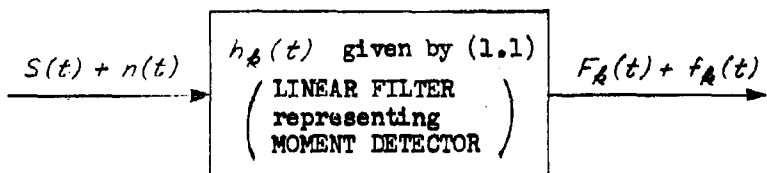
$$S_o(T) = \int_0^T S_i(\tau) \tau^k d\tau = M_k(T, S_i(t))$$

Thus, the output at $t = T$ of a filter having impulse response $h_k(t)$ given by Equation (1.1) is precisely the k th-order moment of the input on the interval $[0, T]$.* Decisions based on the measurement of several moments of different order are equivalent to decisions based on the output of several filters having the appropriate impulse responses.

* Throughout this memorandum, it is assumed that the appropriate time, T , at which to sample the output of the filter(s) is precisely known; this assumption is, of course, equivalent to the precise specification of the interval of integration in moment detection.

In this section, the probability of error in detecting a single pulse by specifying the temporal moment of any order will be investigated, for the case where no filter precedes the moment detector and intersymbol interference (pulse overlap or crowding) is absent. It is assumed throughout this memorandum that the noise is stationary, additive, white and normal with zero mean.

The process of moment detection in the presence of noise is equivalent to passing both the signal $S(t)$ and the noise $n(t)$ through the filter shown in the sketch below.



Thus, the output of the filter at time T due to the signal is

$$\begin{aligned} F_k(T) &= \int_{-\infty}^{\infty} S(t) h_k(T-t) dt \\ &= \int_0^T S(t) t^k dt = \bar{M}_k \end{aligned}$$

and, similarly, the output at time T due to the noise is

$$f_k(T) = \int_0^T n(t) t^k dt = m_k$$

where \bar{M}_k and m_k are the k th-order temporal moments of the signal and noise, respectively.

Designating the noise power density (or, noise power per c.p.s. of one-sided bandwidth) as N_0 , the variance σ_k^2 of m_k (equal to the mean of m_k^2 , since $E[m_k] = 0$) can be expressed as the integral of the power density spectrum of $f_k(t)$ as

$$\sigma_k^2 = \int_{-\infty}^{\infty} \frac{N_0}{2} |H_k(f)|^2 df \text{ where } H_k(f) = \int_{-\infty}^{\infty} h_k(t) e^{-j2\pi ft} dt$$

or, by Parseval's theorem,

$$\sigma_k^2 = \frac{N_0}{2} \int_{-\infty}^{\infty} h_k^2(t) dt \quad (1.2)$$

Substitution of Equation (1.1) in (1.2) yields*

$$\sigma_k^2 = \frac{N_0}{2} \frac{T^{2k+1}}{2k+1} \quad (1.3)$$

* Equation (1.3) can also be obtained as follows:

$$m_k = \int_0^T t^k n(t) dt$$

$$\begin{aligned} \sigma_k^2 &= \int_0^T \int_0^T u^k t^k E[n(t), n(u)] dt du \\ &= \int_0^T \int_0^T u^k t^k \phi_{nn}(t-u) dt du \end{aligned}$$

$$\phi_{nn}(\tau) = \frac{N_0}{2} \int_{-\infty}^{\infty} e^{-j2\pi f\tau} df = \frac{N_0}{2} \delta(\tau)$$

$$\int_0^T t^k \delta(t-u) dt = u^k \quad (0 < u < T)$$

$$\therefore \sigma_k^2 = \frac{N_0}{2} \int_0^T u^k u^k du = \frac{N_0}{2} \frac{T^{2k+1}}{2k+1}$$

Since the probability density of the noise is assumed to be gaussian, the probability density of m_A is also gaussian. If it is assumed that signal pulse is independent and occurs with probability 1/2, it is easily seen that lowest probability of decision error occurs if the decision threshold is set at $\bar{M}_A/2$. The probability of an error, P_e , is then

$$P_e = \frac{1}{\sigma_A \sqrt{2\pi}} \int_{\frac{1}{2} \bar{M}_A}^{\infty} e^{-\frac{m_A^2}{2\sigma_A^2}} dm_A = \frac{1}{\sqrt{\pi}} \int_{x_A}^{\infty} e^{-v^2} dv$$

or, since $\int_0^{\infty} e^{-v^2} dv = \frac{\sqrt{\pi}}{2}$,

$$P_e = \frac{1}{2} (1 - \operatorname{erf} x_A) \quad (1.4)$$

where

$$x_A = \frac{\bar{M}_A}{2 \sqrt{2} \sigma_A} \quad (1.5)$$

and the error function is defined by

$$\operatorname{erf} z = \frac{2}{\sqrt{\pi}} \int_0^z e^{-v^2} dv.$$

Substituting Equation (1.3) into (1.5) yields

$$x_A = \frac{\bar{M}_A}{2 T A} \sqrt{\frac{2 A + 1}{N_0 T}} \quad (1.6)$$

Equation (1.4), with x_A given by (1.6), is the general formula for the probability of error, which is seen to depend on the signal shape through the presence of \bar{M}_A in (1.6).

Consider signal pulses of the form

$$\left. \begin{aligned} S(t) &= \alpha_i \frac{t^i}{\tau^i} && \text{for } 0 \leq t \leq \tau \quad (i \geq 0) \\ &= 0 && \text{elsewhere} \end{aligned} \right\} \quad (1.7)$$

and let E be the average signal energy per symbol. Then

$$E = \frac{1}{2} \left\{ \int_0^\tau \left(\alpha_i \frac{t^i}{\tau^i} \right)^2 dt + 0 \right\} = \frac{\tau}{2(2i+1)} \alpha_i^2 \quad (1.8)$$

$$\alpha_i = \sqrt{2(2i+1) \frac{E}{\tau}} \quad (1.9)$$

$$\begin{aligned} \bar{M}_k &= \int_0^\tau t^k \alpha_i \frac{t^i}{\tau^i} dt = \frac{\tau^{k+i}}{k+i+1} \alpha_i \\ &= \tau^k \frac{1}{k+i+1} \sqrt{2(2i+1) E \tau} \end{aligned} \quad (1.10)$$

By substituting Equation (1.10) into (1.6), one obtains

$$x_k = \frac{\sqrt{(2i+1)(2k+1)}}{k+i+1} \sqrt{\frac{E}{2N_0}} \quad (1.11)$$

from which x_k is maximum when $i = k$ and

$$\text{maximum } x_k = \sqrt{\frac{E}{2N_0}}$$

Then, by Equation (1.4), the corresponding minimum probability of error is

$$P_e = \frac{1}{2} \left(1 - erf \sqrt{\frac{E}{2N_0}} \right) \quad (1.12)$$

or the same as that obtained with coherent matched filter detection of uncorrelated symbols ($\rho = 0$), such as frequency-shift keying. (See Reference 2)

In fact, the impulse response given by Equation (1.1) is also that of a matched filter to a signal of the shape given by (1.7) with $i = k$. It follows that this signal shape is the optimum for detection by the k th moment and (1.12) gives the lowest possible error rate in detecting any order moment.

Instead of Equation (1.11), χ_k can also be expressed in terms of the average signal height. The average signal height is

$$\bar{\alpha} = \frac{1}{T} \int_0^T \alpha_i \frac{t^i}{\tau^i} dt = \frac{1}{i+1} \alpha_i \quad (1.13)$$

Combining this and (1.8),

$$\sqrt{E} = \frac{1+i}{\sqrt{2(2i+1)}} \bar{\alpha} \sqrt{T} \quad (1.14)$$

Substituting in (1.11),

$$\chi_k = \frac{(1+i)\sqrt{2k+1}}{2(k+1+i)} \bar{\alpha} \sqrt{\frac{T}{N_o}} \quad (1.15)$$

which shows the expected result that for a given value of $\bar{\alpha}/\sqrt{N_o}$ the probability of error decreases as T and i increase (except that χ_k is independent of i). It must be realized that for constant $\bar{\alpha}$ increasing i , T or both i and T will result in increased energy per pulse. For this reason, it is felt that the performance of digital systems is more meaningfully portrayed by the functional dependence of error probability P_e (which is related to χ_k through Equation 1.4) on E/N_o than by the dependence on $\bar{\alpha}/N$ where N is the r.m.s. of the noise. The latter approach is, however, used in Reference 1.

2. Moment Detection of Multiple-Pulse Groups

This section will illustrate how to investigate the probability of error in detecting words containing more than one signal pulse. For simplicity, only symbols containing two signal pulses (each of duration T_p) with duration $T = 2T_p$ will be considered. (The extension to longer pulse groups is, at least in principle, straightforward.)

Suppose the pulse shape is

$$\left. \begin{aligned} S(t) &= \alpha_i \frac{t^i}{T_p^i} \quad \text{for } 0 \leq t \leq T_p \quad (i \geq 0) \\ &= 0 \quad \text{elsewhere} \end{aligned} \right\} \quad (2.1)$$

Then, by (1.9),

$$\alpha_i = \sqrt{2(2i+1) \frac{E}{T_p}} \quad (2.2)$$

The k th-order signal moment of word (1, 0), corresponding to the presence of the first pulse and the absence of the second, is

$$\begin{aligned} \bar{M}_k(1,0) &= \int_0^{T_p} t^k \alpha_i \frac{t^i}{T_p^i} dt \\ &= T_p^k \sqrt{2(2i+1) E T_p} \frac{1}{k+i+1} \end{aligned} \quad (2.3)$$

The k th-order signal moment of word (0,1), corresponding to the absence of the first pulse and the presence of the second, is

$$\begin{aligned} \bar{M}_k(0,1) &= \int_0^{T_p} (T_p + t)^k \alpha_i \frac{t^i}{T_p^i} dt \\ &= T_p^k \sqrt{2(2i+1) E T_p} \sum_{r=0}^k \frac{k!}{r!(k-r)!} \frac{1}{r+1+i} \end{aligned} \quad (2.4)$$

3 January 1961

Thus, the expressions for the zero-order and first-order signal moments of the four possible words are:

$$\begin{aligned}
 \bar{M}_0(0,0) &= \bar{M}_1(0,0) = 0 \\
 \bar{M}_0(1,0) &= \bar{M}_0(0,1) = \sqrt{2(2i+1)ET_p} \frac{1}{1+i} \\
 \bar{M}_1(1,0) &= T_p \sqrt{2(2i+1)ET_p} \frac{1}{2+i} \\
 \bar{M}_1(1,0) &= T_p \sqrt{2(2i+1)ET_p} \left(\frac{1}{1+i} + \frac{1}{2+i} \right) \\
 \bar{M}_0(1,1) &= \bar{M}_0(1,0) + \bar{M}_0(0,1) \\
 &= \sqrt{2(2i+1)ET_p} \frac{2}{1+i} \\
 \bar{M}_1(1,1) &= \bar{M}_1(1,0) + \bar{M}_1(0,1) \\
 &= T_p \sqrt{2(2i+1)ET_p} \left(\frac{1}{1+i} + \frac{2}{2+i} \right)
 \end{aligned} \tag{2.5}$$

Let m_0 and m_1 be the zero-order and first-order noise moments. These moments have zero mean and, by (1.3) with $T = 2T_p$, the following variances:

$$\sigma_0^2 = N_0 T_p ; \quad \sigma_1^2 = \frac{4}{3} N_0 T_p^3 \tag{2.6}$$

We will investigate how the decision as to which signal was most likely to have been sent is to be made in terms of the observed moments, $M_0 = \bar{M}_0 + m_0$ and $M_1 = \bar{M}_1 + m_1$. In order to do this, and to find the best decision rule, we must know the joint probability density function $\rho(m_0, m_1)$. The marginal probability density functions are known to be

$$\rho(m_0) = \frac{1}{\sqrt{2\pi}\sigma_0} e^{-m_0^2/(2\sigma_0^2)}$$

and

$$\rho(m_1) = \frac{1}{\sqrt{2\pi}\sigma_1} e^{-m_1^2/(2\sigma_1^2)}$$

3 January 1961

It is more convenient to have the density functions in the normalized coordinates ξ and η .

$$\left. \begin{aligned} \xi &= \frac{m_0}{\sigma_0} = \frac{1}{\sqrt{N_0 T_p}} m_0 \\ \eta &= \frac{m_1}{\sigma_1} = \frac{\sqrt{3}}{2} \frac{1}{\sqrt{N_0 T_p}} \frac{1}{T_p} m_1 \end{aligned} \right\} \quad (2.7)$$

Thus, the marginal probability density functions become

$$\left. \begin{aligned} p(\xi) &= \frac{1}{\sqrt{2\pi}} e^{-\xi^2/2} \\ p(\eta) &= \frac{1}{\sqrt{2\pi}} e^{-\eta^2/2} \end{aligned} \right\} \quad (2.8)$$

If m_0 and m_1 were statistically independent, their covariance would be zero and the joint probability density function $p(\xi, \eta)$ in the normalized coordinates would be $p(\xi) \cdot p(\eta)$ or

$$p(\xi, \eta) = \frac{1}{2\pi} e^{-(\xi^2 + \eta^2)/2} = \frac{1}{2\pi} e^{-r^2/2}.$$

However, the covariance μ of m_0 and m_1 is not zero; in fact, it is given by

$$\begin{aligned} \mu &= E[m_0 m_1] = E \left[\int_0^{2T_p} n(t) dt \int_0^{2T_p} u n(u) du \right] \\ &= \int_0^{2T_p} \int_0^{2T_p} u E[n(t) n(u)] dt du \\ &= \int_0^{2T_p} \int_0^{2T_p} u \frac{N_0}{2} \delta(t-u) dt du \\ &= \frac{N_0}{2} \int_0^{2T_p} u du = N_0 T_p^2 \quad (\text{See also footnote on pg. 5}) \end{aligned}$$

The correlation coefficient of ξ and η (or the normalized covariance of m_0 and m_1) is

$$\rho = E[\xi \eta] = \frac{\mu}{\sigma_0 \sigma_1} = - \frac{N_0 T_p^2}{[(N_0 T_p)(\frac{4}{3} N_0 T_p^3)]^{1/2}} = -\frac{\sqrt{3}}{2} \quad (2.9)$$

So, the random variables m_0 and m_1 have a strong linear dependence and the joint probability density $p(\xi, \eta)$ takes the form

$$p(\xi, \eta) = \frac{1}{2\pi\sqrt{1-\rho^2}} e^{-Q} \quad (2.10)$$

where

$$Q = \frac{1}{2(1-\rho^2)} (\xi^2 - 2\rho\xi\eta + \eta^2) \quad (2.11)$$

The distribution given by Equation (2.10) is seen to be in accord with (2.8) and (2.9); since it yields

$$\int_{-\infty}^{\infty} p(\xi, \eta) d\eta = \frac{1}{\sqrt{2\pi}} e^{-\xi^2/2}, \quad \int_{-\infty}^{\infty} p(\xi, \eta) d\xi = \frac{1}{\sqrt{2\pi}} e^{-\eta^2/2}$$

and

$$\int_{-\infty}^{\infty} \int_{-\infty}^{\infty} \xi \eta p(\xi, \eta) d\xi d\eta = \rho.$$

The joint probability density $p(\xi, \eta)$ given by Equation (2.10) is seen to be symmetric with respect to axes inclined 45° with respect to the ξ, η axes.

Let

$$x_1 = \frac{1}{\sqrt{2}} (\xi + \eta) \quad \text{and} \quad y_1 = \frac{1}{\sqrt{2}} (\eta - \xi)$$

3 January 1961

Then

$$\xi = \frac{1}{\sqrt{2}}(x_1 - y_1) \text{ and } \eta = \frac{1}{\sqrt{2}}(x_1 + y_1)$$

so that

$$Q = \frac{x_1^2}{2(1+\rho)} + \frac{y_1^2}{2(1-\rho)}$$

Thus, lines of constant $\rho(x_1, y_1)$ or constant $Q(x_1, y_1)$ are ellipses with major and minor axes coincident with the x_1 and y_1 axes. That is, x_1, y_1 are independent normally distributed variables with zero mean and unequal variances.

If we now change the scales of x_1 and y_1 such that

$$x_1 = \sqrt{2(1+\rho)} x \quad \text{and} \quad y_1 = \sqrt{2(1-\rho)} y,$$

then

$$Q = x^2 + y^2 \tag{2.12}$$

and the lines of constant $\rho(x, y)$ become circles. x, y are now independent normally distributed variables with zero mean and equal variances.

The transformation from ξ, η to x, y is characterized by

$$x = \frac{1}{2\sqrt{1+\rho}}(\xi + \eta), \quad y = \frac{1}{2\sqrt{1-\rho}}(\eta - \xi) \tag{2.13}$$

$$\xi = \sqrt{1+\rho}x - \sqrt{1-\rho}y, \quad \eta = \sqrt{1+\rho}x + \sqrt{1-\rho}y \tag{2.14}$$

$$\frac{\partial(\xi, \eta)}{\partial(x, y)} = 2\sqrt{1-\rho^2} \tag{2.15}$$

Let R be a region in the ξ, η plane and R' the corresponding region in the x, y plane. Then the probability that ξ, η lie within R equals the probability that x, y lie within R' .

$$P = \int_R \int \rho(\xi, \eta) d\xi d\eta = \int_{R'} \int \rho(\xi, \eta) \frac{\partial(\xi, \eta)}{\partial(x, y)} dx dy$$

and, by Equations (2.10), (2.12) and (2.15), can be expressed as

$$\rho = \frac{1}{\pi} \int_{R'} \int e^{-(x^2 + y^2)} dx dy \quad (2.16)$$

For $\rho = \sqrt{3}/2$, Equations (2.13) and (2.14) become

$$x = \sqrt{\frac{2 - \sqrt{3}}{2}} (\xi + \eta), \quad y = \sqrt{\frac{2 + \sqrt{3}}{2}} (\eta - \xi) \quad (2.17)$$

$$\left. \begin{aligned} \xi &= \sqrt{\frac{2 + \sqrt{3}}{2}} x - \sqrt{\frac{2 - \sqrt{3}}{2}} y \\ \eta &= \sqrt{\frac{2 + \sqrt{3}}{2}} x + \sqrt{\frac{2 - \sqrt{3}}{2}} y \end{aligned} \right\} \quad (2.18)$$

So far, we have been concerned only with the stochastic variables due to the noise with $E(x, y) = (0, 0)$. We must now determine $E_r(x, y)$ from (2.5) for each of the four possible transmitted words. On the assumption that these words are a priori equally probable, the x, y plane is then divided into four decision regions. It is clear that the lowest probability of error will be attained if the four regions in the x, y plane are chosen such that every point in region r is closer to the corresponding $E_r(x, y)$ than to

$E_s(x, y)$, $r \neq s$. $r, s = I, II, III, IV$. The decision regions are readily determined in the x, y plane and can be mapped to ξ, η and M_0, M_1 planes by means of Equations (2.18) and (2.7).

3 January 1961

When the signal moments given by Equation (2.5) are also normalized, by substituting \bar{M}_o for m_o or \bar{M}_i for m_i in (2.7), they become

$$\begin{aligned}\bar{\mathcal{E}}_{(0,0)} &= \bar{\eta}_{(0,0)} = 0 & \lambda &\equiv \sqrt{(2i+1) \frac{E}{N_0}} \\ \bar{\mathcal{E}}_{(1,0)} &= \bar{\mathcal{E}}_{(0,1)} = \lambda \sqrt{2} \frac{1}{1+i} \\ \bar{\eta}_{(1,0)} &= \lambda \frac{\sqrt{6}}{2} \frac{1}{2+i} \\ \bar{\eta}_{(0,1)} &= \lambda \frac{\sqrt{6}}{2} \left(\frac{1}{1+i} + \frac{1}{2+i} \right) \\ \bar{\mathcal{E}}_{(1,1)} &= \lambda \sqrt{2} \frac{2}{1+i} \\ \bar{\eta}_{(1,1)} &= \lambda \frac{\sqrt{6}}{2} \left(\frac{1}{1+i} + \frac{2}{2+i} \right)\end{aligned}$$

When the four points

$$\begin{array}{ll} \text{I } (\bar{\mathcal{E}}_{(0,0)}, \bar{\eta}_{(0,0)}) , & \text{II } (\bar{\mathcal{E}}_{(1,0)}, \bar{\eta}_{(1,0)}) , \\ \text{III } (\bar{\mathcal{E}}_{(0,1)}, \bar{\eta}_{(0,1)}) , & \text{and IV } (\bar{\mathcal{E}}_{(1,1)}, \bar{\eta}_{(1,1)}) , \end{array}$$

representing, respectively, the expectations of the four possible words $(0,0)$, $(1,0)$, $(0,1)$, and $(1,1)$ in the \mathcal{E}, η -system are transformed to the xy -system by (2.17), they become

$$\text{I } (\bar{x}_{(0,0)}, \bar{y}_{(0,0)}) , \quad \text{II } (\bar{x}_{(1,0)}, \bar{y}_{(1,0)}) , \quad \text{etc.}$$

where:

$$\begin{aligned}
 \bar{x}_{(0,0)} &= \bar{y}_{(0,0)} = 0 \\
 \bar{x}_{(1,0)} &= \lambda \sqrt{2-\sqrt{3}} \left(\frac{1}{1+i} + \frac{\sqrt{3}}{2} \frac{1}{2+i} \right) \\
 \bar{y}_{(1,0)} &= -\lambda \sqrt{2+\sqrt{3}} \left(\frac{1}{1+i} - \frac{\sqrt{3}}{2} \frac{1}{2+i} \right) \\
 \bar{x}_{(0,1)} &= \lambda \sqrt{2-\sqrt{3}} \left\{ \left(1 + \frac{\sqrt{3}}{2} \right) \frac{1}{1+i} + \frac{\sqrt{3}}{2} \frac{1}{2+i} \right\} \\
 \bar{y}_{(0,1)} &= \lambda \sqrt{2+\sqrt{3}} \left\{ \frac{\sqrt{3}}{2} \frac{1}{2+i} - \left(1 - \frac{\sqrt{3}}{2} \right) \frac{1}{1+i} \right\} \\
 \bar{x}_{(1,1)} &= \lambda \sqrt{2-\sqrt{3}} \left\{ \left(2 + \frac{\sqrt{3}}{2} \right) \frac{1}{1+i} + \sqrt{3} \frac{1}{2+i} \right\} \\
 \bar{y}_{(1,1)} &= -\lambda \sqrt{2+\sqrt{3}} \left\{ \left(2 - \frac{\sqrt{3}}{2} \right) \frac{1}{1+i} - \sqrt{3} \frac{1}{2+i} \right\}
 \end{aligned}$$

From these coordinates, one obtains the length (in the xy -system) between points I and IV as

$$\begin{aligned}
 \overline{I \text{ IV}} &= \sqrt{\bar{x}_{(1,1)}^2 + \bar{y}_{(1,1)}^2} \\
 &= \frac{\sqrt{(2i+1)(16+16i+7i^2)}}{(1+i)(2+i)} \sqrt{\frac{E}{N_0}} \\
 &= \sqrt{4-i^2} \frac{4i^2+10i+13}{(1+i)^2(2+i)^2} \sqrt{\frac{E}{N_0}}
 \end{aligned}$$

and the length between points II and III as

3 January 1961

$$\begin{aligned}
 \overline{\text{II III}} &= \sqrt{(\bar{x}_{(0,1)} - \bar{x}_{(1,0)})^2 + (\bar{y}_{(0,1)} - \bar{y}_{(1,0)})^2} \\
 &= \frac{\sqrt{3(2i+1)}}{1+i} \sqrt{\frac{E}{N_0}} \\
 &= \sqrt{3 - 3 \left(\frac{i}{1+i}\right)^2} \sqrt{\frac{E}{N_0}}
 \end{aligned}$$

One also observes that

$$\bar{x}_{(1,0)} + \bar{x}_{(0,1)} = \bar{x}_{(1,1)} \quad \text{and} \quad \bar{y}_{(1,0)} + \bar{y}_{(0,1)} = \bar{y}_{(1,1)},$$

therefore, the two lines, $\overline{\text{I IV}}$ and $\overline{\text{II III}}$, bisect each other. Obviously, both the above lengths are maximum when $i = 0$. For $i = 0$, the slope of line $\overline{\text{I IV}}$ is

$$\frac{\bar{y}_{(1,1)}}{\bar{x}_{(1,1)}} = \frac{-\sqrt{2+\sqrt{3}}}{\sqrt{2-\sqrt{3}}} \cdot \frac{2-\sqrt{3}}{2+\sqrt{3}} = -(2-\sqrt{3});$$

while the slope of line $\overline{\text{II III}}$ is

$$\frac{\bar{y}_{(0,1)} - \bar{y}_{(1,0)}}{\bar{x}_{(0,1)} - \bar{x}_{(1,0)}} = \frac{1}{2-\sqrt{3}} \quad \text{for any } i.$$

Thus, since the product of these two slopes is equal to -1 , the two lines are also mutually perpendicular when $i = 0$. Consequently, the case with $i = 0$ (corresponding to rectangular signal pulses) has the four points located farthest apart and will have the lowest error rate when the best decision is made. From now on, we will only consider this case. Then, the lengths $\overline{\text{I IV}}$ and $\overline{\text{II III}}$ become

$$\overline{\text{I IV}} = 2\sqrt{\frac{E}{N_0}} \quad \text{and} \quad \overline{\text{II III}} = \sqrt{3 \frac{E}{N_0}}$$

3 January 1961

The boundaries of the best decision regions are formed by segments of the perpendicular bisectors of lines I III, III IV, IV II, II I, and II III as indicated in Figure 2.1.

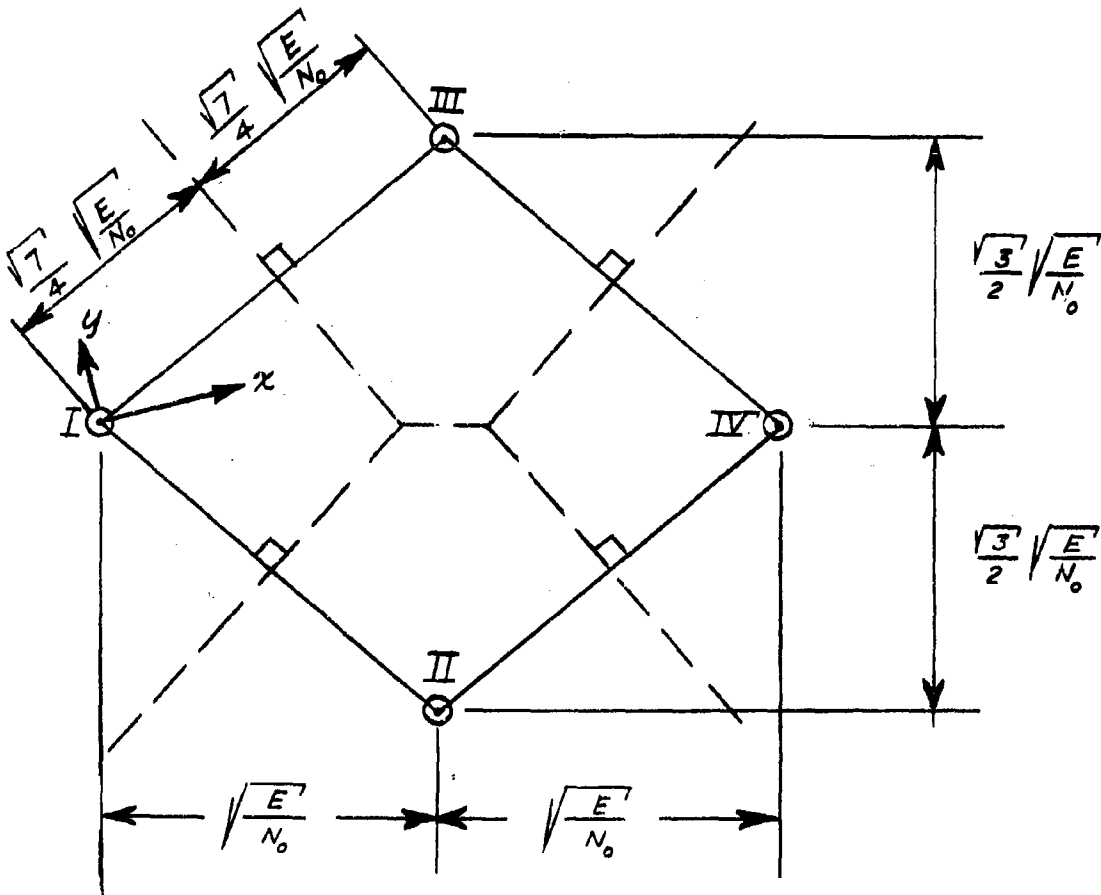


Figure 2.1

We have been unable to obtain a closed form expression for the probability of error when the optimum decision regions are used. However, we have obtained closed form expressions for both an upper and lower bound of this probability. The results are derived below and plotted in Figure 2.4. It will be noted that the lower bound corresponds to the error probability obtained with matched filter detection of uncorrelated binary signals. In this case, each pulse has a probability of error (Reference 2).

$$P_{e1} = \frac{1}{2} \left(1 - \operatorname{erf} \sqrt{\frac{E}{2N_0}} \right) \quad (2.19)$$

and the probability of a group of two pulses to be in error is

$$P_{e2} = 1 - (1 - P_{e1})^2 \quad (2.20)$$

Now, consider the hypothetical case shown in Figure 2.2. Here, the decision regions indicated by the dashed lines are similar to Figure 2.1 but points II and III have been moved farther apart to II' and III' so as to form a square with points I and IV. According to Equation (2.16), the probability of a correct decision for this case is

$$\begin{aligned} P &= \frac{1}{\pi} \int_{-\sqrt{\frac{E}{2N_0}}}^{\infty} \int_{-\sqrt{\frac{E}{2N_0}}}^{\infty} e^{-(x^2+y^2)} dx dy \\ &= \left(\frac{1}{2} + \frac{1}{2} \operatorname{erf} \sqrt{\frac{E}{2N_0}} \right)^2 = (1 - P_{e1})^2 \end{aligned} \quad (2.21)$$

and, hence, the probability of error is

$$1 - P = 1 - (1 - P_{e1})^2 = P_{e2}$$

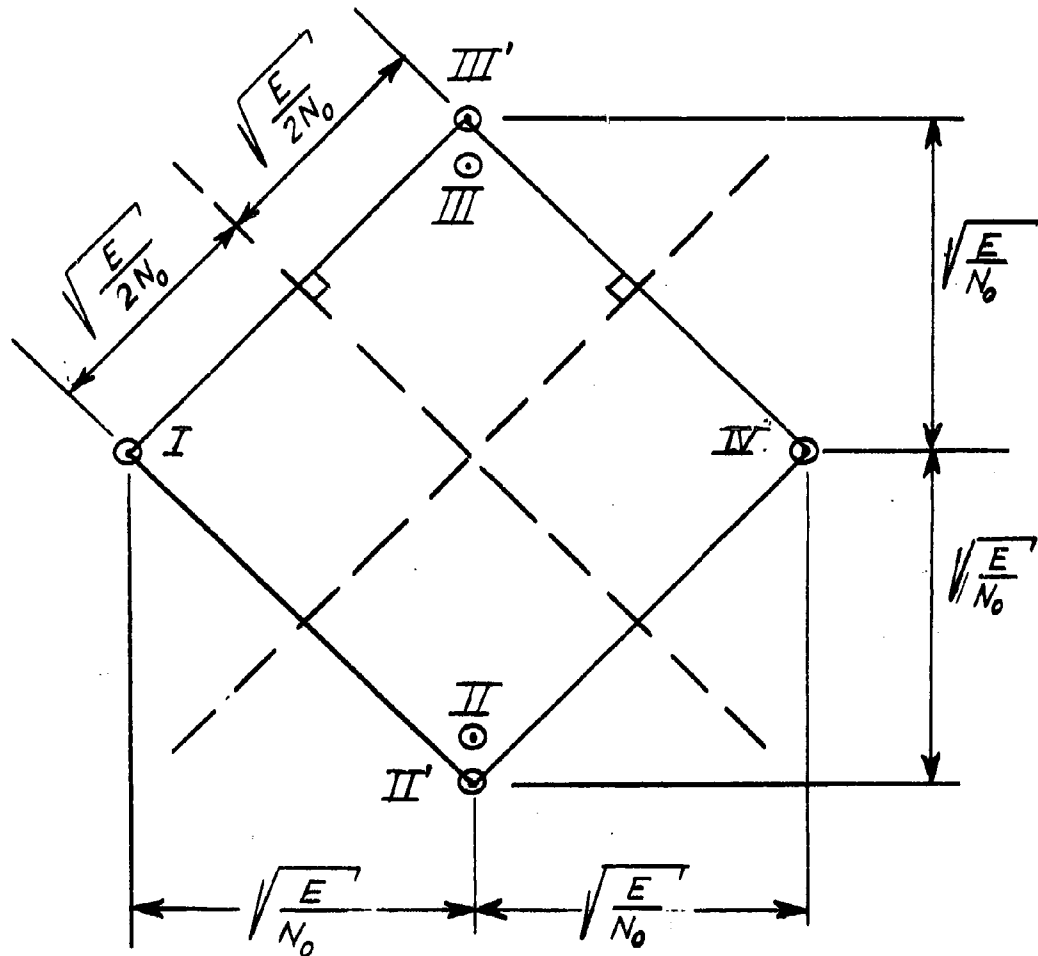


Figure 2.2

Therefore, the probability of error of the actual case shown in Figure 2.1 must be higher than P_{e2} . Next, consider the case shown in Figure 2.3. Here, the locations of the four points are the same as in Figure 2.1 but the boundaries of the decision regions, as indicated by the dashed lines, are

slightly different from the optimum. Consequently, the probability of error, \bar{P}_e , for the boundaries shown in Figure 2.3 must be higher than that for the boundaries of Figure 2.1. By (2.16) and (2.21),

$$\begin{aligned}\bar{P}_e &= \frac{1}{2} \left[\left\{ 1 - (1 - P_{e1})^2 \right\} \right. \\ &\quad \left. + \left\{ 1 - \frac{1}{\pi} \int_{-\frac{\sqrt{3}}{2} \sqrt{\frac{E}{2N_0}}}^{\infty} \int_{-\frac{\sqrt{3}}{2} \sqrt{\frac{E}{2N_0}}}^{\infty} e^{-(x^2+y^2)} dy dx \right\} \right] \\ &= \frac{1}{2} \left[\left\{ 1 - (1 - P_{e1})^2 \right\} + \left\{ 1 - \left(\frac{1}{2} + \frac{1}{2} \operatorname{erf} \frac{\sqrt{3}}{2} \sqrt{\frac{E}{2N_0}} \right)^2 \right\} \right]\end{aligned}$$

Define

$$P'_{e1} = \frac{1}{2} \left(1 - \operatorname{erf} \frac{\sqrt{3}}{2} \sqrt{\frac{E}{2N_0}} \right) \quad (2.22)$$

Then

$$\bar{P}_e = \frac{1}{2} \left[\left\{ 1 - (1 - P_{e1})^2 \right\} + \left\{ 1 - (1 - P'_{e1})^2 \right\} \right] \quad (2.23)$$

3 January 1967

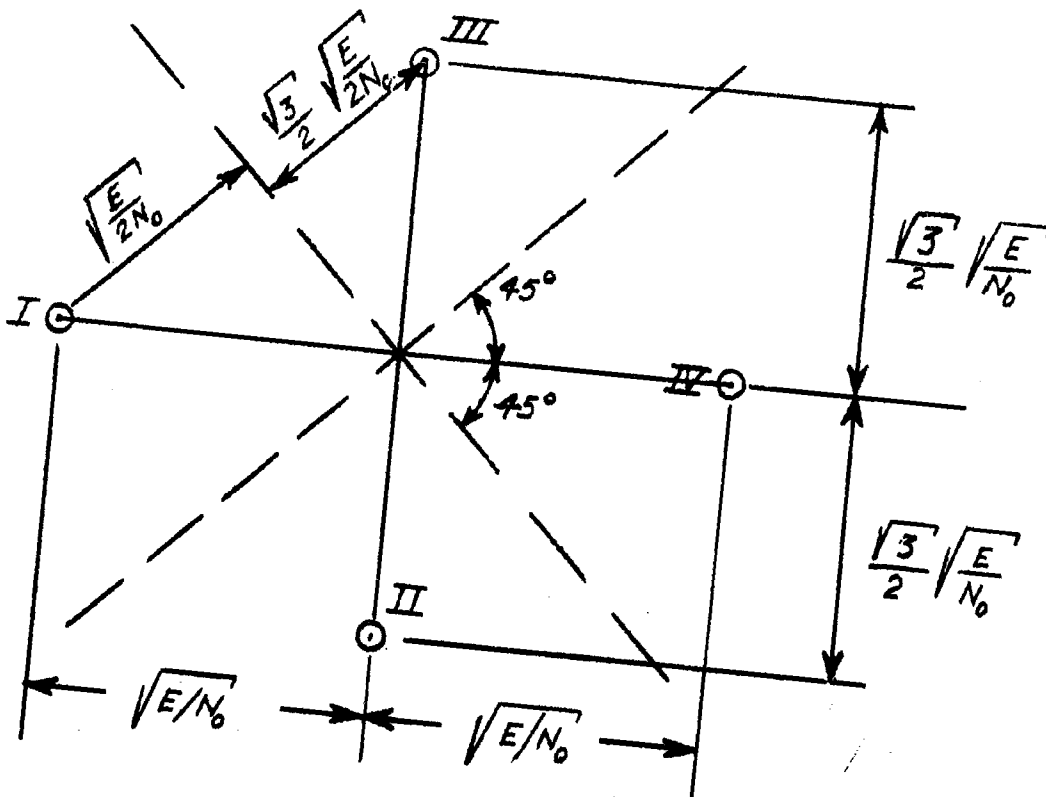


Figure 2.3

The two lower curves of Figure 2.4 marked P_{ol} and P_{ou} are the plots of P_{e_s} , a lower bound, and \bar{P}_e , an upper bound respectively to the probability of error vs. E/N_0 expressed in decibels.

The boundaries of the optimum decision regions, Figure 2.1, and those of Figure 2.3 are shown mapped onto the M_0 , M_1 plane in Figure 2.5 as solid and dashed lines respectively. The implementation of a decision-making circuit based on either of these boundaries is somewhat involved. Slade et al (Ref. 1)

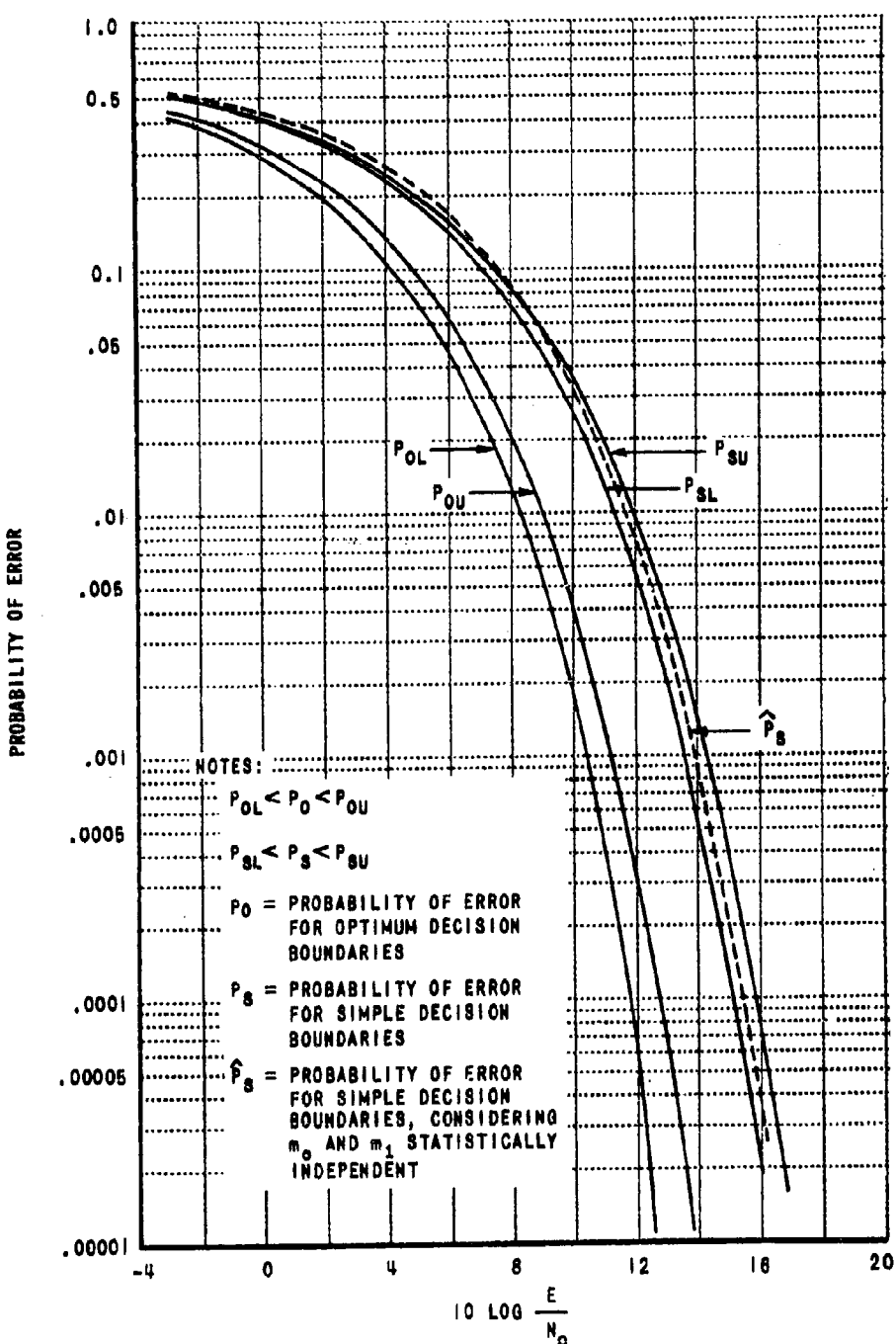


Figure 2.4

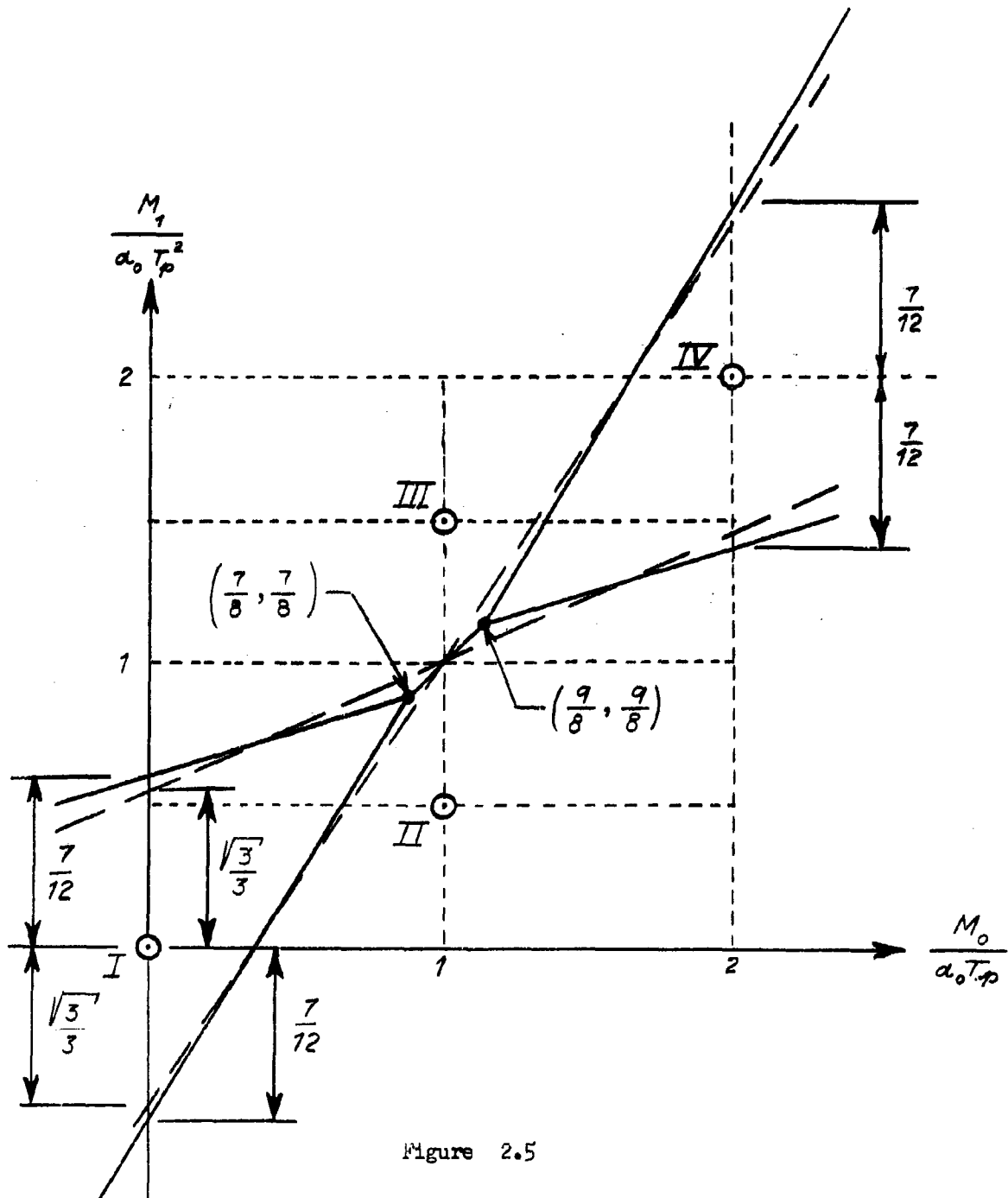


Figure 2.5

use the boundaries shown in Figure 2.6; a decision circuit for these boundaries is, of course, considerably easier to build. In computing the probability of error, Slade, et al, treat m_0 and m_1 as statistically independent. It is of interest to compare the results obtainable with these boundaries to those obtainable with the optimum boundaries and to examine the effect of treating m_0 and m_1 as statistically independent.

When mapped to the x, y plane, the decision boundaries shown in Figure 2.6 appear as the heavy lines shown in Figure 2.7. Let P_α be the conditional probability of error given that either word $(0,0)$ or $(1,1)$ corresponding to points I and IV was sent. Then

$$P_\alpha = \frac{1}{2} \left(1 - \operatorname{erf} \frac{1}{2} \sqrt{\frac{E}{N_0}} \right) \quad (2.24)$$

Let P_β be the conditional probability of error given that either word $(1,0)$ or $(0,1)$ corresponding to points II and III was sent. We have been unable to obtain a closed form expression for P_β . However, we will find an upper bound, $P_{\beta U}$, and a lower bound, $P_{\beta L}$, for P_β . The lower bound is obtained by changing the straight line AB to the broken line 1234 and computing the conditional probability of error given that word $(0,1)$ corresponding to point III was sent.* Thus,

$$\begin{aligned} P_{\beta L} &= 1 - \frac{1}{\pi} \int_0^{\frac{1}{2}\sqrt{E/N_0}} \int_{-\frac{\sqrt{3}}{4}\sqrt{E/N_0}}^{\infty} e^{-(x^2+y^2)} dy dx \\ &\quad - \frac{1}{\pi} \int_{-\frac{1}{2}\sqrt{E/N_0}}^0 \int_{-\frac{3\sqrt{3}}{4}\sqrt{E/N_0}}^{\infty} e^{-(x^2+y^2)} dy dx \\ &= 1 - \frac{1}{4} \left(2 + \operatorname{erf} \frac{3\sqrt{3}}{4} \sqrt{\frac{E}{N_0}} + \operatorname{erf} \frac{\sqrt{3}}{4} \sqrt{\frac{E}{N_0}} \right) \operatorname{erf} \frac{1}{2} \sqrt{\frac{E}{N_0}} \end{aligned} \quad (2.25)$$

* That the contribution of the triangular area A 1 C is less than that of triangular area C 2 D is easily seen by comparing the contribution of triangular area A'1'C to that of area C 2 D and noting that A'1'C is the mirror image of A 1 C about the line IIIC.

3 January 1961

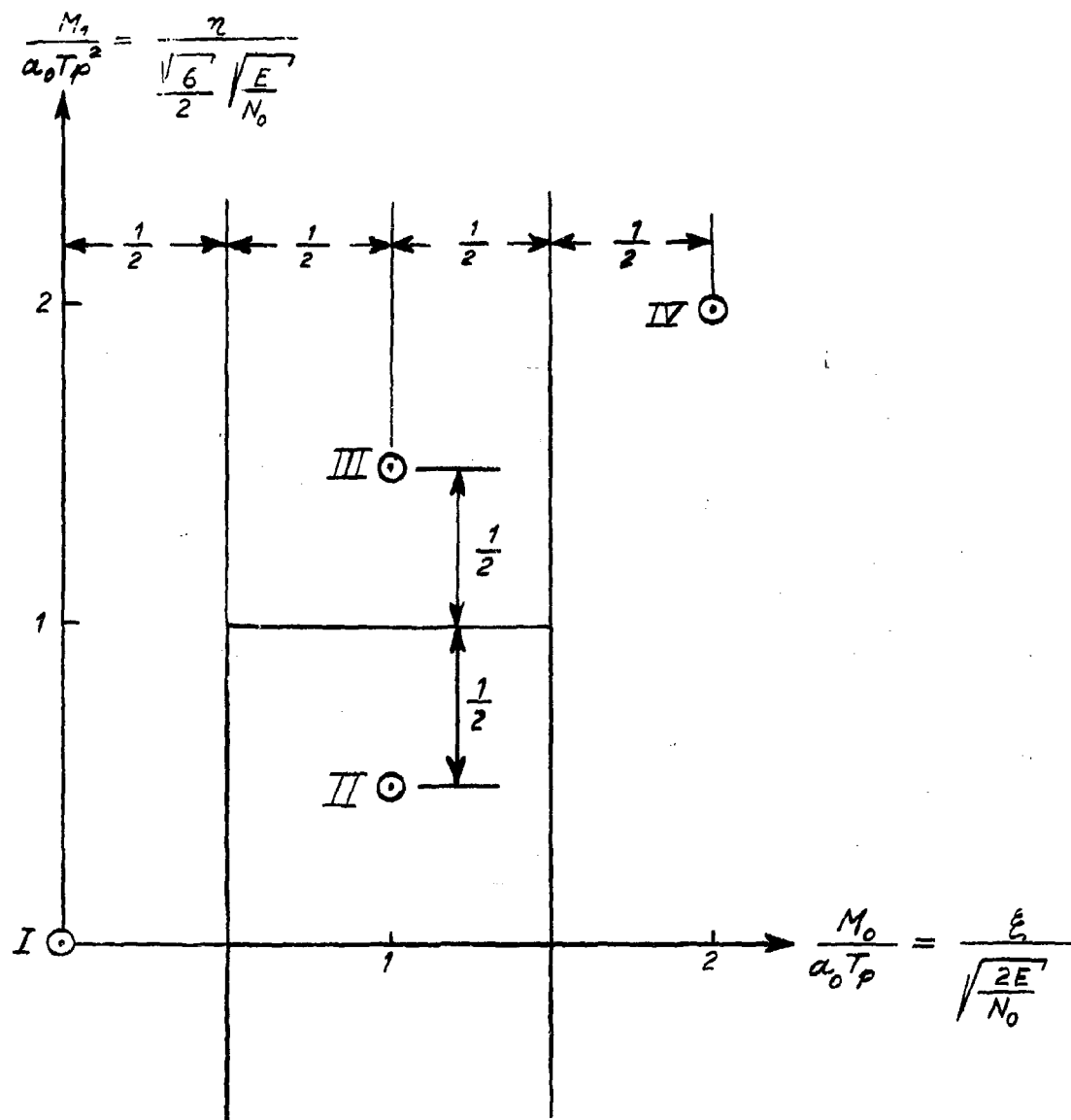


Figure 2.6

3 January 1961

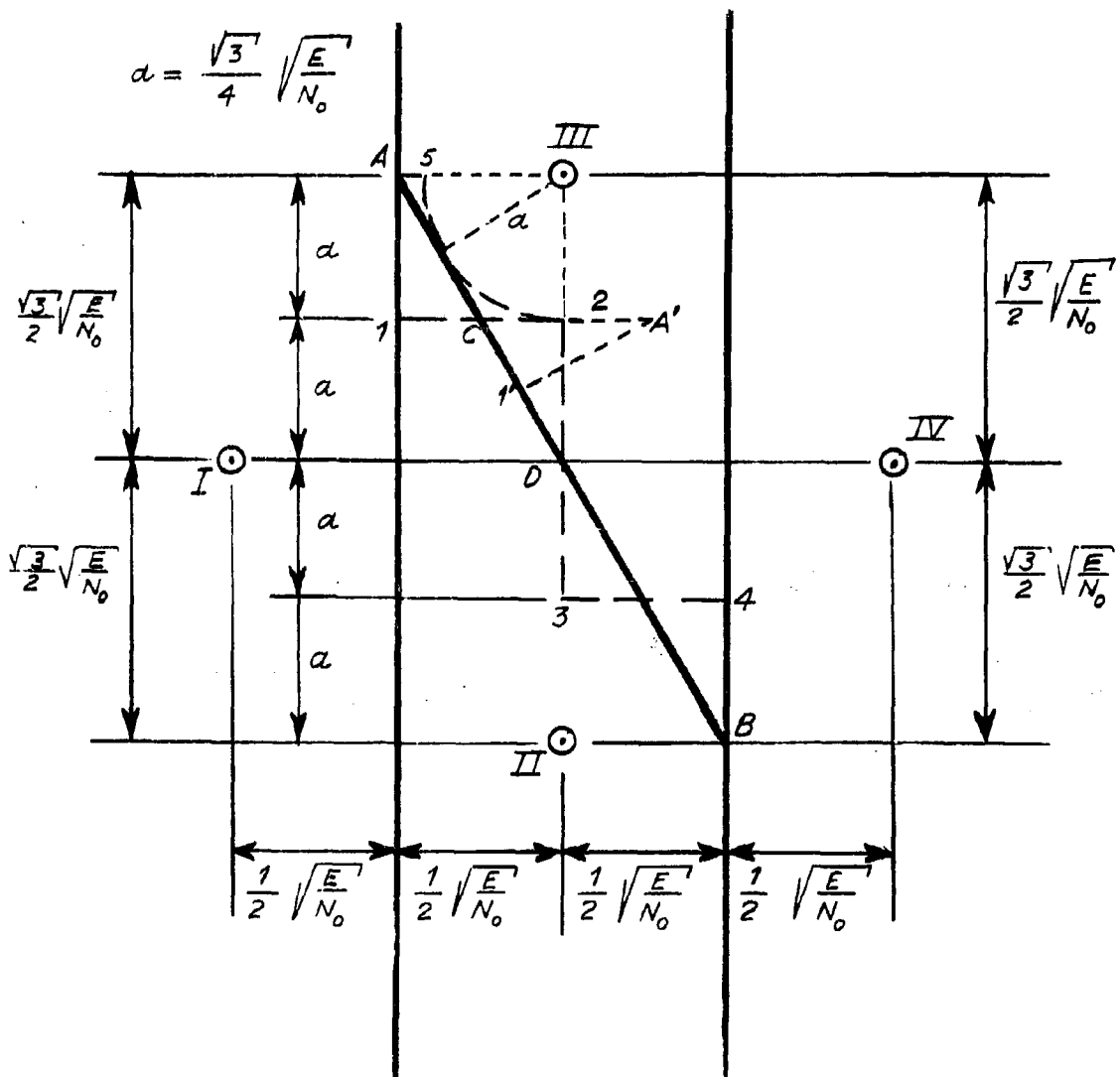


Figure 2.7

The upper bound is obtained by considering the line A5234 as the boundary and again computing the conditional probability of error given that word $(0,1)$ was sent. (The segment 5 to 2 is an arc of a circle with radius $\frac{3}{4}\sqrt{E/N_0}$ and center at point I.I.) Thus,

$$\begin{aligned}
 P_{BU} &= 1 - \frac{1}{\pi} \int_0^{\frac{1}{2}\sqrt{E/N_0}} \int_0^\infty e^{-(x^2+y^2)} dy dx \\
 &\quad - \frac{1}{4} \frac{1}{\pi} \int_0^{\frac{3}{4}\sqrt{E/N_0}} e^{-r^2} 2\pi r dr \\
 &\quad - \frac{1}{\pi} \int_{-\frac{1}{2}\sqrt{E/N_0}}^0 \int_{-\frac{3\sqrt{3}}{4}\sqrt{E/N_0}}^\infty e^{-(x^2+y^2)} dy dx \\
 &= \frac{3}{4} + \frac{1}{4} e^{-\frac{3}{16}\frac{E}{N_0}} - \frac{1}{4} \left(2 + \operatorname{erf} \frac{3\sqrt{3}}{4}\sqrt{\frac{E}{N_0}} \right) \operatorname{erf} \frac{1}{2}\sqrt{\frac{E}{N_0}}
 \end{aligned} \tag{2.26}$$

The probability of error P_S averaged over all 4 words is

$$P_S = \frac{1}{2}(P_\alpha + P_{BU})$$

Define

$$P_{SU} = \frac{1}{2}(P_\alpha + P_{BU}) \quad \text{and} \quad P_{SL} = \frac{1}{2}(P_\alpha + P_{BL})$$

Then

$$P_{SL} < P_S < P_{SU}$$

(2.27)

where, by (2.24) to (2.26),

$$P_{SL} = \frac{3}{4} - \frac{1}{8} \left(4 + \operatorname{erf} \frac{3\sqrt{3}}{4}\sqrt{\frac{E}{N_0}} + \operatorname{erf} \frac{\sqrt{3}}{4}\sqrt{\frac{E}{N_0}} \right) \operatorname{erf} \frac{1}{2}\sqrt{\frac{E}{N_0}} \tag{2.28}$$

$$P_{SU} = \frac{5}{8} - \frac{1}{8} e^{-\frac{3}{16} \frac{E}{N_0}} - \frac{1}{8} \left(4 + \operatorname{erf} \frac{\sqrt{3}}{4} \sqrt{\frac{E}{N_0}} \right) \operatorname{erf} \frac{1}{2} \sqrt{\frac{E}{N_0}} \quad (2.29)$$

and are plotted in Figure 2.4. The probability of error \hat{P}_S based on the assumption that m_0 and m_1 are statistically independent is also plotted for comparison on Figure 2.4. From Figure 2.6 it is seen that

$$\hat{P}_S = \frac{1}{2} (P_S + P_\alpha) \quad (2.30)$$

with

$$\begin{aligned} P_S &= \int_{\frac{1}{2} \sqrt{2 \frac{E}{N_0}}}^{\infty} \int_{-\infty}^{+\infty} p(\xi) p(\eta) d\eta d\xi \\ &= \frac{1}{2} \left(1 - \operatorname{erf} \frac{1}{2} \sqrt{\frac{E}{N_0}} \right) = P_\alpha \end{aligned} \quad (2.31)$$

$$\begin{aligned} P_S &= 1 - \int_{-\frac{1}{2} \sqrt{2 \frac{E}{N_0}}}^{\frac{1}{2} \sqrt{2 \frac{E}{N_0}}} \int_{-\frac{1}{2} \sqrt{\frac{E}{2}}}^{\frac{1}{2} \sqrt{\frac{E}{2}}} \sqrt{\frac{E}{N_0}} p(\xi) p(\eta) d\eta d\xi \\ &= 1 - \frac{1}{2} \left(1 + \operatorname{erf} \frac{\sqrt{3}}{4} \sqrt{\frac{E}{N_0}} \right) \operatorname{erf} \frac{1}{2} \sqrt{\frac{E}{N_0}} \end{aligned} \quad (2.32)$$

It is interesting to note that

$$P_{SL} < \hat{P}_S < P_{SU} \text{ for } \frac{E}{N_0} > 8 \text{ db.}$$

3 January 1961

On Figure 2.4 the upper and lower bounds to P_e obtained with the optimum decision boundaries are also plotted. It will be noted that the difference in db between the optimum and the simple (Figure 2.6) decision rules amounts to approximately 4 db for $E/N_0 > 12$ db. This difference corresponds to about 100:1 ratio in error probability at $E/N_0 = 13$ db and this ratio increases without limit as E/N_0 is further increased.

3. Effect of a Filter Preceding the Moment Detector

This section will illustrate how the probability of error will be affected if a filter precedes the moment detector. The filter to be considered has the simple low pass frequency response

$$H(f) = \frac{W}{W+jf} = \frac{W}{\sqrt{W^2+f^2}} e^{-j \tan^{-1} f/W} \quad (3.1)$$

(W being the 3 db bandwidth) and, consequently, its impulse response is

$$\begin{aligned} h(t) &= 2\pi W e^{-2\pi W t} \text{ for } t \geq 0 \\ &= 0 \text{ for } t < 0 \end{aligned} \quad (3.2)$$

The variance of m_a may be written

$$\begin{aligned} \sigma_a^2 &= \int_0^T \int_0^T t^k u^k E[n(t)n(u)] du dt \\ &= \int_0^T \int_0^T t^k u^k \phi_{nn}(t-u) du dt \end{aligned} \quad (3.3)$$

where $\phi_{nn}(t-u)$ is the noise autocorrelation at the output of the filter. Since the noise power density spectrum at the filter output is $N_o |H(f)|^2$, one has

$$\begin{aligned} \phi_{nn}(t-u) &= \frac{1}{2} \int_{-\infty}^{\infty} N_o \frac{W^2}{W^2+f^2} e^{j2\pi f(t-u)} df \\ &= \frac{\pi}{2} N_o W e^{-2\pi W |t-u|} \end{aligned} \quad (3.4)$$

Substitution of (3.4) into (3.3) yields

$$\sigma_4^2 = \frac{\pi}{2} N_0 W \int_0^T t^4 \left\{ \int_0^t u^2 e^{-2\pi W(t-u)} du + \int_t^T u^2 e^{-2\pi W(t-u)} du \right\} dt \quad (3.5)$$

Thus, by performing the integrations, one obtains:

$$\sigma_0^2 = \frac{N_0}{2} T \left\{ 1 - \frac{1}{2\pi WT} (1 - e^{-2\pi WT}) \right\} \quad (3.6)$$

$$\begin{aligned} \sigma_1^2 &= \frac{N_0}{2} T^3 \left[\frac{1}{3} - \frac{1}{2} \frac{1}{2\pi WT} + \frac{1}{(2\pi WT)^3} \right. \\ &\quad \left. - \left\{ \frac{1}{(2\pi WT)^2} + \frac{1}{(2\pi WT)^3} \right\} e^{-2\pi WT} \right] \end{aligned} \quad (3.7)$$

$$\begin{aligned} \sigma_2^2 &= \frac{N_0}{2} T^5 \left[\frac{1}{5} - \frac{1}{2} \frac{1}{2\pi WT} + \frac{2}{3} \frac{1}{(2\pi WT)^2} - 4 \frac{1}{(2\pi WT)^5} \right. \\ &\quad \left. + \left\{ 2 \frac{1}{(2\pi WT)^3} + 4 \frac{1}{(2\pi WT)^4} \right. \right. \\ &\quad \left. \left. + 4 \frac{1}{(2\pi WT)^5} \right\} e^{-2\pi WT} \right] \end{aligned} \quad (3.8)$$

As $WT \rightarrow \infty$ the variance is asymptotic to the white noise value given by (1.3). This result is not surprising, since: on the one hand, if we hold T fixed and let $W \rightarrow \infty$ the effect of the filter disappears; on the other hand, if we hold W fixed and let $T \rightarrow \infty$ the effective bandwidth W_k of the filter representing the moment detector (see Section 1) approaches zero.*

* Since $W_k = \frac{1}{2\pi H_k(0)} \int_{-\infty}^{\infty} H_k(\omega) d\omega = \frac{1}{H_k(0)} h_k(0)$ and $H_k(0) = \int_{-\infty}^{\infty} h_k(t) dt$, for $h_k(t)$ given by (1.1) one obtains $W_k = \frac{k+1}{T}$.

For the present application, the most important effect of the filter is to add an exponential decay to an originally time-limited pulse. By proper choice of the transmitted signal, however, it is possible to obtain a signal at the output of the filter of limited duration. Thus, the input signal $S_i(t)$ shown in Figure 3.1 results in the output signal $S_o(t)$ shown in the same figure.

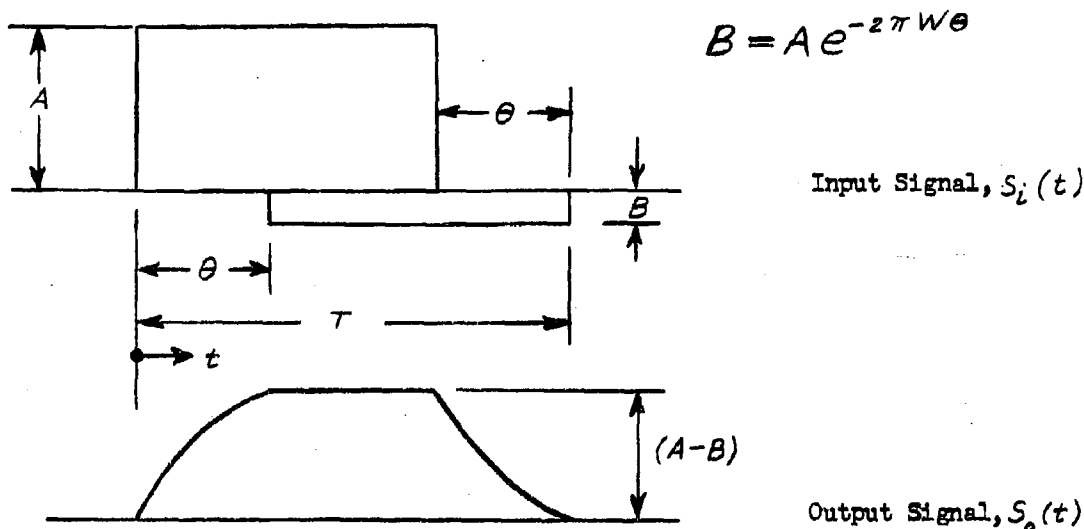


Figure 3.1

Using (3.2) and the relation

$$S_o(t) = \int_{-\infty}^{\infty} S_i(\tau) h(t-\tau) d\tau,$$

one obtains

$$\begin{aligned}
 S_o(t) &= A(1 - e^{-2\pi W t}) && \text{for } 0 \leq t \leq \theta \\
 &= A(1 - e^{-2\pi W \theta}) && \text{for } \theta \leq t \leq (T-\theta) \\
 &= A e^{-2\pi W \theta} \left\{ e^{2\pi W(T-t)} - 1 \right\} && \text{for } (T-\theta) \leq t \leq T \\
 &= 0 \text{ elsewhere}
 \end{aligned} \tag{3.9}$$

The optimum value of θ , i.e., that value of θ which results in the lowest probability of error for a given pulse energy, is a function of peak amplitude A , filter bandwidth W and symbol duration T . Since the input pulse shape (Figure 3.1) cannot match the impulse response of the filter-zero-moment detector combination (except in the limit as $W \rightarrow \infty$), it follows that this system will have a higher error probability with the filter than without it if rectangular pulses are used.*

* For the case of $\theta = T/2$, it is easily shown that the performance degradation exceeds 3 db. Thus,

E = average energy per input signal (It can be shown that for Figure 3.1 the average energy per output signal is equal to $(E - \frac{A^2 - B^2}{4\pi W})$, where E is the average energy per input signal.)

$$= \frac{1}{2} \left\{ \left(A^2 + B^2 \right) \frac{T}{2} + \dots \right\}, \quad A^2 = \frac{T}{4} (1 + e^{-2\pi WT})$$

$$\begin{aligned} \bar{M}_o &= \int_0^T \left\{ S_o(t) \right\}_{\theta=T/2} dt \\ &= A (1 - e^{-\pi WT}) \frac{T}{2} = \frac{1 - e^{-\pi WT}}{\sqrt{1 + e^{-2\pi WT}}} \sqrt{ET} \end{aligned}$$

$$x_o = \frac{\bar{M}_o}{2\sqrt{2} \sigma_o} \left[\text{By (1.5); } \sigma_o \text{ given by (3.6)} \right]$$

$$\begin{aligned} &= \frac{1 - e^{-\pi WT}}{\sqrt{1 + e^{-2\pi WT}} - \frac{1}{2\pi WT} (1 - e^{-4\pi WT})} \sqrt{\frac{E}{4N_o}} \\ &\leq \sqrt{E/4N_o} \quad (\text{Equal sign for } WT \rightarrow \infty) \end{aligned}$$

and the probability of error with the filter present is

$$\begin{aligned} P_{ef} &= \frac{1}{2} (1 - \operatorname{erf} x_o) \quad [\text{By (1.4)}] \\ &\geq \frac{1}{2} (1 - \operatorname{erf} \sqrt{\frac{E}{4N_o}}) > \frac{1}{2} (1 - \operatorname{erf} \sqrt{\frac{E}{2N_o}}) = P_e \end{aligned}$$

where P_e is the probability of error without the filter as given by (1.12), which is valid for zero-order moment detection of unfiltered rectangular signals. Thus, it is seen that for the same probability of error, the E/N_o ratio for the case with the filter must be more than twice that for the case without a filter.

4. Effect of Pulse Overlap (Intersymbol Interference)

When there exists a minimum duration T_p below which the signal pulse duration cannot be reduced, higher signalling speeds can be achieved only by overlapping the pulses such that $\tau < T_p$, where τ is the time between two adjacent pulses, as well as the interval of moment integration. It is clear that under these conditions, intersymbol interference is unavoidable. In this section, the deterioration, as measured by the increase in error probability, will be investigated for a simple case in which the pulses are triangular in shape and the decisions are based on zero-order moments in which case closed form results may be obtained.

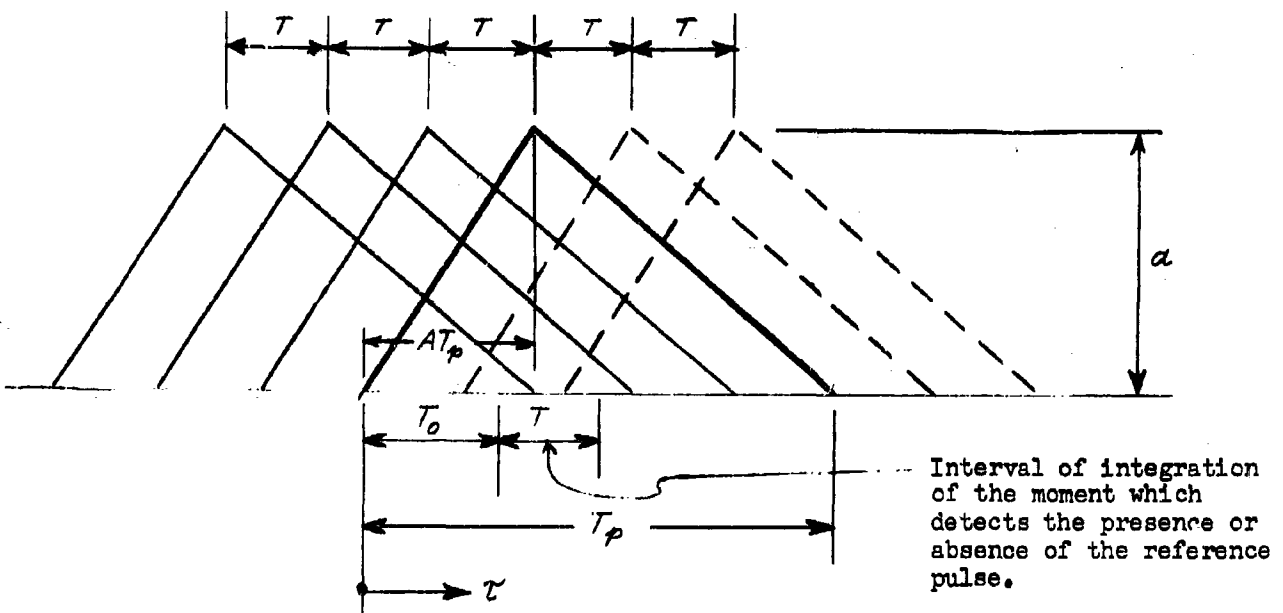


Figure 4.1

The assumed pulse shape and nomenclature are illustrated on Figure 4.1. The reference pulse is shown by the heavier solid lines. The origin of τ , the time variable which describes the pulse shape, is chosen such that

$$\begin{aligned} \bar{\tau}(\tau) &= \alpha \frac{\tau}{AT_p} \quad \text{for } 0 \leq \tau \leq AT_p \\ &= \alpha \frac{T_p - \tau}{(1-A)T_p} \quad \text{for } AT_p \leq \tau \leq T_p \end{aligned} \quad \left. \right\} \quad (4.1)$$

where α is the value of $\frac{\tau}{T_p}$ when the triangular pulse attains its peak value, α . The interval of moment integration of duration T starts at $\tau = T_0$. The pulses shown by the lighter solid lines are called "the possible preceding pulses" and are the possible pulses preceding the reference pulse which cover a portion of the specified interval of moment integration. Similarly, the dashed lines show "the possible succeeding pulses". All other pulses are entirely outside the specified interval of integration and are not shown in Figure 4.1. Let N_p and N_s be, respectively, the number of all possible preceding pulses and all possible succeeding pulses. Then, N_p and N_s are integers satisfying

$$\frac{1}{T}(T_p - T_0) - 1 \leq N_p < \frac{1}{T}(T_p - T_0) \quad (4.2)$$

and

$$\frac{1}{T}T_0 \leq N_s < \frac{1}{T}T_0 + 1 \quad (4.3)$$

respectively.

Let M_0 , M_p and M_s be the zero-order moments contributed respectively by the reference pulse, all possible preceding pulses, and all possible succeeding pulses. Then, for $T_0 < AT_p$ and $T_0 + T > AT_p$,

$$\begin{aligned} M_0 &= (AT_p - T_0) \frac{\alpha}{2} \left(1 + \frac{T_0}{AT_p} \right) + (T_0 + T - AT_p) \frac{\alpha}{2} \left[1 + \frac{T_p - (T_0 + T)}{(1-A)T_p} \right] \\ &= \frac{\alpha T_p}{2A(1-A)} \left[1 \left\{ 1 - A - \left(1 - \frac{T}{T_p} \right)^2 \right\} + 2A \left(1 - \frac{T}{T_p} \right) \frac{T_0}{T_p} - \frac{T_0^2}{T_p^2} \right] \end{aligned} \quad (4.4)$$

$$M_p = (T_p - T - T_0) \frac{\alpha}{2} \frac{T_p - T - T_0}{(1-A)T_p}$$

$$= \frac{\alpha T_p}{2(1-A)} \left(1 - \frac{T}{T_p} - \frac{T_0}{T_p}\right)^2 \quad (4.5)$$

$$M_s = T_0 \frac{\alpha}{2} \frac{T_0}{AT_p} = \frac{\alpha T_p}{2A} \left(\frac{T_0}{T_p}\right)^2 \quad (4.6)$$

and, hence, the total contribution of all possible preceding and succeeding pulses is*

$$M'_0 = M_p + M_s$$

$$= \frac{\alpha T_p}{2A(1-A)} \left\{ A \left(1 - \frac{T}{T_p}\right)^2 - 2A \left(1 - \frac{T}{T_p}\right) \frac{T_0}{T_p} + \frac{T_0^2}{T_p^2} \right\} \quad (4.7)$$

Figure 4.2 is a (hypothetical) sketch of the probability density distribution of the observed zeroth moment due to signal on the assumption that the pulses occur independently with probability 1/2. It consists of two identical symmetric parts, each of which consists of $(N_p + N_s + 1)$ delta functions of strength $1/\{2(N_p + N_s + 1)\}$. The location of each delta function corresponds

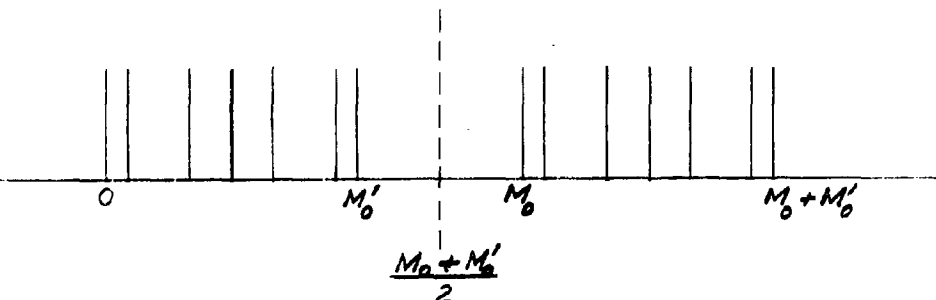


Figure 4.2

* One reason for the choice of triangular pulses for this analysis was that M_p , M_s are independent of N_p , N_s with this shape.

3 January 1961

to a particular combination of presence and absence of the reference pulse and possible preceding and succeeding pulses.

If it is desired to make each decision independently (clearly, succeeding moments are not independent when overlapping pulses are used), the optimum threshold is at $\frac{1}{2}(M_o + M_o')$. We, therefore, adopt the decision rules:

$$\begin{aligned} \text{measured value of zeroth moment } &> \frac{1}{2}(M_o + M_o') \dots \text{reference pulse} \\ &\quad \text{present} \quad (4.8) \\ \text{measured value of zeroth moment } &\leq \frac{1}{2}(M_o + M_o') \dots \text{reference pulse} \\ &\quad \text{absent} \end{aligned}$$

Since the number of the actual preceding and succeeding pulses may vary from zero to $(N_p + N_s)$, the moment due to the actual preceding and succeeding pulses may be less than M_o' and is designated M_o'' . (M_o'' is measured, not M_o' .) Thus, with the reference pulse actually present, an error will be committed when the noise moment, m_o , is such that

$$M_o + M_o'' + m_o \leq \frac{1}{2}(M_o + M_o')$$

or

$$m_o \leq -\frac{1}{2} \left\{ (M_o - M_o') + 2M_o'' \right\} \quad (4.9)$$

Similarly, with signal actually absent, an error will be committed when

$$m_o > \frac{1}{2} \left\{ (M_o - M_o') + 2(M_o' - M_o'') \right\} \quad (4.10)$$

From the fact that M_o'' and $(M_o' - M_o'')$ have the same possible values (which have been assumed to be equally probable), (4.9) and (4.10) show that the probability of error is the same when a signal is either actually present or actually absent. In other words, the probability of error can be calculated as follows: first, by (1.6),

$$x_o = \frac{1}{2\sqrt{N_o T}} \left\{ (M_o - M_o') + 2M_o'' \right\} \quad (4.11)$$

for each possible M_o'' (χ_o will have repeated values if M_o'' has repeated values); then, by the use of (4.4), the probability of error is

$$P_e = \frac{1}{\ell} \sum_{k=1}^{\ell} \frac{1}{2} (1 - \operatorname{erf} \chi_o) \quad (4.12)$$

where

$$\ell = 2^{N_p + N_s} \quad (4.13)$$

is the number of possible M_o'' or χ_o .

From (4.11) and (4.12) and noting that zero is a possible value of M_o'' , one can see that it is desirable to have $(M_o - M_o')$ as high as possible. From (4.4) and (4.7), one finds that M_o is maximum and M_o' is minimum when

$$T_o = A (T_p - T) \quad (4.14)$$

Therefore, we choose this value for T_o . Then (4.4) and (4.7) yield

$$(M_o - M_o') = \frac{a T_p}{2} \left\{ 1 - 2 \left(1 - \frac{T}{T_p} \right)^2 \right\} \quad (4.15)$$

It follows that $(M_o - M_o')$ decreases from $\frac{1}{2} a T_p$ to zero as $\frac{T}{T_p}$ decreases from 1 to $(1 - \frac{1}{2})$.

If $\frac{T}{T_p} = 1$ (i.e., there is no overlap), $M_o' = M_o'' = 0$ and one obtains from (4.15), (4.11) and (4.12) the simple expression for the probability of error

$$P_e = \frac{1}{2} (1 - \operatorname{erf} \frac{a}{4} \sqrt{\frac{T}{N_o}}) \quad (4.16)$$

or, since the average signal energy per signal for the present case is

$$\begin{aligned} E &= \frac{1}{2} \left[\int_0^{AT} \left(a \frac{t}{AT} \right)^2 dt + \int_0^{(1-A)T} \left\{ a \frac{t}{(1-A)T} \right\}^2 dt + \dots \right] \\ &= \frac{1}{6} a^2 T, \\ P_e &= \frac{1}{2} (1 - \operatorname{erf} \frac{\sqrt{6}}{4} \sqrt{\frac{E}{N_o}}) \end{aligned} \quad (4.17)$$

For the case with $\frac{T}{T_p} = \frac{1}{2}$, $A = \frac{1}{2}$ and, by (4.14), $\frac{T_e}{T_p} = \frac{1}{4}$:

$$(M_0 - M'_0) = \frac{1}{4} a T_p = \frac{1}{2} a T \quad [\text{By (4.15)}]$$

$$M''_0 = 0, \frac{1}{8} a T, \frac{1}{8} a T \text{ and } \frac{1}{4} a T$$

$$(M_0 - M'_0) + 2M''_0 = \frac{1}{2} a T, \frac{3}{4} a T, \frac{3}{4} a T \text{ and } a T$$

$$x_0 = \frac{2}{4} \sqrt{\frac{T}{N_0}}, \frac{3a}{8} \sqrt{\frac{T}{N_0}}, \frac{3a}{8} \sqrt{\frac{T}{N_0}} \text{ and } \frac{a}{2} \sqrt{\frac{T}{N_0}} \quad [\text{By (4.11)}]$$

$$\begin{aligned} P_e = & \frac{1}{4} \left\{ \frac{1}{2} (1 - \operatorname{erf} \frac{a}{4} \sqrt{T/N_0}) + 2 \cdot \frac{1}{2} (1 - \operatorname{erf} \frac{3a}{8} \sqrt{T/N_0}) \right. \\ & \left. + \frac{1}{2} (1 - \operatorname{erf} \frac{a}{2} \sqrt{T/N_0}) \right\} \quad [\text{By (4.12)}] \\ & - \frac{1}{2} \cdot \frac{1}{8} (\operatorname{erf} \frac{a}{4} \sqrt{\frac{T}{N_0}} + 2 \operatorname{erf} \frac{3a}{8} \sqrt{\frac{T}{N_0}} + \operatorname{erf} \frac{a}{2} \sqrt{\frac{T}{N_0}}) \end{aligned} \quad (4.18)$$

$$E = \frac{1}{4} \left\{ \int_0^T a^2 dt + 2 \int_0^T (a \frac{t}{T})^2 dt + 0 \right\} - \frac{5}{12} a^2 T$$

$$P_e = \frac{1}{2} - \frac{1}{8} (\operatorname{erf} \frac{\sqrt{5}}{10} \sqrt{\frac{E}{N_0}} + 2 \operatorname{erf} \frac{3\sqrt{5}}{20} \sqrt{\frac{E}{N_0}} + \operatorname{erf} \frac{\sqrt{5}}{5} \sqrt{\frac{E}{N_0}}) \quad (4.19)$$

For the case $\frac{T}{T_p} = \frac{1}{3}$, $A = \frac{1}{2}$ and $\frac{T_e}{T_p} = \frac{1}{3}$, the following results are obtained:

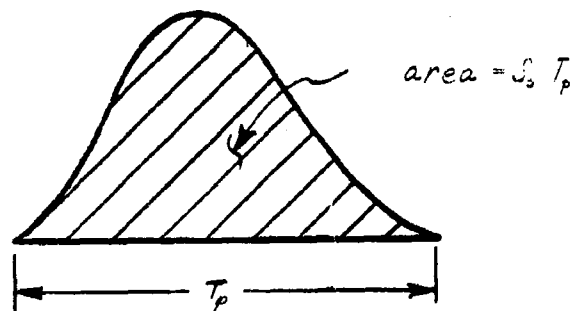
$$P_e = \frac{1}{2} - \frac{1}{8} (\operatorname{erf} \frac{a}{12} \sqrt{\frac{T}{N_0}} + 2 \operatorname{erf} \frac{5a}{12} \sqrt{\frac{T}{N_0}} + \operatorname{erf} \frac{3a}{4} \sqrt{\frac{T}{N_0}}) \quad (4.20)$$

$$E = \frac{169}{216} a^2 T$$

$$P_e = \frac{1}{2} - \frac{1}{8} (\operatorname{erf} \frac{16}{26} \sqrt{\frac{E}{N_0}} + 2 \operatorname{erf} \frac{5\sqrt{6}}{26} \sqrt{\frac{E}{N_0}} + \operatorname{erf} \frac{9\sqrt{6}}{26} \sqrt{\frac{E}{N_0}}) \quad (4.21)$$

The probabilities of error given by (4.17), (4.19) and (4.21) are plotted in Figure 4.3 versus E/N_0 expressed in decibels. The effect of overlap on the error probability is thus made clear. For the cases $T/T_p < 1$, it may be noted that the error probabilities shown in Figure 4.3 are the average values for all possible situations and that the conditional error probabilities at high E/N_0 may be as high as four times for the following two particular conditions: (a) the reference pulse is present and all possible preceding and succeeding pulses absent; (b) the reference pulse is absent and all possible preceding and succeeding pulses present.

It is of interest to compare the results obtained above with those of Slade, et al (Ref. 1). Slade, et al, investigated the effect of pulse rate on error probability in detecting output pulses of an ideal low-pass filter of one-sided bandwidth W . But they neglected the effect of the filter on the variance of noise moment so that (1.3) was assumed to hold*. The output pulses they considered have the shape shown below,



with T_p so selected that

$$\begin{aligned} T_p &\geq \frac{3}{2}W \quad \text{when} \quad \frac{T}{T_p} = 1 \quad (\text{no pulse overlap}) \\ T_p &= \frac{3}{2}W \quad \text{when} \quad \frac{T}{T_p} < 1 \quad (\text{with overlap}) \end{aligned} \quad \left. \right\} \quad (4.22)$$

*By substituting $\frac{N^2}{W}$ for N_0 , (1.3) becomes the same as Equation (19) of Ref. 1.

3 January 1961

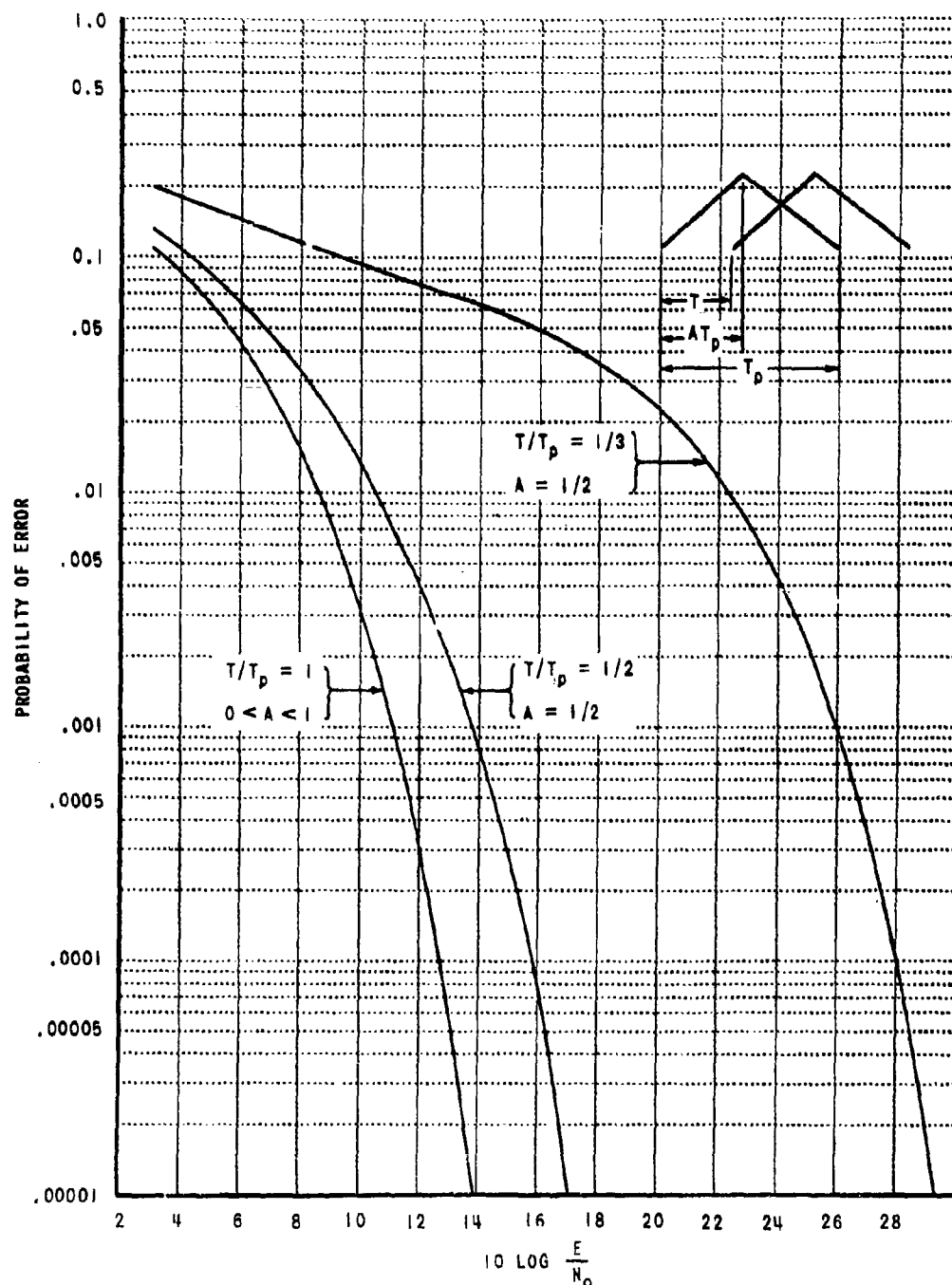


Figure 4-3

Their results are expressed in terms of S_o/N , where S_o is the average pulse amplitude and N is the r.m.s. of the filtered white Gaussian noise.

N^2 is the total noise power at the filter output (or in the bandwidth W) so that it is related to our N_o by

$$N_o = \frac{N^2}{W} \quad (4.23)$$

Our equations (4.16), (4.18) and (4.20) for triangular pulses are readily converted to correspond to their results by the use of (4.22), (4.23) and $\alpha = 2S_o$, yielding

$$P_e = \frac{1}{2} (1 - \operatorname{erf} \frac{S_o}{N} \frac{1}{2} \sqrt{\pi W}) \quad \text{for } T \geq \frac{3}{2W} \quad (4.24)$$

$$P_e = \frac{1}{2} - \frac{1}{8} \left(\operatorname{erf} \frac{S_o}{N} \frac{\sqrt{3}}{4} + 2 \operatorname{erf} \frac{S_o}{N} \frac{3\sqrt{3}}{8} + \operatorname{erf} \frac{S_o}{N} \frac{\sqrt{3}}{2} \right) \quad \text{for } T = \frac{3}{4W} \quad (4.25)$$

$$P_e = \frac{1}{2} - \frac{1}{8} \left(\operatorname{erf} \frac{S_o}{N} \frac{\sqrt{2}}{12} + 2 \operatorname{erf} \frac{S_o}{N} \frac{5\sqrt{2}}{12} + \operatorname{erf} \frac{S_o}{N} \frac{3\sqrt{2}}{4} \right) \quad \text{for } T = \frac{1}{2W} \quad (4.26)$$

From these, the following table, which corresponds to similar tables in the reference, is obtained for $P_e = \text{constant} = 10^{-4}$.

3 January 1961

2 TW	Pulse Per Second	$20 \log \frac{S_o}{N}$
100	$\frac{1}{50} \text{ W}$	-2.6
20	$\frac{1}{10} \text{ W}$	4.4
10	$\frac{1}{5} \text{ W}$	7.4
4	$\frac{1}{2} \text{ W}$	11.4
3	$\frac{2}{3} \text{ W}$	12.7
$\frac{3}{2}$	$\frac{4}{3} \text{ W}$	14.8
1	2 W	26.1

no pulse overlap }
 pulses overlap }

The upper part of the table (no pulse overlap) agrees exactly with Table I of Reference 1. This would be expected, since the probability of error in detecting zero-order moment does not depend on the pulse shape (it depends only on S_o) when the pulses do not overlap. With overlap, however, the

S_o/N values given in the lower part of the above table are about 3.5 decibels lower than the corresponding values given in Table II of Reference 1. This rather appreciable difference is probably due in part to the difference in pulse shape and in part to the choice of T_o which determines the location of the interval of moment integration with respect to the pulse shape. (The manner in which T_o was chosen is not described in Reference 1.)

REFERENCES

1. Slade, J. J., Jr., et al Moment Detection and Coding
Transactions AIEE, Pt. I, pp. 275-279 July 1957
2. Lawton, J. G. Comparison of Binary Data Transmission Systems
Proceedings 1958 IRE Second National Convention on Military Electronics,
pp. 54-61 16 June 1958

1 August 1960

IV(b) DETECT MEMO NO. 4

Subject: "Optimum Decision Based on Multiple Moment-Detection"

By: T. T. Chang

Consider the problem of deciding which of q possible signals was actually transmitted when the only available data consist of a set of n temporal moments derived from the received waveform which consists of signal and stationary, additive, white, Gaussian noise.* q distinct signals, all of equal duration, T , may be transmitted.

The present analysis solves the problem of which decision rule results in the smallest probability of error if the zeroth, first and second order moments are available (the analysis may readily be modified for other order moments). Since the observed moments constitute the sum of the signal and noise moments, one may proceed as follows: First, find the joint probability density distribution of the three noise moments. It is convenient to think of the distribution of a signal point in three-dimensional (moment) space. Since the moments are not independent, an orthogonal transformation** is next performed which yields the probability density of the signal point in independent variables; these variables are then normalized to have identical (Gaussian) distributions. Finally, the decision is made by comparing the distances in this space, between the point represented by the observed moments and the q points representing the q sets of moments of the possible words in the absence of noise.

Without losing any generality, the stationary, additive, white, Gaussian noise may be assumed to have zero mean.*** Then the noise temporal moment of any order also has zero mean. Let m_0 , m_1 and m_2 be the zeroth, first and second order noise moments, all with zero mean. For the analysis, we need to evaluate the following quantities.

* Throughout this memo, $n = 3$ is assumed. The extension to $n > 3$ can be carried through in analogous manner.

** See, e.g., Middleton's "Introduction to Statistical Communication Theory," McGraw-Hill 1960, pg. 349.

*** If the noise has a given mean different from zero, this mean can be added to the signal in computing the expected moments of each word.

1 August 1960
 DETECT MEMO NO. 4
 AF 30(602)-2210

$$\mu_{kh} = E[m_k m_h] \quad k, h = 0, 1, 2$$

For $h = k$, the quantity is the variance or mean square of m_k ; for $h \neq k$, it is the covariance of m_k and m_h . (We avoid the term "second moment" here, so that we can reserve "moment" for "temporal moment" only.) By definition, the k th order noise moment

$$m_k = \int_0^T t^k n(t) dt$$

where $n(t)$ is the noise and T is the duration of one word. Thus,

$$\begin{aligned} \mu_{kh} &= E\left[\int_0^T t^k n(t) dt \int_0^T u^h n(u) du\right] \\ &= \int_0^T \int_0^T t^k u^h E[n(t) n(u)] du dt \\ &= \int_0^T \int_0^T t^k u^h \phi_{nn}(u-t) du dt \end{aligned}$$

Designating the noise power per cps of one-sided spectrum as N_0 , the auto-correlation of the noise is

$$\phi_{nn}(u-t) = \frac{N_0}{2} \int_{-\infty}^{\infty} e^{-j2\pi f(u-t)} df = \frac{N_0}{2} \delta(u-t)$$

Hence,

$$\int_0^T u^h \phi_{nn}(u-t) du = \frac{N_0}{2} t^h \quad (0 < t < T)$$

and

$$\mu_{kh} = \frac{N_0}{2} \int_0^T t^{k+h} dt = \frac{N_0}{2} \frac{T^{k+h+1}}{k+h+1} \quad (1)$$

1 August 1960
 DETECT MEMO NO. 4
 AF 30(602)-2210

From this we obtain:

$$\begin{aligned}
 \mu_{00} &= \frac{N_0}{2} T & = \sigma_0^{-2} \\
 \mu_{11} &= \frac{N_0}{2} \frac{T^3}{3} & = \sigma_1^{-2} \\
 \mu_{22} &= \frac{N_0}{2} \frac{T^5}{5} & = \sigma_2^{-2} \\
 \mu_{01} &= \frac{N_0}{2} \frac{T^2}{2} & = \mu_{10} \\
 \mu_{02} &= \frac{N_0}{2} \frac{T^3}{3} & = \mu_{20} \\
 \mu_{12} &= \frac{N_0}{2} \frac{T^4}{4} & = \mu_{21}
 \end{aligned} \tag{2}$$

We now form the matrix

$$\mu = \begin{bmatrix} \mu_{00} & \mu_{01} & \mu_{02} \\ \mu_{10} & \mu_{11} & \mu_{12} \\ \mu_{20} & \mu_{21} & \mu_{22} \end{bmatrix} \tag{3}$$

Using the elements as given by (2), the determinant of μ is found to be

$$D = \left(\frac{N_0 T^4}{24} \right)^2 - \frac{N_0 T}{30} \tag{4}$$

1 August 1960
 DETECT MEMO NO. 4
 AF 30(602)-2210

and the inverse matrix of μ is found to be

$$\nu = \begin{bmatrix} \nu_{00} & \nu_{01} & \nu_{02} \\ \nu_{10} & \nu_{11} & \nu_{12} \\ \nu_{20} & \nu_{21} & \nu_{22} \end{bmatrix} \quad (5)$$

where

$$\begin{aligned} \nu_{00} &= \frac{18}{N_0 T} & = 9 \frac{1}{\sigma_0^2} \\ \nu_{11} &= \frac{384}{N_0 T^3} & = 64 \frac{1}{\sigma_1^2} \\ \nu_{22} &= \frac{360}{N_0 T^5} & = 36 \frac{1}{\sigma_2^2} \\ \nu_{01} &= -\frac{72}{N_0 T^2} = \nu_{10} & = -12\sqrt{3} \frac{1}{\sigma_0 \sigma_1} \\ \nu_{02} &= \frac{60}{N_0 T^3} = \nu_{20} & = 6\sqrt{5} \frac{1}{\sigma_0 \sigma_2} \\ \nu_{12} &= -\frac{360}{N_0 T^4} = \nu_{21} & = -12\sqrt{15} \frac{1}{\sigma_1 \sigma_2} \end{aligned} \quad (6)$$

Since the noise is assumed to be Gaussianly distributed, the noise moments are also Gaussianly distributed and the joint probability density distribution of any three noise moments of different orders is a 3-dimensional normal distri-

1 August 1960
 DETECT MEMO NO. 4
 AF 30(602)-2210

bution. Consequently, the distribution of m_0 , m_1 and m_2 in the m_0 , m_1 , m_2 space is*

$$p(m_0, m_1, m_2) = \frac{1}{\sqrt{D}} \frac{1}{(\sqrt{2\pi})^3} e^{-R/2} \quad (7)$$

where

$$\begin{aligned} R = & \nu_{00} m_0^2 + \nu_{11} m_1^2 + \nu_{22} m_2^2 \\ & + 2 (\nu_{01} m_0 m_1 + \nu_{02} m_0 m_2 + \nu_{12} m_1 m_2) \end{aligned} \quad (8)$$

Introducing normalized variables,

$$\begin{aligned} \xi &= \frac{m_0}{\sigma_0} = \sqrt{\frac{2T}{N_0}} \frac{m_0}{T} \\ \eta &= \frac{m_1}{\sigma_1} = \sqrt{\frac{2T}{N_0}} \sqrt{3} \frac{m_1}{T^2} \\ \varsigma &= \frac{m_2}{\sigma_2} = \sqrt{\frac{2T}{N_0}} \sqrt{5} \frac{m_2}{T^3} \end{aligned} \quad (9)$$

Then the joint distribution of ξ , η and ς in the ξ , η , ς space is

$$\begin{aligned} p(\xi, \eta, \varsigma) &= \frac{\partial(m_0, m_1, m_2)}{\partial(\xi, \eta, \varsigma)} p(m_0, m_1, m_2) \\ &= \sigma_0 \sigma_1 \sigma_2 p(m_0, m_1, m_2) \end{aligned}$$

*For instance, see J.H. Laning and R. H. Battin "Random Processes in Automatic Control," 1956, McGraw-Hill Book Company, Eq. (2.13-31) on p. 78.

1 August 1960
DETECT MEMO NO. 4
AF 30(602)-2210

or, by (7), (2) and (4),

$$P(\xi, \eta, \zeta) = \frac{12}{(\sqrt{2\pi})^3} e^{-R/2} \quad (10)$$

where, by (8), (9) and (6),

$$\begin{aligned} R = & 9\xi^2 + 64\eta^2 + 36\zeta^2 \\ & + 2(-12\sqrt{3}\xi\eta + 6\sqrt{5}\xi\zeta - 12\sqrt{15}\eta\zeta) \end{aligned} \quad (11)$$

Our next step is to find a linear transformation

$$\begin{bmatrix} x \\ y \\ z \end{bmatrix} = [L] \begin{bmatrix} \xi \\ \eta \\ \zeta \end{bmatrix} \quad (\text{L being a square matrix}) \quad (12)$$

which transforms (11) to

$$R = x^2 + y^2 + z^2 \quad (13)$$

so that x, y, z are orthogonalized normal coordinates. The usual way of obtaining this kind of transformation is to rotate the ξ, η, ζ axes to the principal axes of the central quadric surface represented by (11) with R equal to any real constant and, then, to change the scales of the principal axes.* In doing this for the present case, however,

*For method of obtaining the principal axes, see, for instance, F. B. Hildebrand "Methods of Applied Mathematics," Prentice-Hall, Inc., Article 1.13.

1 August 1960
 DETECT MEMO NO. 4
 AF 30(602)-2210

fairly cumbersome numerical computations are encountered. By a method described in the APPENDIX, the following transformation has been obtained.

$$x = \sqrt{\frac{5}{7}} (\sqrt{3} \xi) - \sqrt{\frac{2}{7}} (\sqrt{6} \zeta)$$

$$y = a \left[\sqrt{\frac{1}{2}(1 + \sqrt{\frac{14}{23}})} \eta - \sqrt{\frac{1}{2}(1 - \sqrt{\frac{14}{23}})} \{ \sqrt{\frac{5}{7}} (\sqrt{6} \zeta) + \sqrt{\frac{2}{7}} (\sqrt{3} \xi) \} \right] \quad (14)$$

$$z = b \left[\sqrt{\frac{1}{2}(1 + \sqrt{\frac{14}{23}})} \{ \sqrt{\frac{5}{7}} (\sqrt{6} \zeta) + \sqrt{\frac{2}{7}} (\sqrt{3} \xi) \} + \sqrt{\frac{1}{2}(1 - \sqrt{\frac{14}{23}})} \eta \right]$$

where

$$a = \sqrt{36 + 2\sqrt{14 \times 23}}, \quad b = \sqrt{36 - 2\sqrt{14 \times 23}} \quad (15)$$

The correctness of (14) is readily verified by substituting (14) into (13) to obtain (11). The Jacobian of the transformation (14) is

$$\frac{\partial(x, y, z)}{\partial(\xi, \eta, \zeta)} = \sqrt{3} \sqrt{6} a b = 12 \quad (16)$$

as would be expected.* Then, from (10), (13) and (16), the joint distribution of the normalized independent random variables, x , y and z in the x , y , z space is

$$P(x, y, z) = \frac{1}{(\sqrt{2\pi})^3} e^{-(x^2 + y^2 + z^2)/2} \quad (17)$$

* Any transformation (12) satisfying (13) identically for R given by (11) must have the Jacobian equal to 12 to cancel that factor appearing in (10), since (17) must be true for such a transformation.

1 August 1960
 DETECT MEMO NO. 4
 AF 30(602)-2210

Let the signal moments of any word i among the q possible transmitted words be M_{0i} , M_{1i} and M_{2i} ($i = 1, 2, \dots, q$); and let the observed moments be M_0 , M_1 and M_2 . Then, if i is the actually transmitted word, we have

$$m_0 = M_0 - \bar{M}_{0i}, \quad m_1 = M_1 - \bar{M}_{1i}, \quad m_2 = M_2 - \bar{M}_{2i} \quad (18)$$

Substituting (18) in (9), one obtains

$$\begin{aligned} \xi &= \sqrt{\frac{2T}{N_0}} (u - \bar{u}_{0i}) \\ \eta &= \sqrt{\frac{2T}{N_0}} (\sqrt{3}v - \sqrt{3}\bar{v}_{1i}) \\ \zeta &= \sqrt{\frac{2T}{N_0}} (\sqrt{5}w - \sqrt{5}\bar{w}_{2i}) \end{aligned} \quad (19)$$

where

$$u = \frac{M_0}{T} \quad v = \frac{M_1}{T^2} \quad w = \frac{M_2}{T^3} \quad (20)$$

and

$$\bar{u}_i = \frac{\bar{M}_{0i}}{T} \quad \bar{v}_i = \frac{\bar{M}_{1i}}{T^2} \quad \bar{w}_i = \frac{\bar{M}_{2i}}{T^3} \quad (21)$$

Substituting (19) in (14), one obtains

1 August 1960
DETECT MEMO NO. 4
AF 30(602)-2210

$$\left. \begin{array}{l} x = \sqrt{\frac{2T}{N_0}} (X - \bar{X}_i) \\ y = \sqrt{\frac{2T}{N_0}} (Y - \bar{Y}_i) \\ z = \sqrt{\frac{2T}{N_0}} (Z - \bar{Z}_i) \end{array} \right\} \quad (22)$$

where

$$\left. \begin{array}{l} X = a_1(u - 2w) \\ Y = -b_1(u + 5w) + b_2 v \\ Z = c_1(u + 5w) + c_2 v \end{array} \right\} \quad (23)$$

$$\left. \begin{array}{l} \bar{X}_i = a_1(\bar{u}_i - 2\bar{w}_i) \\ \bar{Y}_i = -b_1(\bar{u}_i + 5\bar{w}_i) + b_2 \bar{v}_i \\ \bar{Z}_i = c_1(\bar{u}_i + 5\bar{w}_i) + c_2 \bar{v}_i \end{array} \right\} \quad (24)$$

$$\left. \begin{array}{ll} a_1 = \sqrt{\frac{15}{7}} & = 1.463850109 \\ b_1 = \sqrt{\frac{30}{7}} \left(\frac{4}{5} + \sqrt{\frac{14}{23}} \right) & = 2.602352917 \\ b_2 = \sqrt{123} \left(\frac{32}{41} + \sqrt{\frac{14}{23}} \right) & = 13.85508240 \\ c_1 = \sqrt{\frac{30}{7}} \left(\frac{4}{5} - \sqrt{\frac{14}{23}} \right) & = .2913797404 \\ c_2 = \sqrt{123} \left(\frac{32}{41} - \sqrt{\frac{14}{23}} \right) & = .1915510233 \end{array} \right\} \quad (25)$$

1 August 1960
DETECT MEMO NO. 4
AF 30(602)-2210

For an observed set of moments m_0, m_1, m_2 corresponding to a particular set of x, y, z , the likelihood of that word is greatest for which

$$f_i = (x - \bar{x}_i)^2 + (y - \bar{y}_i)^2 + (z - \bar{z}_i)^2 \quad (26)$$

is a minimum. Consequently, the optimum decision rule, in the sense of resulting in the lowest probability of error, may be stated as follows. Designate that signal j as having been sent for which

$$f_j = \min_i \{ f_i \} .$$

Implementation of this decision rule is probably most readily achieved through the use of a digital computer.

1 August 1960
DETECT MEMO NO. 4
AF 30(602)-2210

APPENDIX

Consider the quadratic form of three variables*,

$$R = A_{11} x_1^2 + A_{22} x_2^2 + A_{33} x_3^2 + 2(A_{12} x_1 x_2 + A_{13} x_1 x_3 + A_{23} x_2 x_3) \quad (A1)$$

Let

$$\begin{aligned} x_1 &= Ay_1 + By_2 \\ x_2 &= \alpha y_1 + \beta y_2 \end{aligned} \quad \left. \begin{array}{l} \\ \end{array} \right\} \quad (A2)$$

Then

$$\begin{aligned} R &= (A_{11} A^2 + A_{22} \alpha^2 + 2A_{12} A\alpha) y_1^2 \\ &\quad + (A_{11} B^2 + A_{22} \beta^2 + 2A_{12} B\beta) y_2^2 + A_{33} x_3^2 \\ &\quad + \{2A_{11} AB + 2A_{22} \alpha\beta + 2A_{12}(A\beta + B\alpha)\} y_1 y_2 \\ &\quad + (2A_{13} A + 2A_{23} \alpha) y_1 x_3 + (2A_{13} B + 2A_{23} \beta) y_2 x_3 \end{aligned} \quad (A3)$$

Setting the coefficients of $y_2 x_3$ and $y_1 y_2$ to zero and the coefficient of y_2^2 to unity, one obtains the following three conditions for determining A , B , α and β :

*It is assumed that the coefficients satisfy the conditions:

$$A_{11}(A_{23})^2 + A_{22}(A_{13})^2 > 2A_{12}A_{13}A_{23},$$

$$A_{12}A_{23} \neq A_{13}A_{22}, \quad A_{23} \neq 0.$$

1 August 1960
 DETECT MEMO NO. 4
 AF 30(602)-2210

$$\left. \begin{array}{l} \beta = -\frac{A_{13}}{A_{23}} B \\ B = \pm \frac{1}{\sqrt{A_{11} - \frac{A_{13}}{A_{23}} (2A_{12} - \frac{A_{13}}{A_{23}} A_{22})}} \\ \alpha = \gamma A \quad \gamma = \frac{A_{11} - \frac{A_{13}}{A_{23}} A_{12}}{\frac{A_{13}}{A_{23}} A_{22} - A_{12}} \end{array} \right\} \text{(A4)}$$

The value of A may be chosen arbitrarily. With conditions (A4) satisfied, (A3) becomes

$$R = y_2^2 + K y_1^2 + A_{33} x_3^2 + H y_1 x_3 \quad \text{(A5)}$$

where

$$\left. \begin{array}{l} K = (A_{11} + A_{22} \gamma^2 + 2A_{12} \gamma) A^2 \\ H = (2A_{13} + 2A_{23} \gamma) A \end{array} \right\} \text{(A6)}$$

1 August 1960
DETECT MEMO NO. 4
AF 30(602)-2210

Let y_1' , y_3' be axes which are obtained by rotating the y_1 , x_3 axes through an angle θ about the y_2 axis, where

$$\left. \begin{aligned} \tan 2\theta &= \frac{H}{A_{33} - K} = \lambda \\ \cos \theta &= \sqrt{\frac{1}{2}(1 + \frac{1}{\sqrt{1+\lambda^2}})} \\ \sin \theta &= \frac{\lambda}{|\lambda|} \sqrt{\frac{1}{2}(1 - \frac{1}{\sqrt{1+\lambda^2}})} \end{aligned} \right\} \quad (\text{A7})$$

so that

$$\left. \begin{aligned} y_1 &= \sqrt{\frac{1}{2}(1 + \frac{1}{\sqrt{1+\lambda^2}})} y_1' + \frac{\lambda}{|\lambda|} \sqrt{\frac{1}{2}(1 - \frac{1}{\sqrt{1+\lambda^2}})} y_3 \\ x_3 &= \sqrt{\frac{1}{2}(1 + \frac{1}{\sqrt{1+\lambda^2}})} y_3 - \frac{\lambda}{|\lambda|} \sqrt{\frac{1}{2}(1 - \frac{1}{\sqrt{1+\lambda^2}})} y_1' \end{aligned} \right\}, \quad (\text{A8})$$

and (A5) becomes

$$R = y_2^2 + b^2 y_1'^2 + a^2 y_3^2 \quad (\text{A9})$$

where

$$\left. \begin{aligned} a^2 &= \frac{A_{33} + K}{2} + \frac{A_{33} - K}{2} \sqrt{1 + \lambda^2} \\ b^2 &= K + A_{33} - a^2 \end{aligned} \right\} \quad (\text{A10})$$

Putting

$$x = y_2 \quad y = a y_1' \quad z = b y_3 \quad (\text{A11})$$

(A9) becomes

$$R = x^2 + y^2 + z^2 \quad (\text{A12})$$

1 August 1960
 DETECT MEMO NO. 4
 AF 30(602)-2210

From (A2),

$$\left. \begin{aligned} y_1 &= \frac{1}{A\beta - B\alpha} (\beta x_1 - Bx_2) \\ y_2 &= \frac{1}{A\beta - B\alpha} (Ax_2 - \alpha x_1) \end{aligned} \right\} \quad (A13)$$

From (A8),

$$\left. \begin{aligned} y_3 &= \frac{\lambda}{|\lambda|} \sqrt{\frac{1}{2} \left(1 - \frac{1}{\sqrt{1+\lambda^2}} \right)} y_1 + \sqrt{\frac{1}{2} \left(1 + \frac{1}{\sqrt{1+\lambda^2}} \right)} x_3 \\ y'_3 &= \sqrt{\frac{1}{2} \left(1 + \frac{1}{\sqrt{1+\lambda^2}} \right)} y_1 - \frac{\lambda}{|\lambda|} \sqrt{\frac{1}{2} \left(1 - \frac{1}{\sqrt{1+\lambda^2}} \right)} x_3 \end{aligned} \right\} \quad (A14)$$

Combining (A11), (A13) and (A14), one finally obtains

$$\left. \begin{aligned} x &= \frac{1}{A\beta - B\alpha} (Ax_2 - \alpha x_1) \\ y &= a \left\{ \frac{\lambda}{|\lambda|} \sqrt{\frac{1}{2} \left(1 - \frac{1}{\sqrt{1+\lambda^2}} \right)} \frac{1}{A\beta - B\alpha} (\beta x_1 - Bx_2) \right. \\ &\quad \left. + \sqrt{\frac{1}{2} \left(1 + \frac{1}{\sqrt{1+\lambda^2}} \right)} x_3 \right\} \\ z &= b \left\{ \sqrt{\frac{1}{2} \left(1 + \frac{1}{\sqrt{1+\lambda^2}} \right)} \frac{1}{A\beta - B\alpha} (\beta x_1 - Bx_2) \right. \\ &\quad \left. - \frac{\lambda}{|\lambda|} \sqrt{\frac{1}{2} \left(1 - \frac{1}{\sqrt{1+\lambda^2}} \right)} x_3 \right\} \end{aligned} \right\} \quad (A15)$$

In applying the above results to

$$\begin{aligned} R = & 9\zeta^2 + 64\eta^2 + 36\zeta^2 \\ & + 2(-12\sqrt{3}\xi\eta + 6\sqrt{5}\xi\zeta - 12\sqrt{15}\eta\zeta) \end{aligned} \quad (A16)$$

1 August 1960
 DETECT MEMO NO. 4
 AF 30(602)-2210

it is found that the transformation A13 permits a simple geometric interpretation if we take

$$x_1 = \xi \quad x_2 = \xi \quad x_3 = \eta \quad (\text{A17})$$

Then

$$\begin{aligned} A_{11} &= 36 & A_{22} &= 9 & A_{33} &= 64 \\ A_{12} &= 6\sqrt{5} & A_{13} &= -12\sqrt{15} & A_{23} &= -12\sqrt{3} \end{aligned} \quad \left. \right\} \quad (\text{A18})$$

and conditions (A1) give

$$\begin{aligned} B &= -\frac{1}{\sqrt{21}} & \beta &= \sqrt{\frac{5}{21}} \\ \gamma &= \frac{\alpha}{A} = \frac{2}{\sqrt{5}} \end{aligned} \quad (\text{A19})$$

If we choose A in such a way that

$$\frac{-B}{A} = \frac{\alpha}{\beta} (= \tan \varphi) = \frac{\gamma A}{\beta},$$

we obtain

$$A = \sqrt{-\frac{1}{\gamma} B \beta} = \sqrt{\frac{5}{42}}.$$

Hence,

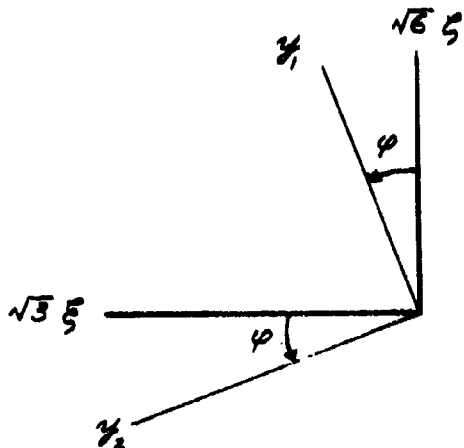
$$\alpha = \sqrt{\frac{2}{21}} \quad A\beta - B\alpha = \frac{\sqrt{2}}{6}$$

and, by the use of (A17), equations (A13) give

$$\begin{aligned} y_1 &= \sqrt{\frac{5}{7}} (\sqrt{6} \xi) + \sqrt{\frac{2}{7}} (\sqrt{3} \xi) \\ y_2 &= \sqrt{\frac{5}{7}} (\sqrt{3} \xi) - \sqrt{\frac{2}{7}} (\sqrt{6} \xi) \end{aligned} \quad \left. \right\} \quad (\text{A20})$$

1 August 1960
 DETECT MEMO NO. 4
 AF 30(602)-2210

The geometric interpretation of this transformation is that the y_1, y_2 axes are obtained by first increasing the scales of the ζ, ξ axes by $\sqrt{6}$ and $\sqrt{3}$, respectively, and then rotating these axes about the η axis through an angle φ .



Using the values of B , β , γ , A and α as determined above, one obtains

$$K = 8 \quad H = -12\sqrt{14} \quad [\text{By (A6)}]$$

$$\lambda = -\frac{3}{\sqrt{14}} \quad [\text{By (A7)}]$$

Then, by (A15) and (A17), one obtains equations (14) on page 7.

1 December 1960

IV(c) DETECT MEMO NO. 9

Subject: "Analysis of the Effects of Impulse Noise on Moment Detection"

By: T. T. Chang

INTRODUCTION

By far the major portion of the literature dealing with the effects of impulse noise on communications systems is concerned with some form of statistical estimation based on experimental data which is often very voluminous. The reasons for this state of affairs are undoubtedly the analytic difficulties which are encountered when one attempts to analyze what the effects of impulse noise on a particular communications system are going to be. This memo presents the results of an attempt to predict how the performance of a moment detection system would be affected by impulse noise. In order to carry the analysis through, it was necessary to make several restrictive assumptions regarding the nature of the impulse noise as well as of the decision technique.

1. GENERAL DISCUSSION

It is assumed that the impulses are true delta functions which are spread due to the finite bandwidth of the transmission system, so that the interfering pulses at the receiver all have the shape $h(t)$ of the impulse response of the transmission system.* If the over-all frequency response of the transmission system can be adequately characterized by the low-pass function $H(\omega) = \frac{\omega_0}{\omega_0 + j\omega}$ then the unit impulse response is given by

* It is known that the observed shape of interfering pulses received over the telephone circuits is highly variable, depending on the distance between the receiver and the location at which the interference originates.

$$h(t) = \begin{cases} \omega_0 e^{-\omega_0 t} & (t \geq 0) \\ 0 & (t < 0) \end{cases} \quad \} \quad (1.1)$$

where $t = 0$ designates the "time of arrival" of the pulse at the receiver.
 (For convenience we will henceforth speak of $t = 0$ as the occurrence of the impulse.)

The temporal moments due to a unit impulse is obtained by integration of the impulse response weighted by the appropriate time function over the duration T of a word. The value of the moment thus obtained will depend on the time of occurrence of the unit impulse relative to the start of the word, this time increment will be treated as a stochastic variable in the sequel. Two distinct cases may be distinguished depending on whether the unit impulse which affects a word occurs after or before the beginning of the word.

(It is clear that any one impulse can occur only during one word but may be the last impulse to occur prior to several words. Thus, the probability of error of adjacent words will not be independent. This dependence of error probabilities will, however, not be treated analytically.)

Case \bar{A} will designate that the impulse occurs after the beginning of the word (obviously since $h(t) = 0$ for $t < 0$ the impulse must occur before the end of the word if it is to affect the moments of that word). Let y designate the time from the beginning of the word until the occurrence of the impulse and m'_k the corresponding k^{th} order moment. Then

$$m'_k = \int_0^{T-y} (t+y)^k h(t) dt \quad (0 \leq y \leq T) \quad (1.2)$$

Case \bar{B} will designate that the unit impulse which affects the word occurs prior to the start of the word. In this case, let \bar{z} be the time from the impulse to the beginning of the word and m''_k the corresponding k^{th} order moment. Then

$$m''_k = \int_{\bar{z}}^{T+\bar{z}} (t-\bar{z})^k h(t) dt \quad (\bar{z} \geq 0) \quad (1.3)$$

Substituting $h(t)$ as given by (1.1) and changing to the normalized (and non-dimensional) variables

$$\tau = \frac{t}{T} \quad \eta = \frac{y}{T} \quad s = \frac{\theta}{T}$$

Equations (1.2) and (1.3) take the form

$$m'_k = aT^k \int_0^{1-\eta} (\tau + \eta)^k e^{-a\tau} d\tau \quad (0 \leq \eta \leq 1) \quad (1.4)$$

$$m''_k = aT^k \int_s^{1+s} (\tau - s)^k e^{-a\tau} d\tau \quad (s \geq 0) \quad (1.5)$$

where $a = \omega_0 T$ (1.6)

Taking k as a positive integer,

$$m'_k(\eta) = aT^k \sum_{r=0}^k \frac{1}{r!} \frac{k!}{(k-r)!} \eta^{k-r} \int_0^{1-\eta} \tau^r e^{-a\tau} d\tau \quad (1.7)$$

$$m''_k(s) = aT^k \sum_{r=0}^k \frac{(-1)^{k+r}}{r!} \frac{k!}{(k+r)!} s^{k+r} \int_s^{1+s} \tau^r e^{-a\tau} d\tau \quad (1.8)$$

Using

$$\begin{aligned} \int \tau^r e^{-a\tau} d\tau &= -\frac{e^{-a\tau}}{a} \left(\frac{r!}{a^r} + \sum_{s=0}^r \frac{r!}{s!} \frac{\tau^s}{a^{r-s}} \right)^*, \\ m'_k(\eta) &= T^k \left\{ \sum_{r=0}^k \frac{k!}{(k-r)!} \frac{1}{a^r} \eta^{k-r} \right. \\ &\quad \left. - e^{-a(1-\eta)} \sum_{r=0}^k \frac{k!}{(k-r)!} \frac{\eta^{k-r}}{a^r} \sum_{s=0}^r \frac{a^s}{s!} (1-\eta)^s \right\} \\ m''_k(s) &= T^k e^{-as} \sum_{r=0}^k (-1)^{k+r} \frac{k!}{(k+r)!} \frac{s^{k+r}}{a^r} \sum_{s=0}^r \frac{a^s}{s!} \{s^s - e^{-a}(1+s)^s\} \end{aligned}$$

* With the understanding that $\tau^s = 1$ when $\tau = s = 0$, one may use

$$\int \tau^r e^{-a\tau} d\tau = -\frac{e^{-a\tau}}{a} \sum_{s=0}^r \frac{r!}{s!} \frac{\tau^s}{a^{r-s}}$$

Interchanging the order of summation ($\sum_{r=0}^k \sum_{s=0}^r \rightarrow \sum_{s=0}^k \sum_{r=s}^k$) and substituting r' for $(k-r)$ (and then dropping the primes) yields

$$m'_k(\eta) = T^k \left\{ \sum_{r=0}^k \frac{k!}{r!} \frac{\eta^r}{a^{k-r}} - e^{-a(1-\eta)} \sum_{s=0}^k \frac{a^s}{s!} (1-\eta)^s \sum_{r=0}^{k-s} \frac{k!}{r!} \frac{\eta^r}{a^{k-r}} \right\} \quad (1.9)$$

$$m''_k(s) = T^k e^{-as} \sum_{s=0}^k \frac{a^s}{s!} \left\{ s^s - e^{-a} (1+s)^s \right\} \sum_{r=0}^{k-s} (-1)^r \frac{k!}{r!} \frac{s^r}{a^{k-r}} \quad (1.10)$$

Define $m''_{k\eta n}$ and $m''_{k\zeta n}$ as follows:

$$m''_{k\eta n} = m''_k (s = \sum_{i=1}^n \lambda_i - \eta) \quad (1.11)$$

$$m''_{k\zeta n} = m''_k (s = \sum_{i=1}^n \lambda_i + \zeta) \quad (1.12)$$

(where the λ_i 's may be identified with the spacing between impulses. See Figure 1.) Then the k th order moment due to all the impulses (I_0, I_1, I_2, \dots , and I_N) which affect the word concerned is equal to

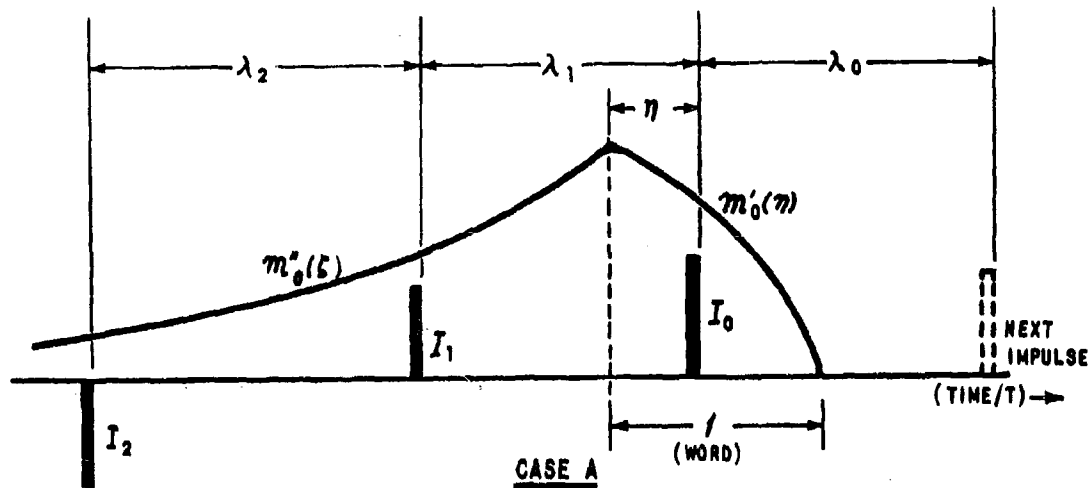
$$I_0 m'_k(n) + \sum_{n=1}^N I_n m''_{k\eta n} \quad \text{for Case A} \quad (1.13)$$

and

$$I_0 m''_k(s) + \sum_{n=1}^N I_n m''_{k\zeta n} \quad \text{for Case B} \quad (1.14)$$

The two cases, A and B, are illustrated schematically in Figure 1. They are differentiated by the time of occurrence, with respect to the word, of the last impulse (indicated by I_0) which affects the word. The total range of

$$\lambda_2 > 1, 0 \leq \eta \leq 1$$



$$\lambda_2 > 1, 0 \leq \xi \leq \lambda_0 - 1$$

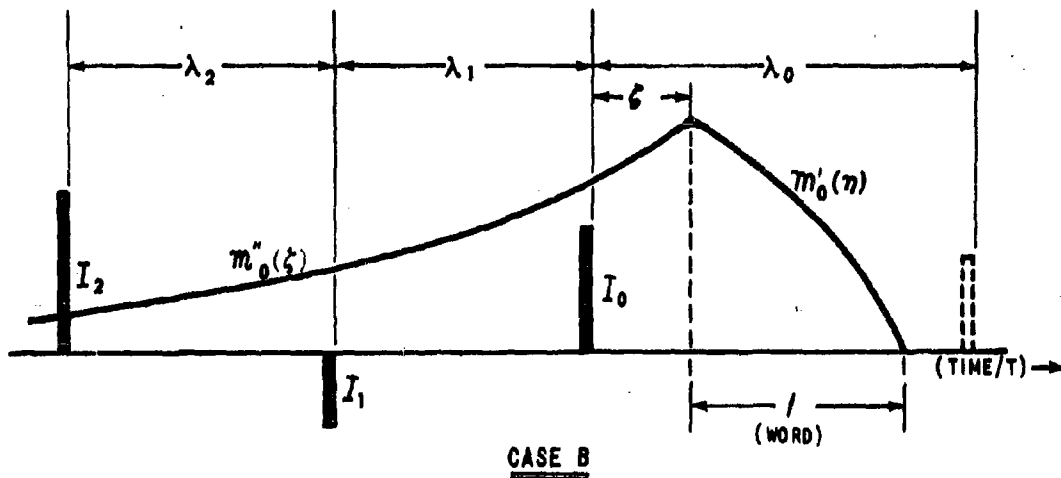


Figure 1

NOTE: λ_2 IS THE LAST IMPULSE THAT AFFECTS THE WORD CONCERNED.
 $\lambda_2 > 1$ REQUIRES THAT THE SPACING BETWEEN IMPULSES IS
 GREATER THAN THE WORD DURATION.

this "time of occurrence" when normalized (by dividing by the word duration T) is equal to λ_0 , the nondimensional spacing from I_0 to the next impulse. Since I_0 does not affect the word when $\eta > 1$, the range of η (Case A) is $0 \leq \eta \leq 1$. This leaves $0 \leq \zeta \leq \lambda_0 - 1$ (Case B). Also shown in the sketches on page 5 are the typical graphs of m'_k and m''_k as functions of η and ζ , respectively.

Let M_k^+ , M_k^- be the largest amount by which the kth order moment may be increased or decreased respectively without causing an error in decision. In general, $M_k^+ \neq M_k^-$ and M_k^+, M_k^- are functions of the particular word which is transmitted. We further assume that the decision logic is such that an error will occur whenever the received moment differs from the interference-free moment by more than M_k^+ or M_k^- (this assumption is justified whenever decisions are based on only these two thresholds). There will be no error if

$$-M_k^- < I_0 m'_k(\eta) + \sum_{n=1}^N I_n m''_{kn} \eta_n < M_k^+ \quad \text{for Case A} \quad (1.15)$$

$$-M_k^- < I_0 m''_k(\zeta) + \sum_{n=1}^N I_n m''_{kn} \zeta_n < M_k^+ \quad \text{for Case B} \quad (1.16)$$

In accordance with Ref. (1) it is assumed that the impulse intensity I (I may be I_0 , I_1 , I_2 , ..., or I_N) has a symmetric hyperbolic distribution such that its probability density is given by

$$\rho(I) = \frac{K-1}{2} \frac{C^{K-1}}{(|I| + C)^K} \quad (1.17)$$

where K and C are positive constants.

From (1.17) the probability that I be in the range $I^- < I < I^+$ is

$$\begin{aligned} P\{I^- < I < I^+\} &= \int_{I^-}^{I^+} \rho(I) dI \\ &= \frac{1}{2} \left\{ \frac{I^+}{|I^+|} \left[1 - \left(\frac{C}{|I^+| + C} \right)^{K-1} \right] - \frac{I^-}{|I^-|} \left[1 - \left(\frac{C}{|I^-| + C} \right)^{K-1} \right] \right\} \quad (1.18) \end{aligned}$$

Even for the case where λ_i is a constant, an analysis based on (1.15) to (1.18) leading to an expression for the probability of error for any k th order moment is found to be mathematically very cumbersome. For this reason, further work will be restricted to the cases of zeroth and first order moments. (It also appears unlikely that if decisions are based on only one moment, a high order moment would be chosen for this purpose.)

2. ZEROOTH ORDER MOMENT

For $k = 0$, Equations (1.9) to (1.12) yield :

$$m'_0(\eta) = 1 - e^{-a(1-\eta)} \quad (2.1)$$

$$m''_0(\zeta) = (1 - e^{-a}) e^{-a\zeta} \quad (2.2)$$

$$m''_{0\eta n} = (1 - e^{-a}) e^{a\eta} e^{-a \sum^n \lambda_i} \quad (2.3)$$

$$m''_{0\zeta n} = (1 - e^{-a}) e^{-a\zeta} e^{-a \sum^n \lambda_i} \quad (2.4)$$

Then, by (1.15) and (1.16), there will be no error if

$$-M_0^- < I_0 \{1 - e^{-a(1-\eta)}\} + \Delta e^{a\eta} < M_0^+ \quad \text{for Case A} \quad (2.5)_A$$

$$-M_0^- < I_0 (1 - e^{-a}) e^{-a\zeta} + \Delta e^{-a\zeta} < M_0^+ \quad \text{for Case B} \quad (2.5)_B$$

where

$$\Delta = (1 - e^{-a}) \sum_{n=1}^N I_n e^{-a \sum^n \lambda_i} \quad (2.6)$$

Note that Δ is the contribution to the zeroth order moment due to I_1 , I_2 , ..., and I_N when $\gamma = \varsigma = 0$.

Let

$$\left. \begin{aligned} I_{\gamma}^+ &= \frac{M_0^+ - \Delta e^{a\gamma}}{1 - e^{-a(1-\gamma)}} & I_{\gamma}^- &= - \frac{M_0^- + \Delta e^{a\gamma}}{1 - e^{-a(1-\gamma)}} \\ I_{\varsigma}^+ &= \frac{M_0^+ e^{a\varsigma} - \Delta}{1 - e^{-a}} & I_{\varsigma}^- &= - \frac{M_0^- e^{a\varsigma} + \Delta}{1 - e^{-a}} \end{aligned} \right\} \quad (2.7)$$

Then, by (2.5), there will be no error if

$$I_{\gamma}^- < I_o < I_{\gamma}^+ \quad \text{for Case A} \quad (2.8)_A$$

$$I_{\varsigma}^- < I_o < I_{\varsigma}^+ \quad \text{for Case B} \quad (2.8)_B$$

Let $P(c|\Delta, \lambda_o)$ be the conditional probability of being correct for given values of Δ and λ_o . If the interference is independent of the information being transmitted, we may assume that the beginning of the word is uniformly distributed with respect to the last interfering pulse I_o . The probability of event A is then

$$P(A) = \frac{1}{\lambda_o} \quad \text{and the probability of event B is}$$

$$P(B) = \frac{\lambda_o - 1}{\lambda_o}; \quad \text{and the probability densities of } \gamma \text{ and } \varsigma \text{ are}$$

$$P(\gamma) = 1 \quad \text{and}$$

$$P(\varsigma) = \frac{1}{\lambda_o - 1}.$$

So that

$$\begin{aligned}
 P(c/\Delta, \lambda_0) &= P(A)P(c/A) + P(B)P(c/B) \\
 &= \frac{1}{\lambda_0} \int_0^1 P(c/\eta) p(\eta) d\eta + \frac{\lambda_0 - 1}{\lambda_0} \int_0^{\lambda_0 - 1} P(c/\xi) p(\xi) d\xi \\
 &= \frac{1}{\lambda_0} \int_0^1 P(c/\eta) d\eta + \frac{\lambda_0 - 1}{\lambda_0} \int_0^{\lambda_0 - 1} P(c/\xi) \frac{1}{\lambda_0 - 1} d\xi \\
 &= \frac{1}{\lambda_0} \left[\int_0^1 P(I_\eta^- < I_0 < I_\eta^+) d\eta + \int_0^{\lambda_0 - 1} P(I_\xi^- < I_0 < I_\xi^+) d\xi \right] \quad (2.9)
 \end{aligned}$$

Equation (1.18) may now be substituted into (2.9) to yield

$$\begin{aligned}
 P(c/\Delta, \lambda_0) &= \frac{1}{2\lambda_0} \left\{ \int_0^1 \frac{M_0^+ - \Delta e^{a\eta}}{|M_0^+ - \Delta e^{a\eta}|} \left[1 - \left(\frac{c - ce^{-a(1-\eta)}}{|M_0^+ - \Delta e^{a\eta}| + c - ce^{-a(1-\eta)}} \right)^{K-1} \right] d\eta \right. \\
 &\quad + \int_0^1 \frac{M_0^- + \Delta e^{a\eta}}{|M_0^- + \Delta e^{a\eta}|} \left[1 - \left(\frac{c - ce^{-a(1-\eta)}}{|M_0^- + \Delta e^{a\eta}| + c - ce^{-a(1-\eta)}} \right)^{K-1} \right] d\eta \\
 &\quad \left. + \int_0^{\lambda_0 - 1} \frac{M_0^+ e^{a\xi} - \Delta}{|M_0^+ e^{a\xi} - \Delta|} \left[1 - \left(\frac{c - ce^{-a}}{|M_0^+ e^{a\xi} - \Delta| + c - ce^{-a}} \right)^{K-1} \right] d\xi \right. \\
 &\quad \left. + \int_0^{\lambda_0 - 1} \frac{M_0^- e^{a\xi} + \Delta}{|M_0^- e^{a\xi} + \Delta|} \left[1 - \left(\frac{c - ce^{-a}}{|M_0^- e^{a\xi} + \Delta| + c - ce^{-a}} \right)^{K-1} \right] d\xi \right\} \quad (2.10)
 \end{aligned}$$

Evaluation of integrals of the type appearing in Equation (2.10) is readily performed by numerical, graphical, or machine methods, but is tedious to perform in closed form. Nevertheless, it can be done, and the method is outlined in the Appendix.

Examination of (2.10) shows $P(c/\Delta, \lambda_0)$ to be a function of $\frac{\Delta}{c}, \frac{M_0^+}{c}, \frac{M_0^-}{c}, \lambda_0$.

Once $P(c/\Delta, \lambda_0)$ is known, the probability of no error $P(c)$ can (in principle) be found from

$$P(c) = \iint P(c/\Delta, \lambda_0) p(\Delta, \lambda_0) d\Delta d\lambda_0 \quad (2.11)$$

where $p(\Delta, \lambda_0)$ is the joint probability density of Δ, λ_0 . Because of the lack of data on which to base realistic assumptions, this final step has not been undertaken except for the limiting case of $\omega_0 = \infty$.

In order to be able to carry through the analysis of an illustrative example, we assume that the strength of each impulse and the spacing from the preceding impulse occur independently of the strength and spacing of all other impulses, with $p(I)$ as given by (1.17) and

$$\begin{aligned} p(\lambda) &= \frac{1}{\lambda_L - \lambda_S}, \quad \lambda_S < \lambda < \lambda_L \\ &= 0, \quad \text{elsewhere} \end{aligned} \quad \} \quad (2.12)$$

Δ and λ_0 are then independent so that

$$\begin{aligned} p(\Delta, \lambda_0) &= \frac{1}{\lambda_L - \lambda_S} p(\Delta) \quad \text{for } \lambda_S \leq \lambda_0 \leq \lambda_L \\ &= 0 \quad \text{for elsewhere} \end{aligned} \quad \} \quad (2.13)$$

and, hence, (2.11) becomes

$$P(c) = \frac{1}{\lambda_L - \lambda_S} \int_{-\infty}^{\infty} p(\Delta) \left\{ \int_{\lambda_S}^{\lambda_L} P(c/\Delta, \lambda_0) d\lambda_0 \right\} d\Delta \quad (2.14)$$

To get a feeling for $\rho(\Delta)$, we consider the simplest case where $N = 1$ (i.e., there is only one impulse, I_1 , preceding I_0). For this case, (2.6) becomes

$$\Delta = (1 - e^{-\alpha}) I_0 e^{-\alpha \lambda_1} \quad (2.15)$$

From (2.15):

$$I_1 = \frac{e^{\alpha \lambda_1}}{1 - e^{-\alpha}} \Delta$$

$$\lambda_1 = \frac{1}{\alpha} \log \frac{(1 - e^{-\alpha}) I_1}{\Delta}$$

$$\frac{\partial I_1}{\partial \Delta} = \frac{e^{\alpha \lambda_1}}{1 - e^{-\alpha}}$$

$$\frac{\partial \lambda_1}{\partial \Delta} = -\frac{1}{\alpha \Delta}$$

$$\rho(\Delta | I_1) = \rho(\lambda_1 = \frac{1}{\alpha} \log \frac{(1 - e^{-\alpha}) I_1}{\Delta}) / \left| \frac{\partial \lambda_1}{\partial \Delta} \right|$$

$$= \begin{cases} \frac{1}{\alpha(\lambda_1 - \lambda_s)/\Delta}, & \frac{e^{\alpha \lambda_s}}{1 - e^{-\alpha}} \leq \frac{I_1}{\Delta} \leq \frac{e^{\alpha \lambda_e}}{1 - e^{-\alpha}} \\ 0, & \text{elsewhere} \end{cases} \quad (2.16)$$

and

$$\begin{aligned} \rho(\Delta | \lambda_0) &= \rho(I_1 = \frac{e^{\alpha \lambda_1}}{1 - e^{-\alpha}} \Delta) / \left| \frac{\partial I_1}{\partial \Delta} \right| \\ &= \rho(I_1 = \frac{e^{\alpha \lambda_1}}{1 - e^{-\alpha}} \Delta) \frac{I_1}{\Delta} \end{aligned} \quad (2.17)$$

Then, since I_1 and λ_1 are assumed to be independent, we may write either

$$\rho(\Delta) = \int_{-\infty}^{\infty} \rho(\Delta/I_1) \rho(I_1) dI_1, \quad (2.18)$$

or

$$\rho(\Delta) = \int_{-\infty}^{\infty} \rho(\Delta/\lambda_1) \rho(\lambda_1) d\lambda_1, \quad (2.19)$$

Both (2.18) and (2.19), upon using (2.12), (2.16), (2.17) and $d\lambda_1 = \frac{1}{aI_1} dI_1$, yield

$$\rho(\Delta) = \frac{1}{a(\lambda_L - \lambda_S)/|\Delta|} \int_{\frac{S}{|\Delta|}}^{\frac{L}{|\Delta|}} \rho(I_1) dI_1, \quad (2.20)$$

where

$$L = \frac{1 - e^{-a}}{e^{a\lambda_L}}, \quad S = \frac{1 - e^{-a}}{e^{a\lambda_S}} \quad (2.21)$$

With $\rho(I_1)$ as given by (1.17), (2.20) yields

$$\rho(\Delta) = \frac{1}{2a(\lambda_L - \lambda_S)/|\Delta|} \left\{ \left(\frac{Sc}{|\Delta| + Sc} \right)^{K-1} - \left(\frac{Lc}{|\Delta| + Lc} \right)^{K-1} \right\} \quad (2.22)$$

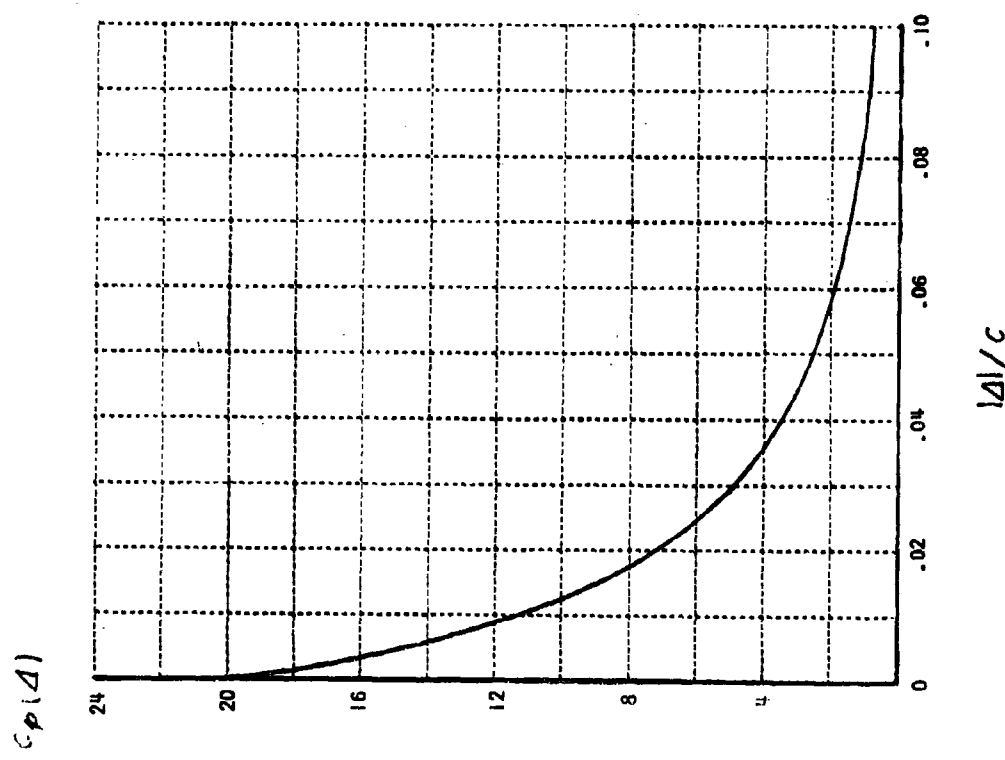
Note that

$$\rho(\Delta=0) = \frac{1}{2a(1-e^{-a})} \frac{e^{a\lambda_L} - e^{a\lambda_S}}{\lambda_L - \lambda_S} \frac{K-1}{c}$$

Figure 2 is a plot of $c\rho(\Delta)$ vs. $|\Delta|/c$ as given by (2.22) for $K = 3$, $a = 1$, $\lambda_S = 2$ and $\lambda_L = 3$.

For $K = 3$, (2.22) yields

$$\begin{aligned} P(0 < \Delta < \bar{\Delta}) &= \int_0^{\bar{\Delta}} \rho(\Delta) d\Delta \\ &= \frac{1}{2a(\lambda_L - \lambda_S)} \left[\left(\frac{Sc}{\bar{\Delta} + Sc} - \frac{Lc}{\bar{\Delta} + Lc} \right) - \log \frac{\bar{\Delta} + Sc}{\bar{\Delta} + Lc} + a(\lambda_L - \lambda_S) \right] \end{aligned}$$



13

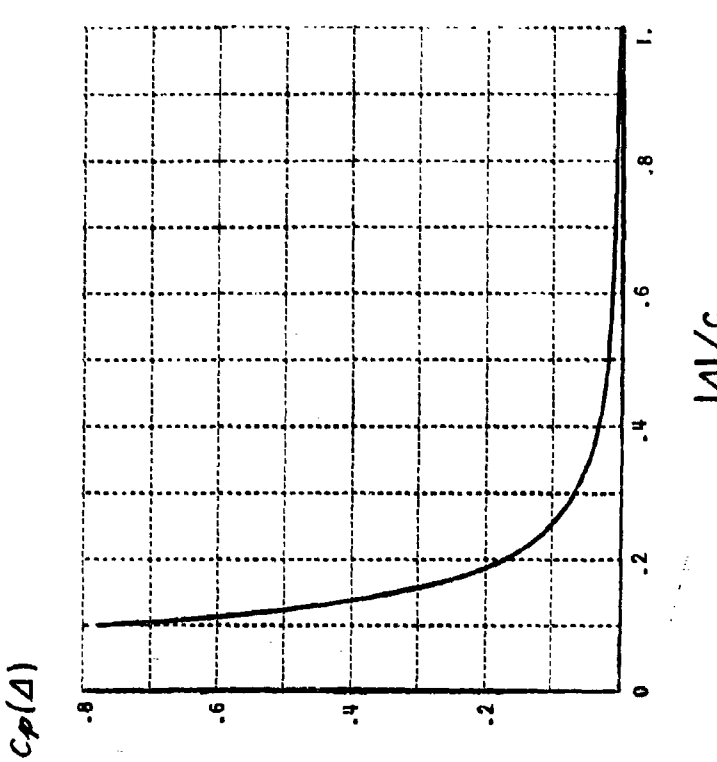


Figure 2 ($\kappa=3, \alpha=1, \lambda_3=2, \lambda_2=3$)

For $K = 4$, (2.22) yields

$$P(0 < \Delta < \bar{\Delta}) = \frac{1}{2a(\lambda_s - \lambda_L)} \left[\frac{1}{2} \left\{ \left(\frac{Sc}{\bar{\Delta} + Sc} \right)^2 - \left(\frac{Lc}{\bar{\Delta} + Lc} \right)^2 \right\} \right.$$

$$\left. + \left(\frac{Sc}{\bar{\Delta} + Sc} - \frac{Lc}{\bar{\Delta} + Lc} \right) - \log \frac{\bar{\Delta} + Sc}{\bar{\Delta} + Lc} + a(\lambda_s - \lambda_L) \right]$$

For $K = 3$,

$$\frac{P(0 < \Delta < \bar{\Delta})}{P(0 < \Delta < \infty)} = 1 - \frac{1}{a(\lambda_s - \lambda_L)} \left[\log \frac{\bar{\Delta} + Sc}{\bar{\Delta} + Lc} \right. \\ \left. - \left(\frac{Sc}{\bar{\Delta} + Sc} - \frac{Lc}{\bar{\Delta} + Lc} \right) \right] \quad (2.23)$$

and this ratio is larger for $K > 3$. For $a = 1$, $\lambda_s = 2$ and $\lambda_L = 3$, (2.23) gives

$$\frac{P(0 < \Delta < \bar{\Delta})}{P(0 < \Delta < \infty)} = .954 \text{ for } \frac{\bar{\Delta}}{c} = .20$$

For the case where $N = 2$, one may write (2.6) as

$$\Delta = (1 - e^{-a}) \Phi e^{-a\lambda_1}$$

which is similar to the Equation (2.15) for Δ for the case $N = 1$. Where:

$$\Phi = I_1 + Q$$

$$Q = I_2 e^{-a\lambda_2}$$

By comparing Q with the Δ given by (2.15) one can see that

$$\rho(Q) = \rho(\Delta = (1 - e^{-a})Q) / \left| \frac{\partial \Delta}{\partial Q} \right| \quad \left(\begin{array}{l} \rho(\Delta) \text{ given by (2.22);} \\ \frac{\partial \Delta}{\partial Q} = 1 - e^{-a} \end{array} \right)$$

or

$$\rho(Q) = \frac{1}{2a(\lambda_s - \lambda_L)|Q|} \left\{ \left(\frac{ce^{-a\lambda_s}}{|Q| + ce^{-a\lambda_s}} \right)^{K-1} \right. \\ \left. - \left(\frac{ce^{-a\lambda_L}}{|Q| + ce^{-a\lambda_L}} \right)^{K-1} \right\}$$

Then, since I_1 and Q are independent according to our assumptions,

$$p(\Phi) = \int_{-\infty}^{\infty} p(Q) p(I = \Phi - Q) dQ$$

Using (1.17),

$$p(\Phi) = \frac{(K-1)c^{K-1}}{4a(\lambda_s - \lambda_L)} \int_{-\infty}^{\infty} \frac{1}{(1\Phi - Q + c)^K} \left\{ \left(\frac{ce^{-a\lambda_s}}{|Q| + ce^{-a\lambda_s}} \right)^{K-1} - \left(\frac{ce^{-a\lambda_L}}{|Q| + ce^{-a\lambda_L}} \right)^{K-1} \right\} \frac{1}{|Q|} dQ$$

or

$$\begin{aligned} p(\Phi) &= \frac{(K-1)c^{K-1}}{4a(\lambda_s - \lambda_L)} \left[\int_{|\Phi|}^{\infty} \frac{1}{(Q - |\Phi| + c)^K} \left\{ \left(\frac{ce^{-a\lambda_s}}{Q + ce^{-a\lambda_s}} \right)^{K-1} - \left(\frac{ce^{-a\lambda_L}}{Q + ce^{-a\lambda_L}} \right)^{K-1} \right\} \frac{1}{Q} dQ \right. \\ &\quad + \int_0^{|\Phi|} \frac{1}{(-Q + |\Phi| + c)^K} \left\{ \left(\frac{ce^{-a\lambda_s}}{Q + ce^{-a\lambda_s}} \right)^{K-1} - \left(\frac{ce^{-a\lambda_L}}{Q + ce^{-a\lambda_L}} \right)^{K-1} \right\} \frac{1}{Q} dQ \\ &\quad \left. + \int_0^{\infty} \frac{1}{(Q + |\Phi| + c)^K} \left\{ \left(\frac{ce^{-a\lambda_s}}{Q + ce^{-a\lambda_s}} \right)^{K-1} - \left(\frac{ce^{-a\lambda_L}}{Q + ce^{-a\lambda_L}} \right)^{K-1} \right\} \frac{1}{Q} dQ \right] \end{aligned} \quad (2.24)$$

Substituting this expression for $\rho(\Phi)$ into (2.20) finally yields for the present case

$$\rho(\Delta) = \frac{1}{\alpha(\lambda_L - \lambda_S)/|\Delta|} \int_{\frac{-1}{|\Delta|}}^{\frac{1}{|\Delta|}} \rho(\Phi) d\Phi \quad (2.25)$$

The above method can be extended to higher N without difficulty, but the computations become more and more elaborate as N increases. If $\rho(\Delta)$ as computed using Equation (2.25) which is based on $N = 2$ differs only slightly from $\rho(\Delta)$, as computed using Equation (2.20) which is based on $N = 1$, one intuitively feels that the $\rho(\Delta)$ for $N = 2$ is a reasonable approximation for that which would be obtained using larger values of N .

3. FIRST ORDER MOMENT

For $k = 1$, Equations (1.9) to (1.12) yield:^{*}

$$m'_1(\eta) = \frac{T}{a} \left\{ 1 + a\eta - (1+a)e^{-a(1-\eta)} \right\} \quad (3.1)$$

$$m''_1(\xi) = \frac{T}{a} \left(1 - \frac{1+a}{e^a} \right) e^{-a\xi} \quad (3.2)$$

$$m''_{1,\eta n} = \frac{T}{a} \left(1 - \frac{1+a}{e^a} \right) e^{a\eta} e^{-a \sum_i^2 \lambda_i} \quad (3.3)$$

$$m''_{1,\xi n} = \frac{T}{a} \left(1 - \frac{1+a}{e^a} \right) e^{-a\xi} e^{-a \sum_i^2 \lambda_i} \quad (3.4)$$

^{*}Note that m'_1 is not maximum at $\eta = 0$. In fact, it is maximum at $\eta = -\bar{\xi}$, where $\bar{\xi} = \frac{1}{a} \log(1+a)$. Substituting $(1 - \bar{\xi} + \xi)$ for η , (3.1) becomes

$$m'_1 = \frac{T}{a} \left\{ 1 + a - \log(1+a) + a\xi - e^{a\xi} \right\}$$

so that m'_1 is obviously maximum when $\xi = 0$.

Then, by (1.15) and (1.16), there will be no error if

$$-M_i^- < I_0 \frac{T}{a} \left\{ 1 + a\eta - (1+a)e^{-a(1-\eta)} \right\} + \theta e^{a\eta} < M_i^+ \text{ for Case A } (3.5)_A$$

$$-M_i^- < I_0 \left(1 - \frac{1+a}{e^a} \right) e^{-a\zeta} + \theta e^{-a\zeta} < M_i^+ \text{ for Case B } (3.5)_B$$

where $\theta = \frac{T}{a} \left(1 - \frac{1+a}{e^a} \right) \sum_{n=1}^N I_n e^{-a \sum_{i=1}^n \lambda_i}$ (3.6)

Note that the relation between θ given by (3.6) and Δ given by (2.6) is

$$\theta = \frac{T}{a} \left(1 - \frac{a}{e^{a-1}} \right) \Delta$$

and that θ is the contribution to the first order moment due to I_1, I_2, \dots, I_N when $\eta = \zeta = 0$. Let

$$\left. \begin{aligned} I_\eta^+ &= \frac{a}{T} \frac{M_i^+ - \theta e^{a\eta}}{1 + a\eta - (1+a)e^{-a(1-\eta)}}, & I_\eta^- &= -\frac{a}{T} \frac{M_i^- + \theta e^{a\eta}}{1 + a\eta - (1+a)e^{-a(1-\eta)}} \\ I_\zeta^+ &= \frac{a}{T} \frac{M_i^+ e^{a\zeta} - \theta}{1 - (1+a)e^{-a}}, & I_\zeta^- &= -\frac{a}{T} \frac{M_i^- e^{a\zeta} + \theta}{1 - (1+a)e^{-a}} \end{aligned} \right\} (3.7)$$

Then, Equation (2.9) applies to the present case with I_η^\pm and I_ζ^\pm as given by (3.7) and plots of $P(c/\Delta, \lambda_0)$ vs. $\frac{\theta}{Tc}$ for various desired λ_0 , K and $\frac{M_i^\pm}{Tc}$ can be obtained by numerical or graphical integrations.

To obtain closed-form expressions of this probability for the present case is more involved than for the previous case, and has not been attempted.

4. LIMITING CASE OF $\omega_0 = \infty$.

For the limiting case where $\omega_0 = \infty$, we have $\Delta = 0$ and there will be no error for Case B. There will also be no error for Case A if the moment due to I_0 lies between $-M_k^-$ and M_k^+ or

$$-\frac{\bar{M}_k^-}{\eta^k} < I_0 < \frac{\bar{M}_k^+}{\eta^k} \quad (\bar{M}_k^\pm \equiv \frac{M_k^\pm}{T^k})$$

Consequently, we have

$$P(C|O, \lambda_0) = \frac{\lambda_0 - 1}{\lambda_0} + \frac{1}{\lambda_0} \int_0^1 P\left(-\frac{\bar{M}_k^-}{\eta^k} < I < \frac{\bar{M}_k^+}{\eta^k}\right) d\eta$$

or, by using (1.18),

$$P(C|O, \lambda_0) = 1 - \frac{1}{2\lambda_0} \int_0^1 \left\{ \left(\frac{\eta^k}{B_k^+ + \eta^k} \right)^{K-1} + \left(\frac{\eta^k}{B_k^- + \eta^k} \right)^{K-1} \right\} d\eta$$

where

$$B_k^\pm = \frac{\bar{M}_k^\pm}{C} = \frac{M_k^\pm}{CT^k}$$

Let

$$X_{k,K} = 2\lambda_0 \{1 - P(C|O, \lambda_0)\} \quad (4.1)$$

Then we may write

$$X_{k,K} = X_{k,K}^+ + X_{k,K}^- \quad (4.2)$$

where

$$X_{k,K}^+ = \int_0^1 \left(\frac{\eta^k}{B_k^+ + \eta^k} \right)^{K-1} d\eta \quad (4.3)$$

$$X_{k,K}^- = \int_0^1 \left(\frac{\eta^k}{B_k^- + \eta^k} \right)^{K-1} d\eta \quad (4.4)$$

For $k = 0$,

$$X_{0,K} = \left(\frac{1}{B_k^+ + 1} \right)^{K-1} + \left(\frac{1}{B_k^- + 1} \right)^{K-1} \quad (4.5)$$

For $k > 0$ and K an integer > 2 , the values of $X_{k,K}^+$ and $X_{k,K}^-$ may be computed by using the relation*

$$\begin{aligned} X_{k,K} &= \int_0^1 \left(\frac{\eta^k}{B_k + \eta^k} \right)^{K-1} d\eta \\ &= -\frac{1}{k(K-2)} \sum_{r=0}^{K-3} \frac{\eta^{k(K-2-r)+1}}{(B_k + \eta^k)^{K-2-r}} \prod_{i=1}^r \left\{ \frac{k(K-1-i)+1}{k(K-2-i)} \right\} \Big|_{\eta=0}^{q=1} \\ &\quad + \frac{k+1}{k(K-2)} \left[- \prod_{i=1}^k \left\{ \frac{k(K-1-i)+1}{k(K-2-i)} \right\} \right] \int_0^1 \frac{\eta^k}{B_k + \eta^k} d\eta \end{aligned}$$

This yields:

$$X_{k,3} = -\frac{1}{k} \frac{1}{B_k + 1} + \frac{k+1}{k} \int_0^1 \frac{\eta^k}{B_k + \eta^k} d\eta \quad (4.6)$$

* In using the relation, one must use $\prod_{i=1}^0 \{ \} = 1$.

$$\begin{aligned} Y_{k,4} = & -\frac{1}{2k} \left\{ \frac{1}{(B_k+1)^2} + \frac{2k+1}{k} \frac{1}{B_k+1} \right\} \\ & + \frac{k+1}{2k} \frac{2k+1}{k} \int_0^1 \frac{\eta^k}{B_k+\eta^k} d\eta \end{aligned} \quad (4.7)$$

$$\begin{aligned} Y_{k,5} = & -\frac{1}{3k} \left\{ \frac{1}{(B_k+1)^3} + \frac{3k+1}{2k} \frac{1}{(B_k+1)^2} \right. \\ & \left. + \frac{3k+1}{2k} \frac{2k+1}{k} \frac{1}{B_k+1} \right\} \\ & + \frac{k+1}{3k} \frac{3k+1}{2k} \frac{2k+1}{k} \int_0^1 \frac{\eta^k}{B_k+\eta^k} d\eta \end{aligned} \quad (4.8)$$

Using

$$\int_0^1 \frac{\eta}{B_1+\eta} d\eta = 1 - B_1 \log \frac{B_1+1}{B_1}$$

and

$$\int_0^1 \frac{\eta^2}{B_2+\eta^2} d\eta = 1 - \sqrt{B_2} \tan^{-1} \frac{1}{\sqrt{B_2}}$$

one obtains

$$\left. \begin{aligned} Y_{1,3} &= 1 + \frac{B_1}{B_1+1} - 2B_1 \log \frac{B_1+1}{B_1} \\ Y_{1,4} &= 1 + \frac{B_1(4B_1+5)}{2(B_1+1)^2} - 3B_1 \log \frac{B_1+1}{B_1} \\ Y_{1,5} &= 1 + \frac{B_1(9B_1^2+21B_1+13)}{3(B_1+1)^3} - 4B_1 \log \frac{B_1+1}{B_1} \end{aligned} \right\} \quad (4.9)$$

and

$$\left. \begin{aligned} \Sigma_{2,3} &= 1 + \frac{1}{2} \frac{B_1}{B_1+1} - \frac{3}{2} \sqrt{B_2} \tan^{-1} \frac{1}{\sqrt{B_2}} \\ \Sigma_{2,4} &= 1 + \frac{B_2(7B_2+9)}{8(B_2+1)^2} - \frac{15}{8} \sqrt{B_2} \tan^{-1} \frac{1}{\sqrt{B_2}} \\ \Sigma_{2,5} &= 1 + \frac{B_2(57B_2^2+136B_2+87)}{48(B_2+1)^3} - \frac{35}{16} \tan^{-1} \frac{1}{\sqrt{B_2}} \end{aligned} \right\} \quad (4.10)$$

The probability of no error for the present case is

$$P(c) = \int_{\lambda_s}^{\lambda_L} P(c|o, \lambda_o) \rho(\lambda_o) d\lambda_o$$

or, by (4.1),

$$P(c) = \int_{\lambda_s}^{\lambda_L} \left(1 - \frac{1}{2\lambda_o} \Sigma_{k,K} \right) \rho(\lambda_o) d\lambda_o \quad (4.11)$$

where λ_s and λ_L are the possible smallest and largest values of λ_o .
 (Since we assumed that the spacing between impulses is greater than the word duration, $\lambda_s > 1$.) If we assume

$$\rho(\lambda_o) = \frac{1}{\lambda_L - \lambda_s} \text{ for } 1 < \lambda_s \leq \lambda_o \leq \lambda_L$$

$$= 0 \text{ for elsewhere}$$

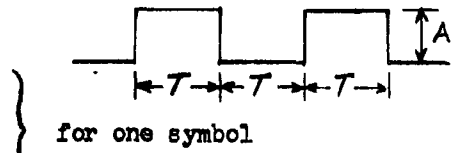
then (4.11) yields

$$P(c) = 1 - \Sigma_{k,K} \frac{1}{2(\lambda_L - \lambda_s)} \log \frac{\lambda_L}{\lambda_s}$$

To illustrate the application of the above results, we consider the on-off binary case where

$$M_0^+ = \frac{1}{2} AT, \quad M_0^- = \infty$$

$$M_k^+ = \frac{T^k}{k+1} M_0^+, \quad M_k^- = \infty$$



for one symbol

and M^+ and M^- are interchanged for the other symbol. Since $X_{k,K}^+ = 0$ for $B_k^+ = \infty$, $X_{k,K}^- = 0$ for $B_k^- = \infty$, and $X_{k,K}^+ = X_{k,K}^-$ for $B_k^+ = B_k^-$; we have for the present

$$X_{k,K} = X_{k,K}^+ = X_{k,K}^- = Y_{k,K}$$

in which the values of B_k to be used for computing $Y_{k,K}$ are, by $B_k^\pm = M_k^\pm / (CT^k)$, as follows:

$$B_0 = \frac{AT}{2C} \quad B_1 = \frac{1}{2} B_0 \quad B_2 = \frac{1}{3} B_0$$

Then by using (4.5), (4.9) and (4.10) one obtains:

$$X_{0,K} = \left(\frac{1}{B_0 + 1} \right)^{K-1} \quad (4.12)$$

$$\begin{aligned} X_{1,3} &= 1 + \frac{B_0}{B_0 + 2} - \varphi \\ X_{1,4} &= 1 + \frac{B_0(2B_0 + 5)}{(B_0 + 2)^2} - \frac{3}{2} \varphi \\ X_{1,5} &= 1 + \frac{B_0(9B_0^2 + 42B_0 + 52)}{3(B_0 + 2)^3} - 2\varphi \end{aligned} \quad \left. \right\} \quad (4.13)$$

and

$$\left. \begin{aligned} X_{2,3} &= 1 + \frac{1}{2} \frac{B_0}{B_0+3} - \frac{3}{2} \psi \\ X_{2,4} &= 1 + \frac{B_0(7B_0+27)}{8(B_0+3)^2} - \frac{15}{8} \psi \\ X_{2,5} &= 1 + \frac{B_0(19B_0^2+136B_0+261)}{16(B_0+3)^3} - \frac{35}{16} \psi \end{aligned} \right\} \quad (4.14)$$

where

$$\varphi = B_0 \log \frac{B_0+2}{B_0}, \quad \psi = \sqrt{\frac{B_0}{3}} \tan^{-1} \sqrt{\frac{3}{B_0}}$$

The Table shown hereunder compares the values of $X_{k,K}$ as given by (4.12), (4.13), or (4.14) for six different combinations of k and K at various B_0 . This table shows higher order moment detection superior to zeroth order moment detection only when

$$\left\{ \begin{array}{l} \frac{AT}{2c} < 2 \text{ if } K=3 \\ \frac{AT}{2c} < 1 \text{ if } K=4 \end{array} \right.$$

$B_0 = \frac{AT}{2c}$	VALUES OF $X_{k,K}$					
	K = 3			K = 4		
	$k = 0$	$k = 1$	$k = 2$	$k = 0$	$k = 1$	$k = 2$
0	1	1	1	1	1	1
1/2	.44444	.3953	.3469	.2963	.2729	.2499
1	.2500	.2347	.2181	.1250	.1299	.1320
2	.1111	.1137	.1148	.03704	.04556	.05348
4	.04000	.04481	.04951	.008000	.01165	.01597
20	.02268	.002887		.000108	.000199	
100	.000980	.0001294		.00000097	.00000190	

REFERENCES

1. Mertz, P. "Model of Impulsive Noise for Data Transmission"
RAND Corporation Report No. P-1761 July 27, 1959.

APPENDIX

Method of Evaluation of $P(c/\Delta, \lambda_0)$.

In this Appendix a method of evaluating $P(c/\Delta, \lambda_0)$ in closed form will be indicated.

Let

$$F(M_0^+, \Delta) = \int_0^1 \frac{M_0^+ - \Delta e^{a\eta}}{|M_0^+ - \Delta e^{a\eta}|} \left\{ 1 - \left(\frac{c - ce^{-a} e^{a\eta}}{|M_0^+ - \Delta e^{a\eta}| + c - ce^{-a} e^{a\eta}} \right)^{\lambda_0 - 1} \right\} d\eta$$

$$+ \int_0^{\lambda_0 - 1} \frac{M_0^+ e^{a\eta} - \Delta}{|M_0^+ e^{a\eta} - \Delta|} \left\{ 1 - \left(\frac{c - ce^{-a}}{|M_0^+ e^{a\eta} - \Delta| + c - ce^{-a}} \right)^{\lambda_0 - 1} \right\} d\eta \quad (A1)$$

Then (2.10) becomes

$$P(c/\Delta, \lambda_0) = \frac{1}{2\lambda_0} \{ F(M_0^+, \Delta) + F(M_0^-, -\Delta) \} \quad (A2)$$

and it is required to express $F(M_0^+, \Delta)$, as given by (A1), in closed form.*

Due to the presence of $|M_0^+ - \Delta e^{a\eta}|$ and $|M_0^+ e^{a\eta} - \Delta|$ in the integrals appearing in (A1), $F(M_0^+, \Delta)$ takes a different form for each of the following four ranges of Δ :

$$\begin{aligned} \Delta &\leq M_0^+ e^{-a} \\ M_0^+ e^{-a} &\leq \Delta \leq M_0^+ \\ M_0^+ &\leq \Delta \leq M_0^+ e^{a(\lambda_0 - 1)} \\ \Delta &\geq M_0^+ e^{a(\lambda_0 - 1)} \end{aligned}$$

For the first range:

* Note that $F(\infty, \Delta) = F(\infty, -\Delta) = \lambda_0$.

$$|M_0^+ - \Delta e^{a\eta}| = M_0^+ - \Delta e^{a\eta} \text{ for } 0 \leq \eta \leq 1$$

$$|M_0^+ e^{a\zeta} - \Delta| = M_0^+ e^{a\zeta} - \Delta \text{ for } 0 \leq \zeta \leq \lambda_0 - 1$$

For the second range:

$$\begin{aligned} |M_0^+ - \Delta e^{a\eta}| &= M_0^+ - \Delta e^{a\eta} \text{ for } 0 \leq \eta \leq \frac{1}{a} \log \frac{M_0^+}{\Delta} \\ &= \Delta e^{a\eta} - M_0^+ \text{ for } \frac{1}{a} \log \frac{M_0^+}{\Delta} \leq \eta \leq 1 \end{aligned}$$

$$|M_0^+ e^{a\zeta} - \Delta| = M_0^+ e^{a\zeta} - \Delta \text{ for } 0 \leq \zeta \leq \lambda_0 - 1$$

For the third range:

$$|M_0^+ - \Delta e^{a\eta}| = \Delta e^{a\eta} - M_0^+ \text{ for } 0 \leq \eta \leq 1$$

$$\begin{aligned} |M_0^+ e^{a\zeta} - \Delta| &= \Delta - M_0^+ e^{a\zeta} \text{ for } 0 \leq \zeta \leq \frac{1}{a} \log \frac{\Delta}{M_0^+} \\ &= M_0^+ e^{a\zeta} - \Delta \text{ for } \frac{1}{a} \log \frac{\Delta}{M_0^+} \leq \zeta \leq \lambda_0 - 1 \end{aligned}$$

For the fourth range:

$$|M_0^+ - \Delta e^{a\eta}| = \Delta e^{a\eta} - M_0^+ \text{ for } 0 \leq \eta \leq 1$$

$$|M_0^+ e^{a\zeta} - \Delta| = \Delta - M_0^+ e^{a\zeta} \text{ for } 0 \leq \zeta \leq \lambda_0 - 1$$

To illustrate the procedure in further detail, we will only consider the second range. For this range, $M_0^+ e^{-\alpha} \leq \Delta \leq M_0^+$, we have

$$F(M_0^+, \Delta) = \int_0^{\frac{1}{\alpha} \log \frac{M_0^+}{\Delta}} \left\{ 1 - \left(\frac{c - ce^{-\alpha} e^{a\eta}}{c + M_0^+ - (ce^{-\alpha} + \Delta)e^{a\eta}} \right)^{K-1} \right\} d\eta$$

$$- \int_{\frac{1}{\alpha} \log \frac{M_0^+}{\Delta}}^1 \left\{ 1 - \left(\frac{c - ce^{-\alpha} e^{a\eta}}{c - M_0^+ - (ce^{-\alpha} - \Delta)e^{a\eta}} \right)^{K-1} \right\} d\eta$$

$$+ \int_0^{\lambda_0 - 1} \left\{ 1 - \left(\frac{c - ce^{-\alpha}}{c - ce^{-\alpha} - \Delta + M_0^+ e^{a\zeta}} \right)^{K-1} \right\} d\zeta$$

or

$$F(M_0^+, \Delta) = \lambda_0 - 2 + \frac{2}{\alpha} \log \frac{M_0^+}{\Delta}$$

$$- \int_0^{\frac{1}{\alpha} \log (M_0^+ / \Delta)} \left(\frac{c - ce^{-\alpha} e^{a\eta}}{c + M_0^+ - (ce^{-\alpha} + \Delta)e^{a\eta}} \right)^{K-1} d\eta$$

$$+ \int_{\frac{1}{\alpha} \log (M_0^+ / \Delta)}^1 \left(\frac{c - ce^{-\alpha} e^{a\eta}}{c - M_0^+ - (ce^{-\alpha} - \Delta)e^{a\eta}} \right)^{K-1} d\eta$$

$$- \int_0^{\lambda_0 - 1} \left(\frac{c - ce^{-\alpha}}{c - ce^{-\alpha} - \Delta + M_0^+ e^{a\zeta}} \right)^{K-1} d\zeta \quad (A3)$$

The integrals appearing in (A3), and in similar expressions for other ranges, can be integrated by change of variable (namely, $y = e^{ax}$ and $dx = \frac{1}{ay} dy$) if K is an integer. Thus, for K = 3 or 4 one obtains, respectively,

$$\int \left(\frac{A + Be^{ax}}{\alpha + \beta e^{ax}} \right)^2 dx = \frac{1}{a} \int \left\{ \frac{A}{\alpha} + \left(B - \frac{A}{\alpha} \beta \right) \frac{y}{\alpha + \beta y} \right\}^2 \frac{dy}{y}$$

$$= \frac{A^2}{\alpha^2} x + \frac{1}{a} \left(\frac{A}{\alpha} - \frac{B}{\beta} \right)^2 \frac{\alpha}{\alpha + \beta y}$$

$$- \frac{1}{a} \left(\frac{A^2}{\alpha^2} - \frac{B^2}{\beta^2} \right) \log(\alpha + \beta e^{ax}) \quad (A4)$$

or

$$\begin{aligned}
 & \int \left(\frac{A + Be^{\alpha x}}{\alpha + \beta e^{\alpha x}} \right)^3 dx \\
 &= \frac{A^3}{\alpha^3} x + \frac{1}{\alpha} \left(\frac{A}{\alpha} - \frac{B}{\beta} \right)^2 \left(\frac{A}{\alpha} + 2 \frac{B}{\beta} \right) \frac{\alpha}{\alpha + \beta e^{\alpha x}} \\
 &+ \frac{1}{2\alpha} \left(\frac{A}{\alpha} - \frac{B}{\beta} \right)^3 \frac{\alpha^2}{(\alpha + \beta e^{\alpha x})^2} \\
 &- \frac{1}{\alpha} \left(\frac{A^3}{\alpha^3} - \frac{B^3}{\beta^3} \right) \log(\alpha + \beta e^{\alpha x}) \tag{A5}
 \end{aligned}$$

By using (A4) and $C' = C(1 - e^{-a})$, (A3) yields

$$\begin{aligned}
 F(M_0^+, \Delta) &= \lambda_0 - 2 - \frac{1}{a} \left[\frac{M_0^+ - \Delta}{C' + M_0^+ - \Delta} \left(\frac{C}{C + M_0^+} - \frac{C}{C + \Delta e^a} \right) \right. \\
 &+ \frac{C}{C - M_0^+} - \frac{C}{C - \Delta e^a} \\
 &- \frac{C'}{C' - \Delta} \left(\frac{C'}{C' - \Delta + M_0^+} - \frac{C'}{C' - \Delta + M_0^+ e^{a(\lambda_0 - 1)}} \right) \\
 &- 2 \log \frac{M_0^+}{\Delta} + \left\{ \left(\frac{C}{C + M_0^+} \right)^2 + \left(\frac{C}{C - M_0^+} \right)^2 \right\} \log \frac{M_0^+}{C} \\
 &+ \left\{ \left(\frac{C}{C + M_0^+} \right)^2 - \left(\frac{C}{C + \Delta e^a} \right)^2 \right\} \log \frac{C' + M_0^+ - \Delta}{\Delta - M_0^+ e^{-a}} \\
 &- \left(\frac{C}{C + \Delta e^a} \right)^2 \log \frac{\Delta}{C} - \left(\frac{C}{C - \Delta e^a} \right)^2 \log \frac{\Delta e^a}{C} \\
 &\left. + \left(\frac{C'}{C' - \Delta} \right)^2 \log \frac{M_0^+ + C' - \Delta}{M_0^+ + (C' - \Delta) e^{-a(\lambda_0 - 1)}} \right]
 \end{aligned}$$

for $M_0^+ e^{-a} \leq \Delta \leq M_0^+$ and $K = 3$.

21 February 1961

IV(d) DETECT MEMO NO. 14

Subject: "Experimental Investigation of Moment Detection"

By: Ned B. Smith

ABSTRACT

Moment detection is a technique which may be used to "detect" information expressed in pulse code form. An obvious application is the decoding of pulse code groups used in binary data transmission. This memo describes the experimental evaluation of moment detection as used with a binary data transmission system. Only a limited amount of data was obtained since early tests indicated that moment detection, to be used successfully, would require such complicated equipment as to make this technique totally unsuitable for use in a practical communications system.

I. INTRODUCTION

In digital data transmission one is interested in the detection of information expressed in pulse code form. Moment detection can be used to determine the absence or presence and the position of a pulse or series of pulses.

As indicated in Ref. 3, a simple pulse code group of 5 pulses occupying T seconds may be uniquely specified by the first three temporal moments which are defined as follows:

$$M_0 = \int_0^T v(t) dt$$

$$M_1 = \int_0^T t v(t) dt$$

$$M_2 = \int_0^T t^2 v(t) dt$$

Table I gives the first 3 moments for each of the 32 possible code groups which can be formed from a 5-digit binary code utilizing 5 equal-width, constant amplitude spaces which may or may not be filled with rectangular pulses. Referring to this table, it will be noted that only the second-order moment is needed to specify any code group. Further, except in six instances, the combinations of zero and first-order moments are sufficient to specify any of the code groups. The theoretically best manner of utilizing these redundant data is discussed in Appendices IVa and b.

Conceptually, the temporal moments may be most easily computed by multiplying the given function and the required power of time and integrating the product. Unfortunately, most of the known schemes of "electronic multiplication" are rather complex as well as frequency-limited and, after a brief investigation of this method of obtaining the temporal moments, it was discarded in favor of the iterated integration method described in Ref. 1.

TABLE I

LEVEL	CODE	H_0	H_1	$H_2 \times 3$
0	_____	0	0	0
1	█	1	0.5	1
2	█ █	1	1.5	7
3	██	2	2.0	8
4	█ █	1	2.5	19
5	██	2	3.0	20
6	██	2	4.0	26
7	███	3	4.5	27
8	██	1	3.5	37
9	█ █	2	4.0	38
10	█ █	2	5.0	44
11	███	3	5.5	45
12	███	2	6.0	56
13	█	3	6.5	57
14	███	3	7.5	63
15	███	4	8.0	64
16	███	1	4.5	61
17	█	2	5.0	62
18	█	2	6.0	68
19	███	3	6.5	69
20	█ █	2	7.0	80
21	█ █	3	7.5	81
22	███	3	8.5	87
23	███	4	9.0	88
24	███	2	8.0	98
25	█	3	8.5	99
26	█ █	3	9.5	105
27	███	4	10	106
28	███	3	10.5	117
29	█ █	4	11	118
30	█ █	4	12	120
31	███	5	12.5	125

The zero-order moment, which is simply the area under the waveform, requires only one integrator, thus

$$M_0 = \int_0^T v(t) dt$$

The first and second temporal moments may be calculated from definite integrals by integration by parts.

$$M_1 = T \int_0^T v(t) dt - \int_0^T \int_0^t v(\tau) d\tau dt$$

$$M_2 = T^2 \int_0^T v(t) dt - 2T \int_0^T \int_0^t v(\tau) d\tau dt$$

$$+ 2 \int_0^T \int_0^t \int_0^\tau v(u) du d\tau dt$$

It should be noted that moment computation by this method is not without attendant difficulties since it may require the subtraction of very large values to obtain a comparatively small answer.

For example, consider the iterated integration method in obtaining the second moment of the word 5.

If $T = 5$ and the amplitude of $v(t)$ is 1, then the waveform corresponding to this word is

$$v_5(t) = \begin{cases} 1, & 0 \leq t < 1 \\ 1, & 2 \leq t < 3 \\ 0, & elsewhere \end{cases}$$

and the second moment is found from

$$\begin{aligned}
 M_2(v_s) &= 25 \left[\int_0^1 dt + \int_2^3 dt \right] - 10 \int_0^5 \int_0^t v_s(\tau) d\tau dt \\
 &\quad + 2 \int_0^T \int_0^t \int_0^\tau v(u) du d\tau dt \\
 &= 25 \{ 1 + 1 \} - 10 \int_0^5 h(t) dt + 2 \int_0^5 \int_0^t h(\tau) d\tau dt
 \end{aligned}$$

$$\begin{aligned}
 \text{where } h(t) &= \begin{cases} t, & 0 \leq t < 1 \\ 1, & 1 \leq t < 2 \\ 1 + (t-2), & 2 \leq t < 3 \\ 2, & 3 \leq t < 5 \end{cases} \\
 &= 50 - 10 \left[\int_0^1 t dt + \int_1^2 dt + \int_2^3 [1 + (t-2)] dt + \int_3^5 2 dt \right] \\
 &\quad + 2 \int_0^5 \int_0^t h(\tau) d\tau dt \\
 &= 50 - 10 \left\{ \frac{1}{2} + 1 + 1 + \frac{1}{2} + 4 \right\} + 2 \int_0^5 g(t) dt
 \end{aligned}$$

$$\begin{aligned}
 \text{where } g(t) &= \begin{cases} \frac{t^2}{2}, & 0 \leq t < 1 \\ \frac{1}{2} + (t-1), & 1 \leq t < 2 \\ \frac{3}{2} + (t-2) + \frac{(t-2)^2}{2}, & 2 \leq t < 3 \\ 3 + 2(t-3), & 3 \leq t < 5 \end{cases} \\
 &= 50 - 70 + 2 \left\{ \int_0^1 \frac{t^2}{2} dt + \int_1^2 \left[\frac{1}{2} + (t-1) \right] dt + \int_2^3 \left[\frac{3}{2} + (t-2) + \frac{(t-2)^2}{2} \right] dt \right. \\
 &\quad \left. + \int_3^5 [3 + 2(t-3)] dt \right\} \\
 &= 50 - 70 + 2 \left\{ \frac{1}{6} + \frac{1}{2} + \frac{1}{2} + \frac{3}{2} + \frac{1}{2} + \frac{1}{6} + 6 + 4 \right\} \\
 &= 50 - 70 + 2 \left\{ \frac{40}{3} \right\} = \frac{20}{3}.
 \end{aligned}$$

Similarly, for the word "l," the waveform of which is $v_1(t) = \begin{cases} t, & 0 \leq t < 1 \\ 0, & \text{elsewhere} \end{cases}$

the second moment is found from $M_2(v_1) = 25 - 45 + \frac{61}{3} = \frac{1}{3}$.

The primary purpose of this investigation was to determine the error probability attainable with moment detection used with a practical remote binary data transmission system using conventional telephone line transmission bandwidths. Probability of error was determined as system parameters were varied, including received signal-to-thermal noise, signal-to-impulse noise, transmission line bandwidth, and signaling speeds. Since

it was obviously impractical to test all combinations of pulse code groups and system parameters because of the tremendous amount of data reduction which would be required, only a set of representative words and variable system parameters were used. The scope of these tests was thus limited to what seemed practical from a data reduction standpoint and still yield sufficient test data for an evaluation of the expected system performance using moment detection.

II. EXPERIMENTAL APPROACH

The experimental approach taken in the evaluation of the performance of moment detection was as follows:

1. Record thermal noise and impulse noise on magnetic tape.
2. Generate coded signals with noise added from the magnetic tape.
3. Transmit the composite signal (noise plus signal) by FSK over a simulated telephone line.
4. Compute the three moments of each word, using the unfiltered detected output of the FSK Receiver as the input to the moment computer.*
5. Record the moments on a magnetic tape and slow down the magnetic tape 32:1 because of the limitations of the digitizing equipment used.
6. Digitize the analog moment outputs of the slowed-down magnetic tape by an analog-to-digital converter and record on digital paper tape.
7. Transfer the digitized moment data on the paper tape to IBM cards in the 704 computer format.
8. Compute the error probability on the IBM 704 computer.

* The unfiltered output was used because moment detection inherently performs a low-pass filtering action and it was desired to avoid phase shifts due to an additional low-pass filter. However, it was noted that use of the filtered instead of the unfiltered output did not result in an observable change in the performance of the moment computer.

III. EQUIPMENT DESCRIPTION

A. General

Figure 1 is a detailed block diagram of the digital data transmission system and evaluator assembled to investigate moment detection experimentally. Figures 2 and 3 are photographs of the experimental equipment which was used.

The equipment consisted of a thermal noise generator, an impulse noise generator, and a clock generator whose outputs were recorded on three channels of an Ampex tape recorder. A series of master tapes were made, using these three inputs, in order that repetitive tests could be made under almost identical conditions of words, thermal noise and impulse noise. The clock generator, impulse noise generator and thermal noise generator were used only to make the master tapes. The recorded clock pulses were fed to the encoder which consists of a word and synchronizing generator capable of repetitively generating any selected one of the 32 possible words of a 5-bit binary code. The output of the word generator was fed to an FSK modulator (Model 3000 Tele-Signal) which was used to convert the binary input data to frequency shift-keyed signals suitable for remote data transmission. The output of the FSK modulator was then fed to a simulated telephone line which consisted of variable filters. The impulse noise and thermal noise channels of the master tape were also used as inputs to the simulated telephone line. The composite signal output of the telephone line (FSK signals plus thermal and impulse noise) was then fed to the FSK demodulator (Model 3000 Tels-Signal). The unfiltered discriminator output of the FSK demodulator (receiver) was then fed to the input of the moment computer.* Synchronizing signals required by the moment computer were obtained directly from the synchronizing generator. The three moment outputs of the computer, together with the synchronizing signals, were then recorded on an Ampex FR-100 FM tape recorder. The recorded moments were next digitized by means of an Epsco analog-to-digital converter, the output of which was recorded on paper tape by means

* See Footnote, page 6.

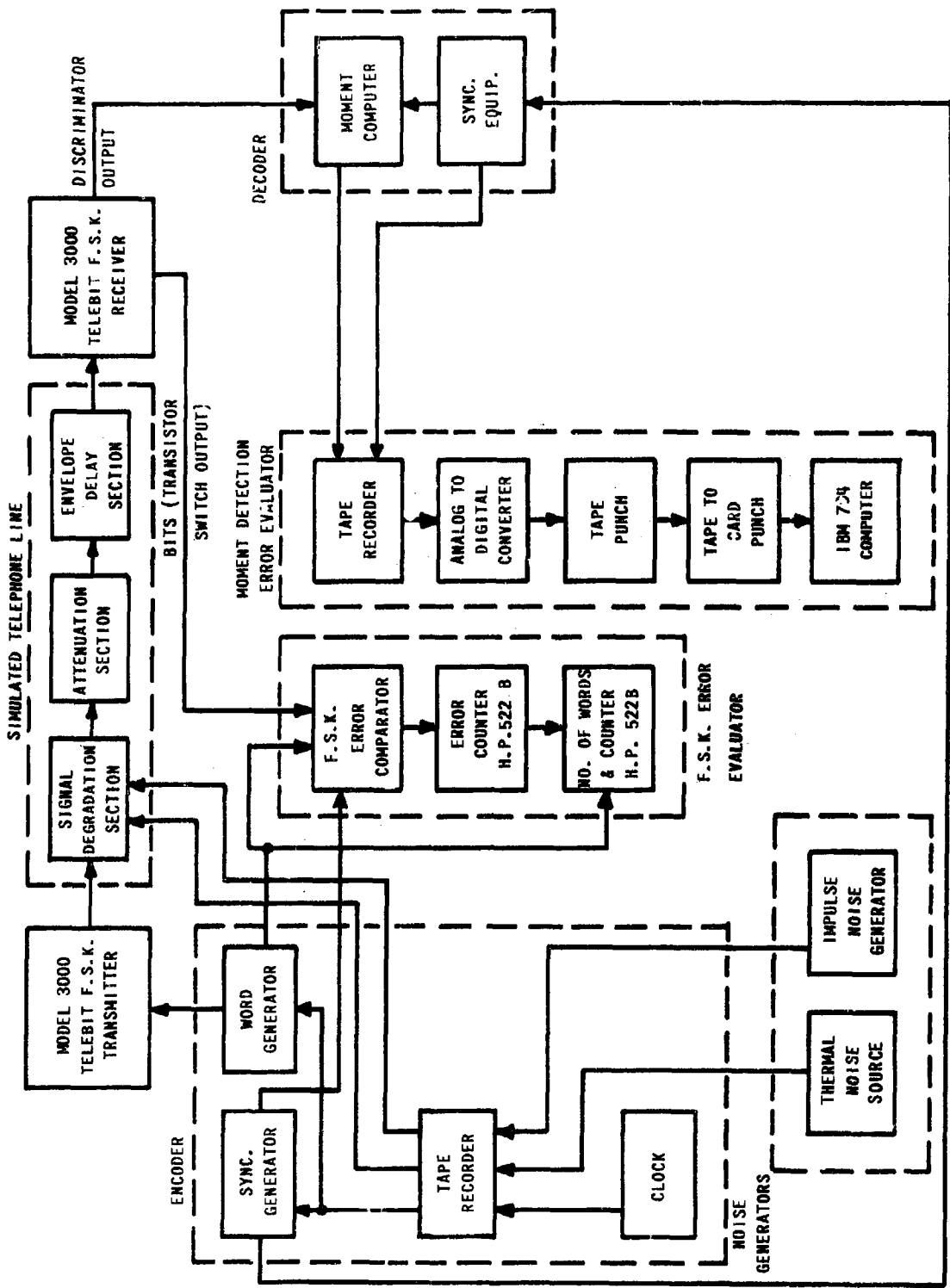


FIGURE I BLOCK DIAGRAM, F.S.K. AND MOMENT DETECTION EVALUATOR

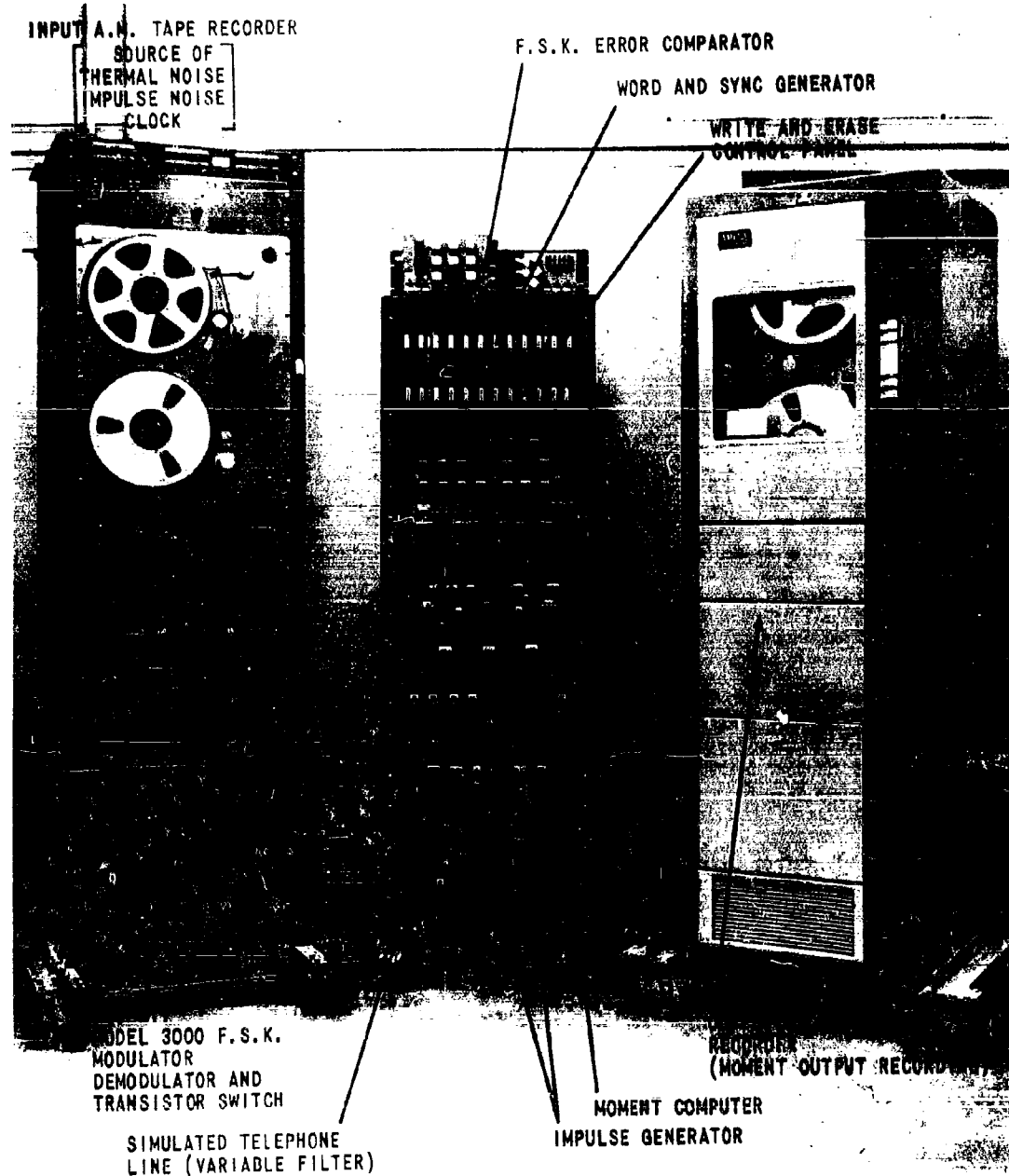
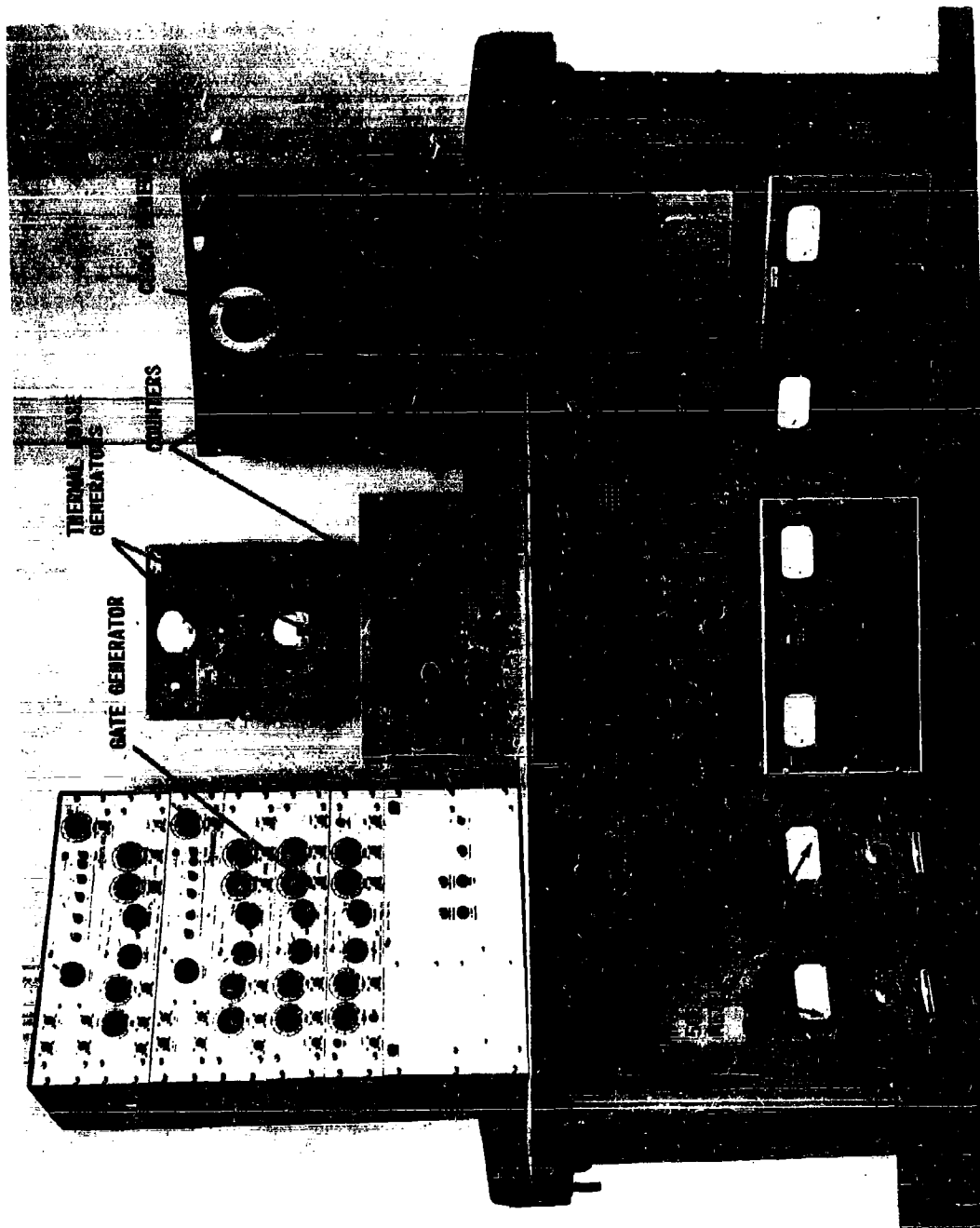


FIGURE 2 EXPERIMENTAL EQUIPMENT USED DURING EVALUATION

FIGURE 3 EXPERIMENTAL EQUIPMENT USED DURING EVALUATION



of a Tally punch. Since the Tally digital paper tape punch was incapable of operating in real time, the tape containing the three recorded moments was "slowed down" 32:1. The digital paper tape was then used to prepare the IBM cards that were used to introduce the data into the IBM 704 computer where the error probability was computed.

Since a comparison of FSK performance with that of moment detection was desired, the filtered output of the FSK discriminator was fed in the normal fashion to the transistor switch, which is a part of the FSK receiver. The output of the FSK transistor switch, together with the output of the word generator, were then used as inputs to an error comparator and the number of bit errors were recorded on a Hewlett-Packard 522B counter. The number of words sent during each run was recorded by another H-P 522B counter. The probability of bit error for each run was then computed as one-fifth of the ratio of these counts.

B. Detailed Description of the Equipment

1. Thermal Noise Generator

A General Radio 1390B Random Noise Generator was used as a source of thermal noise. This uses a gas tube as a noise source and has an "essentially Gaussian"** output when used in the 20 kc/s bandwidth position.

Figure 4 is a photograph of the waveform at the output of the telephone filter when it is driven by the thermal noise generator; Figure 5 of the output of the FSK transmitter with a steady space input, and Figure 6 of the combined thermal noise and FSK signal at the output of the simulated telephone line.

2. Impulse Generator

Figure 7 is a block diagram of the impulse noise generator used. The design of the impulse generator was based, in part, on the data presented by Mertz in Reference 2.

The impulse generator consists of a pulse generator controlled by a

* See General Radio Catalog for qualification of "essentially Gaussian."

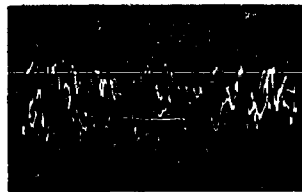


FIGURE 4

OUTPUT OF FILTER DRIVEN
WITH THERMAL NOISE

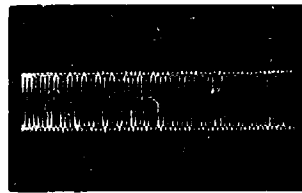


FIGURE 5

OUTPUT FSK TRANSMITTER,
STEADY SPACE INPUT

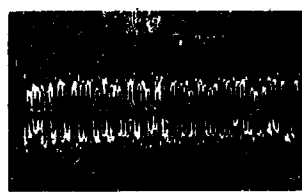


FIGURE 6

COMBINED THERMAL NOISE
AND FSK SIGNAL AT TELEPHONE
LINE OUTPUT

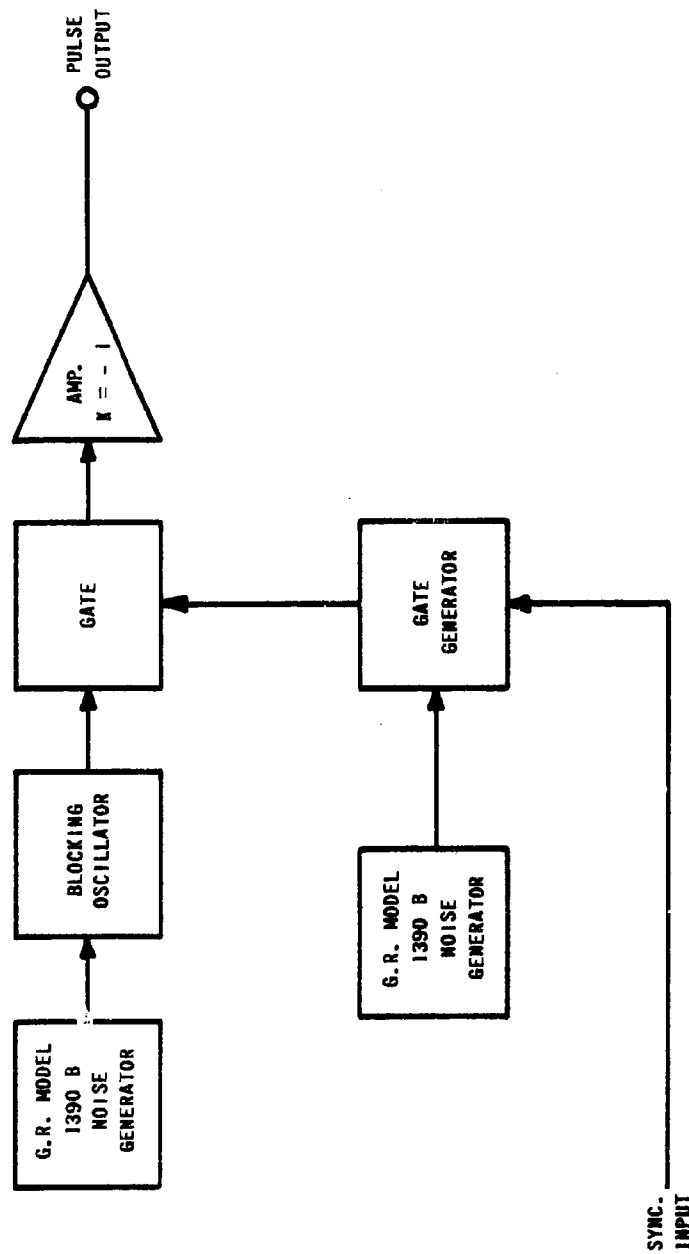


FIGURE 7 BLOCK DIAGRAM, IMPULSE GENERATOR

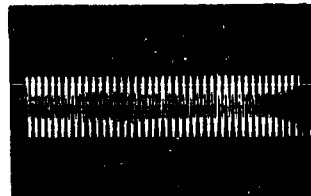


FIGURE 8

FSK SIGNAL (STEADY SPACE INPUT)
AT TELEPHONE LINE OUTPUT



FIGURE 9

IMPULSE BURST AT
TELEPHONE LINE OUTPUT



FIGURE 10

COMBINED FSK SIGNAL AND
IMPULSE BURST AT TELEPHONE
LINE OUTPUT

random noise source. The output pulses were shaped and then fed to a gate. The gate duration was varied randomly by another controlling noise source.

Provision was made in the design of the impulse generator to vary the frequency and duration of the bursts by adjusting the output of the controlling noise generators. Figure 8 is a photograph of the signal output from the telephone line filter with a steady space. Figure 9 shows a burst from the impulse generator, and Figure 10 shows the combined signal and impulse burst at the output of the filter. It should be noted that Figure 10 is a photograph of the combined signal and an impulse burst which is not the same impulse burst pictured in Figure 9.

3. Clock

A Hewlett-Packard Model 212A pulse generator was used as a source of clock pulses. The clock pulses were used for basic timing of all digital and control operations.

4. Master Control Tapes

A series of master control magnetic tapes were prepared using the outputs of the clock, thermal noise generator and impulse noise generator as inputs to three of the tracks.

These tapes were then used as sources of clock pulses, thermal noise and impulse noise for all of the test runs made in evaluating moment detection and FSK performance. These master control tapes were used to reduce the possibilities of variations of input conditions between runs which were to be made under similar input conditions. For instance, this permitted one to evaluate the effects of changing bandwidth while maintaining the same signals and noise.

5. Word and Synchronizing Generator

Figure 11 is a block diagram of the word and synchronizing generator. The word generator was used for the selective generation of any one of the 32 words. The word generator consisted of an eight-stage serial shift register. Write switches were used to permit the introduction of any one of the 32 possible words into the register.

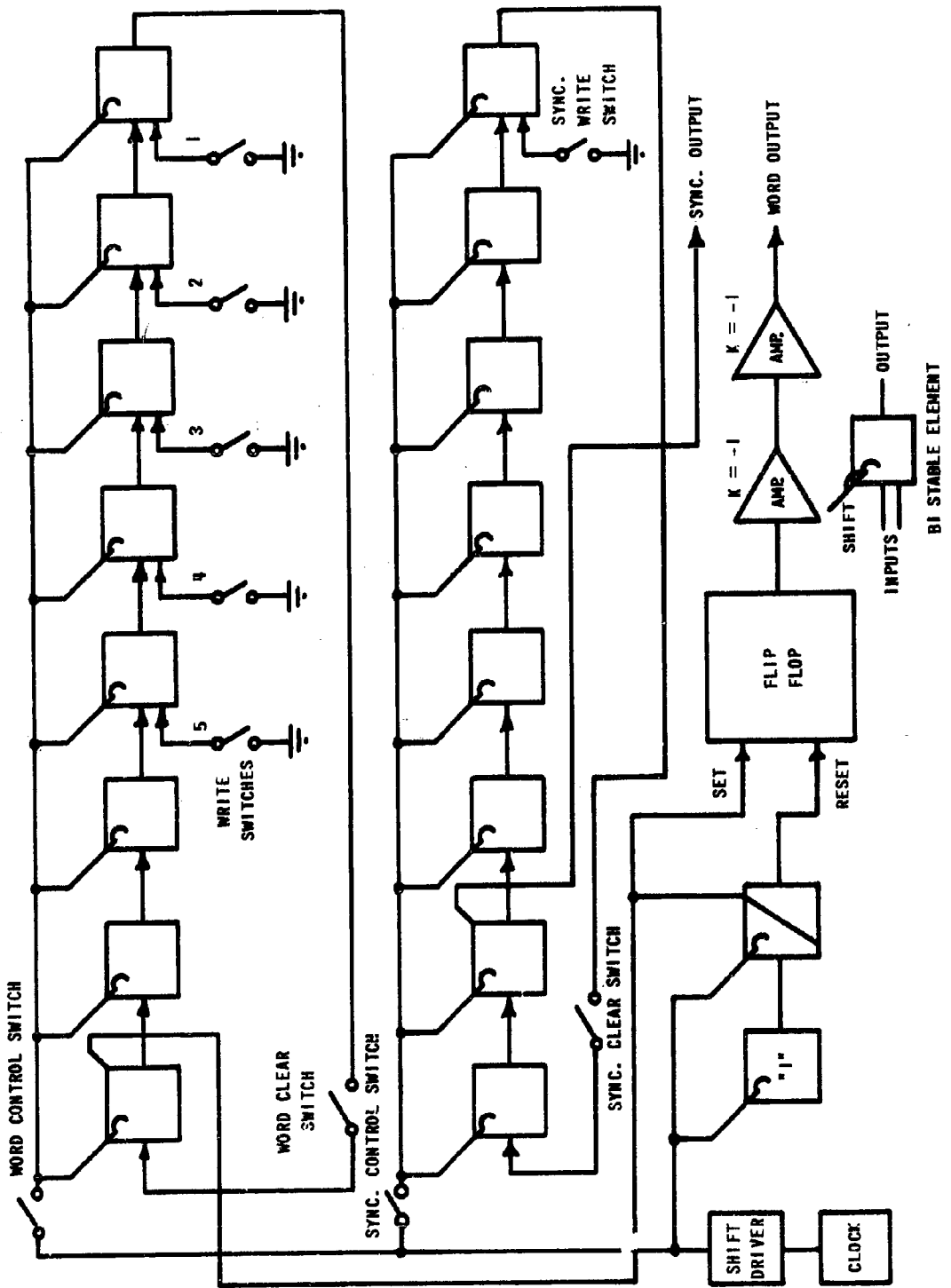


FIGURE II WORD AND SYNC. GENERATOR

The synchronizing generator was used to control operations which occur at word rate. The synchronizing generator was also an eight-stage serial shift register. The outputs of the synchronizing generator were used to control both the transmitting and receiving digital logic equipment.

Figures 12, 13 and 14 are photographs of the waveforms of the words 1, 2 and 5 respectively, existing at the output of the word generator.*



FIGURE 12

WORD 1 AT OUTPUT
OF WORD GENERATOR



FIGURE 13

WORD 2 AT OUTPUT
OF WORD GENERATOR



FIGURE 14

WORD 5 AT OUTPUT
OF WORD GENERATOR

6. Modulator and Demodulator (Transmitter and Receiver)

A Tele-Signal Corporation, Model 3000, FSK High Speed Digital Terminal set was used both as a modulator and demodulator. The modulator was used as supplied by the manufacturer. The unfiltered output of the frequency discriminator output of the receiver was used as the signal input to the moment computer.

* Refer to Section III.1.1. and Figure 26 for an explanation of the eight spaces allocated for each 5-bit word as shown in Figures 12, 13 and 14.

7. Simulated Telephone Line

Figure 15 is a block diagram of the variable filter used to simulate the transmission characteristics of various commercial telephone lines. The filter was divided into three parts, one section consisting of additive mixers to permit variable signal degradation, the second section having variable attenuation characteristics, as shown in Figure 16, and the third section having variable envelope delay characteristics, as shown in Figure 17. The attenuation section consisted of low and high-pass sections having variable cut-off frequencies. The envelope delay section consisted of all pass sections which permitted control of phase characteristics. The signal degradation section consisted of two signal-plus-noise mixers of the conventional resistive matrix type. Amplifiers were used to restore the signal to its original amplitude. The thermal noise and impulse noise signals obtained from the master tapes, together with the input signal obtained from the output of the FSK modulator, were used as inputs to the signal-plus-noise mixers. Controls permitted the adjustment of the signal-to-thermal-noise and signal-to-impulse-noise ratios over a wide ranges.

8. Demodulator

The demodulator was part of the equipment discussed in Item 6.

Figure 18, 19 and 20 are photographs of the waveforms of the words 1, 2 and 5 respectively, taken at the output of the FSK receiver (demodulator) discriminator with the FSK filter connected and the simulated telephone line in its nominal condition. Figures 21, 22 and 23 are the waveforms obtained with the FSK filter disconnected. Figures 24, 25 and 26 are photographs of the waveforms of the words 1, 2 and 5 with the FSK filter disconnected and thermal noise added.

9. Moment Computer

Figure 27 is a block diag of the moment computer. The design follows closely the technique descri : in Ref. 1. The three moments were computed by means of the iterated integration scheme previously described. Figure 28 is a timing chart of the inputs to the computer. It will be noted that three blank spaces existed after each word, i.e., an eight-bit word was actually used instead of a five-bit word and the last three bits of each word were always "0". This was done to permit resetting the computer after each computation.

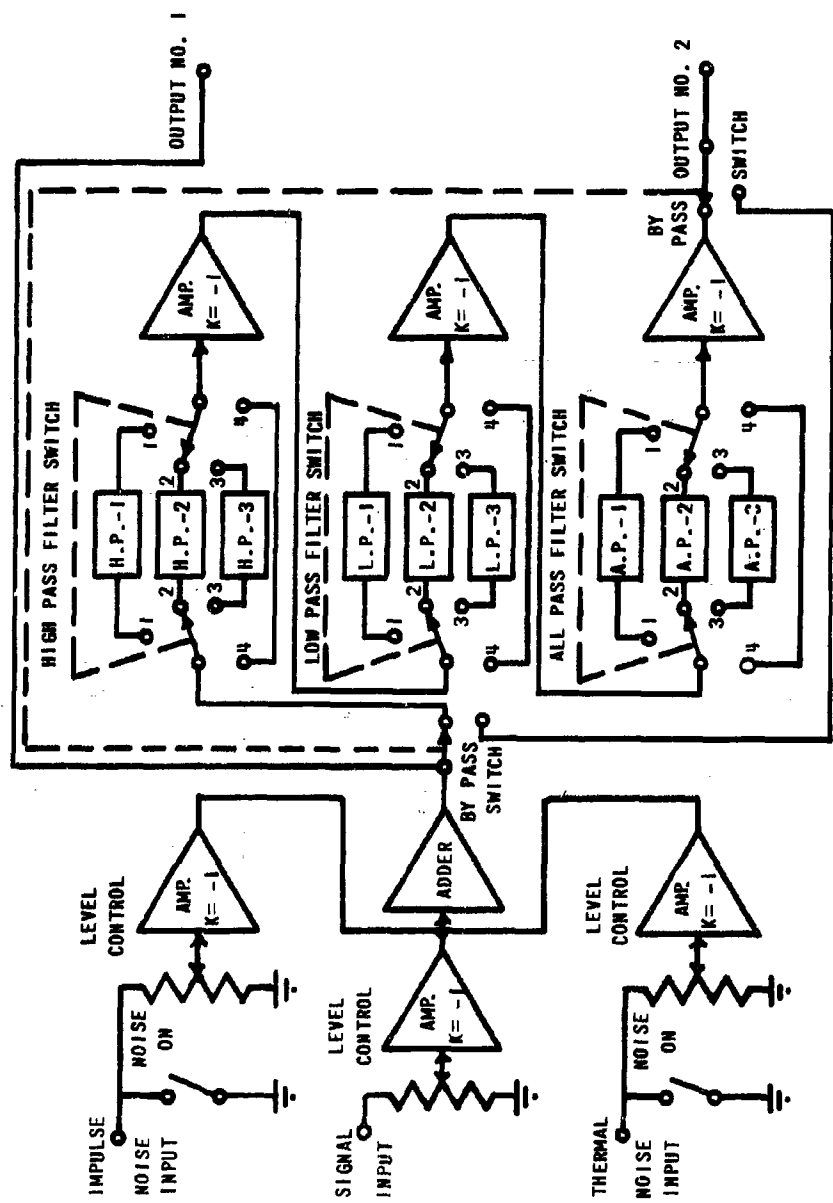


FIGURE 15 BLOCK DIAGRAM, SIMULATED TELEPHONE LINE

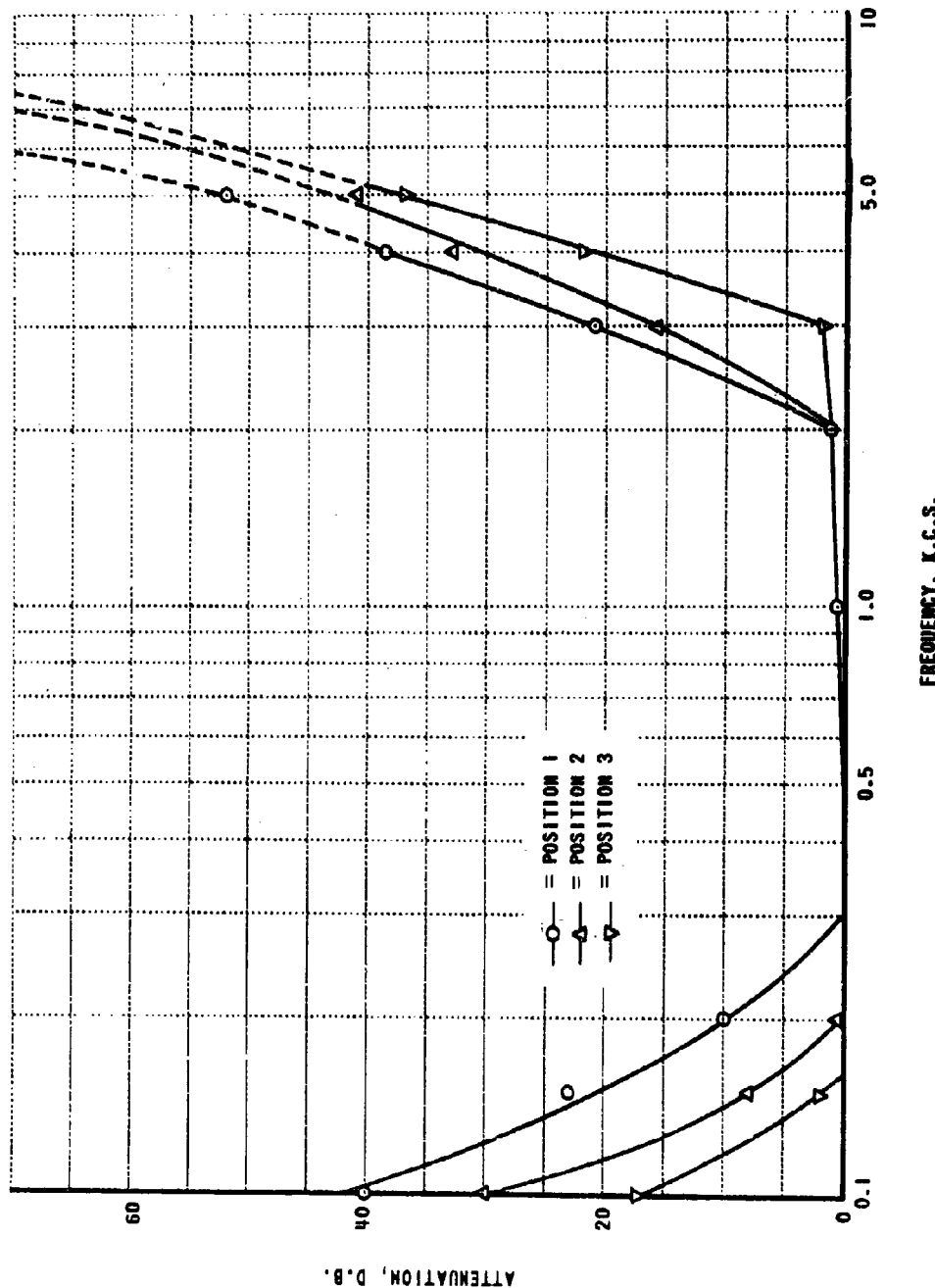


FIGURE 16 ATTENUATION CHARACTERISTICS OF THE SIMULATED TELEPHONE LINE
(VARIABLE FILTER)

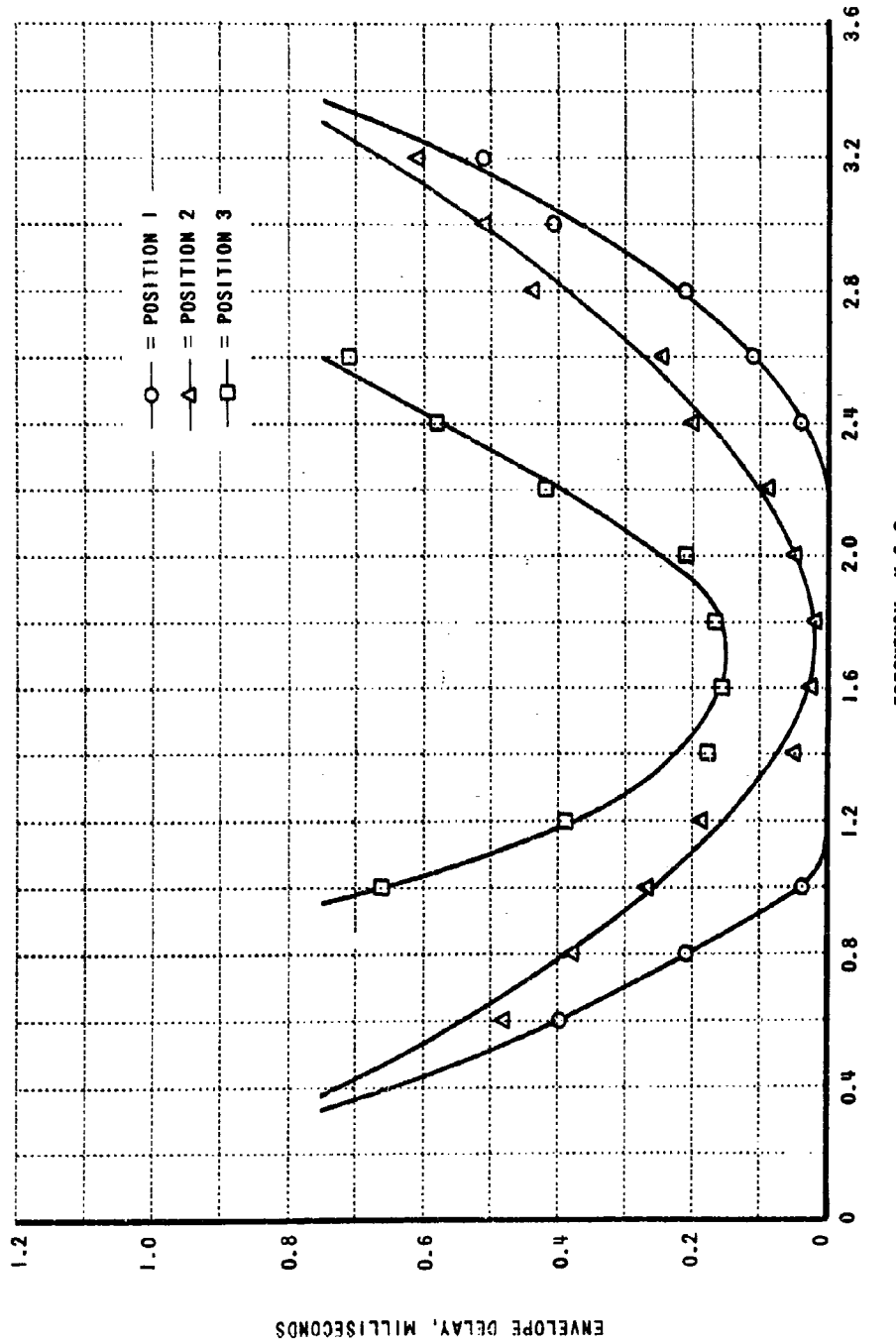


FIGURE 17 ENVELOPE DELAY CHARACTERISTICS OF THE SIMULATED TELEPHONE LINE
(VARIABLE FILTER)

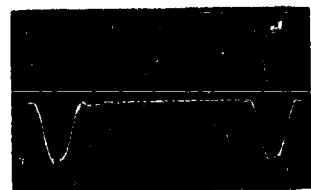


FIGURE 18
DISCRIMINATOR OUTPUT,
WORD 1

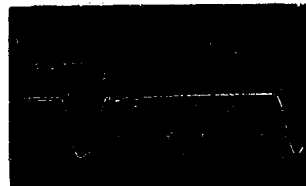


FIGURE 19
DISCRIMINATOR OUTPUT,
WORD 2

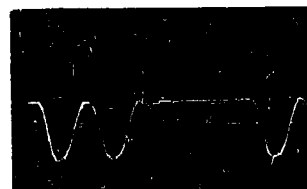


FIGURE 20
DISCRIMINATOR OUTPUT,
WORD 5

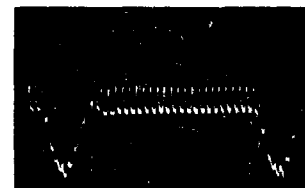


FIGURE 21

DISCRIMINATOR OUTPUT,
FSK FILTER DISCONNECTED,
WORD 1



FIGURE 22

DISCRIMINATOR OUTPUT,
FSK FILTER DISCONNECTED,
WORD 2



FIGURE 23

DISCRIMINATOR OUTPUT,
FSK FILTER DISCONNECTED,
WORD 5

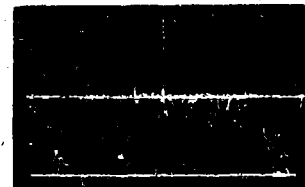


FIGURE 24

FSK DISCRIMINATOR OUTPUT,
WORD 1 PLUS THERMAL NOISE,
FSK FILTER DISCONNECTED

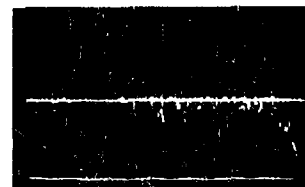


FIGURE 25

FSK DISCRIMINATOR OUTPUT,
WORD 2 PLUS THERMAL NOISE,
FSK FILTER DISCONNECTED



FIGURE 26

FSK DISCRIMINATOR OUTPUT,
WORD 5 PLUS THERMAL NOISE,
FSK FILTER DISCONNECTED

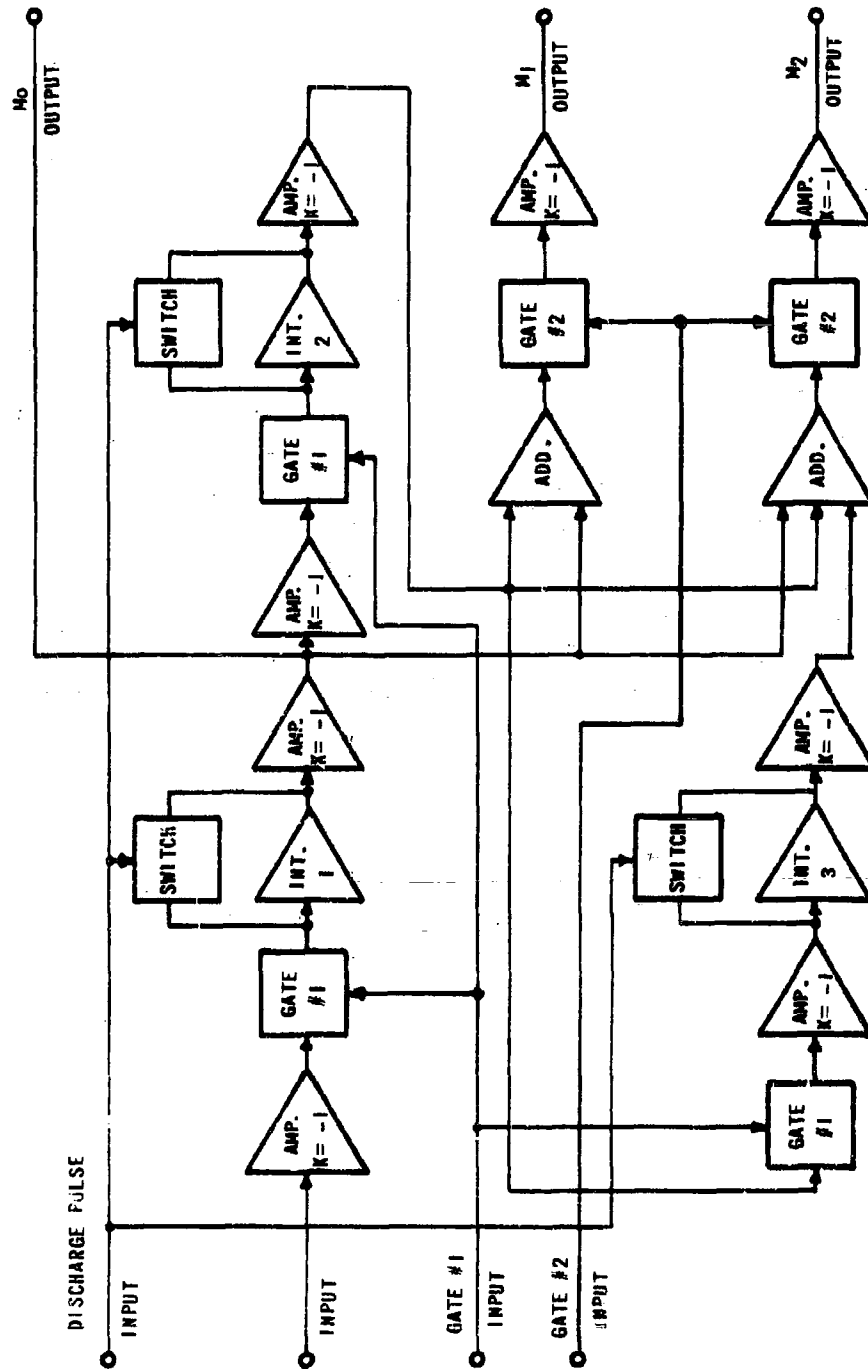


FIGURE 27 BLOCK DIAGRAM, MOMENT COMPUTER

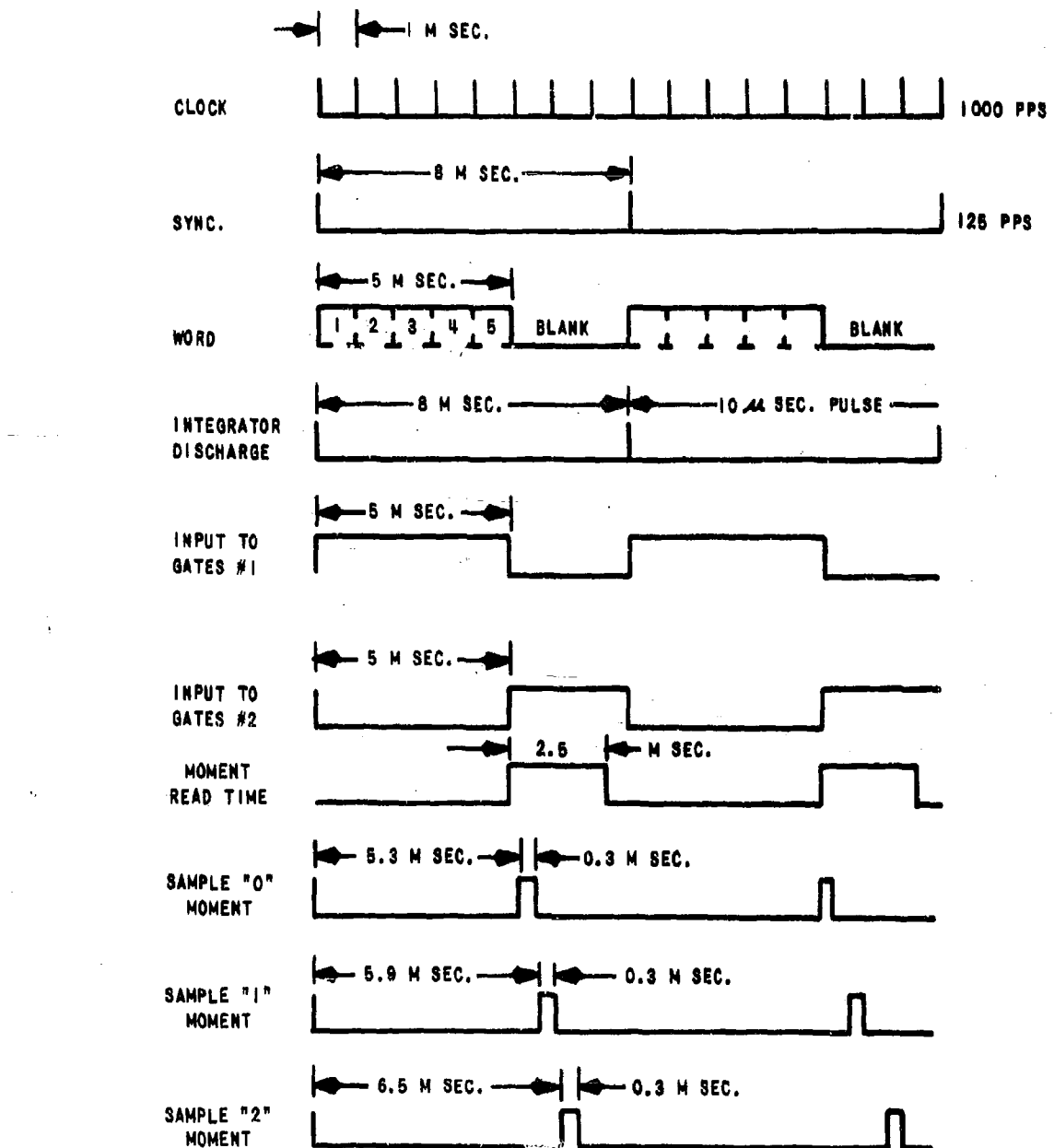


FIGURE 28 TIMING CHART, MOMENT DETECTION

Figure 29 is a photograph taken of the waveform of the word 31 (base band) at the input to the computer. Figure 30 was taken at the input to the first integrator. Figure 31 was taken at the output of the first integrator (M_0).

Figure 32 shows the I_1 input to the M_1 adder; Figure 33 shows the I_2 input to the M_1 adder and Figure 34 shows the sum of I_1 and I_2 at the output of the M_1 adder. This waveform attains a value proportional to the first moment M_1 at time $t = T$.

Figure 35 shows the I_1 input to the M_2 adder; Figure 36 shows the I_2 input to the M_2 adder; Figure 37 shows the I_3 input to the M_2 adder, and Figure 38 the sum of $I_1 + I_2 + I_3$ at the output of the M_2 adder. This waveform attains a value proportional to M_2 at time $t = T$.

FIGURE 29

INPUT TO COMPUTER,
WORD 31



FIGURE 30

INPUT TO 1ST INTEGRATOR,
WORD 31



FIGURE 31

OUTPUT, 1ST INTEGRATOR,
WORD 31





FIGURE 32

1ST INTEGRATOR INPUT
TO M₁ ADDER,
WORD 31



FIGURE 33

2ND INTEGRATOR INPUT
TO M₁ ADDER,
WORD 31



FIGURE 34

SUM, 1ST AND 2ND INTEGRATORS
AT OUTPUT, M₁ ADDER,
WORD 31

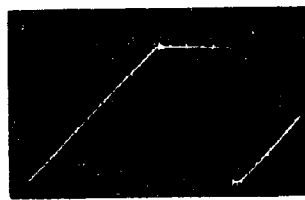


FIGURE 35

1ST INTEGRATOR INPUT
TO M₂ ADDER,
WORD 31

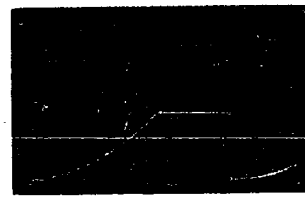


FIGURE 36

2ND INTEGRATOR INPUT
TO M₂ ADDER,
WORD 31



FIGURE 37

3RD INTEGRATOR INPUT
TO M₂ ADDER,
WORD 31



FIGURE 38

SUM 1ST, 2ND AND 3RD
INTEGRATORS AT OUTPUT
OF M₂ ADDER, WORD 31

10. Error Rate Evaluation, Moment Detection

An Ampex FR-100 FM magnetic tape recorder was used to record the three analog outputs of the moment computer plus a synchronizing signal to indicate correct sampling time. The analog outputs of the tape recorder were then digitized by an Epsco analog-to-digital converter and then recorded on digital-punched paper tape. The digital-punched paper tape data were then transferred to IBM input format on punched cards and finally the data were evaluated by an IBM 704 computer.

11. Error Rate Evaluation, FSK Equipment

The filtered output of the FSK demodulator was fed to the FSK transistor switch. The outputs of the FSK transistor switch and the output of the word generator were then used as inputs to an error comparator. Word count and FSK error bit count were made by two H-P 522B counters.

IV. TEST PROCEDURES

A. Selection of Test Conditions

As pointed out in the introduction, it was necessary to limit the number of combinations of system parameters used in order to reduce the data reduction task to reasonable proportions. It was therefore decided to select a set of nominal parameter values and to investigate the sensitivity of the error probability to deviations from these values.

1. Words

A physical three-dimensional model (Figure 39), representing all 32 possible 5-bit words in the orthonormalized three space in which variations of the output due to white Gaussian noise have a normal three-dimensional spherical distribution (refer to Appendix IV.b), was constructed. It was found that in this space there exists zero point symmetry so that only 16 words need be considered. The distances between every word and all other words was tabulated and three words, viz., 1, 2 and 5, were selected as being representative of the set.

2. Signal-to-Thermal-Noise Ratios and Signal-to-Impulse-Noise Ratios

These ratios were selected on the basis of bit-for-bit FSK error comparisons with a criterion of at least ten errors in 20 seconds of real time.

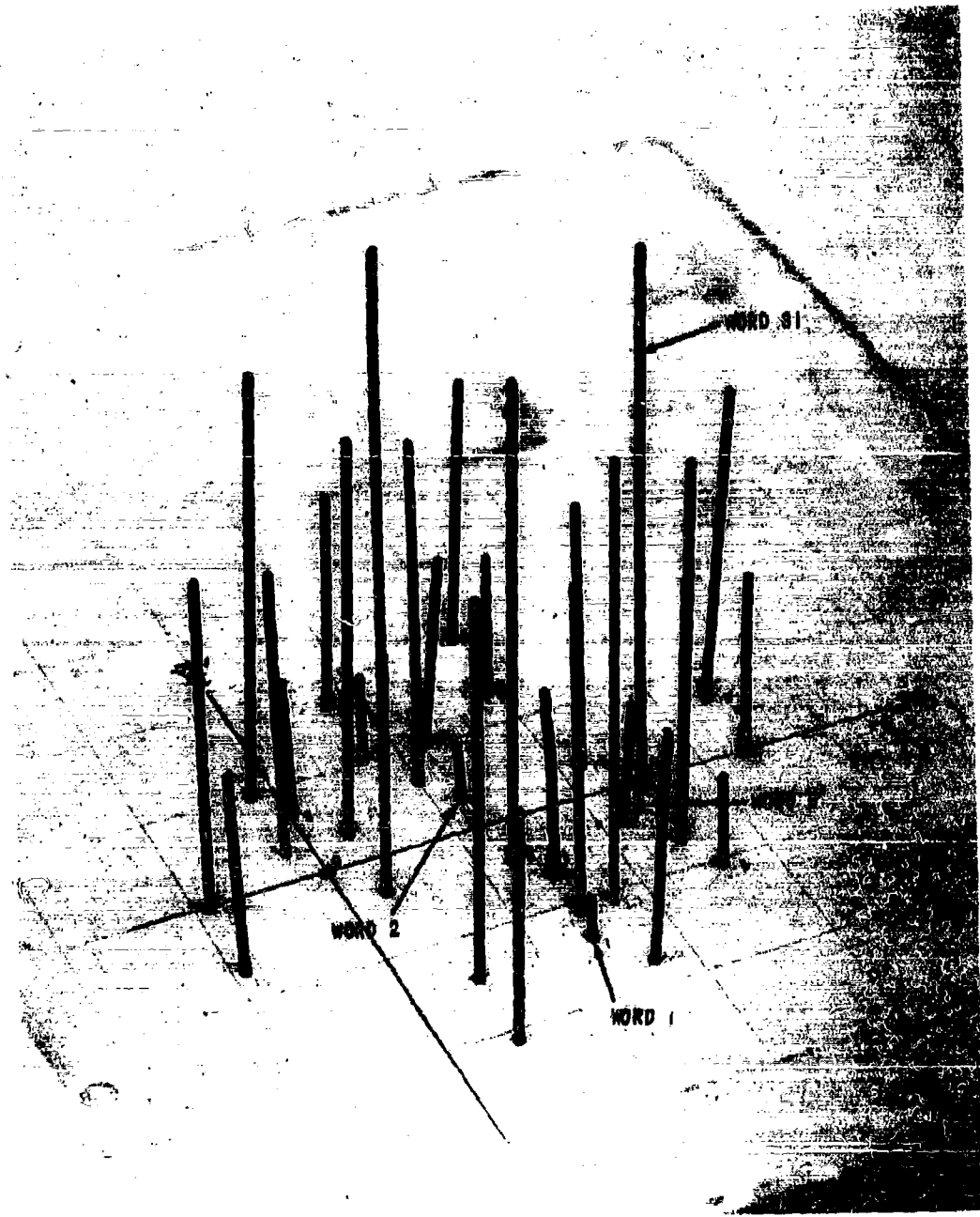


FIGURE 39 MODEL OF 32 POSSIBLE 5 BIT WORDS

(At much lower error rates an unreasonable amount of time would be required for the experiment and for reduction of the data.)

3. Signaling Speed

A 1000-bits/second, 125-words/second nominal rate was selected on the basis of reasonable FSK (Model 3000 Tele-Signal) equipment performance. If a signal of alternate "0's" and "1's" is sent at this rate through the nominal telephone line filter, the output of the discriminator approximates a 500-cps sine wave.

4. Telephone Line Bandwidth and Envelope Delay

Reference to Figures 16 and 17, and Ref. 1, shows that the band-pass and envelope delay characteristics obtained with the corresponding controlling switches set at positions 2 are about half-way between the minimum and maximum bandwidths and envelope delays of 90% of the telephone lines in the United States.

Nominal settings of the simulated telephone line as used in these tests were those obtained with all controlling switches except the low pass in switch positions 2. Nominal setting of the low-pass switch was at position 3 (highest cut-off frequency) to avoid severe amplitude differences between mark and space frequencies at the input of the FSK receiver.

5. Moment Computer Integration Time, Discharge Pulse Timings and Gate Positions

Adjustments were made for best computer performance under nominal conditions. These adjustments were not changed except when the signaling speeds were altered during the tests.

6. Synchronizing

Since an evaluation of synchronization was not of interest per se, and in order to avoid additional complexity, simple external synchronization was used to synchronize the moment computer. It should be noted that the same external synchronization system was used with the FSK error comparator for determining FSK bit error rates.

B. Master Tape Recordings

A series of master tapes were made on an Ampex, Model S 3449 magnetic tape recorder. Clock pulses, thermal noise and impulse noise were recorded, each on a separate channel of the tape. During the tests, the clock generator, thermal noise generator, and impulse noise generator were replaced by the three outputs of the tape recorder to insure similar inputs to the equipment during repetitive runs (e.g., same thermal noise and impulse noise for each word 1, 2 and 5).

C. Initial Tests (base band only)

In order to check performance of the computer against mathematically predicted results at various signal energy/thermal noise power density (E/N_0) ratios, preliminary base band tests were made.

V. TEST RESULTS

A. Base Band Tests

Figure 40 is a plot of the probability of error vs. signal energy/thermal noise power density. Only the zero-order moment was recorded and only words 0 and 31 were sent. The theoretical curve of error probability vs. E/N_0 is also shown on this figure and is seen to be in good agreement with the experimental points.

B. Experimental Error Probability of the FSK Equipment

Figure 41 is a plot of the probability of bit error vs. signal energy/thermal noise power density for the words 1, 2 and 5. For purposes of comparison, the theoretical curve for a wide deviation noncoherent FSK system operating in the presence of additive white Gaussian noise is also shown. In this case the probability of error is given by $P_e = \frac{1}{2} e^{-E/2N_0}$ (Ref. 4). It is to be noted that this equation can not be expected to describe the performance of the experimental equipment for several reasons, e.g., the restricted bandwidth of the telephone line filters, narrow deviation FSK, use of a discriminator rather than two matched filters. As will be discussed later, the FSK equipment showed a variation in mark and

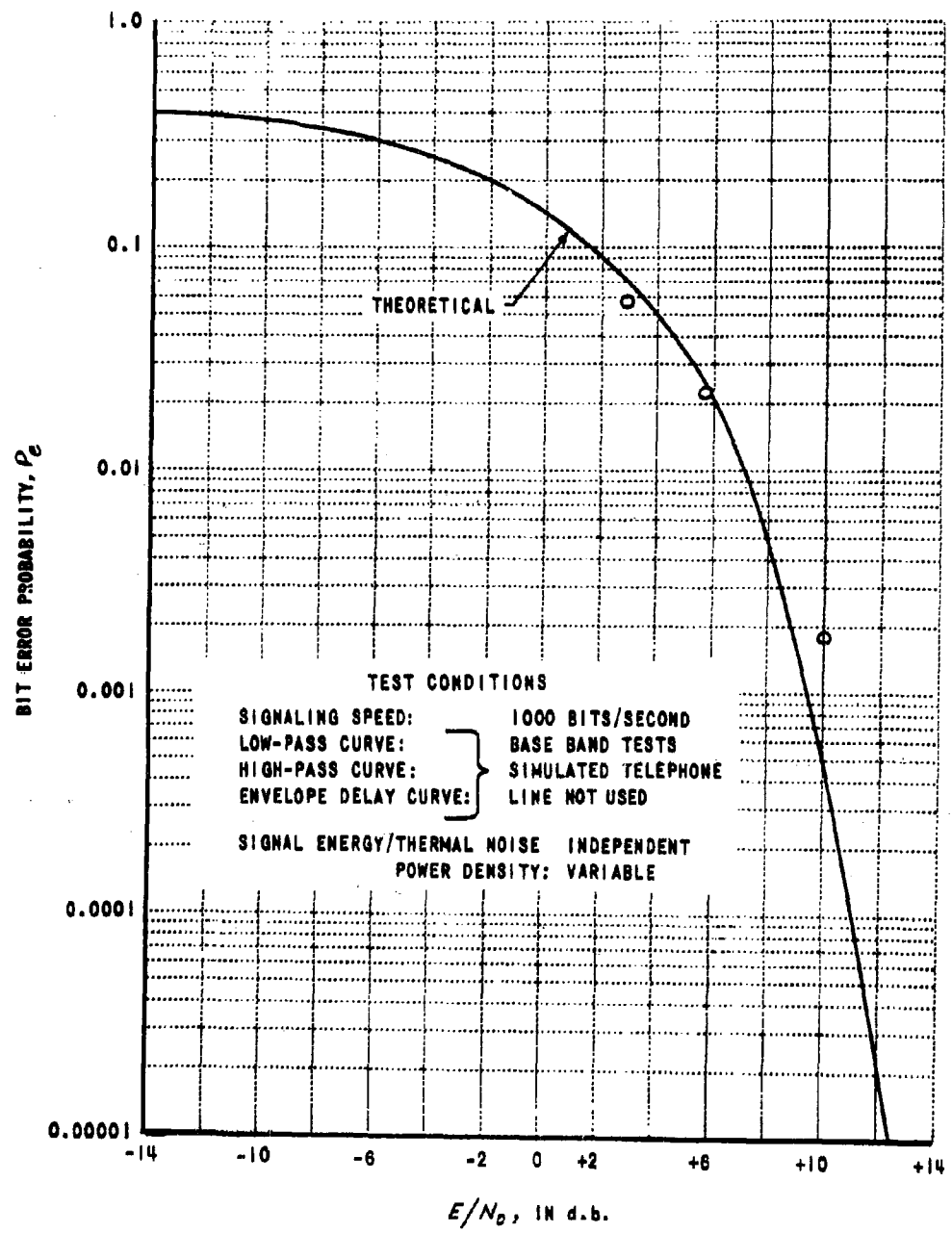


FIGURE 40 PROBABILITY OF ERROR VS SIGNAL ENERGY/ THERMAL NOISE POWER DENSITY

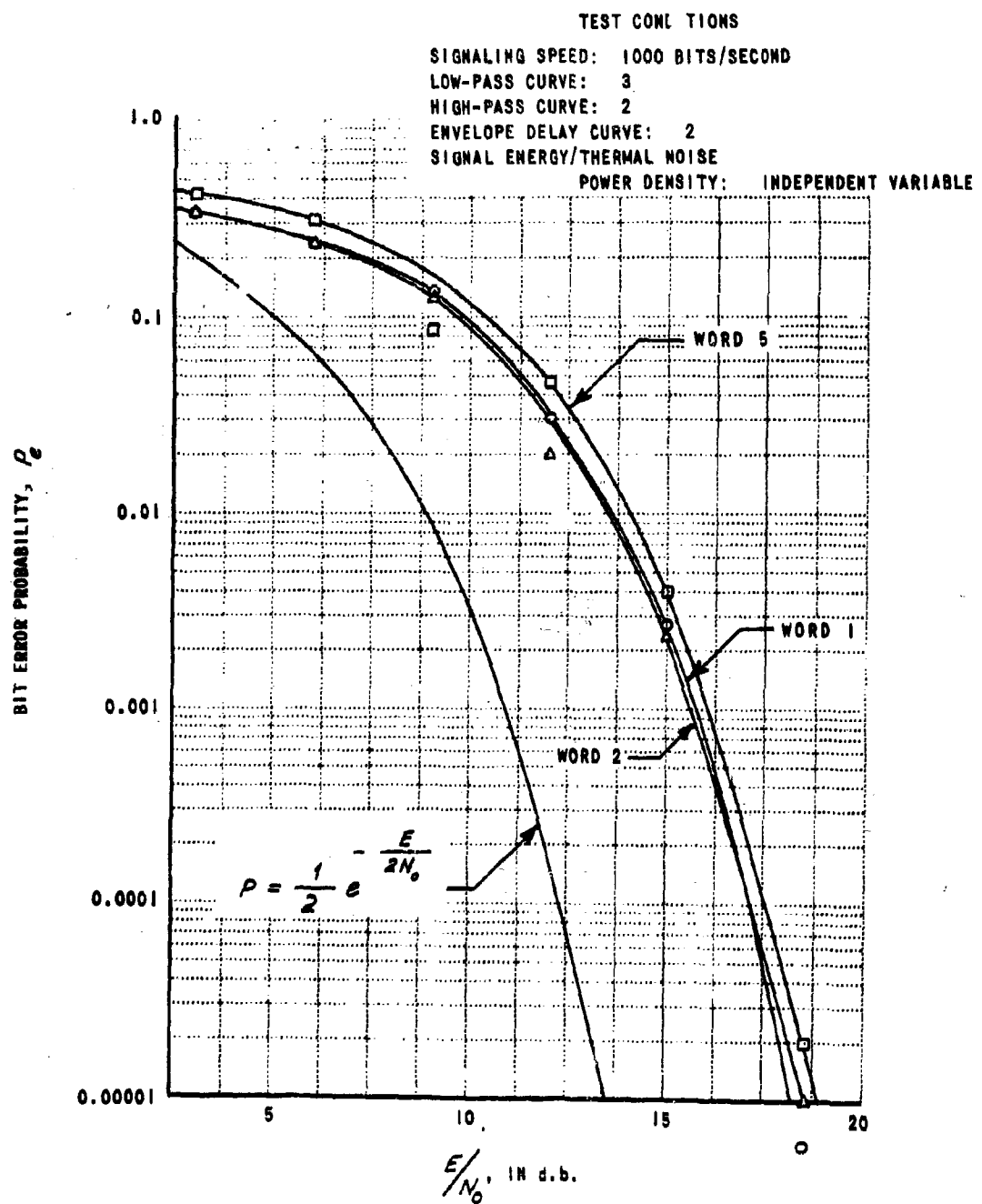


FIGURE 41 F.S.K. PROBABILITY OF BIT ERROR S VS SIGNAL ENERGY/THERMAL NOISE POWER DENSITY, WORDS 1, 2, 5

space output levels, depending on the particular word sent. It is believed that the dependence of error probability on the transmitted word which is apparent in Figure 41, is related to this phenomenon.

Figure 42 is a plot of the probability of error vs. signal amplitude/impulse amplitude at the input to the simulated telephone line. The impulses which were used were essentially rectangular and of 2- μ sec. duration. No errors were observed when the signal-to-impulse noise amplitude ratio was -16 db. The curves in the lower right region of Figure 42 have therefore been extrapolated and are shown dashed.

Table 2 shows the error probability obtained as the high-pass and low-pass cut-off characteristics were varied with a signal energy/thermal noise power density ratio of 15 db at the input to the telephone line filter.

Table 3 was obtained under the same conditions as Table 2 except impulse noise was fed to the input of the filter at a signal-to-impulse amplitude ratio of -21.4 db. (The rms signal was .08 volts and the peak impulse level was 1-1/3 volts.) Again, the high-pass and low-pass cut-off frequencies of the simulated telephone line were varied.

Table 4 was obtained with the filter at nominal settings and a signal energy/thermal noise power density of 15 db and a signal-to-impulse amplitude ratio of -21.4 db at the input to the filter.

Figure 43 is a plot of error probability vs. average impulse spacing at a constant -21.4 db signal-to-input amplitude ratio at the input to the simulated telephone line.

C. Experimental Error Probability of the Moment Detector Equipment

Figure 44 shows the measured word error probability obtained by means of moment detection plotted versus the ratio of signal energy/thermal noise power density (E/N_0). On this figure, upper and lower bounds of the word error probability obtained by the FSK equipment are also shown. The upper bound is obtained on the assumption that there occurs only one bit error per word in error. Since each word contains 5 bits, it is seen that the probability of word error is then 5 times the measured probability of bit error.

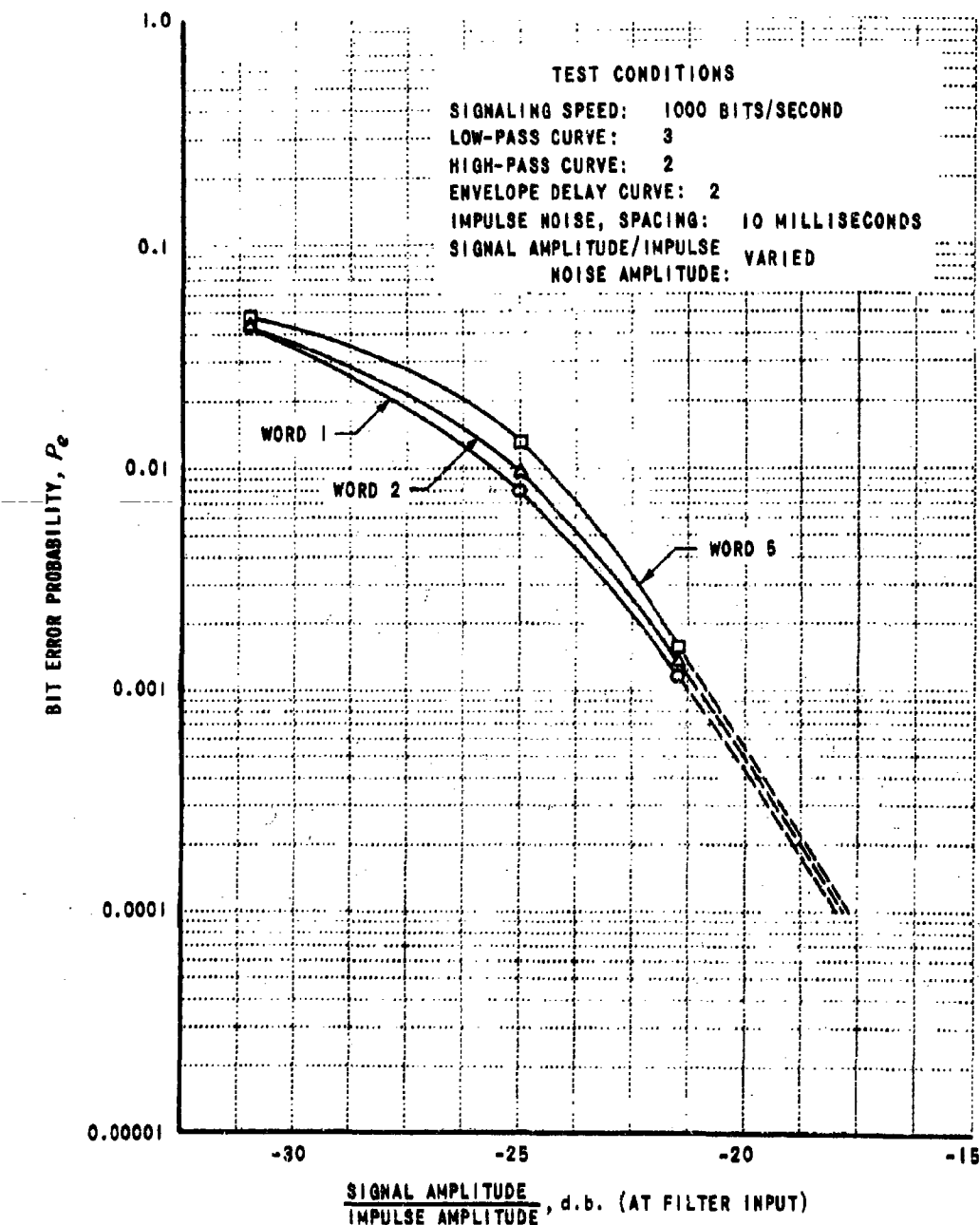


FIGURE 42 F.S.K. PROBABILITY OF BIT ERROR VS SIGNAL AMPLITUDE/IMPULSE AMPLITUDE, WORDS 1, 2, 5

TABLE 2
FSK BIT "ERROR PROBABILITY" AS A FUNCTION OF LINE FILTER HIGH PASS CUT OFF FREQUENCY WITH
LOW PASS CUT OFF AT 2.2 K.C.S. (3 db), SIGNAL ENERGY/ THERMAL NOISE POWER DENSITY = 15 db
(SEE FIG. 16)

HIGH PASS CUT OFF, C.P.S. (AT 3 db)	ERROR PROBABILITY		
	WORD 1	WORD 2	WORD 5
0	0.0070	0.00695	0.0069
145	0.0032	0.00217	0.0046
180	0.055	0.050	0.180
280	0.089	0.101	0.212

FSK BIT "ERROR PROBABILITY" AS A FUNCTION OF LINE FILTER LOW PASS CUT OFF FREQUENCY WITH
HIGH PASS CUT OFF AT 145 C.P.S. (3 db), SIGNAL ENERGY/ THERMAL NOISE POWER DENSITY = 15 db
(SEE FIG. 16)

LOW PASS CUT OFF, K.C.S. (AT 3 db)	ERROR PROBABILITY		
	WORD 1	WORD 2	WORD 5
∞	0.0053	0.0047	0.0087
2.10	.0032	0.0030	0.0052
3.05	.0032	0.0025	0.0044

TABLE 3
BIT ERROR PROBABILITY AS A FUNCTION OF LINE HIGH PASS CHARACTERISTICS WITH LOW PASS CUT OFF
AT 2.2 K.C.S. (3 db), SIGNAL TO IMPULSE NOISE AMPLITUDE RATIO = -21.4 db (SEE CURVES FIG. 16)

HIGH PASS CUT OFF, C.P.S. (AT 3 db)	ERROR PROBABILITY		
	WORD 1	WORD 2	WORD 5
0	0.044	0.043	0.052
145	0.0036	0.0034	0.0050
180	0.0142	0.0158	0.025
280	0.038	0.0410	0.112

ERROR PROBABILITY AS A FUNCTION OF LINE LOW PASS CHARACTERISTICS WITH HIGH PASS CUT OFF AT
145 C.P.S. (3 db), SIGNAL TO IMPULSE NOISE AMPLITUDE RATIO = -21.4 db (SEE CURVES FIG. 16)

LOW PASS CUT OFF, K.C.S. (AT 3 db)	ERROR PROBABILITY		
	WORD 1	WORD 2	WORD 5
∞	0.0095	0.0096	.0149
2.10	0.00212	0.0027	.0085
3.05	0.0056	0.0060	.0044

TABLE 4
ERROR PROBABILITY OF WORDS, SIGNAL ENERGY/ THERMAL NOISE POWER DENSITY = 15 db, SIGNAL TO
IMPULSE NOISE AMPLITUDE RATIO = -21.4 db, FILTER AT NOMINAL SETTINGS (SEE CURVES FIG. 16)

WORD	ERROR PROBABILITY
1	0.0156
2	0.0224
5	0.0238

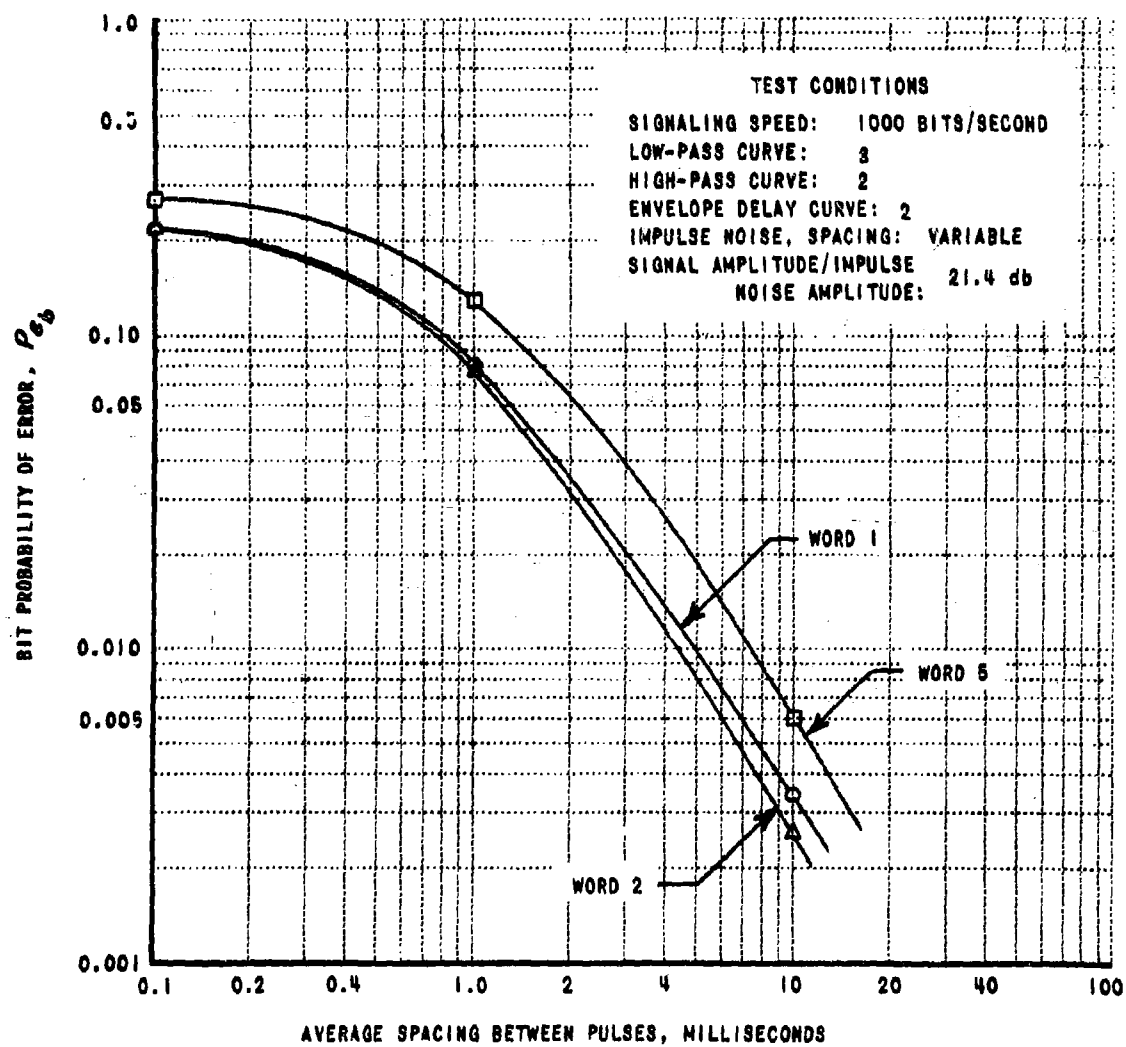


FIGURE 43 F.S.K. PROBABILITY OF BIT ERROR VS AVERAGE IMPULSE SPACING

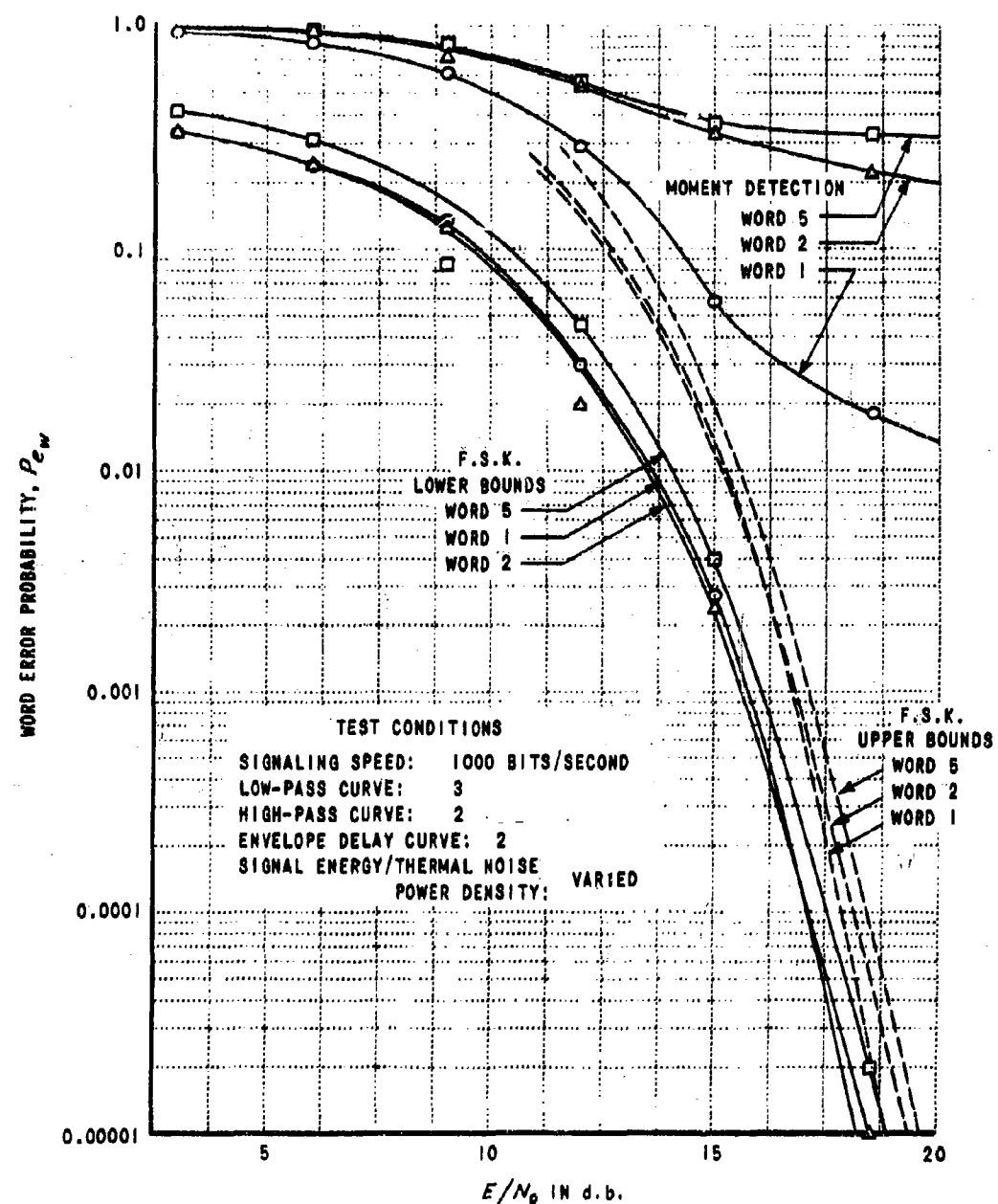


FIGURE 44 MOMENT DETECTION PROBABILITY OF ERROR VS SIGNAL ENERGY/THERMAL NOISE POWER DENSITY, WORDS 1, 2, 5

The lower bound is obtained on the assumption that there occur 5-bit errors per word in error so that the probability of word error equals the probability of bit error. Figure 45 shows the measured word error probability obtained by moment detection plotted versus signal amplitude impulse amplitude. The bounds on word error probability obtained by the FSK system under these conditions are also plotted in Figure 45 for comparison purposes.

Inspection of Figures 44 and 45 shows that the performance attainable with the moment detection equipment was far inferior to that obtainable with the FSK equipment. Under these circumstances, it did not appear warranted to investigate moment detection further.

VI. DISCUSSION OF TEST RESULTS

A. FSK Equipment

A complete set of runs was made on the FSK equipment. The probabilities of error obtained were reasonably compatible with theory. While the error rates were somewhat higher than would be expected of an optimum noncoherent FSK system, it was felt that this was due mainly to the FSK equipment deficiencies noted in the following section.

For purposes of comparison with moment detection, which yields word error probability, the word error probability obtained with FSK would be desirable. In Section V.C., it was shown how upper and lower bounds on word error probabilities may be obtained from the measured bit error probabilities.

B. Moment Detection

Although a complete set of runs were made and recorded on magnetic tape, only two sets of data were reduced by the IBM 704 computer and error rates computed. Data reduction was discontinued after these two runs when the error rates were found to be far greater than those produced by the FSK equipment or mathematically predicted. It was felt that little, if any, information would be obtained by further data reduction. It was believed that the poor results of these two runs justified the suspension of further investigations. Reasons for the lack of correlation between mathematically predicted error rates and actual error rates are discussed in the following section.

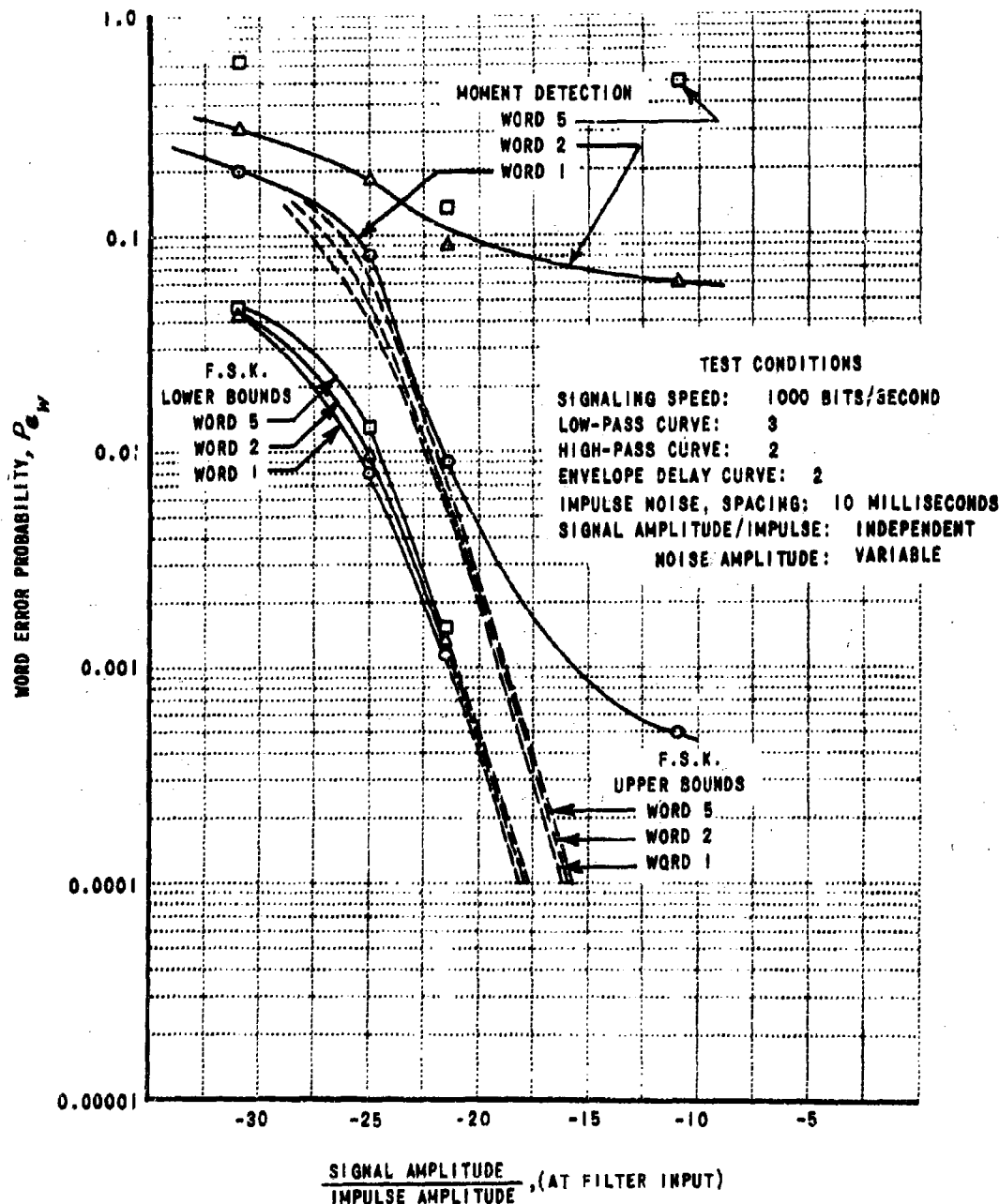


FIGURE 45 MOMENT DETECTION PROBABILITY OF ERROR VS SIGNAL ENERGY/NOISE POWER DENSITY WORDS 1, 2, 5

VII. CONCLUSIONS

In general, the failure to obtain data completely compatible with theory was due to performance limitations of both the FSK equipment and the moment computer.

From a practical point of view, the equipment needed to implement moment detection is inordinately complicated. The computation of the k^{th} -order moment by the "multiple definite integral method" requires the computation of $k + 1$ integrals. This method, which was used because it seemed to be the most practical, obtains the required moments as the weighted sum and difference of these integrals. Since the resulting moment may be of much smaller magnitude than the various inputs of which it is composed, it is extremely sensitive to gain variations and drift of the equipment used (i.e., the small differences of two large numbers is very sensitive to small fractional changes of the large numbers). The example given in the introduction of this memo where the computation of the second moment of the word 1 is obtained from $25 - 45 + \frac{61}{3} = \frac{1}{3}$ illustrates this problem very clearly. Tests of the accuracy obtained with the experimental moment computer showed that the values of all moments were computed to approximately $\pm 1\%$ of full-scale values; this accuracy is in accord with what one can reasonably expect from the type of equipment employed. Considerably more sophisticated electronic circuitry would be needed to obtain much better than 1% of full-scale accuracy. However, $\pm 1\%$ of full-scale errors are sufficient to cause errors in the determination of the received word. To this computer error must be added the error of the tape recorder which is used to record the moments. The Ampex tape recorder accuracy is about $\pm 1\%$ of full scale. This, too, can give an error in the determination of the received word.

Because of the t^k weighting, moment detection computation is very seriously affected by deviations from ideal behavior of the associated communications equipment, such as d.c. components due to nonlinearities or gain variations.

The FSK equipment used in conjunction with the moment computer is believed to be fairly representative of the performance that may be expected from noncoherent FSK equipment. Reference to Figure 4 reveals severe d.c.

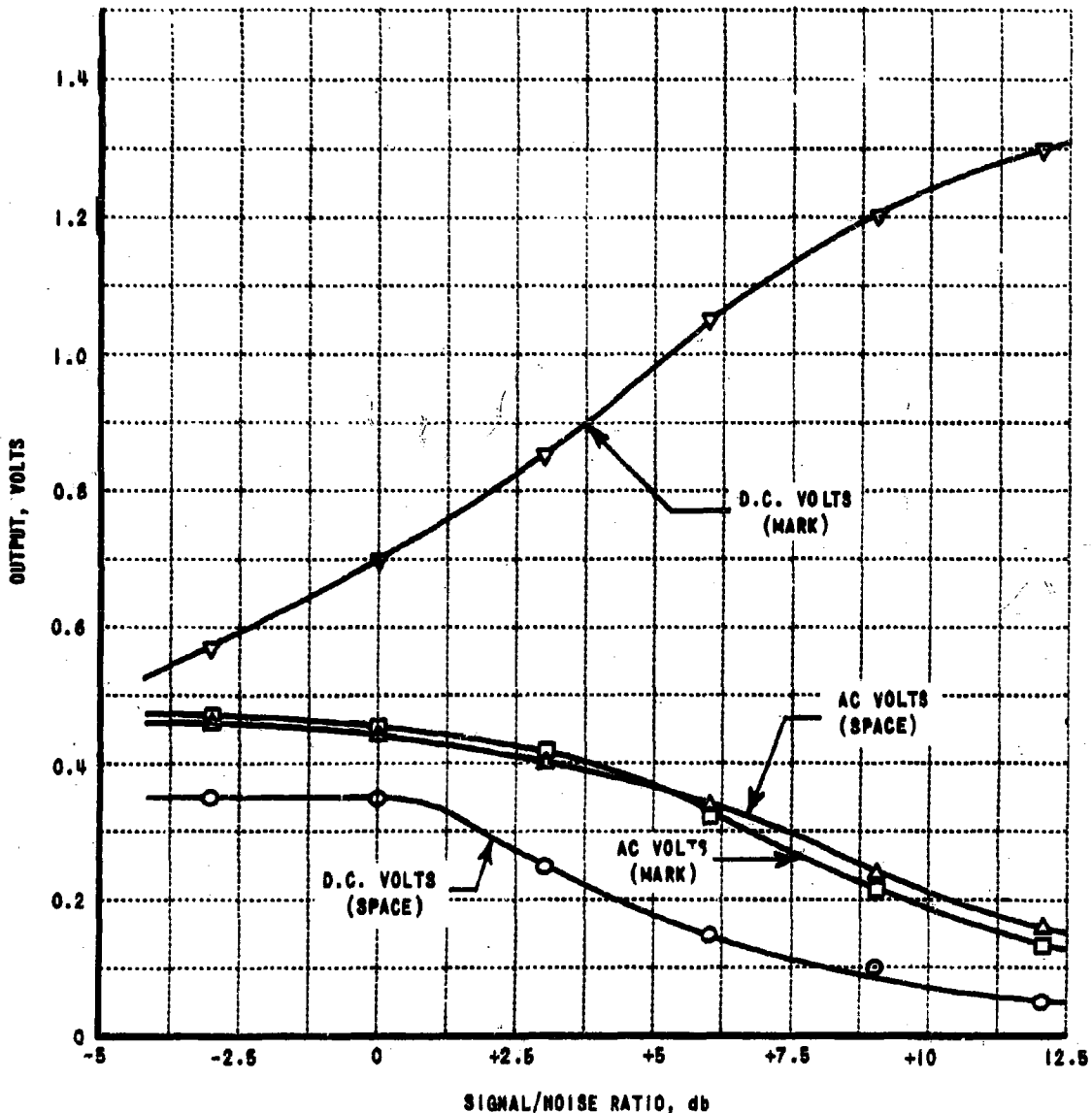


FIGURE 46 F.S.K. DISCRIMINATOR SHIFT VS SIGNAL/THERMAL NOISE

shifts of both mark and space outputs with thermal noise. In addition, the variation of the output levels of both mark and space with word content is clearly indicated in the accompanying photographs, Figures 47a, b and c. The two horizontal lines in each photo are the output levels obtained when a steady mark and space signal is received; the traces within are the output amplitudes obtained when the words 1, 2 and 5 respectively, are sent.



FIGURE 47a

OUTPUT OF FSK DISCRIMINATOR,
FSK FILTER CONNECTED,
WORD 1



FIGURE 47b

OUTPUT OF FSK DISCRIMINATOR,
FSK FILTER CONNECTED,
WORD 2



FIGURE 47c

OUTPUT OF FSK DISCRIMINATOR,
FSK FILTER CONNECTED,
WORD 5

Figures 47a, b and c indicate the difference in output amplitudes of the FSK discriminator when the word 1 without noise is sent, the word 31 without noise is sent, and when the word 31 without noise is sent when the carrier filter of the FSK equipment is disabled.

Figures 49a, b and c clearly indicate the assymetrical noise output of the FSK discriminator when thermal noise is inserted at the receiver input. (Comparison with Figure 4 indicates that the noise at the output of the telephone line filter is symmetric.) Again, the horizontal lines are the output amplitudes when a steady mark and space signal is sent without noise.

It should be noted that the paragraphs above are not written in condemnation of the particular FSK equipment used in conjunction with the moment computer. Quite the contrary; these differences are of little import in normal FSK operation but are inherently very serious when used with moment detection.

The experimental investigation has shown that in order for the moment detection technique to be properly implemented, electronic equipment of unusual, and it is felt impractical, complexity and accuracy is required. Further, it is found that even if the terminal moment detection equipment were ideal, the technique is extremely sensitive to gain variations and nonlinearities (d.c. offset) of the associated communications equipment. Moment detection therefore appears to hold little promise as a decision technique in a practical communications system.

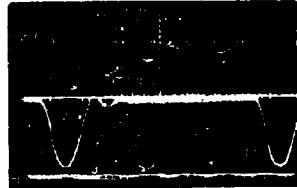


FIGURE 48a

OUTPUT OF FSK DISCRIMINATOR,
FSK FILTER CONNECTED,
WORD 1



FIGURE 48b

OUTPUT OF FSK DISCRIMINATOR,
FSK FILTER CONNECTED
WORD 3

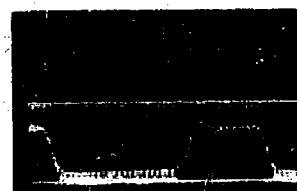


FIGURE 48c

OUTPUT OF FSK DISCRIMINATOR,
FSK FILTER DISCONNECTED,
WORD 3



FIGURE 49a

MARK AND SPACE
OUTPUT OF FSK DISCRIMINATOR,
STEADY INPUT

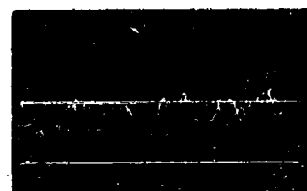


FIGURE 49b

THERMAL NOISE
OUTPUT OF FSK DISCRIMINATOR,
FSK FILTER CONNECTED

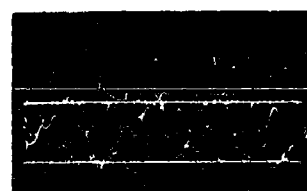


FIGURE 49c

THERMAL NOISE
OUTPUT OF FSK DISCRIMINATOR,
FSK FILTER DISCONNECTED

REFERENCES

1. Alexander, A. A., Nast, D. W., and Gryb, R. M., Capabilities of the Telephone Network for Data Transmission, AIEE Conference Papers CP60-266, CP60-413, and CP60-336.
2. Mertz, Pierre, Model of Impulse Noise for Data Transmission, Rand Corporation Report P-1761, 27 July 1959.
3. Slade, T. T., Jr., Fisch, S., and Maloney, D. A., Detection of Information by Moments, Convention Record - Part 8 - IRE National Convention, 1953.
4. Becker, H. D., and Lawton, J. G., Theoretical Comparison of Binary Data Transmission Systems, Cornell Aeronautical Laboratory, Inc., Report No. CA-1172-S-1, May 1958.

APPENDIX

Difficulties Encountered with The FSK Equipment

Some of the difficulties experienced with the Tele-Signal, Model 3000, FSK equipment may be of interest and are listed below.

1. Extremely high error probabilities observed during early FSK test runs were found to be due to a partially shorted input transformer and a defective transistor V103 in the high-speed network of the FSK Receiver.
2. After the defective parts were replaced, the FSK test runs were repeated. Although the error probabilities were greatly reduced, they were still much higher than expected. The reason was found to be the large ripple components on the d.c. output voltages from the power supplies. Since reduction of the ripple components would have entailed equipment redesign, the power supplies were disconnected and the FSK equipment was supplied with external d.c. power during the actual evaluation.
3. As noted in Section VII of this report, severe d.c. discriminator shifts with additive thermal noise was encountered. Again, equipment redesign would have been necessary to correct this condition; however, an attempt was made to minimize this effect by adjustment of the discriminator. It is believed that this d.c. shift had much more serious effects on the error probabilities obtained with moment detection than during normal FSK detection.
4. In the process of correcting and/or alleviating these difficulties, many differences between the schematics and the actual equipment were noted. In prototype equipment of this kind, it is not unusual to encounter discrepancies of this type and in all cases it was considered that the equipment components and wiring rather than the schematics were correct.

DISTRIBUTION LIST

No. of Copies

RADC (RAUAT) Griffiss AFB, New York	15
RADC (RAAT) Griffiss AFB, New York	1
RADC (RAOYL-2) Griffiss AFB, New York	1
Armed Services Technical Information Agency Arlington Hall Station Arlington 12, Virginia	13
ESD (CRQSL-1) L. G. Hanscom Field, Massachusetts	1
AUL (AUL-7736) Maxwell AFB, Alabama	1
WADD (WWAD) Wright-Patterson AFB, Ohio	1
Chief Naval Research Laboratory Attn: Code 2021 Washington 25, D. C.	1
Air Force Field Representative Naval Research Laboratory Attn: Code 1010 Washington 25, D. C.	1
Commanding Officer U. S. Army Signal Research and Development Laboratories Attn: SIGRA/SL-ADT Fort Monmouth, New Jersey	1
Chief Bureau of Ships Attn: Code 312 Washington 25, D. C.	1
Signal Corps Liaison Officer RADC (RAOYL, Capt. Norton) Griffiss AFB, New York	1

GEEIA (ROZMSTL, Technical Library)
Griffiss AFB, New York 1

Chief
Research & Development Office of Chief Signal Officer
Washington 25, D. C. 1

RADC (RAOUA, Mr. Malloy)
Griffiss AFB, New York 1

AF Section
MAAG, Germany
Box 810
APO 80
New York, New York 1

AF Plant Representative Office
United States Air Force
Attn: RCRCA
General Electric Company
P. O. Box 91
Cincinnati 15, Ohio 1

John Kelly
Mitre Corporation
Box 208
Lexington 73, Mass. 1

ESD (SCSD, Col. O'Hearn)
L G Hanscom Field
Bedford, Mass. 1

RADC (RAUO)
Griffiss AFB, New York 2

Mr. L. DeRosa
ITT Communication System, Inc.
Garden State Plaza
Routes 4 & 17, Paramus, New Jersey 1

ESD (ESRR, Colonel Sheets)
L G Hanscom Field
Bedford, Mass. 1

AFSC (Major Nowakowski, SCSPE)
Andrews AFB, Washington 25, D. C. 1